

To=NWS-LIBRARY

QC
807.5
U66
no. 354
c.1

NOAA Technical Report ERL 354-WMPO 6

U.S. DEPARTMENT OF COMMERCE
NATIONAL OCEANIC AND ATMOSPHERIC ADMINISTRATION
Environmental Research Laboratories

The Florida Area Cumulus Experiment: Rationale, Design, Procedures, Results, and Future Course

WILLIAM L. WOODLEY
ROBERT I. SAX

BOULDER, COLO.
JANUARY 1976



U.S. DEPARTMENT OF COMMERCE

Rogers C. B. Morton, Secretary

NATIONAL OCEANIC AND ATMOSPHERIC ADMINISTRATION

Robert M. White, Administrator

ENVIRONMENTAL RESEARCH LABORATORIES

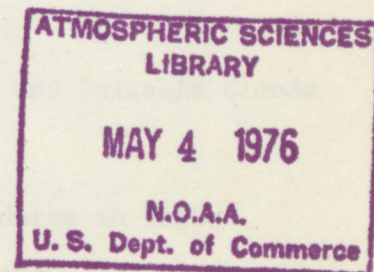
Wilmot N. Hess, Director

QC
807.5
U66
no. 354
c.1

NOAA TECHNICAL REPORT ERL 354-WMPO 6

The Florida Area Cumulus Experiment: Rationale, Design, Procedures, Results, and Future Course

WILLIAM L. WOODLEY
ROBERT I. SAX



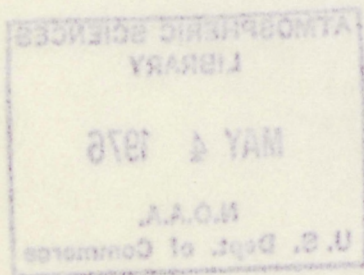
BOULDER, COLO.
January 1976



For sale by the Superintendent of Documents, U. S. Government Printing Office, Washington, D. C. 20402

NOTICE

The Environmental Research Laboratories do not approve, recommend, or endorse any proprietary product or proprietary material mentioned in this publication. No reference shall be made to the Environmental Research Laboratories or to this publication furnished by the Environmental Research Laboratories in any advertising or sales promotion which would indicate or imply that the Environmental Research Laboratories approve, recommend, or endorse any proprietary product or proprietary material mentioned herein, or which has as its purpose an intent to cause directly or indirectly the advertised product to be used or purchased because of this Environmental Research Laboratories publication.



CONTENTS

	Page
ILLUSTRATIONS	v
TABLES	viii
ABSTRACT	x
1. HISTORICAL OVERVIEW	1
2. PHYSICAL HYPOTHESIS	4
2.1 Chain of Reasoning	4
2.2 Concept of Seedability	8
2.3 Weak Links in the Reasoning Chain	13
2.3.1 Distribution of Nucleating Material	13
2.3.2 Concentration of Natural Ice	17
2.3.3 Uncertainty in the Nature of Entrainment	22
2.3.4 Lack of Understanding of Cloud-Cloud Interactions and Failure to Model a Cloud System	23
2.3.5 Cloud System Interaction with the Mesoscale Boundary Layer Flow Pattern	23
2.3.6 Lack of Documentation of the Natural Evolution of In-cloud Microphysical Processes	24
2.3.7 Extended Area and Persistence Effects	29
2.4 Problems in Verifying the Physical Hypothesis	32
2.4.1 Convective Rainfall Variability and Measurement Errors	32
2.4.2 Proper Instrumentation to Detect Microphysical and Dynamical Changes	33
2.4.3 Proper Instrumentation to Detect Kinematic Changes and to Characterize the Boundary Layer Flow	36
2.4.4 Proper Timing of Data Collection	39
3. MERGER PROCESS	41
4. DESIGN OF FACE	45
5. EXPERIMENTAL PROCEDURES	49
5.1 Determination of a Suitable "GO" Day and Suitable Clouds	49
5.2 Idealized Flight Patterns	52
5.3 FACE Seeding Procedures	56
5.3.1 General	56
5.3.2 Two Examples of Seeding Procedures in FACE	57
6. MEASUREMENT OF RAINFALL IN FACE AND RESULTS	89
6.1 Measurement of Convective Rainfall	89
6.2 Area Rainfall Results from FACE	97
6.3 Results of Single Cloud Analyses in FACE	102

CONTENTS (Continued)

	Page
7. THE 1975 FACE PROGRAM	105
7.1 The Randomized Core Seeding Effort	105
7.2 Intensive Phase Microphysical Investigation	107
7.2.1 Motivation	107
7.2.2 Instrumentation	108
7.2.3 Procedures	109
7.2.4 Impact on Planning	110
8. FUTURE COURSE OF FACE	110
8.1 Should We Continue?	110
8.2 Plans	111
9. CONCLUSIONS	113
10. ACKNOWLEDGMENTS	114
11. REFERENCES	116
APPENDIX A - SEED DECISION: RANDOMIZATION AND INFERENCE	122
APPENDIX B - SUPPLEMENTARY FACE RAIN ANALYSES AND TABULATIONS	127
APPENDIX C - CHARACTERISTICS OF THE NUCLEATING AGENT	164
APPENDIX D - SELECTED DATA FROM THE FACE-73 CLOUD PHYSICS PROGRAM	181
APPENDIX E - SYNOPSIS OF METEOROLOGICAL AND MICROPHYSICAL CONDITIONS JUDGED SUITABLE OR UNSUITABLE FOR DYNAMIC CUMULUS SEEDING IN FLORIDA	196
APPENDIX F - ANSWERS TO QUESTIONS FREQUENTLY ASKED ABOUT FACE	198

ILLUSTRATIONS

Figure		Page
1.	Field design for the Florida Area Cumulus Experiment (FACE).	3
2.	Relationship of model-predicted seedability calculations to an environmental sounding.	9
3.	Mean soundings for four different cumulus growth regimes in the tropics.	12
4.	Cloud photographs illustrating four types of growth behavior.	14
5.	In-cloud microphysical data obtained by penetrating an unseeded growing cumulus tower at three levels.	20
6.	Power function of likelihood ratio test that cloud seeding has no effect for the FACE target.	34
7.	In-cloud microphysical data obtained by penetrating a growing nonseeded cumulus tower at a single level.	40
8.	Before merger (M) photographs of clouds A (seeded) and B (unseeded) on 16 July 1970, taken from the seeder aircraft at 21,000 ft.	42
9.	After merger (M) photographs of clouds A (seeded) and B (unseeded) on 16 July 1970, taken from seeder aircraft at 21,000 ft.	43
10.	Precipitation histories of clouds A and B before and after merger on the University of Miami 10-cm radarscope, 16 July 1970.	44
11.	Flow diagram of the FACE design.	47
12.	Examples of internal cloud microphysical properties of clouds judged suitable for seeding on 20 July 1973.	50
13.	Idealized diagram of seeding flight patterns in relation to a developing convective system.	53
14.	The merging of two seeded clouds into one large convective system on 7 May 1971.	55
15.	Photographs (1/3 n mi resolution) from the Defense Meteorological Satellite Program.	58

ILLUSTRATIONS (Continued)

Figure		Page
16.	Vertical motion field at 1.22 km for a southeast wind as predicted by the Pielke (1974) sea breeze model.	59
17-24.	See extended caption for radar and photographic documentation of target developments on 14 July 1971.	62
25.	Time plots of floating and total target echo areas, and gage-adjusted floating and total target volumetric rainfalls for 14 July 1971.	74
26.	Tracings of the PPI presentation on the scope of the WSR-57 radar of the National Hurricane Center on 20 July 1973.	76
27.	Photograph from the DMSP satellite on 20 July 1973.	77
28-33.	See extended caption for radar and photographic documentation of target developments on 20 July 1973.	79
34.	Time plots of floating and total target echo areas and gage-adjusted floating and total target volumetric rainfalls for 20 July 1973.	90
35.	Comparison between rainfall as calculated by computer (on ordinate) and as calculated manually using filmed observations from the Video Integrator and Processing (VIP) unit.	94
B1.-B37.	Time plots of target variables on FACE "GO" days	141-159
C1.	Size distributions of AgI particles produced from the Olin X-1055/WM105 pyrotechnic; theoretical Khrgran-Mazin distribution included for comparison.	167
C2.	Electron microscope photographs of various magnification showing aerosol produced during burn of Olin X-1055/WM105 pyrotechnic.	169
C3.	Representative elemental composition of relatively large ($>0.2\mu\text{m}$) individual particles produced by burn of Olin X-1055/WM105 pyrotechnics in wind tunnel.	172
C4.	Nucleating effectiveness as a function of temperature for AgI emitted from Olin WM-105 pyrotechnic.	174
C5.	Nucleating effectiveness data for NEI TB-1 and Navy TB-1 pyrotechnic with Olin WM-105 nucleating curve included for comparison.	175

ILLUSTRATIONS (Continued)

Figure		Page
C6.	Electron microscope photograph (magnification 1600X) of silver iodide aerosol emitted by NEI pyrotechnic of TB-1 formulation.	177
C7.	Electron microscope X-ray scan of 0.5 μ m particle emitted from NEI pyrotechnic of TB-1 formulation.	177
D1.	Mean concentration of ice particle concentration (as determined from Mee ice particle instrument) as a function of time for those seeded and unseeded cumulus towers which were penetrated at least twice and had no ice on first penetration.	194
D2.	Maximum concentration of ice particle concentration (as determined from Mee ice particle instrument) as a function of time for those seeded and unseeded cumulus towers which were penetrated at least twice and had no ice on first penetration.	194
D3.	Percentage of the penetration with ice particle concentration (as determined from Mee ice particle instrument) greater than 2.5 crystals per liter as a function of time for those seeded and unseeded cumulus towers which were penetrated at least twice and had no ice on first penetration.	195

TABLES

Table		Page
1.	Variation of Model-Predicted Seedabilities, 1200 GMT Miami, 28 August 1973	11
2.	FACE 1973 Seed Versus No-Seed Microphysical Statistics	26
3.	Comparison of Single Clouds A and B with a Merger on 16 July 1970	45
4.	Unadjusted Radar-Rainfall Calculations (Units in $m^3 \times 10^7$)	93
5.	Adjusted Radar-Rainfall Calculations (Units in $m^3 \times 10^7$)	96
6.	FACE Rain Results	99
7.	FACE Rain Results 1970-1973: Means and Standard Deviations	100
8.	Stratification of Cases into Marching (1) and Stationary (2) Radar Echoes	102
9.	Mean Rainfalls from Single Clouds ($m^3 \times 10^3$) Dissipating Without Merger	104
10.	Mean Rainfalls from Single Clouds ($m^3 \times 10^3$) Merging Clouds	104
A1.	Guessing the Treatment Decision - 1971 Multiple Cloud Seeding Experiment	124
A2.	Attempt to Recognize Seeding Effect in FACE-73	125
B1.	Unadjusted Hourly Rainfall for FACE Target in 1973 (All Times EDT)	128
B2.	1970 - 1973 Rain Table	133
B3.	Hourly Rain Depth Difference (D)	162
C1.	Composition of Olin X-1055/WM105	171
C2.	Expected Exhaust Products of Olin X-1055/WM105	171
C3.	Composition of TB-1	178

TABLES (Continued)

Table		Page
C4.	Expected Exhaust Products of TB-1	178
D1.	Characteristics of Microphysical Instrumentation Used in the FACE Program	182
D2.	FACE 1973 Pass-by-Pass Selected Microphysical Data	185
E1.	Dynamic Seeding Criteria	197

ABSTRACT

All aspects of NOAA's Florida Area Cumulus Experiment (FACE) are treated in this report to provide a summary of current progress and problems, and to serve as a basis for discussion by the scientific community. We realize that this is a ponderous report and that only a fraction of the readers will have both the time and inclination to read it in its entirety. Consequently, this summary is provided at the outset for those who desire a FACE briefing without the attendant details.

The FACE program is an outgrowth of the single cloud seeding experiments in Florida, the results of which demonstrated that "dynamic seeding" can be effective in increasing the sizes and lifetimes of individual cumuli and the localized rainfall resulting from them. The concept of seedability was central to this effort. As presently conceived, the FACE is a program to determine whether dynamic seeding can be used to augment precipitation over an extensive area ($1.3 \times 10^4 \text{ km}^2$) by promoting larger and better organized convective systems. This is a logical progression from the early works on isolated cumuli.

The single cloud seeding experiments began in the Caribbean in 1963 (Malkus and Simpson, 1964) and continued in 1965 (Simpson et al., 1967). Theoretical work and modeling had suggested that, under certain specifiable conditions, massive seeding with an ice nucleating agent, such as silver iodide (AgI), might stimulate cloud growth in supercooled convective clouds through the release of the latent heat of fusion. The Caribbean experimentation, in which vertical-fall AgI rockets were ejected into supercooled convective clouds from aircraft, verified this prediction and helped explain the isolated instances of spectacular cloud growth following seeding that had been reported in the literature (e.g., Kraus and Squires, 1947). The concepts of dynamic seeding and seedability were developed and quantified using a one-dimensional, Lagrangian, numerical model of a rising convective bubble.

The individually seeded clouds exhibited several growth modes following seeding, of which explosive cloud growth was unquestionably the most spectacular. Although there were no formal theoretical foundations for such an expectation, it seemed likely that such impressive cloud growth would be correlated with increases in precipitation. Consequently, the research was moved to Florida to investigate this possibility.

This step required self-consuming pyrotechnics (Simpson et al., 1970). Rain volume from cloud base was measured by ground-based calibrated S-band radar (Woodley, 1970; Woodley and Herndon, 1970). In this series, 52 GO clouds were selected by the randomization procedure; 26 were seeded and 26 were investigated as controls. Randomization was in large blocks, and usually several seeded and control clouds were obtained in close succession on a single day. Careful tests failed to reveal any bias in selection (Brier et al., 1972). Average rain volume from seeded clouds exceeded that from controls by a factor of 3, or by about $3.0 \times 10^5 \text{ m}^3$. The difference was significant at the 5 percent level or better, using several classical statistical tests (Simpson et al., 1973).

Physical studies demonstrated that seeded rainfall was increased because of the larger volume and longer life of the seeded clouds. An important result came from stratification of the data into fair and disturbed days (radar echo coverage > 13 percent at 1400 local time in the experimental region). On fair days, the seeded-control difference was 37 percent greater than the average, while on disturbed, rainy days it was negative (the difference was small and not significant).

Although these results represent one of the few instances in which statistically significant increases in precipitation from summertime convective clouds has been documented, their significance for practical rain enhancement over a larger area is yet to be demonstrated.

Studies of Florida rainfall revealed that most of the precipitation is produced by organized convective systems and not by isolated convective clouds (Woodley et al., 1971). Consequently, dynamic seeding of many isolated individual clouds does not appear to be the answer for practical precipitation enhancement over a large area. Rather, dynamic seeding to promote larger and better organized rain systems is apparently requisite for practical rain increases in Florida. With this realization, the Experimental Meteorology Laboratory commenced research in 1970 on the potential of dynamic seeding for inducing area-wide increases in rainfall.

Although the theoretical foundations for this phase of the research are not as firm as those for the single cloud studies, the disparity is not as great as is believed by some. At the start of the single cloud studies, the interest focused on a test of a physical hypothesis and of model predictions that massive seeding of supercooled convective clouds would stimulate their growth. Only after these predictions were verified did the interest shift to the possibility of rainfall enhancement, and for this phase of the research the theoretical foundations for the expectation of increases in rainfall were open to question. In fact, respected scientists argued persuasively that dynamic seeding might well decrease rainfall despite the increased cloud size. Nevertheless, this matter was pursued based on a physical hypothesis that was founded primarily on scientific intuition. Only after the rain increases from dynamic seeding were documented was the physical basis for these increases better understood.

There is an analogous situation today with respect to the area experiment. The theoretical foundations that would either support or contradict an expectation of area-wide rain increases from dynamic seeding are sadly lacking. Nevertheless, this research has continued, based on a physical hypothesis and intuitive thinking as to how to proceed. This intuitive thought has been founded in careful observations of productive unmodified clouds and their interaction, and on predictions as to how seeding might be used to imitate these natural processes on clouds that are not so disposed.

Dynamic seeding with silver iodide to alter the circulations that sustain the supercooled convective clouds is predicated on the thermodynamic certainty that the conversion of supercooled liquid water to ice releases heat that increases cloud buoyancy. The increased buoyancy

invigorates the cloud and prolongs its lifetime, resulting in increased convergence at cloud base, a greater mass flow through the system and, consequently, a more efficient processing of the available moisture, and an augmentation of the rainfall. It is hypothesized that, under optimum conditions, dynamic seeding eventually leads to a better organization of the low-level inflow, thereby increasing the probability of cloud merger and area-wide enhancement of the rainfall. The theoretical foundations for the chain of reasoning leading to the sequence of events described above are examined in detail in the text.

There are many weak links in this reasoning chain that are brought about by a host of uncertainties and problems. These include: (a) uncertainty as to the distribution of the seeding material, (b) uncertainty as to the amount of natural ice and its evolution in Florida clouds, (c) uncertainty as to the nature of entrainment, (d) a lack of understanding of cloud and environmental interactions and our resultant inability to model convective cloud systems and (e) uncertainty as to the existence and intensity of extended area and persistence effects. These uncertainties and problems are discussed at length in this report.

There are also problem areas in verifying the physical hypothesis. Two of the most formidable are the large variability in space and time of area-mean rainfall, and errors in rain measurement. The magnitude of these problems was quantified by Olsen and Woodley (1975), with rain variability being the greater problem. Although measurement errors are important, the system of convective rain measurement used in Florida that involves conjunctive use of S-band radar and raingages is adequate for evaluation of the area experiment. The importance of covariates and predictors in reducing the magnitude of the rain variability problem is emphasized.

Other problem areas in verifying the physical hypothesis include: (a) a lack of proper instrumentation before 1973 for the detection of microphysical and dynamical changes induced by seeding, (b) a lack of instrumentation to detect kinematic changes and to characterize the boundary layer inflow and, (c) the proper timing of the data collection. These problems and the efforts being made to solve them are discussed. A section detailing the types of physical measurements needed to resolve key aspects of the hypothesis is included.

Cloud merger is apparently the crucial natural process that leads to heavy and extensive convective rainfall. Our studies indicate that much of the rainfall in Florida occurs through merger. Consequently, dynamic seeding must be effective in inducing this natural process if it is to prove useful for augmenting areal rainfall. In designing FACE, we decided to investigate two sequential uncertainties: (1) can dynamic seeding systematically induce cloud merger and rainfall, and (2) will these mergers result in rain increases over a fixed target area. An affirmative resolution of the first uncertainty is apparently a necessary, but not a sufficient, condition for an affirmative resolution of the second.

Two experimental designs were seriously considered in planning for the Florida Area Cumulus Experiment. The first was the random experimental design, which involves randomization of days, over a single target area, into seeded and nonseeded days, with nonseeded as the control. The second was the crossover target-control, which requires random interchange of target and control areas among seeding days. The crossover approach was appealing, because this design minimizes the noise of natural rain variability inherent in the random experimental design. The shower patterns in two adjacent areas (as with crossover) on a particular day are better correlated than the shower patterns in the same area on different days (as with the random experimental design). Furthermore, crossover procedures require less time to verify a particular seeding effect than does the random experimental design (Schickendanz and Huff, 1971). The disadvantages of the crossover design are the possibility of silver iodide contamination between target and control, and the possibility of other effects on the control area because of seeding in the nearby target. Other effects might be reduced isolation due to a cirrus canopy or an altered low-level wind field. The crossover approach also precludes the "floating target" concept that is discussed in detail in the report.

The random experimental design was selected for FACE because of practical considerations (Woodley and Williamson, 1970). At the beginning of this program it was impossible to select two land areas within the range of the research radar (the UM/10-cm) that were free of blind cones produced by obstructions to the radar beam. By 1973, estimates of rainfall by radar were made in FACE using the WSR-57 radar (Woodley et al., 1975). This radar has no obstructions to the energy radiated by its antenna. Because of this development, Woodley et al. (1974) reinvestigated the possibility of changing the FACE design to crossover. They concluded that the lone remaining obstacle was the likelihood of dynamic contamination of the control area by events in the seeded target. Because the magnitude of this factor is unknown, further consideration of the crossover design in Florida was postponed.

With the selection of the random experimental design for FACE, the experiments began on a very limited basis in 1970 and continued in 1971 and 1973. The design features (Woodley and Williamson, 1970) include:

- 1) A fixed target area with randomized seeding instructions.
- 2) Surveillance of the clouds in the target by 10-cm radars of the University of Miami (in 1970 and 1971) and the National Hurricane Center (in 1972 and 1973).
- 3) Suitable days for experimentation. These were days that satisfied a daily suitability criterion of $S - N_e \geq 1.0$ (later increased to ≥ 1.5), where S is the predicted seedability (in km) predicted by the EML model (Simpson and Wiggert, 1971) with the 1200 GMT Miami radiosonde and a hierarchy of horizontal cloud sizes, and N_e is the number of hours between 1300 and 1600 GMT with 10-cm echoes in the target. The maximum possible

value of N_e is 3. The N_e factor is introduced to bias the decision for experimentation against naturally rainy days. Decision time on a day's suitability is 1600 GMT.

4) Flights by the seeder aircraft only on days that satisfied the meteorological suitability factor. The seeding decision was randomly determined in the air when suitable hard, vigorous clouds with top temperatures near -10°C were found in the target, with only the "randomizer" knowing the decision.

5) Final acceptance of a day for inclusion in the area analysis only after expenditure of 60 flares (50 grams of silver iodide each) or after seedings of six clouds, or both.

Multiple seedings of individual clouds that were in proximity were attempted to promote mergers and to enhance the preferred organization patterns evident in the unmodified convection. On days with adequately long cloud lifetimes, these attempts were apparently successful.

Because this experiment is randomized by days in a single target, it is vulnerable to daily fluctuations in radar performance. Woodley et al. (1975) have looked at radar measurement errors and developed methods of correcting them. As discussed herein, Olsen and Woodley (1975) have shown that the existing measurement errors are overwhelmed by the magnitude of the rain variability problem and do not substantially add to the uncertainties.

In the analysis of the FACE experimental days, floating target and total target calculations were made for the 6 hours following the initial seeding. The floating target is composed of the echoes of all experimental clouds and those with which they merge. The total target is made up of the floating target echoes plus the echoes of nonexperimental clouds. All rain calculations are limited to the target area.

The floating target concept was dictated by several considerations. Early work in FACE showed that it was impossible to seed all clouds in the target area at the moment that they became suitable, even with two seeder aircraft. Once a seeding opportunity was missed the cloud either dissipated or grew to massive stature by itself. In either case, seeding was in no way responsible for cloud behavior and its presence in the target area merely diluted any seeding effect there. At the time there was no way of determining the magnitude of this problem, and the floating target was devised to serve as a more sensitive measure of the effect of seeding. It is a means of determining whether dynamic seeding is effective in promoting merger and rainfall, and it is also a safeguard against years of fruitless area experimentation. A seeding effect must appear in the floating target before it is evident in the total target. If it

has not appeared after a reasonable period of experimentation, then the FACE must either be redesigned or discontinued altogether.

The floating target concept has provoked criticism and some of it is justified. The prime concern is whether, in fact, we are conducting two distinct experiments and whether one has been conducted at the expense of the other. In actually carrying out the seedings, we have given more attention to ensuring an untainted floating target, reasoning that it is more important to document an effect here before worrying about the total target. Furthermore, a large effect in the floating target may manifest itself in the total target as well, despite the problem of nonexperimental clouds within the target. Ultimately, it must be demonstrated that dynamic seeding can increase the rainfall over a large area. The floating target is merely an interim, but a very important step in the experimental process.

The FACE planning process, since its inception in 1970, is described. A recounting of experimental procedures is provided, including the sequential decision process to qualify a day for experimentation, idealized flight patterns and generalized seeding procedures. Two detailed case studies illustrating experimental procedures and the selection of the floating target are also included.

The measurement of convective rainfall in FACE using the Miami reflectivity-rainfall rate relation receives extensive treatment. The UM/10-cm radar of the Radar Meteorology Laboratory of the University of Miami was used to evaluate the series of single cloud seeding experiments between 1968 and 1971. The WSR-57 radar of the National Hurricane Center (NHC) was used concurrently with the UM/10-cm radar in 1972. By 1973, EML's primary research radar was the NHC WSR-57. Radar was chosen for the evaluation of the single cloud seeding experiments because gage measurement of rainfall from individual clouds (base echo areas generally 250 km^2) could not have been accomplished without a totally unacceptable expenditure of money and logistic effort. Further, seed and control clouds were obtained on each day of experimentation so, despite radar inaccuracies, intraday relative differences (seed versus control) should still have been valid. With the advent of the area experiment and interday randomization instead of intraday randomization cloud-by-cloud, radar is not as obvious a choice, particularly if the radar exhibits great interday variability. Woodley et al. (1975) treat this problem in detail, concluding that radar is the best tool for the evaluation of rainfall in FACE, provided the radar estimates are adjusted by raingages.

Before 1973, we calculated target rainfall in FACE by manually planimetering scope photographs of the areas within the contours of each radar echo as described by Woodley (1970). In 1973, a conversion was made to computer processing. In 1970, 1971, and for one nonrandom control day in 1972, the UM/10-cm radar (Senn and Courtright, 1971) of the University of Miami's Rosenstiel School of Marine and Atmospheric

Sciences made the reflectivity measurements that were used for rain calculations. For three nonrandom control days in 1972, and for all days of experimentation in 1973, the WSR-57 radar (Rockney, 1958) of NOAA's National Hurricane Center was used for rain calculation. Both radars are capable of the iso-echo contouring that is necessary for manual rain calculation; the UM/10-cm uses a four-level device (Senn and Andrews, 1968) and the WSR-57 is equipped with a six-level video integrator and processor (Shreeve, 1969).

The rain estimates by radar in FACE 1970 were not adjusted by rain-gages and those in FACE 1971 were adjusted uniformly by a factor of 1.75 based on gage and radar comparisons. In 1972 and 1973, the radar rain estimates were adjusted using raingage clusters and the resulting values are certainly more accurate than those of earlier years. Based on the analysis of Woodley et al. (1975), it is likely that the calculations from the first two years (1970 and 1971) of area experimentation are accurate to within a factor of 2. However, one or two undetected outliers may exist in this data sample.

Because of intra-agency cooperation in 1973, we used the NHC WSR-57 radar for our research without compromising the operational requirements of the NHC. Although the basic radar remained the same as in 1972, the radar output was digitally quantized and tape recorded. Wiggert and Ostlund (1975) provide specific details on the EML-NHC digitized radar system, including a description of hardware and a description and listing of the software programs for reading and processing the taped data. Calibration of the radar and digitizer are treated, and comparisons between the manual and computer methods of rain measurement are made. Adjustment by raingages as described improved the agreement between the two methods and their accuracy.

For all FACE experimentation as of the end of 1973 there were 14 seed days and 23 controls (floating target analysis on 22 of the 23) of which 10 are random and 13 nonrandom. Nonrandom controls were obtained using a light aircraft on days suitable for the experiment on which a seeder aircraft was unavailable. The flights were necessary to insure that adequate numbers of seedable clouds were present in the target area, to select floating targets, and to simulate flare releases. Rain calculations were made for floating and total target for the 6 hours following the first seeding. On days screened as suitable for the experiments, natural rain volume varied by a factor of 62 for floating target and by a factor of 25 for total target. Area seed - control rainfall differences are not significant with six classical tests, nor is the difference between random and nonrandom controls.

As of 1973, the sample size in FACE was still too small to determine the effect of seeding. Both Simpson et al. (1973) and Olsen and Woodley (1975) show that at least 50 pairs of cases (seed and control) will be necessary to resolve a seeding effect of 1.5 to 1.7

in total target rainfall. If the seeding effect is less than this, as indicated by our current calculations, more experimental days will be necessary unless suitable covariates and/or predictors are found. The situation is much more hopeful for the floating target.

Scientists studying the FACE problem have worked hard to find covariates in the area experiment. Many covariates that were useful for single clouds in Florida and/or area experiments elsewhere were tried, but they failed to provide significant regressions. Examples are rainfall in the area before seeding time, rain upwind of the area, rain surrounding the area, one-dimensional model-predicted seedability and/or rain production, three-dimensional mesoscale model moisture influx predictions, area echo coverage, and numerous others, singly and in combinations.

Knowledge of the behavior of heated islands (Malkus, 1963) combined with a suggestion that a "heavy-tailed" rain distribution might usefully be treated as two separate distributions, led to a breakthrough in data stratification. Over flat, heated islands, days with strong wind flow generally do not permit the build-up of towering clouds and heavy showers; the Pielke Florida model also shows weak vertical moisture fluxes in the EML target with strong winds impinging on the peninsula.

Upon examining the radar echo motions with these concepts in mind, we found that the GO days were readily separable into "marching" and "stationary" days of radar echo behavior. Days could usually be classified using the radar scope tracings and notes thereon provided routinely by the National Weather Service radar observers. The same category (1 for marching and 2 for stationary) was reached by independent analysis on most occasions before 1400 hours local time, or before the time when the first seeding usually occurred. Examination of the radar film itself resolved the few ambiguous cases.

Recently, Simpson and Woodley (1975) demonstrated that the category, as defined, is a significant covariate for FACE rainfall. Although this finding does not give us direct or immediate information regarding the effects with existing data, it will be useful in the future with expanded data sets.

Analysis of isolated experimental clouds obtained on days of multiple cloud seeding has produced significant findings. Results were stratified depending upon whether the single clouds dissipated in the target area without merger or whether they merged with a neighbor. With the former stratification, the mean seeded rainfall exceeded the mean control rainfall by a factor of 2, a result (one-tailed significance of 3 percent) that is consistent with earlier single cloud studies. No meaningful rainfall comparison was possible with the latter stratification because, on the average, the seeded clouds merged (and were dropped) 13 minutes earlier than the controls. This disparity in mean lifetime before merger (two-tailed significance level of 0.5 percent) suggests that seeding is promoting merger in FACE as intended.

The plans for the FACE 1975 field program (which has now been completed) are detailed. The motivation, instrumentation and procedures for each phase of the program are described. Plans beyond FACE 1975 as a function of several contingencies are also mapped.

Complete tabulations of single cloud and area rainfalls are provided in the appendices for those wishing to work with FACE observations. The characteristics of the pyrotechnic flares used for dynamic seeding and the FACE cloud physics program are also discussed extensively in the appendices. Answers to questions frequently asked about FACE are provided in the final appendix.

THE FLORIDA AREA CUMULUS EXPERIMENT:
RATIONALE, DESIGN, PROCEDURES, RESULTS, AND FUTURE COURSE

William L. Woodley and Robert I. Sax

The Florida Area Cumulus Experiment (FACE) has developed as the logical extension of the successful series of single cloud experiments conducted by NOAA's Experimental Meteorology Laboratory¹ over the Caribbean and Florida. Although the results of FACE studies have been painstakingly reported in the literature, conversations with colleagues have made it obvious that the empirical and theoretical foundations for this experiment are not well understood. Confusion still exists in the minds of some as to the rationale for FACE and its design. The need exists then for a detailed exposition of all aspects of the FACE effort for consideration and discussion by the scientific community. With this report we attempt to fulfill this need.

At the outset we wish to acknowledge the contributions of others. Whenever possible, these contributions are referenced and/or acknowledged in this report. It is appropriate to recognize at this time the major input that Dr. Joanne Simpson made to FACE studies while she was Director of the Experimental Meteorology Laboratory. It was largely her dedication and perseverance that made FACE possible and it is primarily her work and ideas that have served as the impetus for this report.

1. HISTORICAL OVERVIEW

The single cloud seeding experiments began in the Caribbean in 1963 (Malkus and Simpson, 1964) and continued in 1965 (Simpson et al., 1967). Theoretical work and modeling had suggested that under certain specifiable conditions massive seeding with an ice nucleating agent such as silver iodide (AgI) might stimulate cloud growth in supercooled convective clouds through the release of the latent heat of fusion. The Caribbean experimentation, in which vertical-fall AgI rockets were ejected into supercooled convective clouds from aircraft, verified this prediction and helped explain the isolated instances of spectacular cloud growth following seeding that had been reported in the literature (e.g., Kraus and Squires, 1947). The concepts of dynamic seeding and seedability were developed and quantified using a one-dimensional, Lagrangian, numerical model of a rising convective bubble.

¹Now the Cumulus Group of the National Hurricane and Experimental Meteorology Laboratory.

The individually seeded clouds exhibited several growth modes following seeding, of which explosive cloud growth was unquestionably the most spectacular. Although there were no formal theoretical foundations for such an expectation, it seemed likely that such impressive cloud growth would be correlated with increases in precipitation. Consequently, the research was moved to Florida to investigate this possibility.

This step required self-consuming pyrotechnics (Simpson et al., 1970). Rain volume from cloud base was measured by ground-based calibrated S-band radar (Woodley, 1970; Woodley and Herndon, 1970). In this series, 52 GO clouds were selected by the randomization procedure; 26 were seeded and 26 were investigated as controls. Randomization was in large blocks and usually several seeded and control clouds were obtained in close succession on a single day. Careful tests failed to reveal any bias in selection (Brier et al., 1972). Average rain volume from seeded clouds exceeded that from controls by a factor of 3 or by about $3.0 \times 10^5 \text{ m}^3$. The difference was significant at the 5 percent level or better, using several classical statistical tests (Simpson et al., 1973).

Physical studies demonstrated that seeded rainfall was increased because of the larger volume and longer life of the seeded clouds. An important result came from stratification of the data into fair and disturbed days (radar echo coverage > 13 percent at 1400 local time in the experimental region). On fair days, the seeded-control difference was 37 percent greater than the average, while on disturbed, rainy days it was negative (the difference was small and not significant).

Although these results represented one of the few instances in which statistically significant increases in precipitation from summertime convective clouds had been documented, their significance for practical rain enhancement had yet to be demonstrated.

Studies of Florida rainfall revealed that most of the precipitation is produced by organized convective systems and not by isolated convective clouds (Woodley et al., 1971). Consequently, dynamic seeding of many isolated individual clouds does not appear to be the answer for practical precipitation enhancement over a large area. Rather, dynamic seeding to promote larger and better organized rain systems is apparently requisite for practical rain increases in Florida. With this realization, the Experimental Meteorology Laboratory commenced research in 1970 on the potential of dynamic seeding for inducing area-wide increases in rainfall. The target area for the Florida Area Cumulus Experiment (FACE), as this effort is now called, is shown in figure 1.

Although the theoretical foundations for this phase of the research are not as firm as those for the single cloud studies, the disparity is not as great as is commonly believed. At the start of the single

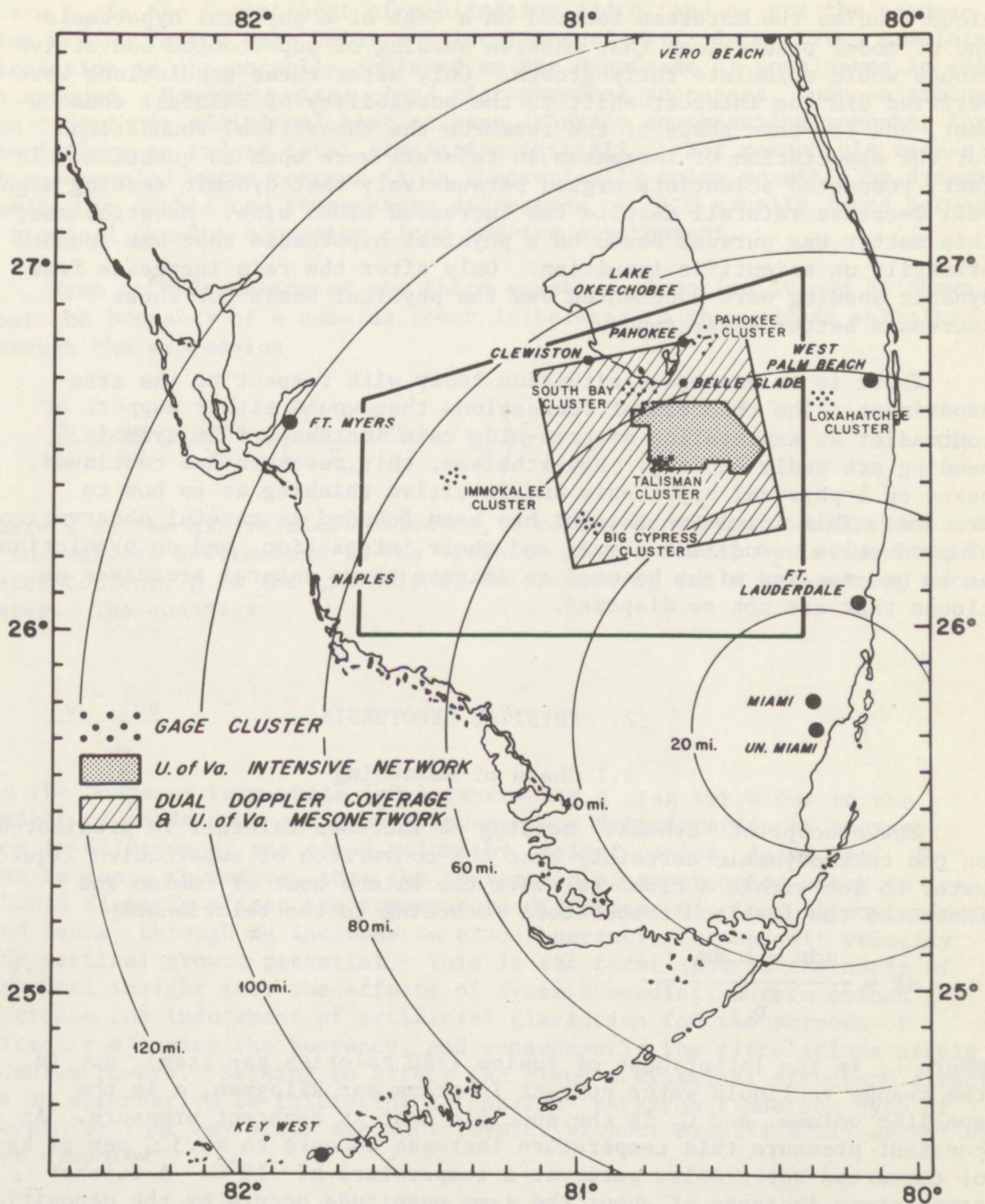


Figure 1. Field design for the Florida Area Cumulus Experiment (FACE). The largest quadrilateral is the EML target area. Contained within are the areas covered by the dual doppler radars, the mesonet (FACE intensive network) and the gage clusters. In the 1972 gaging effort, the mesonet and the Big Cypress clusters were not operative; in 1973 only the Talisman cluster was not operative.

cloud studies the interest focused on a test of a physical hypothesis and of model predictions that massive seeding of supercooled convective clouds would stimulate their growth. Only after these predictions were verified did the interest shift to the possibility of rainfall enhancement, and for this phase of the research the theoretical foundations for the expectation of increases in rainfall were open to question. In fact, respected scientists argued persuasively that dynamic seeding might well decrease rainfall despite the increased cloud size. Nevertheless, this matter was pursued based on a physical hypothesis that was founded primarily on scientific intuition. Only after the rain increases from dynamic seeding were documented was the physical basis for these increases better understood.

There is an analogous situation today with respect to the area experiment. The theoretical foundations that would either support or contradict an expectation of area-wide rain increases from dynamic seeding are sadly lacking. Nevertheless, this research has continued, based on a physical hypothesis and intuitive thinking as to how to proceed. This intuitive thought has been founded in careful observations of productive unmodified clouds and their interaction, and on predictions as to how seeding might be used to imitate these natural processes on clouds that are not so disposed.

2. PHYSICAL HYPOTHESIS

2.1 Chain of Reasoning

The concept of "dynamic" seeding to increase rainfall is predicated on the thermodynamic certainty that the conversion of supercooled liquid water to ice within a cloud releases the latent heat of fusion and increases the in-cloud temperature according to the relationship

$$dT = \frac{\alpha dp - L_f dw_L}{C_p} \quad (1)$$

where L_f is the latent heat of fusion (≈ 80 calories per gram), dw_L is the change in liquid water content in grams per kilogram, α is the specific volume, and C_p is the specific heat at constant pressure. At constant pressure this temperature increase amounts to $\approx 0.3^\circ\text{C}$ per gm kg^{-1} of converted supercooled water at a temperature of -10°C . A further temperature increase of about the same magnitude occurs by the deposition of vapor onto the newly formed ice crystals, so that the optimal total in-cloud temperature increase with complete glaciation can be expressed by

$$dT = \frac{1}{C_p} \left[-L_f dw_L + L_s (q_w - q_i) \right] \quad (2)$$

where L_s is the latent heat of sublimation and q_w and q_i are the saturation mixing ratios over water and ice respectively. In reality, complete glaciation is not normally achieved so the magnitude of both terms in (2) is reduced. However, mixed-cloud microphysical processes, such as riming, can contribute additional heat release, thereby compensating somewhat for the failure to induce total glaciation initially. For reasonable values of supercooled water content it is theoretically quite possible by dynamic seeding to double the temperature difference of $\approx 1^\circ\text{C}$ usually found between a tropical cumulus congestus cloud and its environment.

From transformation of the third equation of motion it can be shown that the buoyancy of a cumulus tower is related to the updraft velocity through the expression

$$\frac{dw}{dt} = \frac{\partial w}{\partial t} + w \frac{\partial w}{\partial z} = \left(\frac{T_v - T_{ve}}{T_{ve}} - Q_T \right) g - \mu w^2 \quad (3)$$

where w is the air vertical velocity, v refers to virtual temperature and e the ambient environment in the vicinity of the cloud, Q_T is the liquid water content, g is the gravitational acceleration, and μ is a mixing parameter. The quantity

$$\frac{T_v - T_{ve}}{T_{ve}}$$

is the buoyancy term while (gQ_T) represents a drag force due to the weight of condensate and (μw^2) represents a deterioration of buoyancy due to dilution of the cloud volume by ambient cooler, drier air. It can be seen, therefore, that the conversion of supercooled water to ice should directly affect the temperature difference of cloud to environment, and hence, through an increase in cloud buoyancy, the updraft velocity and vertical growth potential. This is the first link in the chain of physical insight into the effects of dynamic seeding, a term coined to indicate the inducement of artificial glaciation for the purpose of directly altering the buoyancy, and consequently the circulations within cumulus towers. Seeding to affect the cloud's dynamical structure directly is an alternative to initiating a "passive" Bergeron-Finderson type of mechanism that may alter the microphysics without significantly affecting the dynamics.

The success of dynamic seeding to induce cumulus development is determined largely by two principal considerations. First, as discussed in more detail later in this section, the nucleating material must be effective within the temperature range of interest and must be of sufficient concentration and distribution throughout the supercooled cloud volume to glaciare enough supercooled water to significantly alter the tower buoyancy. Second, the environmental thermodynamic structure

in the vicinity of the cloud must be stable enough to prevent natural growth much beyond the seeding altitude, but unstable enough so that the additional buoyancy realized through seeding will enable the tower to penetrate the capping stable layer and grow to a greater height. Reasoning intuitively, one concludes that this should allow more time for the conversion of cloud water into hydrometeor water and should result in an increase of precipitation from the cloud. If, however, the capping stable layer is too strong, the additional heating resulting from seeding could alter the cloud's internal updraft velocity structure without bringing about an increase in the vertical development of the tower. This could allow less time for the microphysical mechanisms to work to process the moisture into precipitation and could lead to a rainfall decrease from the cloud. The important observation that, depending upon the environmental structure, different results could occur from an identical seeding treatment was perhaps the principal lesson learned from the Caribbean series of experiments in 1963 and 1965.

Allowing that greater cloud development can accrue from dynamic seeding under predefined "proper" environmental conditions, consideration must then be given to the manner in which the cloud processes the available moisture and converts it into precipitation. Two alternative conceptual views are possible. One is that the cloud develops following seeding and the microphysical processes, having more time with which to work, serve to wring the cloud of its moisture much as a sponge might be squeezed to drip water. This analogy, however, ignores the interaction of the developing cloud with its environment and cannot be validly applied to the concept of dynamic seeding. The alternative and more plausible viewpoint is that the developing cumulus cloud acts as a pump to continuously draw in moisture from its surroundings and process it through the precipitation stage. Since pumps are notoriously less than 100 percent efficient, the cloud may lose some moisture to its surroundings at upper levels in the form of an ice crystal anvil.

The question then arises as to how seeding affects the convergent inflow of moisture into the cloud pump. The communication following seeding of a buoyancy increase at mid- or upper levels within the cumulus cloud to the convergent air flow in the subcloud boundary layer containing the bulk of the moisture is the vital second link in the thought chain outlining the physical hypothesis. It seems intuitively reasonable, through the argument of mass continuity², to postulate that any buoyancy gain must be balanced by increased inflow into the thermal envelope, but the fundamental question of just where this increased inflow occurs needs resolution and documentation. On some occasions cloud towers have been observed to pinch in or cut off following seeding, thus supplying visual evidence that there is some increased convergence at an altitude of a

²Expressed by $-\frac{1}{D} \frac{dD}{dt} = \frac{\partial u}{\partial x} + \frac{\partial v}{\partial y} = \text{DIV}_2 V$ where D is the depth of a cylindrical volume of air.

kilometer or so below the cloud turret. However, air at this level is too dry and too cold to provide the thermodynamic impetus for the explosive cloud growth observed on some occasions following seeding. In these cases the convergent air to sustain the pumping action of the cloud must reasonably have come from the moist mixed region of the lower troposphere, probably from the subcloud boundary layer. It is hypothesized, therefore, that the buoyancy gained from the dynamic seeding of a cumulus tower in the middle troposphere is, under some conditions, communicated to the boundary layer in the form of increased convergence of moist air. The exact transfer mechanisms by which such communication takes place are not well understood or documented at present.

The crucial third link in the reasoning chain concerns the organization of convergence and the development of efficiently precipitating convective systems. It has been determined from observation (Woodley et al., 1971) that most of the precipitation occurring over south Florida is produced by organized convective systems and not by isolated cumulus clouds. As will be discussed in detail later, it has also been demonstrated that the total rainfall resulting from the combination of two small cumulonimbi into one convective system is considerably greater than the sum total of the rainfall from both clouds had they not merged. It is theorized that the inflow into isolated, individual cumulus clouds is relatively weak and highly fluctuating so that the updraft structure below cloud base displays considerable "noise" in the form of high frequency oscillations. Following seeding, however, it is hypothesized that the communication of the buoyancy pulse to the boundary layer is likely to be effective in increasing the strength and the organization of the inflow and in concentrating the available energy into a less turbulent, longer wavelength profile of vertical velocity. This postulated enhanced organization of the inflow may well account for the observed increase in the breadth of tropical cumuli following dynamic seeding.

The horizontal expansion of the cumulus cloud provides a greater probability for the merging of two or more neighboring cells into a convective mass capable of better sustaining its buoyancy against the destructive process of entrainment of ambient cold, dry air. The entraining outside environmental air first encounters a "protective" region of dormant cloud mass, which modifies its temperature and humidity characteristics before it reaches the vital updraft region of the cloud body. It follows, therefore, that the better the organization of the low-level inflow, the deeper will be the convective updraft, thus making available more time for the microphysical mechanisms to process the moisture and develop a more efficiently precipitating cloud system. There is little doubt that the most prolific convective precipitation is produced by organized cloud systems (e.g., the hurricane), but the uncertainty as to the intensity and extent of compensating suppression in the vicinity of enhanced convective regions has not been resolved. This uncertainty is crucial to dynamic seeding efforts because convective suppression, if it exists, might well partly or totally negate the localized enhancement of cumulus development and rainfall.

2.2 Concept of Seedability

The concept of "seedability" was developed to quantify the degree to which the growth of a cumulus cloud can be affected by dynamic seeding. Seedability is the model predicted difference (in km) between the maximum height of a cloud if seeded and the same cloud if not seeded. A one-dimensional Lagrangian tower model (Simpson and Wiggert, 1969; 1971) has been developed and used throughout the series of Florida cumulus experiments to predict cloud top heights and to determine seedability potential on a daily basis. The model requires as input data the tower radius, the height of cloud base, and the vertical profile of environmental pressure, temperature, and humidity. Calculations based on a numerical extension of Stommel's (1947) entrainment concept are carried out to compute the tower buoyancy, rise rate, and water content as a function of height. The altitude at which the rise rate decreases to zero is taken to represent the maximum height of the center of the tower. The corresponding cloud top height above ground can be computed by adding the cloud base altitude and the tower radius to the maximum height attained by the center of the tower.

Seedability predictions from the one-dimensional Lagrangian model have been shown to be extremely useful as a tool for evaluating the effectiveness of the dynamic seeding of isolated cumulus towers (Simpson et al., 1967) when the cloud base height and tower radius could be accurately measured and when radiosonde data were available in proximity (space and time) to the experimental event. When used as an operational tool to help determine the advisability of launching aircraft to conduct an experiment on a given day, however, the concept of seedability may have severe limitations. In this case, the input tower radius and cloud base height are not known³, and the radiosonde data, by necessity, will be several hours old by the time of the experiment and may not be representative of current meteorological conditions. The location of the experiment may also be a considerable distance removed from the location of the sounding data, and the validity of assuming a spatially homogeneous lower troposphere is questionable (see discussions by Weinstein, 1972a, 1972b; Sax, 1972; and Cotton and Boulanger, 1974 and 1975). These limitations can be partially overcome by computing seedability for a hierarchy of radii and cloud bases and examining the results in a consistent, objective manner. This is the method used in the FACE program.

Figure 2 illustrates how seedability is related to an environmental profile of pressure, temperature, and humidity. Shown is the 1200 GMT Miami temperature and humidity sounding for 28 August 1973 with three separate model-calculated in-cloud temperature profiles superimposed. The in-cloud profiles were computed assuming a cloud base level of 915 m, but different tower radii were postulated (1250 m and 1500 m). It can be seen that the center of the tower with radius 1250 m would be computed

³The prediction of a cloud base altitude through the computation of a convective condensation level may be of some help.

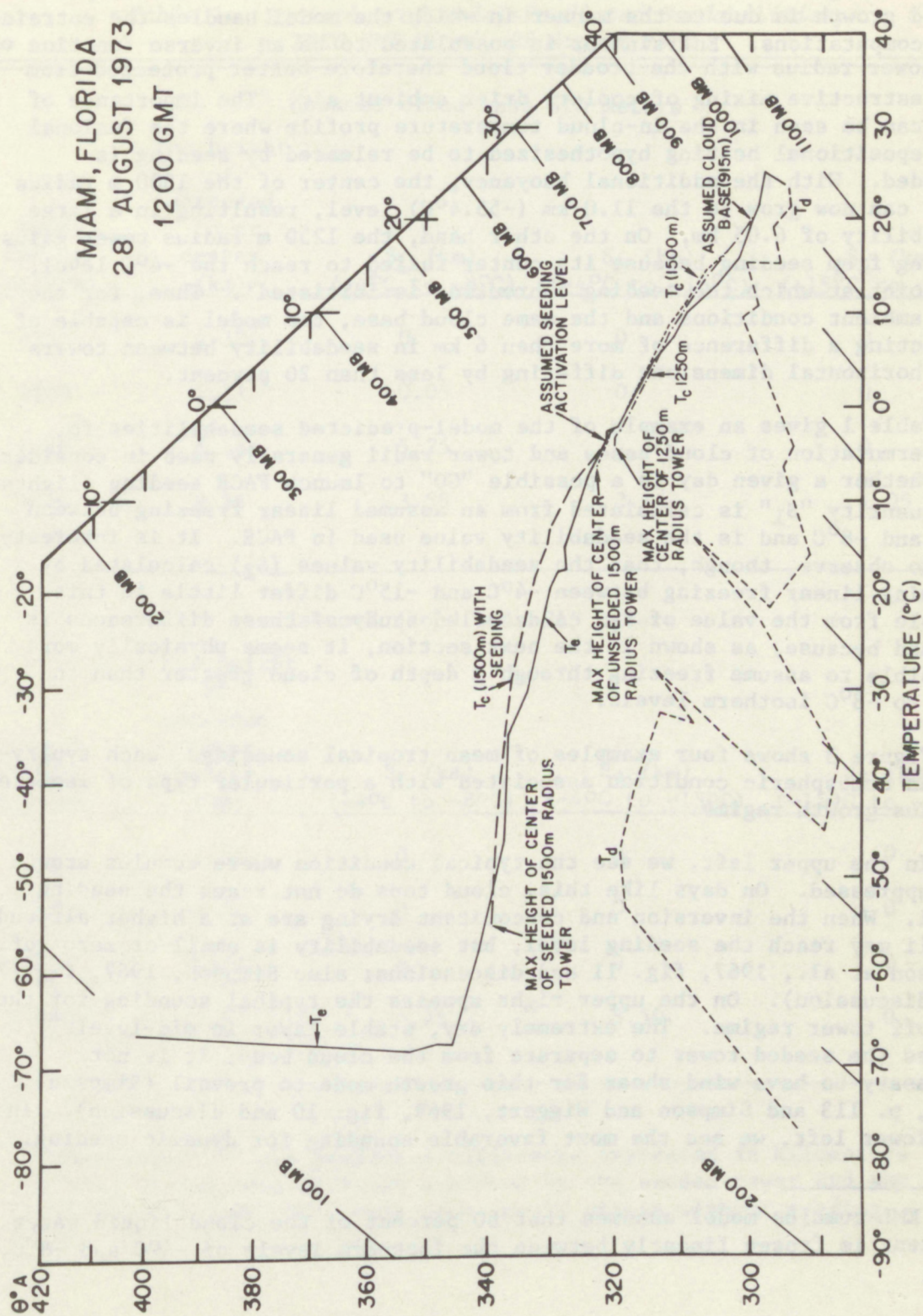


Figure 2. Relationship of model-predicted seedability calculations to an environmental sounding. Note extreme sensitivity of potential cloud growth to cloud radius dimension.

to top at the 4.25 km level (-3.7°C) while that with the unseeded 1500 m radius can grow to the 4.95 km (-7.8°C) level. The difference in predicted growth is due to the manner in which the model handles the entrainment computations. Entrainment is postulated to be an inverse function of the tower radius with the broader cloud therefore better protected from the destructive mixing of cooler, drier ambient air. The importance of this can be seen in the in-cloud temperature profile where the fusional and depositional heating hypothesized to be released by seeding is included. With the additional buoyancy, the center of the 1500 m radius tower can now grow to the 11.0 km (-55.4°C) level, resulting in a large seedability of 6.05 km. On the other hand, the 1250 m radius tower gains nothing from seeding because its center failed to reach the -4°C level, the point at which the seeding subroutine is initiated⁴. Thus, for the same ambient conditions and the same cloud base, the model is capable of predicting a difference of more than 6 km in seedability between towers with horizontal dimensions differing by less than 20 percent.

Table 1 gives an example of the model-predicted seedabilities for the permutation of cloud bases and tower radii generally used in considering whether a given day is a possible "GO" to launch FACE seeding flights. The quantity " S_1 " is calculated from an assumed linear freezing between -4°C and -8°C and is the seedability value used in FACE. It is interesting to observe, though, that the seedability values (S_2) calculated by assuming linear freezing between -4°C and -15°C differ little in this example from the value of S_1 . A detailed study of these differences is planned because, as shown in the next section, it seems physically more plausible to assume freezing through a depth of cloud greater than the -4°C to -8°C isotherm levels.

Figure 3 shows four examples of mean tropical soundings, each typifying an atmospheric condition associated with a particular type of isolated cumulus growth regime.

In the upper left, we see the typical condition where cumulus growth is suppressed. On days like this, cloud tops do not reach the seeding level. When the inversion and concomitant drying are at a higher altitude, cumuli may reach the seeding level, but seedability is small or zero (cf. Simpson et al., 1967, fig. 11 and discussions; also Simpson, 1967, fig. 7 and discussion). On the upper right appears the typical sounding for the cut off tower regime. The extremely dry, stable layer in mid-levels causes the seeded tower to separate from the cloud body; it is not necessary to have wind shear for this growth mode to prevail (Simpson, 1967, p. 113 and Simpson and Wiggert, 1969, fig. 10 and discussion). In the lower left, we see the most favorable sounding for dynamic seeding.

⁴The EML cumulus model assumes that 60 percent of the cloud liquid water content is frozen linearly between the isotherm levels of -4°C and -8°C .

Table 1. Variation of Model-Predicted Seedabilities,
1200 GMT Miami, 28 August 1973

Assumed cloud base 610 meters				
Tower radius (meters)	Max height of unseeded tower center (km)	S ₁ (km) (-4°C to -8°C)	S ₂ (km) (-4°C to -15°C)	S ₃ (km) (-15°C to -40°C)
750	4.30	0	0	0
1000	5.31	0.05	0	0
1250	6.36	5.25	4.70	0
1500	9.36	3.55	3.15	1.05

Assumed cloud base 915 meters				
Tower radius (meters)	Max height of unseeded tower center (km)	S ₁ (km) (-4°C to -8°C)	S ₂ (km) (-4°C to -15°C)	S ₃ (km) (-15°C to -40°C)
750	3.82	0	0	0
1000	4.47	0	0	0
1250	5.17	0	0	0
1500	5.87	6.05	5.50	0

"Seedability" is the predicted difference expressed in kilometers between the maximum altitude achieved by the seeded tower and the maximum altitude the same tower would attain without seeding.

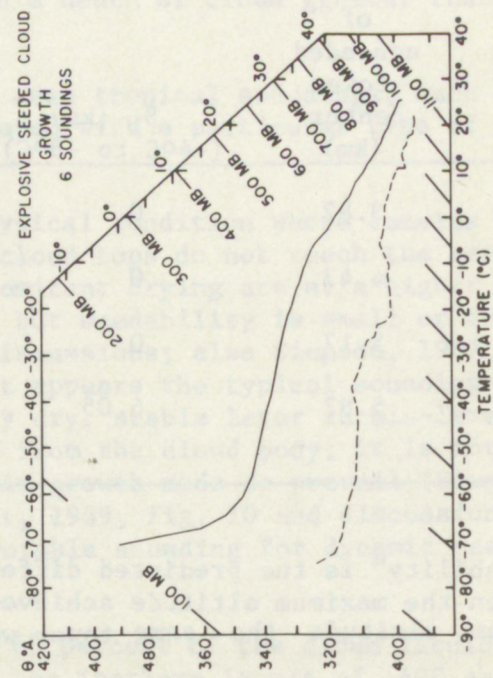
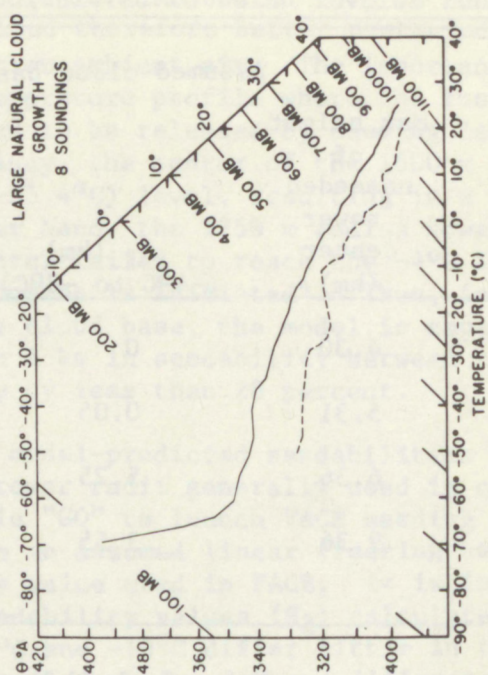
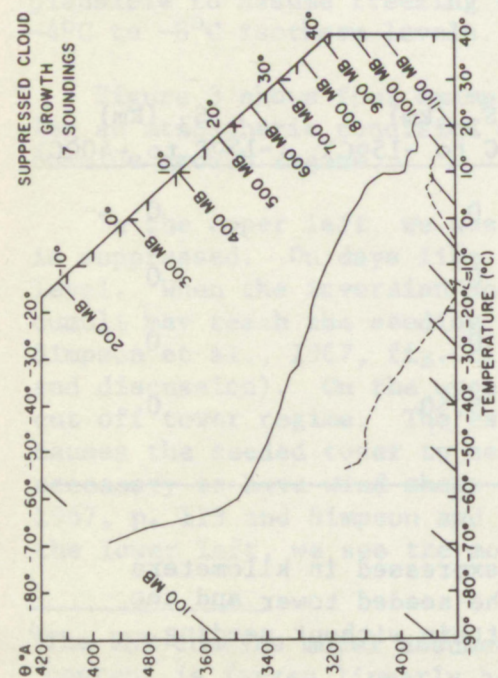
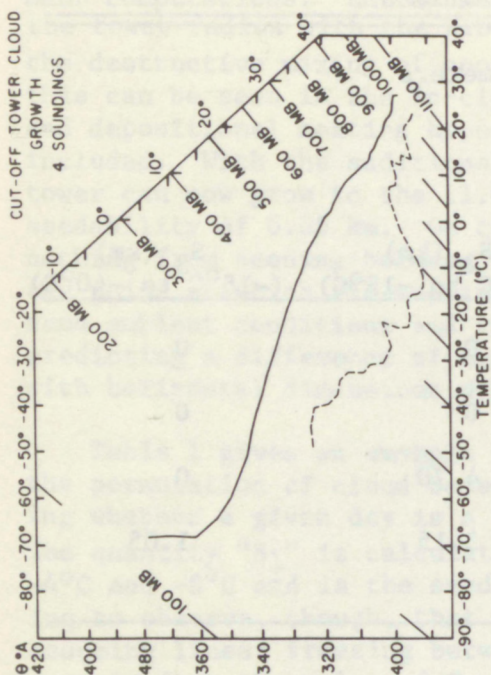


Figure 3. Mean soundings for four different cumulus growth regimes in the tropics. Upper left: suppressed growth. Seven soundings. Upper right: cutoff tower growth. Four soundings. Lower left: explosive growth. Six soundings. Lower right: large, natural cloud growth. Eight soundings.

Here there is a weak, stable, dry layer in mid-levels, restricting natural growth, and an unstable upper troposphere (Simpson, 1967, tables 1 and 2). Seeded clouds with this environment commonly explode in two phases: the first is a vertical growth to 35,000 - 45,000 ft altitude, requiring about 10 to 15 minutes, and the second is a horizontal expansion requiring 15 to 20 minutes (Simpson et al., 1967, fig. 4 and discussion). The resulting giant cumulonimbus may persist for 2 hours or more. The sounding on the lower right is typical of rainy, disturbed conditions where seedabilities are again small, here due to large natural cloud growth. In south Florida, these conditions are often, perhaps usually, accompanied by strong vertical wind shear which inhibits explosive growth.

The photographs in figure 4 illustrate the type of growth regimes associated with the different sounding types. Figures 4a and 4b show views of a cumulus tower before and after seeding on an "explosive growth" day. The cloud grew from 20,000 ft to 42,000 ft within one-half hour following its initial seeding. Figure 4c and 4d show the growth behavior in a "cutoff tower" mode. Figures 4c and 4d show the growth "pressed" day with hazy conditions and only small cumuli, and figure 4f provides an indication of what is meant by a "disturbed" day with cumuli and cumulonimbi imbedded in layers of middle stratiform cloudiness.

It should be appreciated that the less isolated the cumulus development on a given day, the less likely that the seedability results from the one-dimensional Lagrangian model (or any one-dimensional model) can be applied with confidence. Therefore, the occurrence of "acceptable" seedability is a necessary, but not sufficient, prerequisite for declaring an experimental GO day. If the environment is too disturbed and cumulus development rampant, the results of the model seedability predictions are probably not indicative of true seeding potential⁵.

2.3 Weak Links in the Reasoning Chain

2.3.1 Distribution of Nucleating Material

One of the greatest uncertainties facing scientists involved in dynamic cloud seeding is the decision of how frequently to release pyrotechnics while in the moist updraft regions of the convective tower. There are at least two schools of thought on this matter. St. Amand and Elliott (1972) describe a technique whereby one or two flares, each emitting 25 gm of AgI nucleant, are released into updrafts of radius 1 to 2 km. They reason that restraint is necessary both to preclude too rapid localized growth which can cause some spindly towers to break off at mid-cloud level and separate (cutoff tower growth mode) and to

⁵This is the rationale for introducing an additional criterion based on degree of disturbance as manifested by radar echo activity. See section 4.



1827 GMT 16 MAY 1968
(a) 3min. after seeding



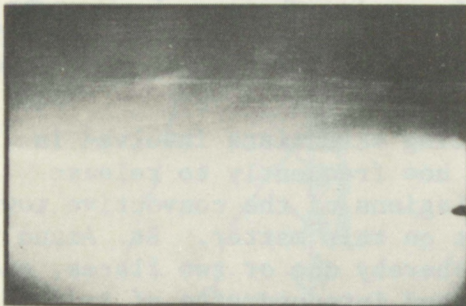
1848 GMT 16 MAY 1968
(b) 24min. after seeding



1850 GMT 18 JULY 1970
(c) 1 min. before seeding



1857 GMT 18 JULY 1970
(d) 6min. after seeding



(e) 1904 GMT 7 MAY 1971



(f) 1843 GMT 30 MAY 1968

Figure 4. Cloud photographs illustrating: (a) and (b) explosive growth behavior; (c) and (d) cutoff tower growth behavior; (e) growth behavior on a suppressed day; and (f) growth behavior on a disturbed day.

prevent overseeding to such an extent that either an outflow shield develops and prevents the insolation necessary to sustain active convection, or the vital cloud downdraft regions are weakened to the extent that the organization of the internal circulation is destroyed. On the other hand, Simpson et al. (1970) typically released 10 to 20 flares, each emitting 50 gm of AgI nucleant, into a convective updraft of radius 1 to 2 km. They reason that the one-dimensional numerical modeling indicates that on most occasions at least 50 percent of the cloud's water content must be nearly instantaneously frozen in order that enough latent heat is released to significantly affect the tower's buoyancy and allow its growth through a capping inversion. The only way to achieve such massive glaciation is to insure that the nucleating material is quickly mixed throughout the updraft, and it has been assumed that the release of one flare every 150 to 200 meters within the updraft is necessary for an acceptable lateral distribution of the silver iodide. Experimental success has been claimed by supporters of both schools of thought.

From turbulent diffusion theory it can be shown that the increase in mean square distance (\overline{D}^2) between pairs of particles as a function of time relative to the dimensions of a container (in this case an updraft) can be expressed by

$$\overline{D}^2 - \overline{D}_0^2 = A\epsilon (t^3 - t_0^3) \quad (4)$$

where the subscript zero refers to initial conditions ϵ is the dissipation rate of turbulent energy which provides a measure of the magnitude of the turbulence, and A is the dimensionless constant of order unity. Both Dye et al. (1975) and Kyle (1974) have used this expression to evaluate the dispersal of pyrotechnically-produced silver iodide in convective updrafts. Kyle's treatment allowed for the computation of $\epsilon^{1/3}$ as a function of the vertical velocity (w) and the updraft radius R by assuming updraft similarity with an entraining jet. Measurements of turbulence intensity can be obtained by aircraft because, at any given airspeed, the rms value of vertical accelerations is proportional to the quantity of $\epsilon^{1/3}$ (MacCready, 1964). Kyle's (1974) computations⁶ of $\epsilon^{1/3}$ indicate a value of 8.1 cm^{2/3} sec for a vertical velocity of 10 m/sec and an updraft radius of 1 km. This compares well with MacCready's (1964) tabulation of $\epsilon^{1/3}$ value between 8 and 10 observed in cumulus congestus clouds. From (4) it can be calculated that the spreading distance (d) is 400 m after about 150 sec, assuming $\epsilon^{1/3}=8$ and an initial line source of negligible width. This will cover less than one-twentieth of the area of an updraft having a diameter of 2.0 km. After nearly 200 seconds, the plume is calculated to have a diameter of 625 m (covering one-tenth the updraft area) and after about 340 seconds will spread to a diameter of 1400 m covering one-half of the above updraft area. These results will not be greatly affected by considering the initial plume diameter to be a significant fraction of the aircraft wingspan because of immediate mixing in the aircraft wake turbulence after ignition of the pyrotechnic. Small variability in the value

⁶Using the formulation: $\epsilon^{1/3} = \left(\frac{3}{2c}\right)^{1/2} \frac{cw}{(2R)^{1/3}}$

with "C" a dimensionless constant having a value of 0.15, and "w" the updraft velocity.

assumed for $\Sigma^{1/3}$ will have a substantial effect on the calculated plume spread. For $\Sigma^{1/3}=6$ and 10, the computed times required for a plume to attain a diameter of 1400 m are about 440 and 270 seconds.

Assuming a bubble rise rate of 10 m/sec and an in-cloud temperature lapse rate of $4^{\circ}\text{C}/\text{km}$, it can be easily calculated that the tower center will pass through the -4°C to -8°C region in 100 seconds. From the previous computations it can be seen that an individual nucleating plume from a pyrotechnic will not have diffused enough during that time to cover even one-twentieth of the area of a reasonably sized cumulus tower. If one is constrained to believe that at least 50 percent of the cloud's water must be converted to ice entirely within the -4°C to -8°C region, it would appear that upwards of 20 flares would have to be distributed homogeneously throughout the cloud tower's cross sectional area. Because an aircraft must penetrate the tower in a straight line, this is clearly impossible to achieve. It would appear that the best that can be achieved within the -4°C to -8°C region, given the above rise rate and lapse rate assumptions, is a rectangular total coverage 400 m by 2000 m, which represents about 30 percent of the area of a 2.0 km tower.

An expenditure rate of one flare released every 200 m of flight (about 2 sec of NOAA C-130 or DC-6 flight time) is required to achieve this blanket coverage with considerable overlap of plumes. An expenditure rate of one flare every 400 m will provide coverage of roughly 20 percent of the tower area in this time frame. With either release rate, the plumes are predicted to diffuse and merge to cover over 90 percent of the tower area after about 5 minutes, at which time the tower temperature will be -16°C at its center (assuming previous conditions). With just the release of two flares, one at the entry point to the 2.0 km updraft and the other 1400 m (14 sec) later, the plumes are predicted to cover 75 percent of the cloud area after 5 minutes. All these calculations, of course, are predicated upon the assumptions that in cloud turbulent diffusion follows the relationship shown by (4), and that $\Sigma^{1/3}$ in the type of towers penetrated for seeding does not vary greatly from a value of about $8 \text{ cm}^{2/3} \text{ sec}^{-1}$.

We have considered only the spread of material following the bubble upward, and have not treated the movement of nucleant upwards from below through a fixed level. This would serve to increase the dispersion within the -4°C to -8°C level because the initial width of the plume rising from below would no longer be negligible in the calculations. This, however, is a very complex problem because the axial and vertical continuity of the updraft velocity may well not be maintained through the fall depth of the pyrotechnic. The dispersion of the plume during the short time the pyrotechnic falls from its -10°C release level through the -8°C to -4°C region can be neglected.

It therefore seems that the modeling requirement to glaciare more than 50 percent of the cloud's water content within the region -4°C to -8°C is inconsistent with the practical realities. A more realistic simulation would be the computation of seedability based on the linear

freezing of water between -4°C and -15°C , by which point the seeding material should be uniformly distributed through most of the tower volume. Considering just the nuclei distribution problem, it would appear that only a few well-placed flares are necessary to achieve a uniform spread of material within most of the tower after 5 minutes.

Early in the Florida single cloud experiments it was assumed that a concentration of nucleating material sufficient to produce the order of 100 ice crystals per liter of cloud volume was required for dynamic seeding to be effective. This was based largely upon some analytical calculations of MacCready (1959). Recently, Cotton (1972) has numerically analyzed in considerable detail the amount of ice crystals necessary to induce a dynamic seeding effect, and his work indicates a critical concentration of about 50 per liter in towers with precipitation to as many as 500 per liter if all the water is contained in cloud-sized droplets. If we assume a one-to-one relationship between AgI nuclei and ice particles (see next section for discussion), then 4×10^{14} nuclei must be released into a spherical bubble of radius 1.0 km to achieve a nuclei concentration of 100 per liter after uniform mixing through the cloud volume is achieved. This criterion can be fulfilled if 10 pyrotechnics, each emitting 40 grams of nucleant (while falling 2 km through the bubble) with a yield of 10^{12} nuclei per gram effective within the temperature range of interest are released with even spacing on the aircraft traverse across the tower diameter. The nucleating characteristics of the pyrotechnics used in FACE are discussed in appendix C. Suffice it to say that a considerable problem apparently exists in producing this concentration of effective nuclei at temperatures warmer than -12°C from the type of pyrotechnic used through the FACE-73 program. With the theoretical uncertainties involved, it remains our best judgment that an evenly spaced expenditure of the order of 10 flares during a traverse of a strong, moist updraft of the type generally found in vigorous Florida cumuli is optimal to induce an effective dynamic response to seeding.

2.3.2 Concentration of Natural Ice

The dynamic seeding hypothesis is predicated upon the overriding assumption that the natural conversion of water to ice inside an updraft at temperatures near -10°C proceeds so slowly and so ineffectively as to be of negligible importance to the life cycle of a cumulus cloud. The preponderance of data relating to the activity of ice-forming nuclei support this assumption. It has been generally accepted that an average worldwide concentration of ice nuclei is about one per liter active at -20°C , with an order of magnitude decrease of active concentration for every 4°C increase in temperature. Therefore, at -12°C it might be expected that the order of 10^{-2} ice nuclei per liter should show activity, and at -4°C , the order of 10^{-4} per liter.

During the past 15 years, however, observational evidence has accumulated that strongly indicates that ice crystal formation in the atmosphere oftentimes bears little direct relationship to the concentration

of active ice nuclei detected by conventional measurement techniques. Koenig (1963) has observed that roughly 30 percent of the Project Whitetop cumulus clouds in Missouri glaciated completely within 10 minutes after the first appearance of ice crystals, and none of these clouds had top temperatures colder than -10°C . Mossop et al. (1968) reported the presence of columnar ice crystals in average concentrations of 35 per liter in a well-documented Australian cumulus cloud with a top temperature of -4°C . This represented a 5 orders of magnitude increase in ice crystal concentration over the active ice nuclei concentration that was measured simultaneously below the cloud base. Hobbs (1974) has summarized an entire series of ice crystal measurements by several investigators and has concluded that in the case of maritime clouds at least, the ratio of observed ice particle concentration to measured active ice nuclei concentration is the order of 10^4 at -4°C decreasing to the order of 10^2 at about -14°C and the order of 10^1 at -20°C . On the other hand, observations obtained in Israeli continental cumuli by Gagin (1975) indicate a fairly small ($<10^1$) discrepancy between ice particle and ice nuclei concentrations over the temperature range -8°C to -20°C . It has been hypothesized by Hallett and Mossop (1974) that the efficiency of a secondary ice crystal production mechanism is dependent upon the presence of large ($>25\mu\text{m}$) drops interacting with rimed particles. They offer laboratory evidence to indicate that such a mechanism is most important in the temperature range -4°C to -6°C .

Figure 5 shows microphysical observations obtained in four separate penetrations of a growing cumulus tower during the FACE-73 program (Sax and Willis, 1974). An attempt was made to follow the bubble upwards in a Lagrangian sense, and some success at this was achieved during the first three penetrations. The bubble was first penetrated at an altitude of 4.6 km (15,000 ft) and then successively at an altitude of 5.2 km (17,000 ft) and twice at an altitude of 5.8 km (19,000 ft). The cloud top was approximately 0.15 km (500 ft) above the first penetration altitude of 4.6 km, but the tower growth slightly outpaced the aircraft ascent so that by the time of the second penetration at 5.2 km, the top was about 0.3 km above. At the start of the initial 5.8 km penetration the cloud top was about 0.5 km above, and this was also the case for the final penetration as the cloud appeared to rapidly lose its buoyancy. The profiles of Rosemount temperature, liquid cloud water content (as measured by a Johnson-Williams device), ice particle concentration (as measured by a Mee optical counter), hydrometeor water content and concentration of hydrometeor drops greater than 0.93 mm diameter (as determined from an analysis of foil impactor data) and vertical velocity (as calculated by the method of Carlson and Sheets, 1971) are shown stacked upon each other as a function of time. There are several interesting features relevant to this discussion. It can be seen that during the first penetration, a concentration of ice crystals of as much as 10 per liter was detected at a temperature of -2°C . Although it is possible for the optical ice crystal instrument to give erroneous results due to its detection of a signal from large water drops ($>\approx 2$ mm diameter), it can be deduced from the drop concentration profile that this introduced an uncertainty of no more than about 20 percent in the ice particle data presented here. Although an

extensive series of instrumentation checks and intercomparisons are planned for FACE-75, the performance of the ice particle instrument in FACE-73 was such as to warrant confidence in the data. It would appear, therefore, that ice particle concentrations of 10 per liter are possible in Florida cumuli with top temperatures no colder than about -4°C . It is more important to observe, however, that the high ice particle concentration appears to be inversely correlated with the strong updraft region in the tower. During the first penetration almost no ice was found in the region of strong updraft, and during the second penetration 4 minutes later, distinct minima in ice particle concentration are observed to correspond to the regions of strongest updrafts. Glaciation appears to proceed markedly after the second penetration, so that by the time of the third pass, the updraft had weakened and practically all of the cloud droplet water content had been converted to ice. No seeding activity was conducted on the day this cloud was studied.

These types of data have very great significance for the verification of the dynamic seeding hypothesis⁷. If a cumulus cloud can glaciate naturally under some conditions in the same time interval that it would glaciate if seeded, there does not appear to be much logic in conducting seeding operations. If, on the other hand, the large concentrations of ice frequently observed in the maritime environment are confined to the stagnant, peripheral regions of the cloud envelope, there would still be good reason to induce glaciation by artificial means in the updraft, since it is the temperature difference between updraft and environment that drives the buoyancy and determines the cloud growth. Sax (1969) has examined the response to seeding of the 1965 Stormfury clouds (Simpson et al., 1967) and has deduced that large-scale rapid glaciation in the manner proposed by Koenig (1966) could not have been occurring, although an analysis of formvar data did reveal pronounced pockets of ice on at least one occasion.

The instrumentation needed to reliably discern the spatial variability of ice in-cloud has not been available in FACE programs before 1973. With the exception of a few dedicated occasions (the results of one shown in fig. 5) efforts in FACE-73 to determine the in-cloud microphysical evolution of the water-ice budget were carried out on a catch-as-catch-can basis during lull periods in the seeding activity. It was only during such periods that the aircraft could be spared to make repeat penetrations through towers for cloud physics purposes. Until the natural glaciating behavior of Florida cumuli is thoroughly understood, it is not possible to ascertain whether the full potential of dynamic seeding is being realized. The FACE-75 program (see section 8) has been designed in part

⁷These types of data are also of tremendous importance in attempts to alter cloud microphysics by a "static" seeding approach that seeks to create ice crystals in about the same concentrations as those observed from these profiles to exist naturally.

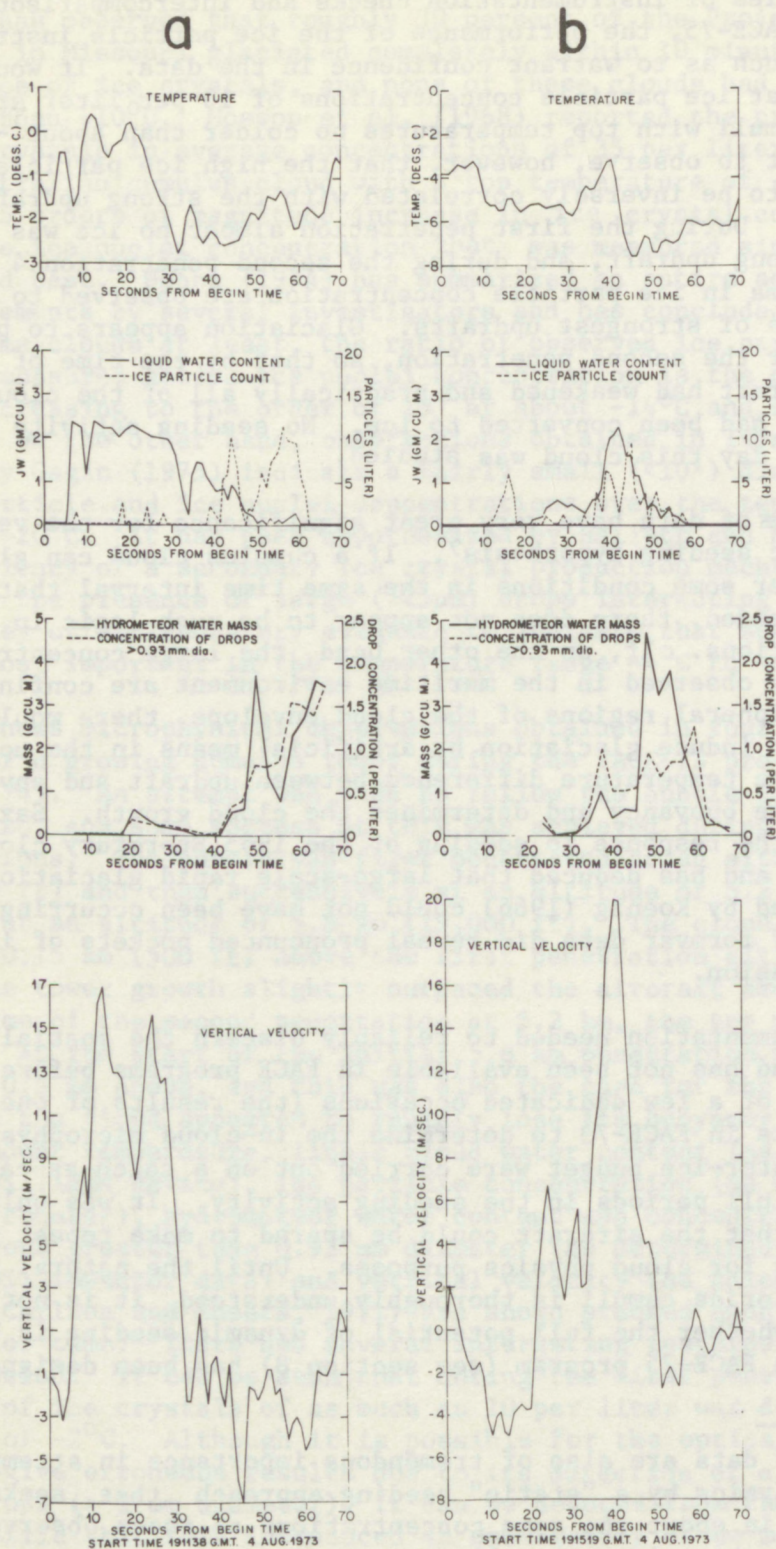


Figure 5. In-cloud microphysical data obtained by penetrating an unseeded growing cumulus tower at three levels: (a) 4.6 km; (b) 5.2 km; (c) and (d) 5.8 km. Note the evolution of the microphysical parameters with time.

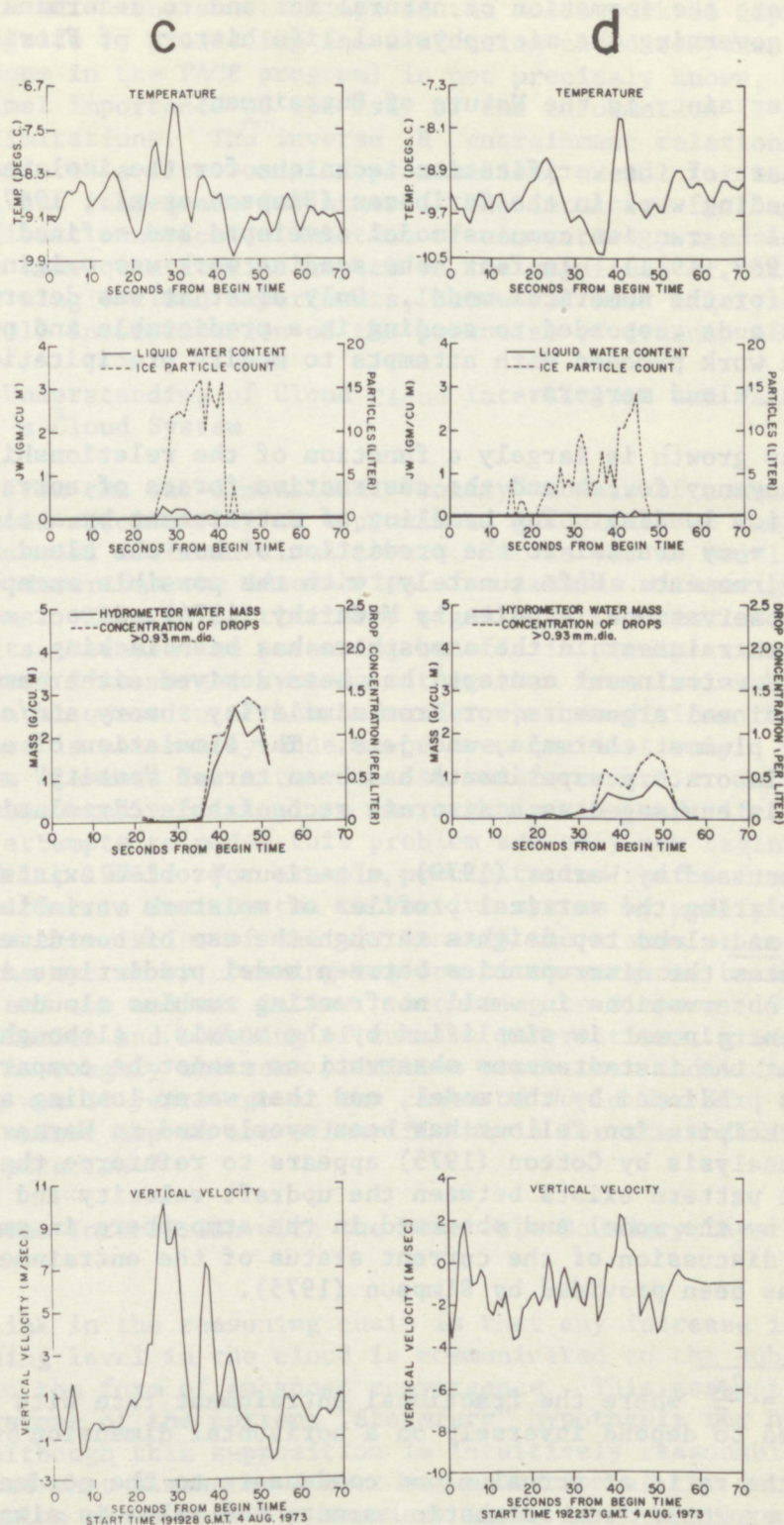


Figure 5. (contd.) Note the intercorrelation of the variables on each penetration. Data are of a Lagrangian nature in that the aircraft was successful in repenetrating at approximately the same distance below cloud top at each altitude. See text for discussion.

to investigate the formation of natural ice and to determine predictor variables governing the microphysical life history of Florida cumuli.

2.3.3 Uncertainty in the Nature of Entrainment

The heart of the verification technique for the isolated single cloud dynamic seeding work in the Caribbean (Simpson et al., 1967) was the one-dimensional Lagrangian cumulus model developed and refined by Simpson and Wiggert (1969, 1971). In fact, the seeding work was originally designed as a test for the numerical model. Only after it was determined that isolated clouds responded to seeding in a predictable and predefinable manner did work proceed with attempts to modify precipitation over an area by inducing cloud mergers.

Cumulus growth is largely a function of the relationship between the driving buoyancy forces and the destructive forces of entrainment and precipitation loading. The handling of entrainment by a cloud model is, therefore, very crucial to the prediction of how the cloud will respond to its environment. Unfortunately, with the possible exception of recent aircraft observational studies by McCarthy (1974), direct evidence of the nature of entrainment in the atmosphere has been lacking. The classical inverse "R" entrainment concept⁸ has been derived either empirically, or from dimensional arguments, or from similarity theory and/or analog with laboratory plumes, thermals, and jets. The simulation of entrainment by analog to laboratory experiments has been termed "entity" modeling, since the cloud is envisaged as a discrete recognizable circulation unit.

As discussed by Warner (1970), a serious problem exists in simultaneously simulating the vertical profiles of moisture variables, updraft velocity, and cloud top heights through the use of one-dimensional models. He attributes the discrepancies between model predictions and his careful series of observations in small nonfreezing cumulus clouds to the manner in which entrainment is simplified by the models. Although it has been argued that the instantaneous observations cannot be compared to the mean properties predicted by the model, and that water loading and the treatment of precipitation fallout has been overlooked in Warner's discussion, a recent analysis by Cotton (1975) appears to reinforce the view that no consistent pattern exists between the updraft velocity and Q/Q_a ⁹ profiles predicted by the model and observed in the atmosphere in small cumuli. An excellent discussion of the current status of the entrainment and modeling problem has been provided by Simpson (1975).

⁸ $\mu = \frac{1}{M} \frac{dM}{dz} = \frac{2\alpha}{R}$ where the fractional entrainment rate with height is postulated to depend inversely on a horizontal dimension or cloud radius R.

⁹ Q/Q_a is the ratio of actual cloud condensate to the condensate which could be expected from adiabatic ascent; the value is always less than unity due to mixing process.

The manner in which the shortcomings of the model work to impair its usefulness as a guide to predicting and evaluating cloud response to seeding (as is done in the FACE program) is not precisely known, but is probably of minimal importance if the user of the information is acutely aware of model limitations. The inverse R entrainment relationship can, perhaps, be considered a first-order approximation, useful for some types of computations, but inadequate for others. The intuitive feeling is that a more realistic numerical simulation of convective processes would undoubtedly have some quantitative impact on the magnitude of the results from the earlier single cloud experiments, but would most likely not alter greatly the overall interpretation of the potential of dynamic seeding.

2.3.4. Lack of Understanding of Cloud-Cloud Interactions and Failure to Model a Cloud System

Predictions from the one-dimensional "entity" models of cumulus convection may be used successfully as approximate guidelines to the behavior of seeded and unseeded isolated cloud towers, but as yet no model exists which adequately describes the interaction of a cumulus with neighboring clouds and systems. This is particularly significant to cumulus modification experiments, because the potential benefit in precipitation alteration probably comes from merged systems rather than from isolated cumuli. The very fundamental question of how and under what conditions the merging process progresses is not really understood even qualitatively. The spacing of convective elements for either mutual reinforcement or mutual destruction is undoubtedly critical to the organization and life system, but rudimentary attempts to model this problem are only now beginning in earnest (e.g., Hill, 1974). For example, precipitation shafts from cumulus clouds can act either to destroy the convective system by modifying the thermodynamic characteristics of the air beneath the clouds or to enhance development of the system by creating regions of convergence between the rain-cooled air and the ambient inflow. According to Simpson (1975) "... the documentation and modeling of cumulus interactions, groups, and systems are now in roughly the same primitive state that individual cumulus modeling was 30 years ago at the close of World War II. This open frontier is the widest gap in the scientific basis for the modification of convective precipitation."

2.3.5 Cloud System Interaction with the Mesoscale Boundary Layer Flow Pattern

The second link in the reasoning chain is that any increase in buoyancy at the seeding level in the cloud is communicated to the subcloud boundary layer in the form of enhanced convergence. This assumption also forms the cornerstone of the current "Stormfury" hypothesis for hurricane modification. Although this supposition is intuitively reasonable, it must be recognized that almost no direct documentation of the interaction of a growing cumulus cloud with its boundary layer is currently available. Attempts were made in FACE-73 to obtain and analyze heat, moisture, and

momentum fluxes data related to the scale of the south Florida peninsula¹⁰ but, because of problems with data recording, no useful information on the scale of individual cumuli was obtained. Hopefully, the flux and microphysical data obtained in the multi-aircraft 1974 GATE program will produce some direct documentation of the transfer processes through the boundary layer.

It is also recognized that the mesoscale boundary layer holds the key to the determination of the spectrum of horizontal sizes of the active towers on a given occasion. Since the horizontal dimension of the perturbation is related to the vertical penetration of convection and dynamic seedability, it is vitally important that attempts be made to fill our knowledge gap in the area. In addition, the mesoscale boundary layer over south Florida has been shown by Pielke (1973) to directly respond to the peninsula heating and to establish initial convergence zones in a semi-predictable and repeatable manner as a function of ambient flow. The Pielke sea breeze model has already proven valuable to the FACE program, but its potential usefulness as presently formulated is limited because of its inability to account for interactions of cloud systems with the boundary layer.

2.3.6 Lack of Documentation of the Natural Evolution of In-cloud Microphysical Processes

Perhaps the most obvious weak link in the reasoning chain is our lack of detailed knowledge of how microphysical processes evolve naturally within Florida cumuli. This problem was referred to in the previous discussion about the concentration of natural ice in the atmosphere. Figure 5 illustrates the type of data that must be collected, cataloged, analyzed, and interpreted from an ensemble of clouds to obtain a reasonable understanding of how the microphysical processes evolve and how the various parameters are interrelated. Until a concerted effort is undertaken to obtain such data, it may be very difficult to discern a "seeding signal" from background noise using a catch-as-catch-can procedure of obtaining single-level microphysical data only once or twice in the cloud's life history. Sax (1974) has demonstrated that the microphysical differences between populations of seeded and nonseeded Florida cumulus clouds are not so blatantly obvious that they can be defined unambiguously in the mean data field. Therefore, apparently it is necessary to construct detailed case studies of the microstructure of individual clouds to detect differences due to seeding.

This uncertainty points out a possible serious discrepancy between what is hypothesized to occur following massive seeding and what actually occurs. Dynamic seeding procedures were designed (and modeled) to glaciare 60 percent of the cloud tower in the temperature range -4°C

¹⁰Results to be published as a NOAA Technical Memorandum.

to -8°C . If this were actually occurring, it would seem reasonable that repeated penetrations at the -10°C isotherm level through an ensemble of seeded and nonseeded cumuli should provide data showing substantial differences in changes in, at least, the mean ice particle concentration and probably also in the mean updraft velocity and mean liquid water content. As we can see from table 2, this was not the case in the rather limited number of repeated passes available for analysis from the FACE-73 program. There can be several reasons advanced by way of explanation:

- 1) The pyrotechnics were not emitting enough ice nuclei active at -10°C or warmer to cause glaciation significantly above background levels. Glaciation may have occurred at levels colder than -10°C and was not sampled by the aircraft penetrations.
- 2) The aircraft did not pass through the area of the tower penetrated previously and therefore missed the plume region.
- 3) The ice particle instrumentation failed to detect all the particles present or was malfunctioning in some other manner.
- 4) The mean values of ice particle concentration and other parameters are not good indicators of glaciation characteristics and cloud response to seeding.
- 5) The conversion of supercooled water to ice does not proceed in the manner described by the seeding hypothesis.

A discussion of reason #4 can be found in appendix D. Suffice it to say here that a more sensitive indicator of glaciating behavior may be the percentage of time during the penetration that the ice particle concentration exceeds a critical threshold value, but even this kind of stratification fails to produce a totally unambiguous distinction between the seed and no-seed populations. Of the remaining possible explanations, it would seem that #2, that of aircraft positioning, and #1, that of glaciation at colder temperatures, are the most reasonable. As we noted earlier, a finite period is required for the nucleating material to be distributed throughout the cloud tower. If the conditions assumed in section 2.3.1 are valid, and if the release of pyrotechnics were optimally spaced throughout the updraft, it would require several minutes for the materials to be distributed to more than 50 percent of the updraft region. Single towers can have multiple updraft regions, and the transfer of nucleant from one region to another certainly proceeds more slowly than it does across a continuous updraft region. Therefore, the possibility exists that an aircraft can be sampling a different region of the cloud tower from that previously penetrated, and the new region may very well have different microphysical characteristics. This is, of course, especially critical in the case of actual seeding because, unless the nucleant has been released evenly through all the updraft areas within a tower, successive penetrations within relatively short periods may encounter nonseeded regions.

Table 2. FACE 1973 Seed Versus No-Seed Microphysical Statistics

	Cloud penetrations					
	First		Second		Third	
	Seed	No seed	Seed	No seed	Seed	No seed
Number of cloud penetrations	12	17	12	17	4	7
Mean pass duration	27.6	26.9	41.1	29.1	32.5	41.1
Mean Δt from first penetration (min)	----	----	6.1	5.0	10.0	8.5
<u>Vertical velocity statistics</u>						
Mean of cloud penetrations	3.5	5.4	2.7	3.4	4.9	0.9
Standard deviation (m/sec)	5.1	7.4	6.8	7.0	5.8	5.0
Mean updraft velocity (m/sec)	6.7	7.8	7.0	6.4	6.2	4.6
Standard deviation (m/sec)	4.8	6.3	5.8	6.3	5.6	3.8
Mean downdraft velocity (m/sec)	-2.8	-3.5	-3.0	-3.1	-1.2	-3.0
Standard deviation (m/sec)	2.1	2.6	2.3	2.6	0.7	2.5
Maximum vertical velocity (m/sec)	21.8	39.3	26.0	33.6	26.0	18.0
Percent pass with updraft	66.2	78.2	57.0	68.4	83.1	51.4
Percent pass with downdraft	33.8	21.8	43.0	31.6	16.9	48.6
<u>Johnson-Williams cloud water statistics</u>						
Mean cloud water content (g/m^3)	1.5	1.0	0.9	0.6	0.2	0.4
Standard deviation (g/m^3)	0.8	0.8	0.9	0.7	0.4	0.6
Maximum cloud water content (g/m^3)	2.5	2.7	2.7	2.4	2.1	2.6
Median cloud water content (g/m^3)	1.8	0.9	0.4	0.2	0.1	0.2
<u>Ice particle statistics</u>						
Mean ice particle concentration (no/l)	2.5	5.3	6.6	8.2	8.7	11.4
Standard deviation (no/l)	5.5	7.1	7.4	8.3	7.3	10.1
Maximum ice particle concentration (no/l)	38.1	34.5	45.7	40.8	31.8	56.7
Median ice particle concentration (no/l)	0.1	1.7	4.2	6.0	6.8	9.8

Table 2. FACE 1973 Seed Versus No-Seed Microphysical Statistics (Continued)

	Cloud penetrations					
	First		Second		Third	
	Seed	No seed	Seed	No seed	Seed	No seed
<u>Foil hydrometeor water statistics</u>						
Mean hydrometeor water content. (g/m^3)	0.3	0.7	1.0	0.8	1.1	0.7
Standard deviation	0.5	1.2	1.3	1.9	1.2	1.0
Maximum hydrometeor water content. (g/m^3)	3.8	6.0	9.7	10.1	3.7	5.1
Mean concentration of drops $d > 0.47 \mu\text{m}$ (no/l)	0.4	0.9	1.3	0.7	1.8	1.1
Mean concentration of drops $d > 0.93 \mu\text{m}$ (no/l)	0.1	0.3	0.4	0.2	0.6	0.3
Median hydrometeor water content (g/m^3)	0.0	0.1	0.5	0.0	0.5	0.2
<u>Lyman-alpha total water statistics</u>						
Mean total water content (g/m^3)	4.2	5.4	3.5	5.6	4.0	5.2
Standard deviation (g/m^3)	1.9	2.1	2.1	1.9	1.5	2.0
Maximum total water content (g/m^3)	8.6	9.9	9.3	9.0	6.5	8.9
Median total water content (g/m^3)	4.5	5.4	2.6	5.8	3.9	5.2
<u>Time percentage statistics</u>						
Vertical velocity $> 7.5 \text{ m/sec}$	25.1	31.9	21.5	20.4	24.6	9.4
J-W cloud water $> 1.0 \text{ g}/\text{m}^3$	71.0	48.3	36.3	24.3	3.8	15.6
Ice particle concentration $< 2.5/\text{liter}$	81.9	57.2	37.3	36.0	24.6	27.1
All three conditions simultaneously	16.6	19.9	10.1	6.7	0.0	5.6
<u>Correlation statistics</u>						
Vertical velocity vs. cloud water content	0.23	0.35	0.69	0.37	0.74	0.54
Vertical velocity vs. hydrometeor water content	-0.13	-0.10	0.37	0.14	0.35	-0.17
Vertical velocity vs. ice particle concentration	0.04	-0.19	-0.16	-0.11	0.45	-0.23
Cloud water content vs. hydrometeor water content	-0.03	-0.21	0.25	-0.43	0.26	-0.19

Table 2. FACE 1973 Seed Versus No-Seed Microphysical Statistics (Continued)

	Cloud penetrations					
	First		Second		Third	
	<u>Seed</u>	<u>No seed</u>	<u>Seed</u>	<u>No seed</u>	<u>Seed</u>	<u>No seed</u>
Cloud water content vs. ice particle concentration	-0.42	-0.60	-0.30	-0.46	0.39	-0.33
Ice particle concentration vs. hydrometeor water content	0.53	0.47	0.22	0.68	0.08	0.18

The possibility that the pyrotechnics were not emitting enough nucleating material active at the proper temperatures cannot be discounted, particularly in view of the requirements posed in section 2.3.1 and the activity characteristics discussed in appendix C. However, if this were the case, the dynamic response of the individual clouds in the earlier Florida seeding experiments (Woodley, 1970) would be difficult to understand. In view of the tremendous ramifications¹¹ of this possibility, the FACE-75 program has been designed, in part to investigate the in-cloud nucleating capabilities of several pyrotechnics (see section 7).

Reasons #3 and #5 are rejected at this point because no evidence yet exists to indicate their possible validity.

In summary, the very first link in the chain of events following seeding, the creation of significantly greater concentrations of ice crystals than exist naturally, has not been documented in the FACE program (nor in a quantitative manner in any other cumulus modification program to the authors' knowledge). On the contrary, the evidence in existence (see appendix D) offers reason to believe that natural glaciation, at least under some conditions in Florida, can produce ice in concentrations not strongly distinguishable from those produced following seeding. This evidence may be misleading, however, because a concerted effort to obtain such data on a repeated basis will be carried out for the first time in FACE-75. Until the evolution of in-cloud microphysical processes is better understood and documented, it will not be possible to confidently assess in detail the effects of seeding on cloud development.

2.3.7 Extended Area and Persistence Effects

It is now known that the rainfall from individual convective clouds can be augmented by seeding. It is not known whether cumulus precipitation can be increased over a large target area. The FACE program is directed at resolving this uncertainty. It is even more uncertain whether attempts at cumulus modification within a target area might have effects outside the target area that might persist for hours, days or even months after the cessation of treatment.

Some scientists have argued that artificially increased rainfall in one area means decreases elsewhere. Others have argued that a net increase in rainfall is possible. The evidence to date is conflicting.

Simpson and Dennis (1972) point out that extended space and time effects of cloud modification need not be confined to rainfall, but could affect radiation and energy budgets, momentum transports, boundary layer processes, severe weather manifestations and wind circulation patterns

¹¹A finding of this sort would require reinterpretation of seeding results from the FACE program.

They also discuss the possible causes of such extended effects. These might include such causes as:

- 1) physical transport of the seeding agent,
- 2) physical transport of ice crystals produced by a seeding agent,
- 3) changes in radiation and thermal balance, as for example, from cloud shadows or wetting of the ground,
- 4) evaporation of water produced,
- 5) changes in the air-earth boundary, such as vegetation changes over land or changes in the structure of the ocean boundary layer following cloud modification,
- 6) dynamic effects, such as:
 - a. intensified subsidence surrounding the seeded clouds, compensating for invigorated updrafts,
 - b. advection or propagation of intensified cloud systems which subsequently interact with orography or natural circulations,
 - c. cold thunderstorm downdrafts, either killing local convection or setting off new convection cells elsewhere,
 - d. extended space-time consequences of enhancement or suppression of severe weather owing to cumulus modification,
 - e. alteration, by means of altered convection, of wind circulation patterns or their transport, or both, which could interact with other circulations, perhaps at great distances.

Observations and calculations make it obvious that transport of the seeding agent and of ice crystals produced by the seeding agent does occur with regularity in seeding efforts, but the effects of these transports have not been determined. The ice crystal anvils from seeded and unseeded clouds appear to have important radiative effects in Florida. In this area, solar radiation striking the ground directly maintains the convection on undisturbed days and the shade of a single anvil often wipes out cumuli over a sizeable fraction of the southern peninsula extending outward in any direction from the target area, depending on winds aloft. An excellent example of this phenomenon is presented in section 5.3 in the discussion of the seeding procedures on 20 July 1973.

Evaporation of water or the wetting of the ground, or both, produced by seeding could have many different, possibly interacting, effects depending upon the locale of the seeding and the initial conditions of the system

(Simpson and Dennis, 1972). In droughts, cloud base could be lowered and CCN production suppressed by these mechanisms. Over a heated island, cooling of the ground by precipitation was found to destroy the island effect. Evaporation of falling rain is a major factor in starting and maintaining the thunderstorm downdraft, while wetting of the ground can change the soil and vegetation. The latter effect is postulated by some Australian scientists as a possible cause of year-to-year persistence in rainfall increases from seeding.

Although extended space-time dynamic effects of cumulus modification are potentially complex, widespread and subtle, many have probably been observed in the dynamic cumulus seeding experiments in Florida. Compensating subsidence may be a mechanism whereby one might be increasing rainfall in one area at the expense of another. However, no one yet knows how to specify where the compensating subsidence will occur; its location and local strength almost surely depend on the meso- and larger scale wind patterns and their convergences. Even where we have observed cleared out areas surrounding seeded complexes in Florida, we cannot be sure whether one area has been robbed of more or received less rainfall than the other area. Preliminary radar results in Florida do not indicate compensating rain decreases surrounding seeded complexes.

In Florida, we have rather clearly documented the propagation of seeded cumulonimbus complexes out of the target area and their interaction with the coastal seabreeze, resulting in heavy rainfall at least 50 miles away from the seeding site up to 5 hours after seeding had ceased. If the seeding did indeed cause the observed explosive growth of the original seeded clouds, the extended space and time effects would follow. More explicitly, we may alternatively postulate that the seeding was a necessary, but not sufficient, condition to cause the observed chain of events, or better perhaps, that the extended effects could be triggered by the seeding because of the special initial conditions of the cloud-environment systems (Simpson and Dennis, 1972).

The effects of cold cumulonimbus downdrafts to suppress or propagate convection have not yet been explicitly studied in connection with modified cumuli. However, they are becoming documented in connection with natural cumulonimbi. Since, in the tropics, no observable differences have been detected between cumulonimbi whose stature has been brought about by dynamic seeding and those created by nature, cold downdrafts could play a role in extending the effects of cumulus modification experiments.

The last two possible extended effects of dynamic seeding are even more in the realm of speculation than the previous discussion and they are not considered here. Further, one could hardly do them more justice than do Simpson and Dennis (1972) in their text on cumulus clouds and their modification.

2.4 Problems in Verifying the Physical Hypothesis

2.4.1 Convective Rainfall Variability and Measurement Errors

There are several obstacles to verification of the area seeding hypothesis; two of the most formidable are the large variability in space and time of area-mean rainfall and errors in rain measurement. The magnitude of these problems was determined by FACE scientists in terms of the number of experimental days necessary to resolve a particular seeding effect. Two independent, but mutually consistent, simulations were made, one by Simpson et al. (1973) in which the importance of natural rain variability was investigated and the other by Olsen and Woodley (1975) in which both rain variability and measurement errors were considered.

In the Olsen and Woodley study, a gamma distribution was fitted to the area-mean rainfalls for the EML target measured by radar and adjusted by gages, and an area seeding experiment was simulated on the computer using these measurements as input. The simulation was designed to study the effects of natural rain variability and multiplicative measurement errors on the ability to detect a seeding effect. The errors for the measurement of rainfall were determined for raingage networks of varying density and also for radar without the benefit of adjusting gages.

The simulation procedure consisted of randomly generating two samples of equal size - the first corresponding to nonseeded area rainfall and the second to seeded area mean rainfall with a specified seeding effect θ . A no seeding effect is given by $\theta = 1$ and a seeding effect of a 40% increase in rainfall is given by $\theta = 1.40$. Selected test statistics (significance level of 0.05) were then calculated to determine whether the hypothesis of no seeding effect is rejected versus the alternative of either a positive or negative effect. This was repeated for 500 simulated experiments for each paired sample and the percent of rejections is tabulated to give the Monte Carlo power as a function of θ , where power in this context is the probability of detecting the seeding effect given that the seeding effect is θ .

The distribution used in the simulation was the gamma distribution fit for area average rainfall for the EML target. The effect of seeding, if any, was postulated to be multiplicative so that the distribution for seeded rainfall was also a gamma with the same slope parameter α , but with a scale parameter depending on θ , i.e. β/θ . The simulations were made for postulated seeding effects of 0.4, 0.6, 0.8, 1.0, 1.2, 1.4 and 1.6 and for sample sizes of 10, 20 and 50 seeded and nonseeded samples.

The second part of the simulation introduces the effect of the measurement error distributions obtained by Woodley et al. (1975) for raingages and radar. The measurement error is assumed to be multiplicative. Therefore, the generation of a rainfall observation with an attached error is accomplished by first generating an observation from the assumed actual rainfall distribution and then multiplying this value

by an observation generated from the assumed error distribution. The resulting set of error-adjusted observations are treated as in the analysis of the first part. This procedure was completed for the same sample sizes and seeding effects for all of the specified error distributions.

The results for the EML target are presented in figure 6 in terms of the power function of the likelihood ratio test. This test and the optimal $C(\alpha)$ were the better of six statistical tests and they performed very much the same. In examining figure 6 one can see that the empirical power increases with an increase in sample size and an increase in seeding effect. Even with 50 pairs of cases and perfect rain measurement (the true gamma line), the empirical power does not reach a respectable 90 percent until we have a total target seeding effect of at least 1.5.

This study, as well as that of Schickedanz and Huff (1971), emphasizes the importance of reducing the natural rain variability. This can be accomplished in several ways. Cumulus Group (CG) scientists have been rather selective in their choice of days for experimentation (Simpson et al., 1973) by applying a suitability criterion. The suitability criterion was designed to eliminate days that were not conducive to effective cloud seeding. These include the days when it is unlikely that there will be clouds in the target area to seed and the days when the target area is very disturbed so that the effect of seeding would be negligible. These restrictions should reduce the natural variability of the area-mean rainfall. However, the basic shape of the distribution should remain the same. Hence, it is felt that the suitability criterion will increase the ability of the tests to detect a seeding effect. The validity of this assumption is currently under investigation.

Alternative methods of circumventing the rain variability problem are stratification of the days of experimentation based on predictor variables and/or outright prediction of target rainfall using a physical model. Search for such predictor variables and model development is now a collaborative program between the CG and the University of Virginia. Once the useful predictors are in hand, predictions of target rainfall, regardless of amount, will be possible on days of experimentation. A measure of the effect of seeding will then be provided by the departure of the rainfall on seed days from that predicted. Should such a scheme be possible, rain variability will be greatly diminished as an obstacle to evaluation of a seeding effort for rain enhancement.

2.4.2 Proper Instrumentation to Detect Microphysical and Dynamical Changes

In the FACE program prior to 1973, the types of instrumentation¹² available to directly detect microphysical and dynamical changes induced

¹²A description of cloud physics instrumentation can be found in appendix D.

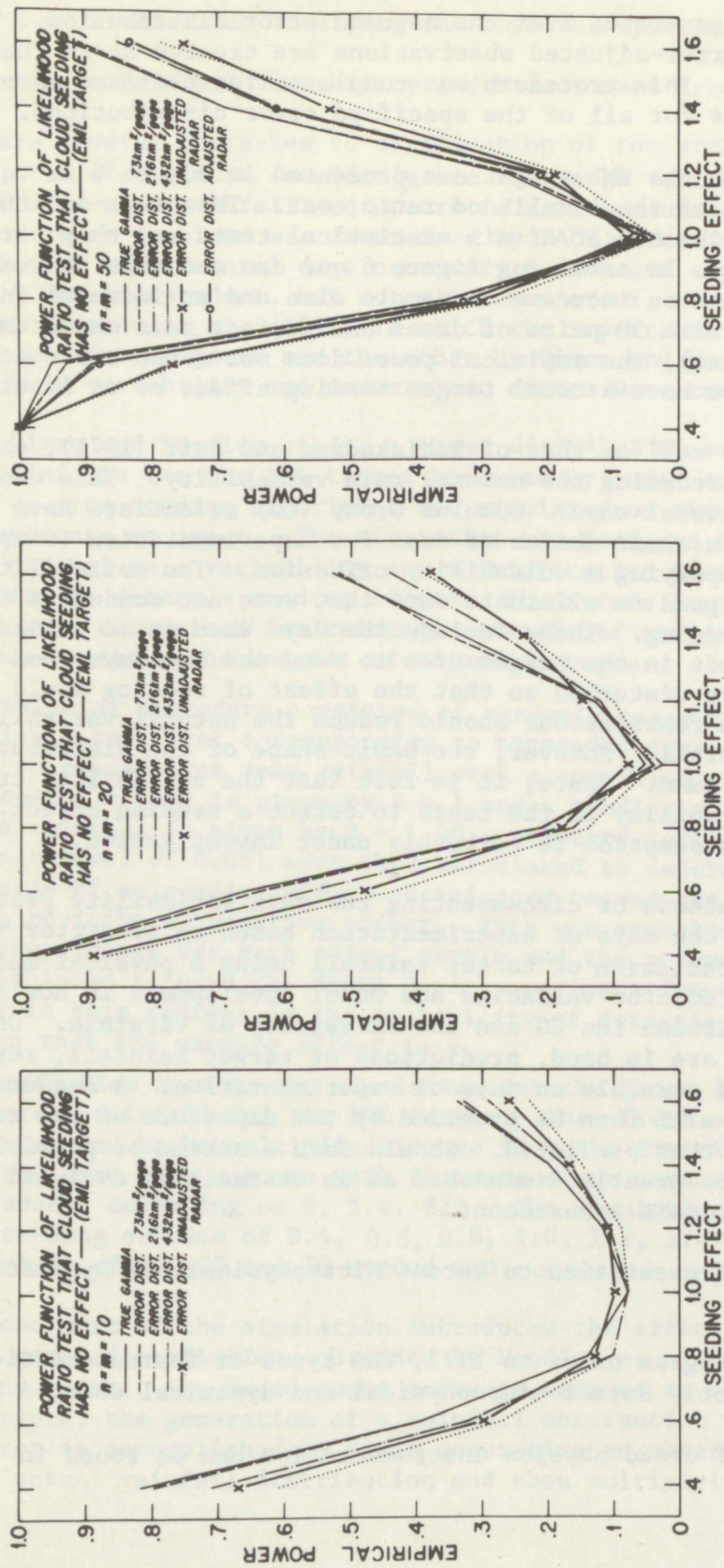


Figure 6. Power function of likelihood ratio test that cloud seeding has no effect for the FACE target.

by seeding were rather limited and quite crude in terms of real-time analysis. It was possible to determine cloud water content in real-time (from the Johnson-Williams device) and also to deduce a very coarse perception of updraft velocity (from the aircraft rate of climb), and these two parameters were used to determine where pyrotechnics should be released in the cloud. The formvar replicator (when operating properly) was used as a means of providing a post analysis¹³ of in-cloud ice crystal concentrations, but these data were never reliable enough in long stretches to obtain quantitative information bearing on the glaciating characteristics of an ensemble of cumuli. Analysis of the formvar data was tedious, time consuming and often very subjective. The proper meshing of the formvar data with other in-cloud data also proved to be a problem on many occasions, and the detailed spatial variability of ice within the cloud as a function of other microphysical parameters (such as updraft velocity) was generally impossible to deduce, except in a very gross manner. Without reliable ice particle data, it was not possible to examine the rate of conversion of water to ice and to draw direct conclusions regarding the first link in the seeding hypothesis.

The introduction of the optical ice particle counter (Sheets and Odencrantz, 1974) into the FACE-73 program provided, for the first time, the opportunity to acquire continuous, real-time data bearing on the evolution of the ice budget. The instrument was very reliable from an operational viewpoint, and a discussion of some of the measurements obtained is provided in appendix D. The use of a newly developed liquid water sensor (Merceret and Schricker, 1975) and the optical particle spectrometer (Knollenberg, 1970) promises to make possible a detailed investigation into the partitioning of cloud and rainwater substance.

The accurate measurement of detailed variations in the in-cloud vertical velocity structure is extremely important to an analysis of how well the seeding hypothesis is verified by observed dynamic response. The conversion of water to ice should significantly increase cloud buoyancy, and this should be detected in changes in strength and organization of the updraft. Unfortunately, in all past FACE programs, including 1973, the updraft structure had to be calculated¹⁴ from the aircraft pitch angle data in the manner described by Carlson and Sheets (1971). This method uses several assumptions in computing angle of attack (when, as in the case of the FACE program before 1975, angle of attack measurements are not directly obtained from aircraft sensors), and, perhaps more importantly, utilizes a 4-second smoothing function because of the sometimes highly fluctuating nature of the w_p component as calculated from nonintegrated radar altimeter data. In the FACE-75 program both problems in using the Carlson-Sheets method will be alleviated (direct angle of attack measurement and integrated radar altimeter data), and the vertical velocity

¹³ Usually many months after conclusion of the project.

¹⁴ $w = v(\alpha - \theta) + w_p$ where w_p is the updraft motion of the aircraft, v the true air speed, α angle of attack in radians and θ the pitch angle in radians.

calculations will be available for real-time use on board the seeding aircraft. In addition, the inertial platform navigational systems enable us to obtain and analyze aircraft acceleration data from which vertical velocities can be calculated and compared with results from the method discussed above. Until the FACE-75 data become available, however, it is realistic to claim that, at best, we have a general description (primarily from FACE-73 data) of the updraft profiles inside Florida cumuli, but the absolute strengths and detailed structure of the updrafts are unknown.

In summary, it is only now that the technology of cloud physics instrumentation has reached the point where it is both possible and feasible to collect the direct in-cloud measurements necessary to confirm several fundamental first responses of the tower to seeding. A real-time continuous record of ice particle concentration, vertical velocity, cloud and hydrometeor water contents, dropsize distribution, and several other microphysical parameters (see section 8) can now be obtained routinely during aircraft penetrations. Digital recording of all microphysical parameters makes it possible to process and analyze the data during the course of the field program and to apply what is learned to the design and execution of the experiment. This has never been possible before, and, as a result, emphasis was correctly placed on other types of measurements related to describing rainfall characteristics and variability.

2.4.3 Proper Instrumentation to Detect Kinematic Changes and to Characterize the Boundary Layer Flow

Four principal types of measurements are applicable to a discussion of the boundary layer flow and cloud kinematics, but all have inherent problems when it comes to verifying the physical hypothesis. Surface systems designed to obtain wind and rainfall information have been incorporated into FACE since its inception, and were expanded in 1973 to include temperature measurements. These systems will be expanded further in 1975 to obtain concurrent humidity and pressure data. The computation of convergence patterns in the mesonet network for several days of interest during FACE-73 has been completed and a careful examination of changes in such patterns during seeding is planned for FACE-75. The inherent difficulties with these types of measurements, however, is that they apply only to a rather limited region of the target area (fig. 1) and only to 6 m above ground level. It is not known how well the convergence characteristics at the 6 m level describe the flow through the boundary layer, but preliminary indications¹⁵ are that under some conditions at least, the flow at several hundred meters can be 180° different from that very close to the surface. A further disadvantage of the data from FACE surface instrumentation is that nearly all of it is analog and requires a long

¹⁵Personal communication with Dr. Roger Lhermitte, University of Miami.

time to process and analyze. Ideally, it would be desirable and very valuable to obtain convergence data in real-time to assess the manner in which clouds are likely to organize. However, the logistical problems of doing this with surface systems are formidable for the FACE target area.

A second category of "kinematic" instrumentation includes pibals and rawinsondes, the latter of which, of course, also provides essential thermodynamic information. Before FACE-73, no data of this type were available from the target area, but in 1973 a program to release pibals and radiosondes was initiated at the Field Observing Site for 1 month. This program has been enlarged for FACE-75 to include the entire period of experimentation and to allow for the possibility of pibal release at more than one location. Also, the release of rawinsondes utilizing an omega signal has been planned, and, if successful, will allow for the routine acquisition of wind information through the depth of the troposphere. However, it is readily apparent that with the resources available to FACE, pibal and rawinsonde data can be obtained at only one or two locations at a given time and, since they can be released only at selected times, provide a discontinuous analysis of the wind flow. The use of this type of data to determine changes from seeding in the boundary layer flow is, therefore, not possible. However, the pibal and rawinsonde wind data will be very useful in determining the representativeness of the winds obtained by the surface network to those existing through the boundary layer.

Remote sensing by X-band dual doppler radar has been used in FACE-73 (Lhermitte and Sax, 1974) to determine the morphology of the kinematics of precipitating convective systems, and this program will be continued (with the possible addition of a third C-band doppler radar during part of the program) in FACE-75¹⁶. The two radars were operated in a coplanar scanning mode, which permitted the acquisition of data at 1.2 km grid points throughout a 60 x 60 km area and through elevation angles from 0° to 18° every 7 minutes. With this system, we can calculate convergence and, through the continuity equation, vertical velocities assuming steady-state conditions¹⁷. This system has the advantages of permitting a continuous description of the flow through a substantial vertical depth (to mid-cloud levels) over a relatively large portion of the FACE target area (see fig. 1). However, the dual doppler is restricted by the physics of its operating principle to obtain data only from systems already precipitating¹⁸. Although these systems are of considerable interest and importance, and should provide essential data bearing on cloud interactions

¹⁶One of the X-band radars used in FACE-73 has been converted to C-band for FACE-75.

¹⁷For FACE-75 the scanning sequence has been made faster so that only 2 minutes are required per complete scan. This will allow for a more confident assumption of steady state conditions.

¹⁸A small pilot project to assess the potential of tracking chaff will be conducted during FACE-75.

with rain-induced downdrafts, it is not clear yet how the information will relate to the fundamental questions of how the effects of seeding are communicated to the boundary layer and how the cloud field becomes favorably organized for mergers.

A final category of instrumentation pertinent to this discussion is the gust probes and related sensors¹⁹ carried by aircraft. No flux measurements were attempted in FACE before 1973. During FACE-73 the vane-type gust sensor and data processing system developed by Grossman and Bean (1973) were flown to acquire heat, moisture, and momentum fluxes through the cloud base level, and some data was successfully acquired on the peninsular scale. However, no useful data was acquired on the scale of individual cumuli because of recording problems and lack of opportunity. In principle, the gust probe measurements should be capable of answering some fundamental questions related to verification of the seeding hypothesis. With repeated aircraft penetrations underneath a subject cumulus cloud group, it should be possible to determine how the updraft structure naturally organizes with time, and how such organization is affected by seeding at upper levels in the cloud tower. If a buoyancy pulse is communicated downward following seeding, it should theoretically show up as enhanced convergence at cloud base accompanied by a better organized (longer wavelength) updraft structure. Both of these should be detectable by gust sensors. Unfortunately, resources devoted to a program do not always permit the use of a dedicated aircraft at cloud base. This is the case in FACE-75 where both research aircraft need to be utilized at upper levels for seeding and for obtaining microphysical data.

A major disadvantage to vane-type gust sensors is their susceptibility to heavy precipitation. In tropical convection, which oftentimes produces rains of intensity greater than 50 mm/hr, the gust sensors can be rendered inoperative and the usefulness of the technique can be greatly impaired. The development of a hot film gust-probe technique (Merceret, 1975) should, theoretically, work in precipitation shafts, but not inside clouds. There have also been problems with proper positioning of the gust probe aircraft underneath seeded clouds, although these will be alleviated to a large degree by the inertial navigation systems.

A proper combination of all the types of measurements described in this section should result in an evaluation of whether dynamic seeding organizes the boundary layer flow in accordance with the seeding hypothesis. The gust probe and doppler radar measurements together are the key to the determination of how buoyancy is communicated downward through the convective thermal. The relegation of priority research areas in FACE-75, dictated by a careful consideration of aircraft and personnel resources, has resulted in the forfeiture of a gust probe program, and means that

¹⁹Such as the microwave cavity for humidity measurements.

this aspect of the seeding hypothesis will not be subject to complete documentation or verification. However, it is expected that future programs will examine the buoyancy communication and subcloud organization problems in detail.

2.4.4 Proper Timing of Data Collection

Possibly the greatest problem in verifying the microphysical and dynamical aspects of the seeding hypothesis is associated with the highly variable nature of the cloud's life cycle. Experience gained from numerous penetrations through Florida cumuli has shown that on some occasions most towers appear to rapidly progress through their life cycle and dissipate, while on other occasions some towers retain a youthful, vigorous appearance for relatively long periods of time. Figure 5 showed microphysical characteristics (in a Lagrangian sense) of a cloud bubble that rose through the 4.6 km level with a strong updraft and a copious supply of cloud water, but by the time it reached 5.8 km, 8 minutes later, it contained almost all ice and was losing its strong updraft characteristics. A little more than 3 minutes later the tower was in the dissipating stage. Figure 7 shows an evolution of the microphysics of another tower at a single level (approximately 5.8 km) during three cloud penetrations spanning almost 9 minutes. Again one can see the initially slow microphysical evolution between passes #1 and #2 followed by rapid glaciation and decay of the updraft between passes #2 and #3. During FACE-73 this type of rapid life cycle appeared to be the rule rather than the exception²⁰, and attempts are being made to correlate microphysical changes with ambient flow and the other possible predictor variables.

As might be appreciated, this type of cloud behavior plays havoc both with seeding procedures and with evaluation of the seeding hypothesis. Since both NOAA research aircraft typically cruise at about 100 m/sec, they can reach any tower within 25 km in less than 4 minutes. However, any promising looking tower developing beyond that distance very often is in a dissipating stage of its life cycle by the time it is reached for penetration by the aircraft. Fortunately, new active towers frequently develop in the region of the old subsiding tower so the repositioning of the aircraft is not necessarily always a wasted maneuver.

During the FACE-73 program, many penetrations were made into clouds which appeared visually suitable for seeding, yet contained very little cloud water and/or strong updrafts. In those cases, the seeding time "window" was obviously quite narrow. Similarly, the data collection time window can also be narrow when it comes to attempting to determine microphysical and dynamical evolution. Departures of only a few minutes in penetration times can lead to totally different impressions of the cloud's life history. This can be a critical factor in properly

²⁰See table D-2 in appendix D.

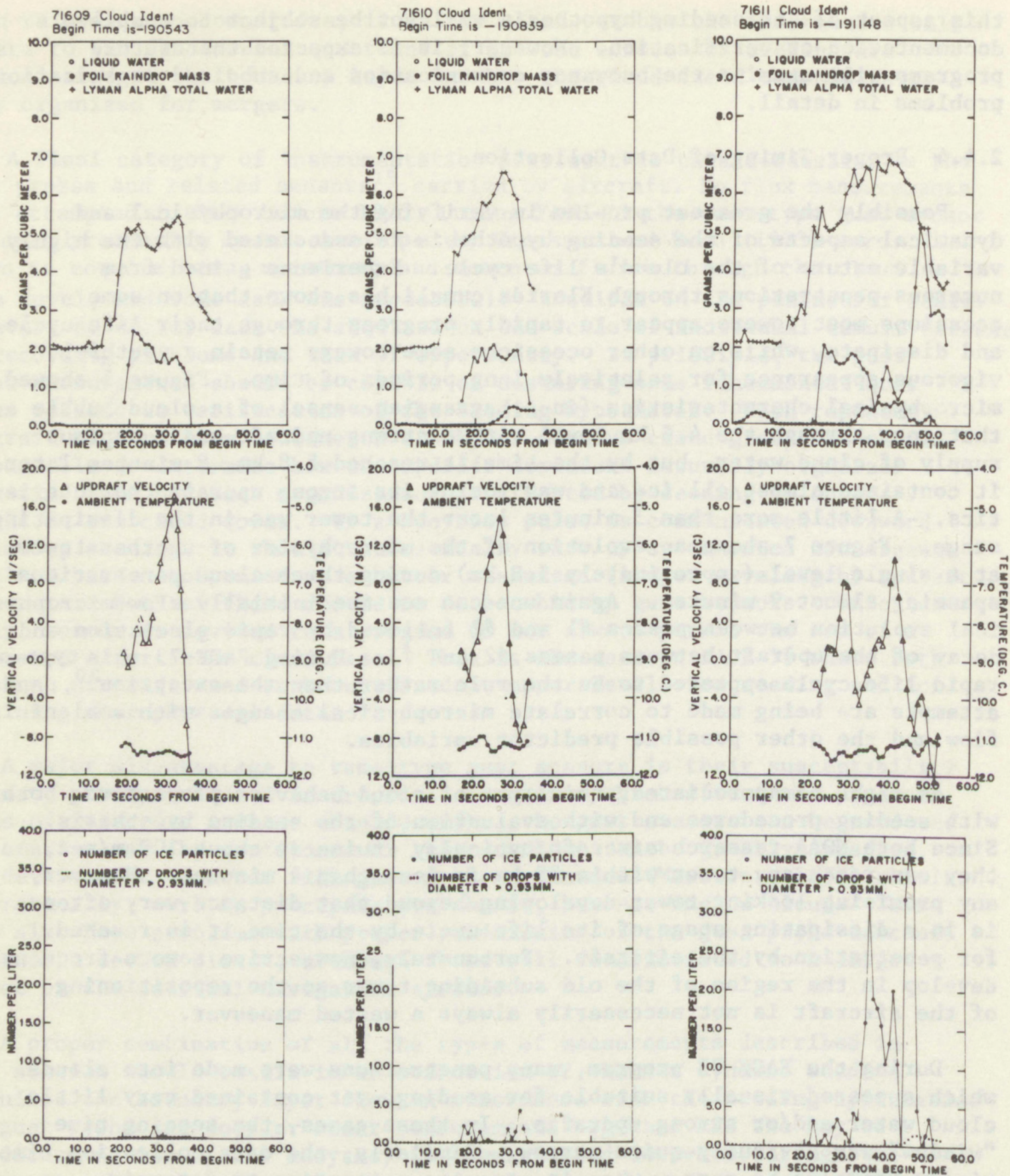


Figure 7. In-cloud microphysical data obtained by penetrating a growing nonseeded cumulus tower at a single level (5.8 km); note the evolution of the microphysical parameters with time (particularly the increase in ice crystal concentration between pass (b) and pass (c) and the inter-correlation of variables on each pass).

evaluating cloud response to seeding. It is, therefore, important that penetrations through the same portion of the tower be made as rapidly and as frequently as possible.

3. MERGER PROCESS

In the design of the Florida single cloud seeding experiments only isolated convective clouds were acceptable for experimentation. This precaution was necessary to insure that the echoes from individual experimental clouds did not become lost among their echo neighbors. Despite these precautions, experimental echoes did merge with their neighbors; the seeded echoes showed a greater tendency for this behavior by virtue of their greater size and duration. Although this was an annoyance in the evaluation of the single cloud experiments, the merger cases proved to be most informative. The most striking feature of the merger of two or more clouds is the great increase in rainfall that frequently follows.

Before illustrating the merger process, it is important that we define merger since there is no universal definition as yet in the meteorological literature. Merger is the joining of two or more formerly independent precipitating cloud systems into one coherent echo mass as viewed by radar. In past studies using photographs of the radar scope, merger of two or more echo entities was not complete until the contours corresponding to a rainfall rate of 2.5 mm/hr had joined. With the digitizer radar product, a merger is now defined as the juncture of echo boundaries at an equivalent rainfall rate of 1 mm/hr. This definition is merely one of convenience and it says nothing about the time at which the clouds physically interact. In fact, it is likely that the clouds interact well before even their visible boundaries join, and it may be this interaction that predisposes them to eventual merger.

An excellent illustration of the merger process was obtained on 16 July 1970 as depicted in figures 8, 9 and 10. Cloud A was seeded; cloud B was not. Both clouds paced one another to great heights with the seeded cloud reaching 12.5 km before merger. After merger, the consolidated cloud system reached 16.2 km. The radar depictions of the two clouds during their merger phase is shown in figure 8 (bottom). The area of the system increased with time, as did the area covered by the innermost intense cores. In its most intense phase the merged system covered over 340 km².

The merger of the seeded cloud with its neighbor resulted in a great increase in precipitation production compared with what the component clouds produced before merger (fig. 10). This merger also produced an order of magnitude more precipitation than isolated clouds on this day. A specific comparison is presented in table 3 for the merger case and the two isolated control clouds. Although all clouds surpassed 12 km, it would have taken 36 isolated clouds to equal the precipitation of the merged system!

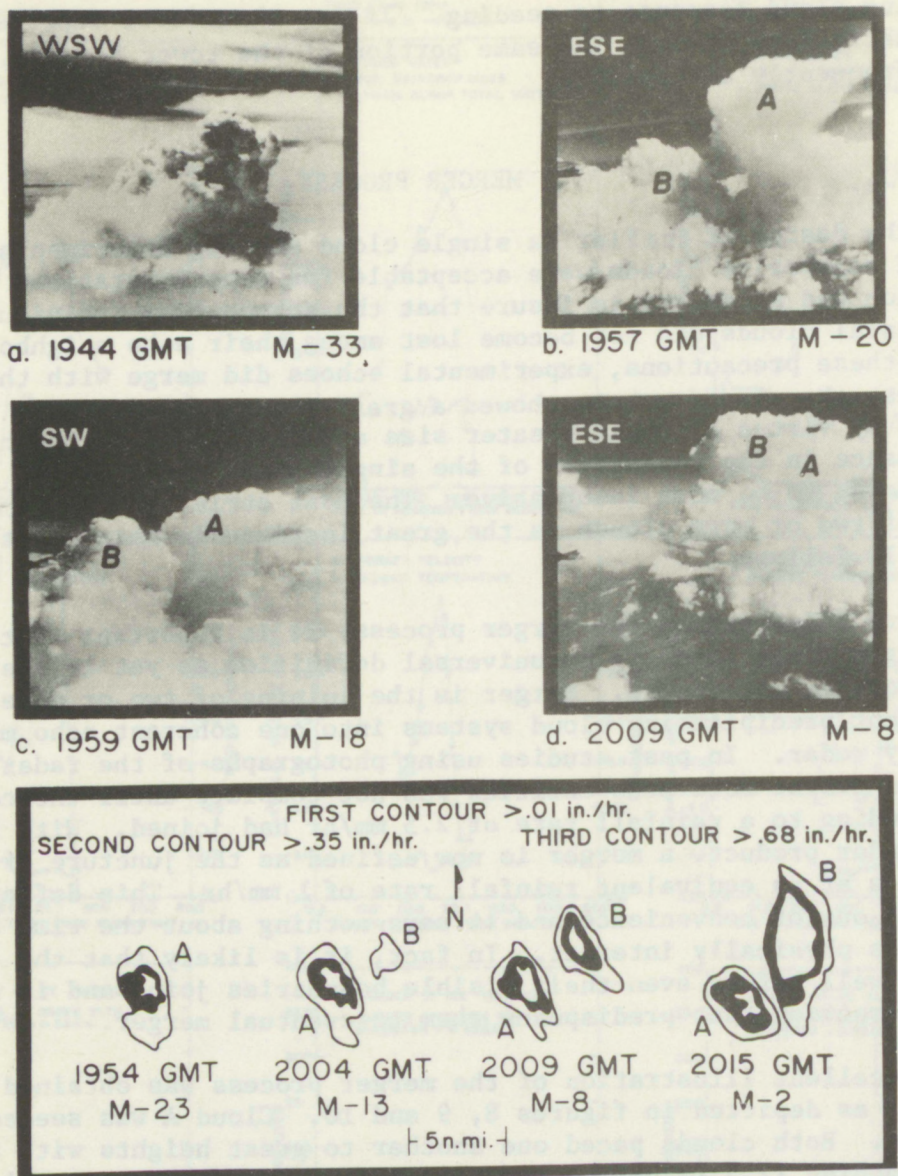


Figure 8. (top) Before merger (M) photographs of clouds A (seeded) and B (unseeded) on 16 July 1970, taken from seeder aircraft at 21,000 ft. The camera direction is indicated in the upper left of each photograph. The numbers below each panel are the times in minutes relative to the time of merger. (a) Seeded cloud A 26 min after seeding and 33 min before merger with cloud B. Cloud A, exhibiting "hesitation growth," is entering its main growth phase. (b) Cloud A has attained miniature cumulonimbus stature. Cloud B is growing rapidly. (c) Cloud B has become the more vigorous cloud. (d) Both clouds have attained cumulonimbus stature, but have not yet merged on radar. (bottom) Precipitation histories of clouds A and B before merger. Depictions were constructed from photographs of the University of Miami 10-cm radarscope as the antenna scanned 0.5° elevation, which corresponds to a beam center altitude of 3500 ft at the range of these clouds. Note rapid growth of cloud B relative to cloud A.

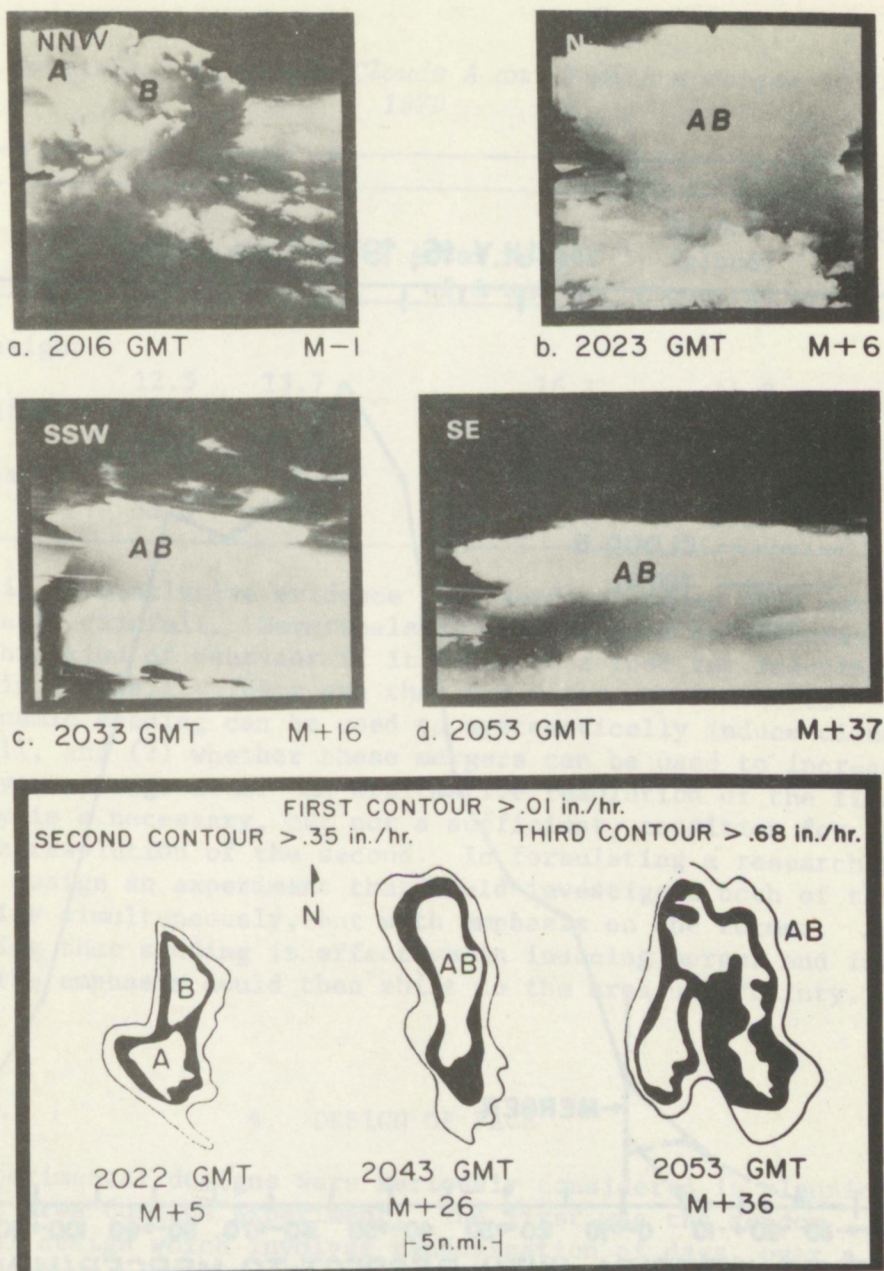


Figure 9. (top) After merger (M) photographs of clouds A (seeded) and B (unseeded) on 16 July 1970, taken from the seeder aircraft at 21,000 ft. The camera direction is indicated in the upper left of each photograph. The numbers below each panel are the times in minutes relative to the time of merger. (a) Clouds 1 min before merger on radar (fig. 9d). Note pileus (cap cloud indicating vigorous growth) near the tops of both clouds. (b) Clouds 6 min after merger seen in the upshear direction under the anvil. (c) Clouds A and B have lost identity as the merger has become a massive thunderstorm complex. (d) The complex 37 min after merger. (bottom) Precipitation history of clouds A and B after merger on the University of Miami 10-cm radar, as in figure 9, bottom.

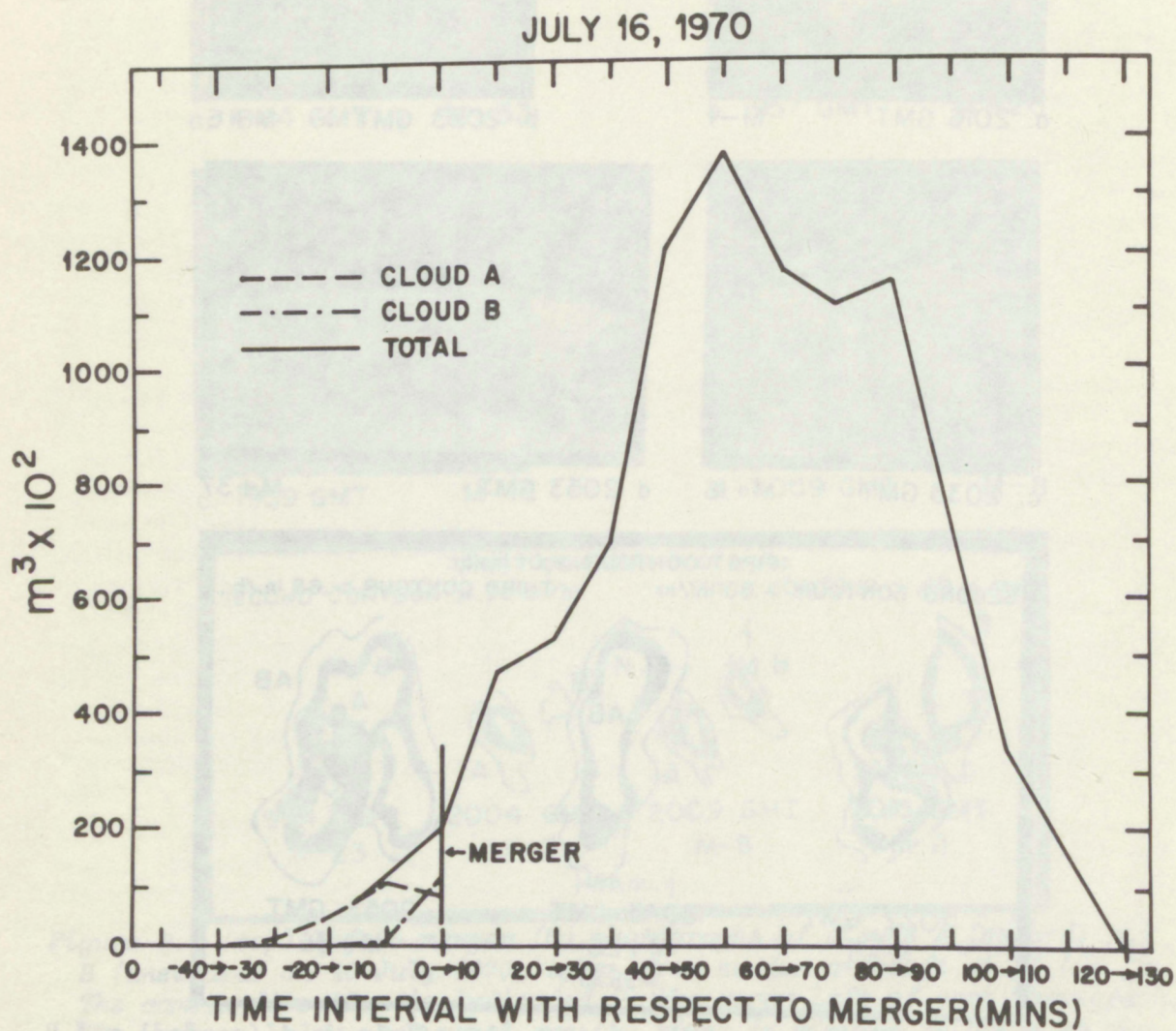


Figure 10. Precipitation histories of clouds A and B before and after merger (vertical line) on the University of Miami 10-cm radarscope, 16 July 1970. Rainfall is plotted against time (10-min intervals relative to seeding cloud A).

Table 3. Comparison of Single Clouds A and B with a Merger on 16 July 1970

Measurements	Before merger		After merger of A and B	Random (cloud) control	Nonrandom (cloud) control
	A	B			
Max. top height (km)	12.5	13.7	16.1	14.3	12.5
Total rainfall ($m^3 \times 10^3$)	298.3	152.5	10,821.0	300.5	181.8
S-band radar (min)	35.0	14.0	112.0	59.0	43.0

There is no conclusive evidence that seeding caused this merger and the subsequent rainfall. Nevertheless, seeding must be effective in inducing this kind of behavior if it is to be a tool for inducing practical increases in rainfall. There are then two major uncertainties: (1) whether dynamic seeding can be used to systematically induce cloud merger and rainfall, and (2) whether these mergers can be used to increase the rainfall over a large area. An affirmative resolution of the first uncertainty is a necessary, but not a sufficient, condition for an affirmative resolution of the second. In formulating a research plan, we decided to design an experiment that would investigate both of these uncertainties simultaneously, but with emphasis on the former. After demonstrating that seeding is effective in inducing merger and increased rainfall, the emphasis could then shift to the area uncertainty.

4. DESIGN OF FACE

Two experimental designs were seriously considered in planning for the Florida Area Cumulus Experiment. The first was the random experimental design which involves randomization of days, over a single target area, into seeded and nonseeded days, with nonseeded as the control. The second was the crossover target-control which requires random interchange of target and control areas among seeding days. The crossover approach was appealing, because this design minimizes the noise of natural rain variability inherent in the random experimental design. The shower patterns in two adjacent areas (as with crossover) on a particular day are better correlated than the shower patterns in the same area on different days (as with the random experimental design). Furthermore, crossover procedures require less time to verify a particular seeding effect than does the random experimental design (Schickendanz and Huff, 1971). The disadvantages of the crossover design are the possibility of silver iodide contamination between target and control, and the

possibility of other effects on the control area because of seeding in the nearby target, such as reduced insolation due to a cirrus canopy or an altered low level wind field. The crossover approach also precludes the "floating target" concept that will be discussed in detail later.

The random experimental design was selected for FACE for practical considerations (Woodley and Williamson, 1970). At the beginning of this program, it was impossible to select two land areas within the range of the research radar (the UM/10-cm) that were free of blind cones produced by obstructions to the radar beam. By 1973, estimates of rainfall by radar were made in FACE using the WSR-57 radar (Woodley et al., 1975). This radar has no obstructions to the energy radiated by its antenna. Because of this development, Woodley et al. (1974) reinvestigated the possibility of changing the FACE design to crossover. They concluded that the lone remaining obstacle was the likelihood of dynamic contamination of the control area by events in the seeded target. Because the magnitude of this factor is unknown, further consideration of the crossover design in Florida was postponed.

With the selection of the random experimental design for FACE, the experiments began on a very limited basis in 1970 and continued in 1971 and 1973. The design of the experiment can best be understood by reference to a flow diagram (fig. 11). The design features (Woodley and Williamson, 1970) were organized as follows:

- 1) A fixed target area (fig. 1) was defined.
- 2) Randomized seeding instructions were prepared.
- 3) Clouds were surveilled in the target by 10-cm radars of the University of Miami (in 1970 and 1971) and the National Hurricane Center (in 1972 and 1973).
- 4) Suitable days for experimentation were necessary. Those were days that satisfied a daily suitability criterion of $S - N_e \geq 1.0$ (later increased to ≥ 1.5), where S is the predicted seedability (in km) predicted by the EML model (Simpson and Wiggert, 1971) with the 1200 GMT Miami radiosonde and a hierarchy of horizontal cloud sizes, and N_e is the number of hours between 1300 and 1600 GMT with 10-cm echoes in the target. The maximum possible value of N_e is 3. The N_e factor is introduced to bias the decision for experimentation against naturally rainy days. Decision time on a day's suitability was 1600 GMT.
- 5) The seeder aircraft flew only on days that satisfied the meteorological suitability factor. The seeding decision was randomly determined in the air when suitable clouds were found in the target, with only the "randomizer" knowing the decision.
- 6) Final acceptance of a day for inclusion in the area analysis was made only after expenditure of 60 flares (50 grams of silver iodide each) or after seedings of six clouds, or both.

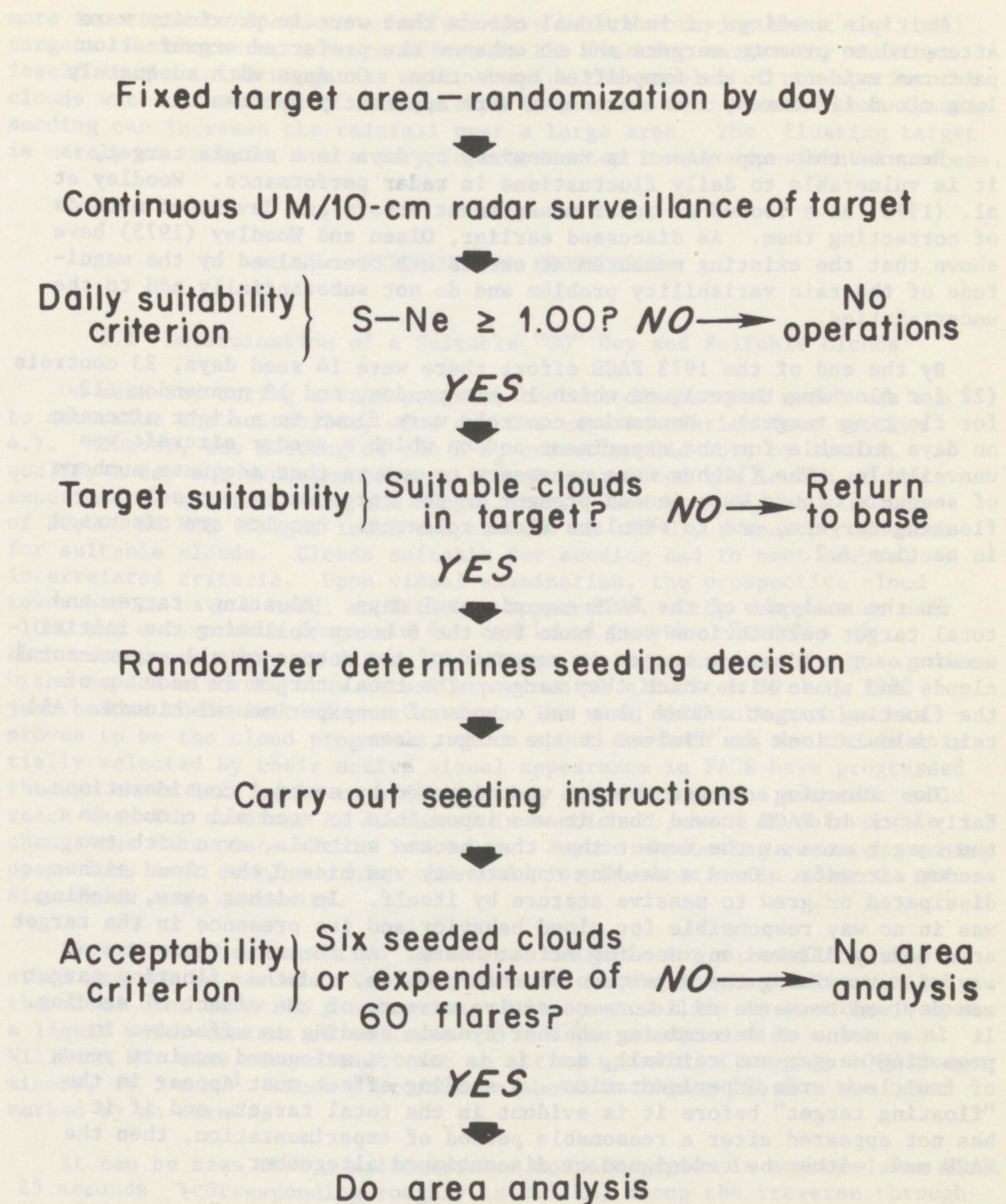


Figure 11. Flow diagram illustrating the design of FACE. The University of Miami 10-cm radar was replaced by the WSR-57 radar of the National Hurricane Center late in 1972. The $S-N_e$ factor for suitability was increased to 1.50 by 1972.

Multiple seedings of individual clouds that were in proximity were attempted to promote mergers and to enhance the preferred organization patterns evident in the unmodified convection. On days with adequately long cloud lifetimes, these attempts were apparently successful.

Because this experiment is randomized by days in a single target, it is vulnerable to daily fluctuations in radar performance. Woodley et al. (1975) have looked at radar measurement errors and developed methods of correcting them. As discussed earlier, Olsen and Woodley (1975) have shown that the existing measurement errors are overwhelmed by the magnitude of the rain variability problem and do not substantially add to the uncertainties.

By the end of the 1973 FACE effort there were 14 seed days, 23 controls (22 for floating target), of which 10 are random, and 13 nonrandom (12 for floating target). Nonrandom controls were flown in a light aircraft on days suitable for the experiment and on which a seeder aircraft was unavailable. The flights were necessary to ensure that adequate numbers of seedable clouds were indeed present in the target area, to select floating targets, and to simulate flare releases. Results are discussed in section 7.2.

In the analysis of the FACE experimental days, floating target and total target calculations were made for the 6 hours following the initial seeding. The floating target is composed of the echoes of all experimental clouds and those with which they merge. The total target is made up of the floating target echoes plus the echoes of nonexperimental clouds. All rain calculations are limited to the target area.

The floating target concept was dictated by several considerations. Early work in FACE showed that it was impossible to seed all clouds in the target area at the moment that they became suitable, even with two seeder aircraft. Once a seeding opportunity was missed, the cloud either dissipated or grew to massive stature by itself. In either case, seeding was in no way responsible for cloud behavior and its presence in the target area merely diluted any seeding effect there. At the time there was no way of determining the magnitude of this problem, and the floating target was devised to serve as a more sensitive measure of the effect of seeding. It is a means of determining whether dynamic seeding is effective in promoting merger and rainfall, and it is also a safeguard against years of fruitless area experimentation. A seeding effect must appear in the "floating target" before it is evident in the total target, and if it has not appeared after a reasonable period of experimentation, then the FACE must either be redesigned or discontinued altogether.

The floating target concept has provoked criticism and some of it is justified. The prime concern is whether, in fact, we are conducting two distinct experiments and whether one has been conducted at the expense of the other. In actually carrying out the seedings, we have given more attention to ensuring an untainted floating target, reasoning that it is

more important to document an effect here before worrying about the total target. Furthermore, a large effect in the floating target may manifest itself in the total target as well, despite the problem of nonexperimental clouds within the target. Ultimately, it must be demonstrated that dynamic seeding can increase the rainfall over a large area. The floating target is merely an interim, but a very important step in the experimental process.

5. EXPERIMENTAL PROCEDURES

5.1 Determination of a Suitable "GO" Day and Suitable Clouds

On each day during a FACE program, the one-dimensional model was run to determine the suitability of a day for experimentation (see section 4.). However, the meeting of the $S-N_e$ criterion did not, by itself, qualify a day for experimentation; it only permitted the launch of the experimental aircraft into the target area. Once at a flight altitude of 20,000 ft MSL (flight level temperature of -10°C), a search commenced for suitable clouds. Clouds suitable for seeding had to meet several interrelated criteria. Upon visual examination, the prospective cloud tower had to have a hard, cauliflower appearance, a top temperature near -10°C and a favorable prognosis for continued growth. Examples of such towers are shown in figure 12. These photographs from the nose camera in the seeder aircraft show actual experimental clouds on 20 July 1973 just before their initial penetration. The most difficult problem has proven to be the cloud prognosis, since about one-half of the clouds initially selected by their active visual appearance in FACE have progressed through their life cycle to a dissipating stage before the aircraft could reach them for seeding. As discussed in section 2., such an unfavorable change can take place within 5 minutes. Anyone conducting research seeding operations must develop a high threshold for frustration in order to persist under such adversity.

Even if a cloud satisfies the visual criteria for suitability, it still may not be seeded. The ultimate test is the internal structure of the cloud upon aircraft penetration. Final suitability is contingent upon a liquid water content of at least 0.5 g m^{-3} as measured with a Johnson-Williams hot wire concomitant with an active updraft of roughly 1000 ft per minute, or 5 m s^{-1} . Such a profile is shown in figure 12b for the tower marked by an arrow.

It can be seen that a multiturreted updraft region is measured for about 25 seconds (corresponding roughly to 2.5 km) along the traverse through the cloud, and the updraft regions are coincident with a broad area in which the Johnson-Williams liquid water content exceeds 1.5 g m^{-3} . Further, no significant ice was found in the three strongest updraft turrets, but the weak fourth updraft area contained ice in concentrations exceeding 10 per liter. Actual seeding of this cloud took place during this penetration.

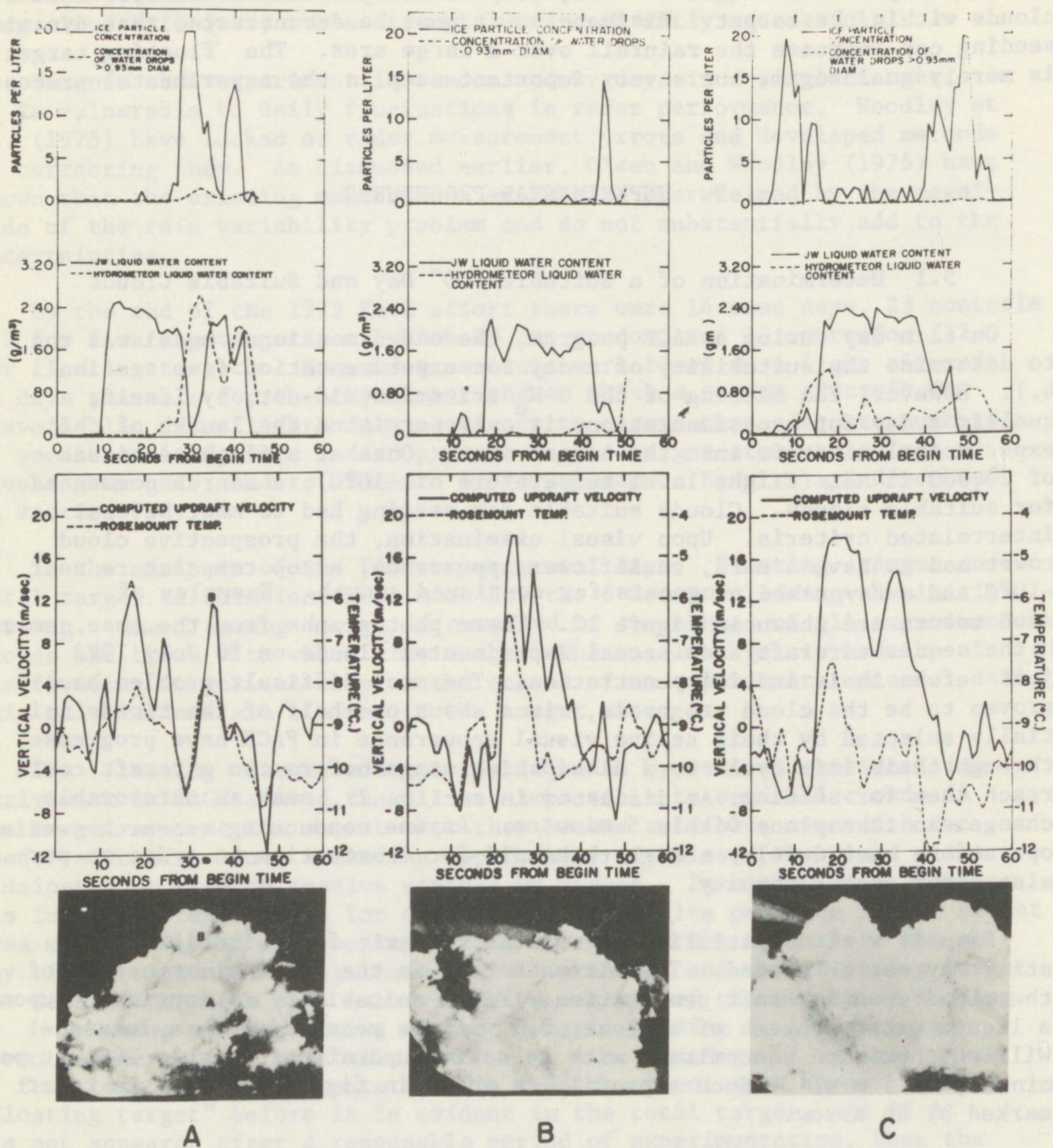


Figure 12. Examples of internal cloud microphysical properties of clouds judged suitable for seeding on 20 July 1973. Note the broad regions of JW liquid water content $>1.0 \text{ g/m}^3$ and the strong ($>7.5 \text{ m/sec}$) vertical velocities. Also, note the low ice crystal concentrations in "active" portions of the cloud, although relatively high ($>10/\text{liter}$) concentrations of ice apparently coexist in dormant regions of the tower; photographs of the selected towers prior to initial penetrations are also shown.

Usually, the appearance of a cloud provides a good clue as to its internal structure, but on some occasions appearances can be deceiving. Consequently, it is important that the seeder remain flexible and base his seeding action on what is measured and not on preconceived notions before cloud penetration. As examples, we examine the appearances and the internal structures of two more clouds on 20 July 1973 in figures 12a and 12c. The cloud pictured in figure 12a had two prominent features, towers A and B, before the first seeding penetration. Tower B was the older and taller, while tower A was below the aircraft altitude, but growing at the time of the photograph. Both towers were penetrated by the aircraft, as is obvious by the plot of microphysical variables in figure 12a. Tower A was actually more suitable than B because of its broad region of high water content, its strong updraft and its negligible ice concentration. Therefore, tower A should (and did) receive greater seeding attention than B.

It is interesting to observe that although extremely large concentrations of ice particles (20 per liter) were measured during this penetration, all of the ice is associated with stagnant or downdraft regions of the cloud. The actual updraft region of the older tower was almost free from ice even though glaciation was obviously proceeding very quickly in its surroundings. This provides strong direct evidence that a dynamic seeding potential can exist in the updraft regions even though the cloud as a whole is found to contain large quantities of ice.

The cloud tower shown in figure 12c easily meets all the visual criteria for seeding suitability and its internal structure certainly confirmed its suitability. The broad expanse (nearly 3 km) of cloud in which strong updraft, high Johnson-Williams liquid water content and low ice particle concentration values coexist should be very responsive to seeding. Nevertheless, there were rather large portions of the cloud area on the periphery of the updrafts that contained a copious quantity of ice and were distinctly unsuitable for seeding. These areas of high ice concentration coincided with areas of weak downdrafts. Apparently there was a skirt of cloud debris from an earlier tower around the new tower and this accounts for the high natural ice concentrations upon entering and leaving what proved to be a vigorous tower.

Finding a group of suitable clouds is but the beginning of the area seeding process. One must then make a prediction as to whether there will be enough seeding opportunities to warrant declaration of a GO day. On one of the experimental days early in the FACE program, all the clouds disappeared from the target area, as if by magic, shortly after the cloud seeding activity had begun. To compensate for this and any other such future problems, an acceptability criterion was invoked to qualify a day for area analysis. By this final criterion (fig. 11), at least six clouds must be seeded and/or 60 flares must be expended in order to qualify a day for analysis (a GO day). This design feature mitigated some problems, but created others. This final stipulation will be modified for FACE-75 for reasons discussed in section 8.1.

Once suitable clouds are found in the target and the prognosis is good for area experimentation, the randomizer is instructed to determine the seeding decision and to arm the racks containing the silver iodide flares. Upon penetration of the first suitable cloud, the flares are sequenced into the active portions of the supercooled cloud and the experiment begins. In FACE, pyrotechnic flares emitting 50 grams of silver iodide nucleant each are ejected into the suitable portions of the cloud at about 100-m intervals. The optimum amount and spacing of the silver iodide flares is still controversial, and the rationale for our procedures is in section 2.3.1. Flights are conducted, regardless of the seeding decision, to guard against bias and to ensure proper definition of the floating target. The individual conducting the seeding never knows for certain whether he is seeding, although in some instances, the seeding action can be inferred from cloud behavior. Inference of the seed decision and its ramifications are discussed in appendix A.

5.2 Idealized Flight Patterns

Figure 13 is an idealized diagram of seeding flight patterns in relation to the development of a convective system. In figure 13a, an isolated, actively growing cumulus cloud is penetrated at the -10°C isotherm level, and AgI pyrotechnics are released in the updraft region at about 100-m intervals. The seeding may be conducted either parallel (as in this example) or normal to the shear vector. As the original seeded tower grows into a small cumulonimbus (fig. 13b) new active towers appear on its upshear side. The general procedure is to seed these in a direction normal to the shear vector to avoid repenetrating the originally seeded large cell²¹. New active towers continue to appear on the upshear side of the maturing older cells, as shown in side view in figure 13c and in top view in figure 13d. These towers are seeded in the optimum direction for penetrating the most active new growth without re-entering the older mature cells. This portion of the seeding procedure requires a tremendous amount of intuition and subjectivity, and there is no substitute here for experience on the part of both the scientists and the aircrew. The seeding of outrigger towers of the convective system continues until it has been determined that either there is no point in attempting to expand the system further, or that there is a requirement elsewhere for the seeding resources.

On many occasions, a new actively growing cumulus cloud develops close to the original system being worked, and it is then that the greatest potential for rainfall enhancement though dynamic seeding theoretically exists. The flight procedure in this case is to

²¹It is often desirable, for data collection, to repenetrated seeded towers; there are many occasions when it is safe to do so.

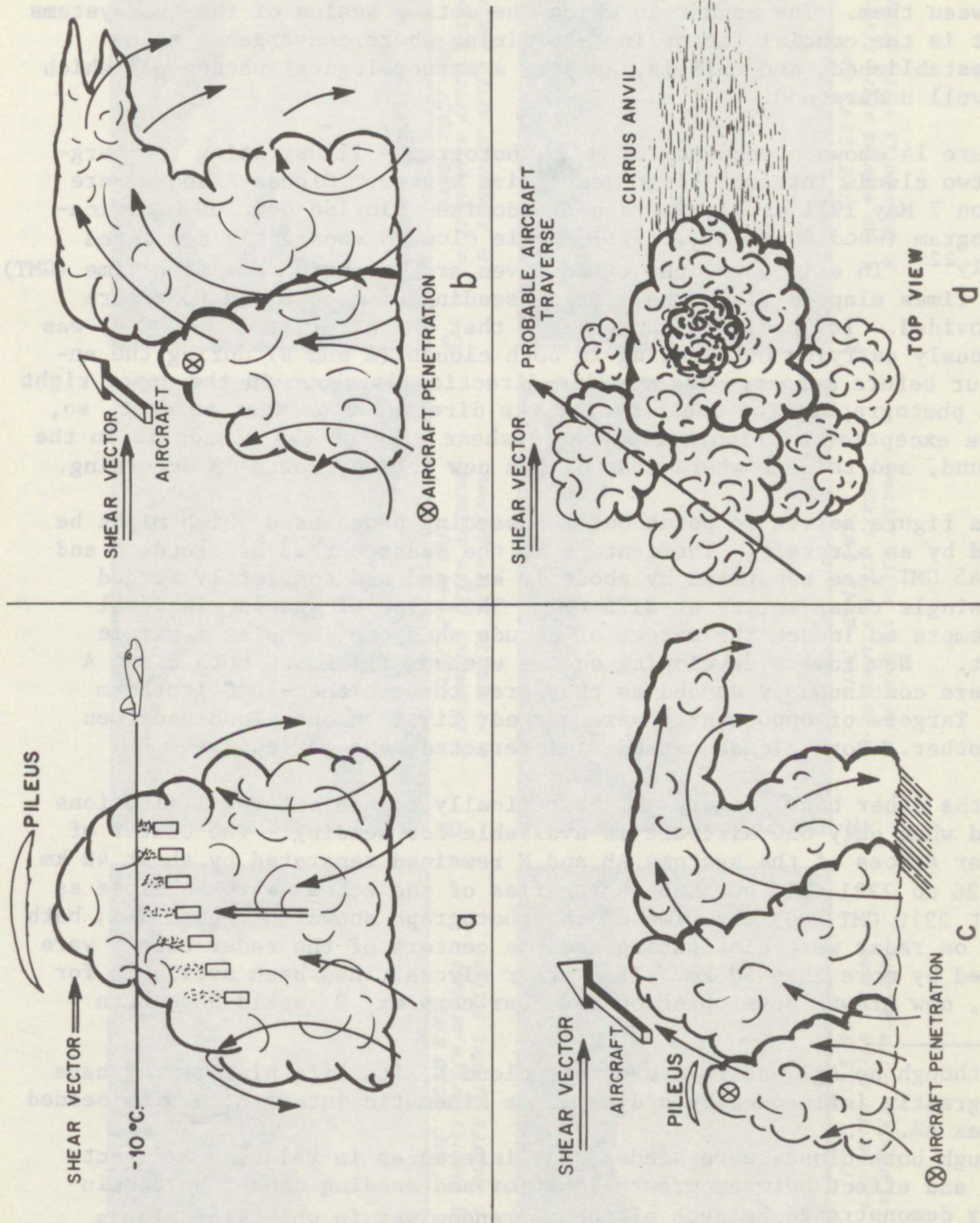


Figure 13. Idealized diagram of seeding flight patterns in relation to a developing convective system; seeding is usually carried out in new towers developing on the upshear flank of the system in the hope that the convection will expand and become better organized.

seed the new cloud in an attempt to expand it into a convective system and narrow the gap to the point where merger is induced. The scientist or crew member conducting the seeding should always be watching for groups of clouds that might be close enough to eventually merge, particularly if an associated region of convection appears to be developing between them. The manner in which the motion scales of the two systems interact is the crucial factor in determining where convergence zones become established, and this is, as yet, a meteorological phenomenon which is not well understood.

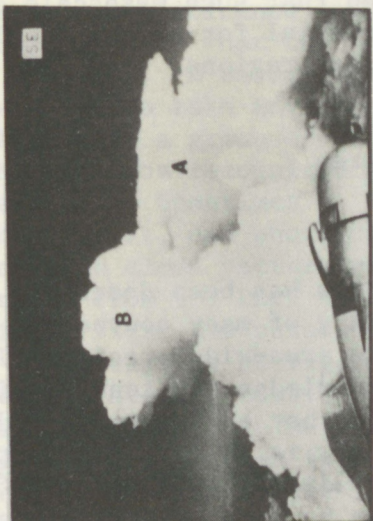
Figure 14 shows a sequence of six photographs illustrating the merging of two clouds into one large convective system. Clouds A and B were seeded on 7 May 1971 as part of a nonrandomized Florida Cumulus modification program (Woodley et al., 1971), while cloud N apparently developed naturally²². In all cases, the times given are Greenwich Meridian Time (GMT) and the times elapsed since the initial seeding of each cloud tower are also provided. It should be appreciated that the aircraft (NOAA DC-6) was continuously carrying out seeding in both clouds (A and B) during the entire hour before merger. The viewing direction is shown in the upper right of each photograph. The shear vector was directed from west to east, so, with the exception of figure 14b, the upshear side of the clouds is in the foreground, and this is where most of the new active growth is occurring.

This figure serves to point out the seeding procedures which might be followed by an aircraft. The centers of the radar echoes of clouds A and B at 2045 GMT were separated by about 10 km, and had completely merged into a single radar entity at 2126 GMT. This type of spacing is ideal for attempts to induce the merger of clouds when one is using a single aircraft. New towers developing on the upshear flanks of both cloud A and B were continuously seeded as they grew through the -10°C isotherm level. Targets of opportunity were worked, first on one cloud and then on the other. Both clouds expanded, interacted, and merged²³.

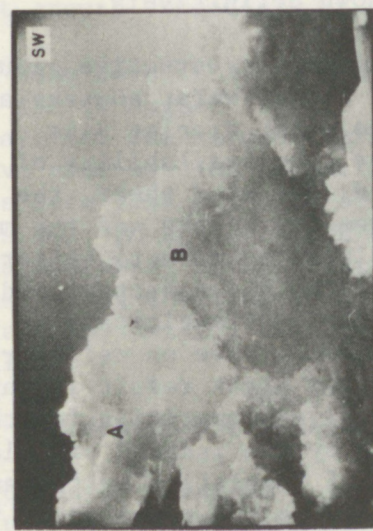
On the other hand, figure 14f dramatically points out the limitations suffered when only one aircraft is available for seeding. The center of the radar echoes of the systems AB and N remained separated by about 40 km from 2126 to 2221 GMT, but the peripheries of the echoes were as close as 10 km at 2210 GMT. By the time of the photograph shown in figure 14f, both systems on radar were dissipating and the centers of the radar echoes were separated by more than 50 km. If another aircraft had been available for seeding, new growth developing on and near complex N would have been

²²Even though no AgI was released into cloud N, its life history may have been greatly influenced by a dynamic or kinematic interaction with seeded complex AB.

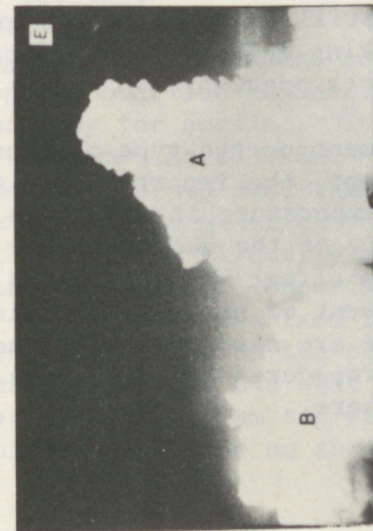
²³Although both clouds were seeded, any inferences in relating a direct cause and effect between growth behavior and seeding cannot be conclusively demonstrated because of the nonrandom way in which the clouds were selected.



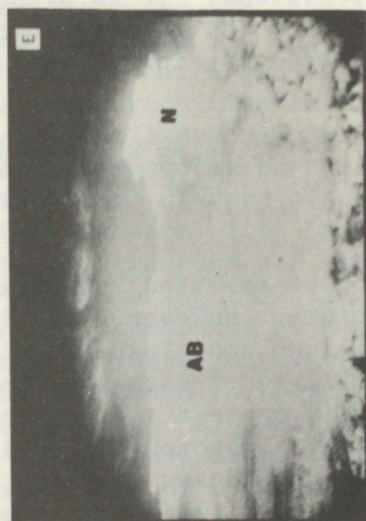
C
TIME 2057 GMT
A: 35 MINUTES AFTER SEEDING
B: 3 MINUTES AFTER SEEDING



B
TIME 2044 GMT
A: 22 MINUTES AFTER SEEDING
B: 2 MINUTES AFTER SEEDING



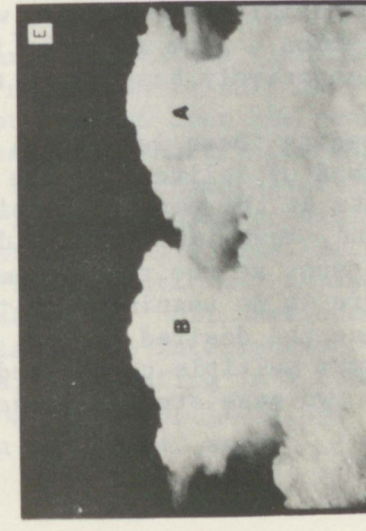
A
TIME 2039 GMT
A: 17 MINUTES AFTER SEEDING
B: 3 MINUTES BEFORE SEEDING



F
TIME 2242 GMT
A: 140 MINUTES AFTER SEEDING
B: 120 MINUTES AFTER SEEDING



E
TIME 2142 GMT
A: 80 MINUTES AFTER SEEDING
B: 60 MINUTES AFTER SEEDING



D
TIME 2125 GMT
A: 63 MINUTES AFTER SEEDING
B: 43 MINUTES AFTER SEEDING

Figure 14. This sequence shows the merging of two seeded clouds into one large convective system on 7 May 1971. Note in 14f that unseeded system (N) also developed well on this day.

seeded at the same time as "AB" in order to attempt to induce a "super-merger" of the two systems. It is hypothesized that such mesoscale organization of convection holds the key to the potential for substantially enhancing the area-wide precipitation in tropical regions.

5.3 FACE Seeding Procedures

5.3.1 General

Dynamic seeding of isolated convective clouds has been described rather well in the literature. However, dynamic seeding of many convective clouds in groups, lines and clusters to enhance area-wide precipitation has received very limited treatment. To our knowledge the lone publication that treats this subject in some detail is that by St. Amand and Elliott (1972). Their approach, as well as ours, is primarily intuitive. In illustrating our procedures with two case studies we will cite references or unpublished findings whenever possible to support our approach. Unfortunately, in some areas very little is known definitively.

As we have seen, successful seeding of individual convective clouds depends on several variables: the supercooled liquid water content and its vertical distribution within the cloud, the water droplet size spectrum, strength and location of the updrafts, the availability of replenishment moisture, the slope of the cloud, the wind shear, the natural ice nuclei distribution, the type of seeding agents and the method of delivery. The successful seeding of many clouds to promote better cloud organization through merger depends upon all of the above factors and others as well. With multiple cloud seeding, one must anticipate in space and time the effect a particular seeding action will have on neighboring clouds. Selection of the wrong seeding candidates might result in any one or a combination of the following: destructive competition for the available moisture, suppression of other clouds by the induced circulation around the seeded cloud group, and suppression of insolation by the anvil canopy streaming from the top of a seeded complex to the point where there is no cloud generation beneath the anvil. Conversely, it may be possible to minimize all potential disadvantages while still enhancing cloud growth and areal precipitation. Firm guidance is lacking and any area approach, by necessity, is intuitively based upon the facts presently in hand.

For dynamic seeding there is general agreement on the type of cloud to be seeded, the method of delivery of the nucleant, the importance of seeding only in updrafts at the warmest possible temperature at which the nucleant is effective and, most importantly, delivery of the nucleant into the cloud at the right spot at the right time to be effective. As stated in section 2.3.1, there is no unanimity on the amount of nucleant that is necessary to produce the desired effect. There are also areas of uncertainty on the optimum multiple cloud seeding procedures and these are illustrated in the two case studies presented here.

Once the experiment has begun, the mapping of seeding strategy takes on increased significance. This requires radar and satellite observations as a supplement to what the scientist sees from his lofty perch in the seeder aircraft. A cardinal rule is to work with and not against natural processes and to take advantage of all opportunities as they present themselves. If a group of clouds takes on linear alignment, it is important that this be recognized and that all seedings be tailored to promote this tendency. Sometimes it is difficult to discern cloud patterning from an aircraft, and photographs from new satellites have assumed great importance in cloud pattern recognition. Examples are presented in photographs from the DAPP satellite taken during 1973 (fig. 15). Examination of the first two panels of figure 15 shows the tendency of convective clouds in Florida to be organized in sea breeze convergence lines. Consequently, a seeding candidate should be chosen in these preferred regions whenever possible. Pielke (1974) shows (fig. 16) that there is general sinking in areas removed from these lines, suggesting that it will be more difficult to promote merger in these areas. With photographic guidance such as this, it is easier to select the right clouds and to avoid those without growth potential.

On some days it is more difficult to map seeding strategy, as shown in figure 15c (6 August 1973). Sea breeze organization is not as strong on this day, but the clouds (marked by arrow) southwest of Lake Okeechobee may have some seeding potential. On very active days, sea breeze organization is even less evident, and synoptic controls take over (fig. 15d). On this day, an active cloud line containing several cumulonimbus masses extends southwest across Florida. An additional complication is the rather obvious strong shearing of the cloud tops. On such days seeding strategy is uncertain, natural rainfall is great, and flight operations are usually cancelled.

5.3.2 Two Examples of Seeding Procedures in FACE

Two nearly ideal days for multiple cloud seeding have been selected to illustrate the seeding procedures used in FACE. Both were days of actual seeding.

14 July 1971 - There were no disturbances in the Florida area and shower development over the peninsula was normal on 14 July 1971. This was nearly an ideal day for seeding. The first showers over the peninsula formed near Ft. Myers at 1530 GMT but dissipated shortly thereafter. The first cumulonimbus formed near the Miami VOR (approximately 25 km northwest of the University of Miami campus) at 1630 GMT. Shower activity elsewhere over the land was virtually nonexistent at this time, although there was a sprinkling of small showers over the Atlantic and in the Florida Keys. Echo motion was from 100° at 10 kt. All development continued over the south part of the peninsula at the intersection of the sea breezes of the west and east coasts, culminating in a cumulonimbus cluster with a maximum top exceeding 50,000 ft (15.2 km) at 1930 GMT. Meanwhile, there were no showers in the target area.

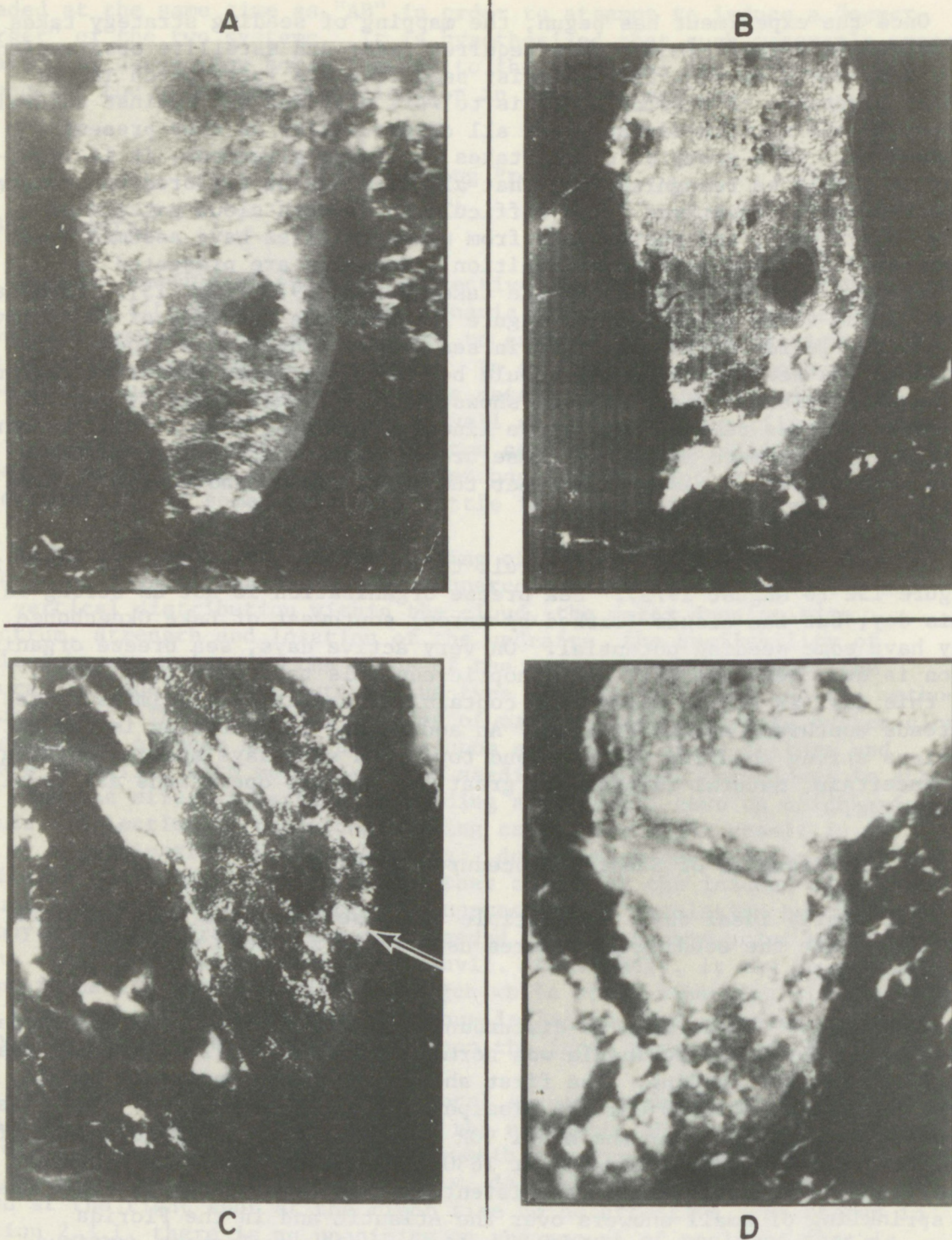
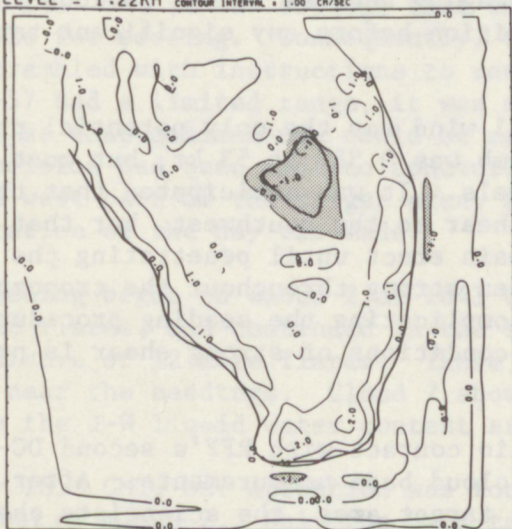
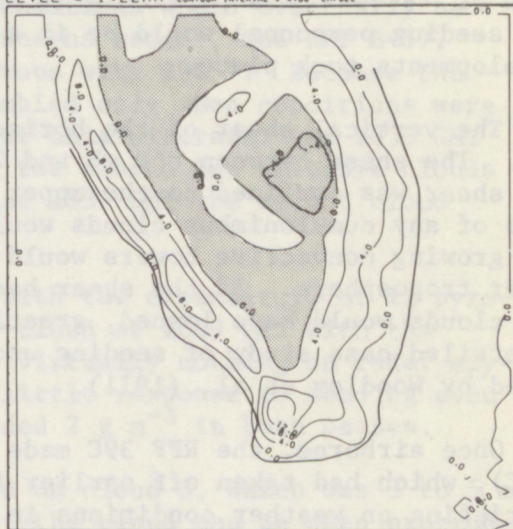


Figure 15. Photographs (1/3 n mi resolution) from the Defense Meteorological Satellite Program. (a) 1807 GMT, 1 July 1973; (b) 1737 GMT, 17 July 1973; (c) 1751 GMT, 6 August 1973; and (d) 1638 GMT, 4 August 1973.

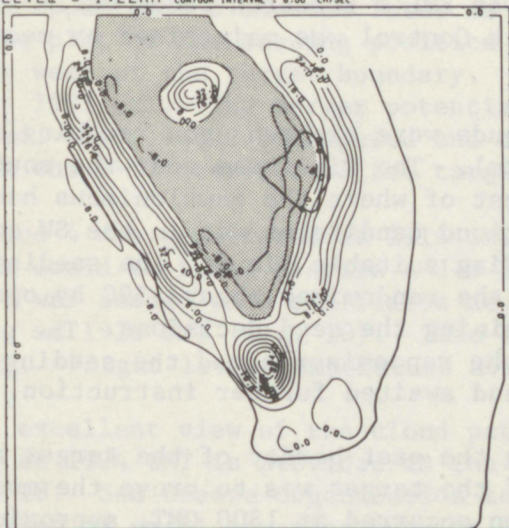
VERTICAL VELOCITY HOUR = 3.01
 USYNOP = 6.0M/SEC ANGLE = 135.
 LEVEL = 1.22KM CONTOUR INTERVAL = 1.00 CM/SEC



VERTICAL VELOCITY HOUR = 5.00
 USYNOP = 6.0M/SEC ANGLE = 135.
 LEVEL = 1.22KM CONTOUR INTERVAL = 4.00 CM/SEC



VERTICAL VELOCITY HOUR = 8.01
 USYNOP = 6.0M/SEC ANGLE = 135.
 LEVEL = 1.22KM CONTOUR INTERVAL = 8.00 CM/SEC



VERTICAL VELOCITY HOUR = 10.00
 USYNOP = 6.0M/SEC ANGLE = 135.
 LEVEL = 1.22KM CONTOUR INTERVAL = 8.00 CM/SEC

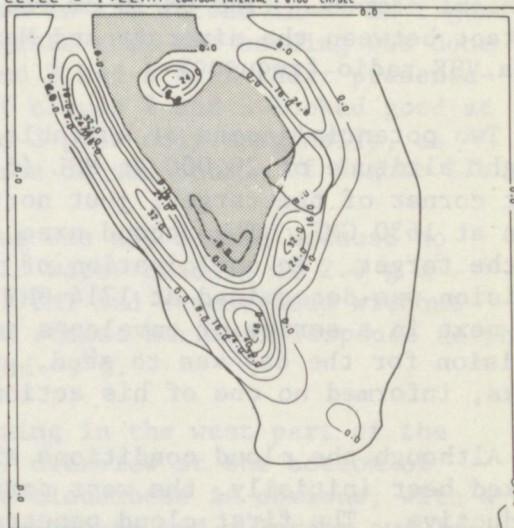


Figure 16. The vertical motion field at 1.22 km for a southeast wind as predicted by the Pielke (1974) sea breeze model after 3, 5, 8, and 10 hours. The stippled areas are regions of sinking motion.

The RFF DC-6 (39C) seeder aircraft took off from Miami International Airport at 1625 GMT with the scientists aboard anticipating a good day. The $S - N_e$ factor was 2.60 satisfying the criterion that $S - N_e \geq 1.50$ for an experimental day. The maximum seedability was 2.60 km, which was obtained by subtracting the maximum predicted top height of the seeded cloud (11.2 km) from the maximum top height (8.6 km) of the same cloud if not seeded. The lack of shower development in the target area at the time of takeoff was particularly encouraging because it was obvious that all seeding personnel would be in a position before any significant target developments took place.

The vertical shear of the horizontal wind was the only potential problem. The shear between 850 mb and 200 mb was 0.58° at 53 kt, but most of the shear was confined to the upper levels. It was anticipated that the tops of any cumulonimbus clouds would shear to the southwest, but that the growing convective towers would remain erect until penetrating the upper troposphere. If the shear had been strong throughout the troposphere, the clouds would have leaned, greatly complicating the seeding procedure. A detailed case study of seeding under conditions of strong shear is provided by Woodley et al. (1971).

Once airborne, the RFF 39C made radio contact with RFF's second DC-6 (40C), which had taken off earlier for cloud base measurements. After a briefing on weather conditions in the target area, the scientists aboard the seeder began to look for suitable clouds. Continual guidance on echo patterning was provided by scientists operating the University of Miami radar (UM/10-cm) that was housed in the Merrick Building on the University of Miami campus. (The UM/10-cm radar was EML's research radar until 1972.) Contact between the aircraft and Merrick Control was maintained by means of a VHF radio frequency.

Two potential areas of suitable clouds were sighted upon reaching a flight altitude of 20,000 ft MSL (6.1 km). The first was near the southeast corner of the target, just northwest of where the cumulonimbus had been at 1630 GMT. The second area of cloud candidates was in the SW corner of the target. In anticipation of finding suitable clouds, the seeding decision was determined at 1714 GMT by the randomizer aboard 39C by opening the next in a series of envelopes containing the seed decisions. The decision for the day was to seed, and the randomizer armed the seeding racks, informed no one of his action, and awaited further instruction.

Although the cloud conditions along the east border of the target area looked best initially, the west part of the target was to prove the most productive. The first cloud penetration occurred at 1800 GMT, approximately 30 n mi north-northeast of the Miami VOR, just east of the target boundary. The maximum in-cloud liquid water content on the Johnson-Williams was 2.2 g m^{-3} but there was no seeding because the cloud was out of the target area.

For the next 40 minutes the scientists aboard 39C waited, as is characteristic for all airborne seeding operations. Several clouds appeared tantalizingly good, but they either collapsed before the aircraft could reach them, or they were out of the area. The lifetimes of the cloud towers were short early in the day, greatly compounding the problem of reaching the clouds at the best time for seeding.

By 1817 GMT it was obvious that the conditions would eventually be suitable for seeding. Consequently, the second seeder, the RFF B-57, was scrambled with instructions to rendezvous with 39C²⁴. Because the RFF B-57 had a limited range, it was scrambled only when conditions were right, so that maximum use could be made of this aircraft. At 1830 GMT the decision had been made to concentrate the search for suitable clouds in the west part of the target area, and at 1837 GMT the second cloud penetration of the day was made.

Seeding began on cloud 2 at 1841 GMT with the expenditure of 11 pyrotechnic flares, and continued in the same cloud at 1849 GMT with the expenditure of 12 more flares. There was virtually nothing on radar anywhere near the seedings. Cloud 2 showed little response to seeding even though the J-W liquid water content exceeded 2 g m^{-3} in both passes.

By 1853 GMT, our attention was focused on cloud 3, which was 3 to 5 mi northwest of cloud 2. Only the hard top of the cloud can be seen protruding above cloud 2 in the inset in the upper left of figure 17. Aircraft heading and camera direction for the picture is as plotted in the radar depiction (on the right). Cloud 3 was seeded with 15 flares at 1853 GMT and its appearance 6 minutes later is shown in the second inset in figure 17. The plot of the seeding position suggests that the seeding was done 2 miles west of the target boundary. Cloud 3 had a weak radar presentation by 1901 GMT. The merger potential of clouds 2 and 3 looked good at the time, but cloud 2 dissipated and cloud 3 grew only marginally, as seen in the B-57 overview of the target area in the bottom of figure 17.

Cloud 4 was penetrated at 1916 GMT, but was not seeded because no updraft could be found despite a J-W liquid water reading of 2.0 g m^{-3} . Cloud 5 was seeded with six flares at 1921 GMT and reentered without seeding at 1928 GMT (fig. 18). This cloud showed marginal response to the seeding. Flight level temperature averaged -9°C .

An excellent view of the cloud patterning in the west part of the target at 1924 GMT is provided in the B-57 overview at the bottom of figure 18. Sea breeze organization to the cloudiness is obvious, with a scattering of small towering cumulus in the center and a larger cumulonimbus about 20 n mi north of Ft. Myers. Out of the picture to the

²⁴A U. S. Air Force B-57 photo-reconnaissance aircraft was already airborne at 16.8 km above the target area on a photographic mission for FACE. Pictures from the aircraft are used in documenting cloud developments in this section of the report.

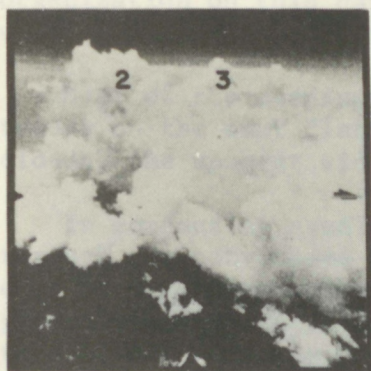
Figures 17 through 24.

*Extended Caption for Radar and Photographic Documentation of Target
Developments on 14 July 1971*

The UM/10-cm radar depictions are for the times shown. Floating target echoes are identified by the solid black MDS contour. The contours correspond to the following approximate rainfall rates: first contour or MDS = trace, second contour = 2.5 mm/hr, third contour = 15.2 mm/hr, and fourth contour = 81.3 mm/hr. Gage and radar comparisons for FACE 1971 suggest that the real rainfall rates for these contours are higher than indicated.

Seeding positions are marked by numbers on the radar depictions. Relevant seeding information for that number can be found in the legend above the radar depiction. Letters on the radar depiction refer to the positions of the aircraft at the times of the inset photographs. The letters on the map correspond to the letters on the photographs. The times and aircraft from which the pictures were taken are as marked. Aircraft heading and camera direction at the time of each photograph are indicated by the long and short arrows, respectively. The photographs from the DC-6 were taken by 35 mm side cameras while the aircraft was flying at 6.1 km. The photographs from the U.S. Air Force Reconnaissance B-57 aircraft were taken from 16.8 km with an F-415P Panoramic Camera System. This camera system is a pulse-operated, high altitude, panoramic daylight camera system capable of providing horizon-to-horizon photographic coverage with 60-percent overlap. Exposure of the film is accomplished by a double dove prism which rotates in front of the camera lens on an axis parallel to the flight direction. At the same time, the unexposed film travels across the focal plane while the automatic exposure control varies the slit opening at the focal plane exposing the film according to terrain brightness. The intervals between exposures can be varied from approximately 30 to 90 sec, depending upon aircraft speed and altitude while the camera operates 1 cycle in 1 sec.

The high altitude photographs have the least distortion at the point in the picture directly below the aircraft, with the distortion increasing to each horizon. For quantitative work, a grid to accommodate the distortion is available. In our work, the photographs are used qualitatively to document cloud developments from a vantage point high above the target area.

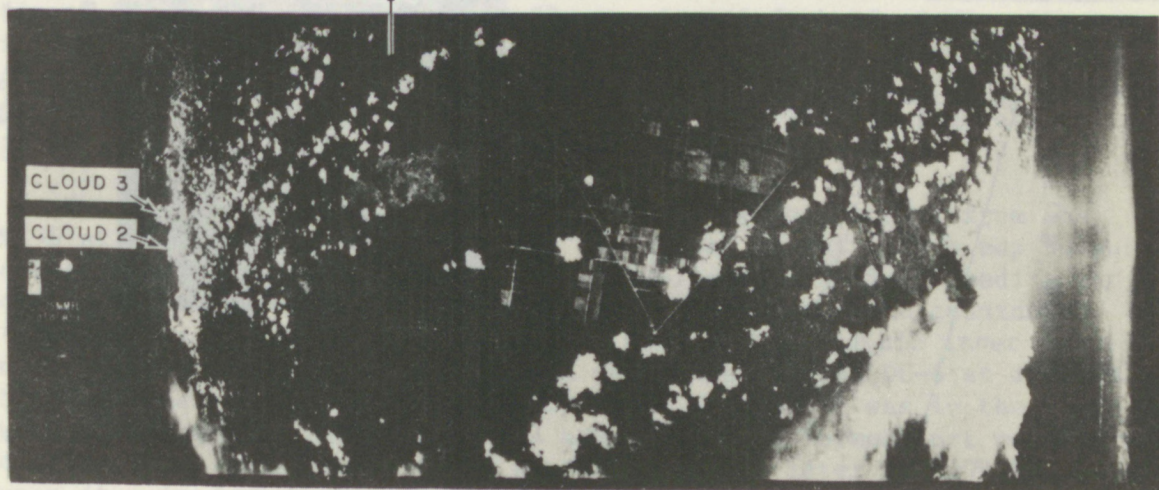
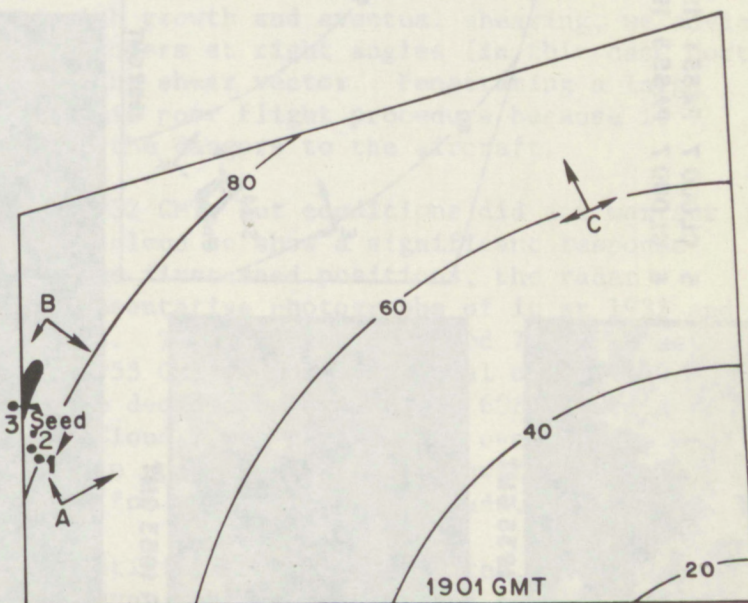


A: 1852 GMT



B: 1859 GMT

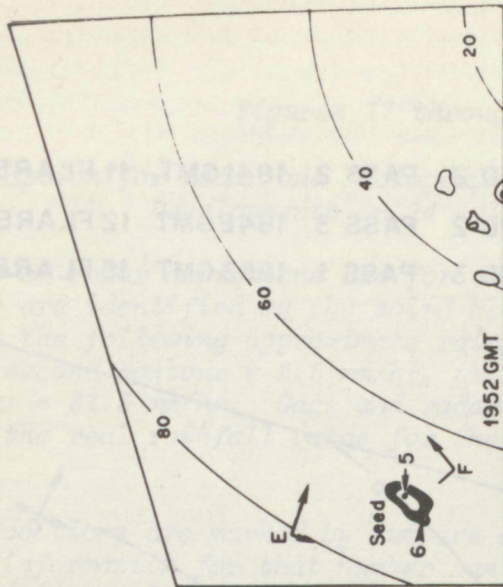
- | | | | | |
|---|---------|--------|---------|-----------|
| 1 | CLOUD 2 | PASS 2 | 1841GMT | 11 FLARES |
| 2 | CLOUD 2 | PASS 3 | 1848GMT | 12 FLARES |
| 3 | CLOUD 3 | PASS 1 | 1853GMT | 15 FLARES |



C: B-57 OVERVIEW AT 1858 GMT

Figure 17. See extended caption, page 62.

5 CLOUD 7 PASS 1 1939 GMT 8 FLARES
6 CLOUD 7 PASS 3 1949 GMT 7 FLARES

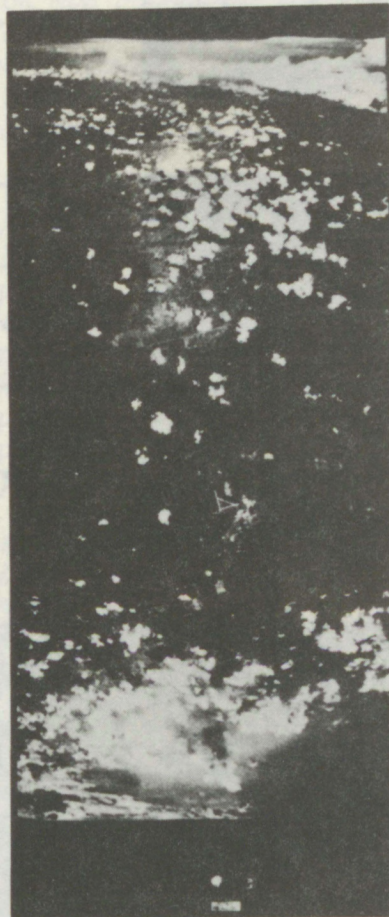
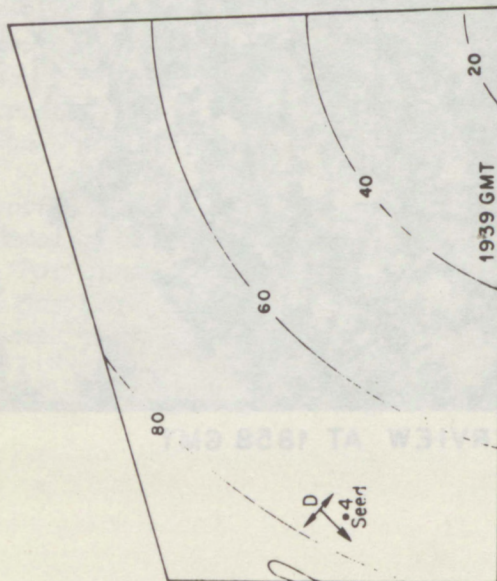


E: 1935 GMT



F: 1953 GMT

4 CLOUD 5 PASS 1 1921 GMT 6 FLARES



D: B-57 OVERVIEW AT 1924 GMT

Figure 18. See extended caption, page 62.

left (south) there was a massive cumulonimbus centered over Everglades National Park. There was certainly nothing random about the cloud organization on this day and it appeared to us at the time that we were working in a favored convective region.

Most of the seedings on 14 July 1971 were done in the new upshear towers on the east flanks of the clouds. Because of the shearing to the clouds, the upshear side is readily found in the photographs.

In conducting seeding operations, we have found that initial traverses through the convective clouds can be made in any direction, as long as the core is penetrated. However, with growth and eventual shearing, we advise penetration of the new upshear towers at right angles (in this case north to south or south to north) to the shear vector. Penetrating a large cloud either upwind or downwind is poor flight procedure because it maximizes the time in cloud and the dangers to the aircraft.

Cloud 6 was penetrated at 1932 GMT, but conditions did not warrant seeding. Cloud 7 was the first cloud to show a significant response following multiple seedings. The first seed positions, the radar depiction at 1952 GMT, and representative photographs of it at 1935 and 1953 GMT, are shown in figure 18. The position of cloud 7 in the sea breeze line is obvious in the 1953 GMT picture. A total of 59 flares had been used. At this point we decided to expend the 60th flare and qualify the day for analysis. Cloud 7 was then turned over to the B-57 for continued seeding in suitable upshear towers. Meanwhile, the scientists in the DC-6 searched for other suitable clouds.

Although there was little activity in the target area, there was considerable cloud development over central Florida and over the southern tip of Florida as shown in the B-57 overview (left half of fig. 19). As is usual for an undisturbed day, Lake Okeechobee was completely devoid of clouds. The relationship of cloud 7 to other clouds in its environment is shown rather well in the second B-57 overview of figure 19. It is in the sea breeze region on the west coast of Florida.

The upper left of figure 20 is a closer view of cloud 7 from the DC-6 at 1959 GMT. It had broadened in lateral extent with a top height exceeding 30,000 ft (9.1 km). The RFF B-57 made its first seeding run of the day on this cloud 2 minutes later. The next cloud candidate (cloud 8) is marked by an arrow in the second photographic inset in the upper left of figure 20. This cloud was seeded by the DC-6 at 2006 GMT. No additional runs were made on this cloud because it was in the north-west corner of the target area. A new small echo formed just northeast of cloud 7 at this time; it was seeded 3 minutes later at 2009 GMT, whereupon it joined with the parent cloud at the MDS. Other seedings of this cloud by the RFF B-57 were made at 2013 and 2023 GMT (lower left and right of fig. 20). Growth in this cloud complex continued, but at a slow rate.



G: 1939 GMT



H: 1953 GMT

Figure 19. See extended caption, page 62.

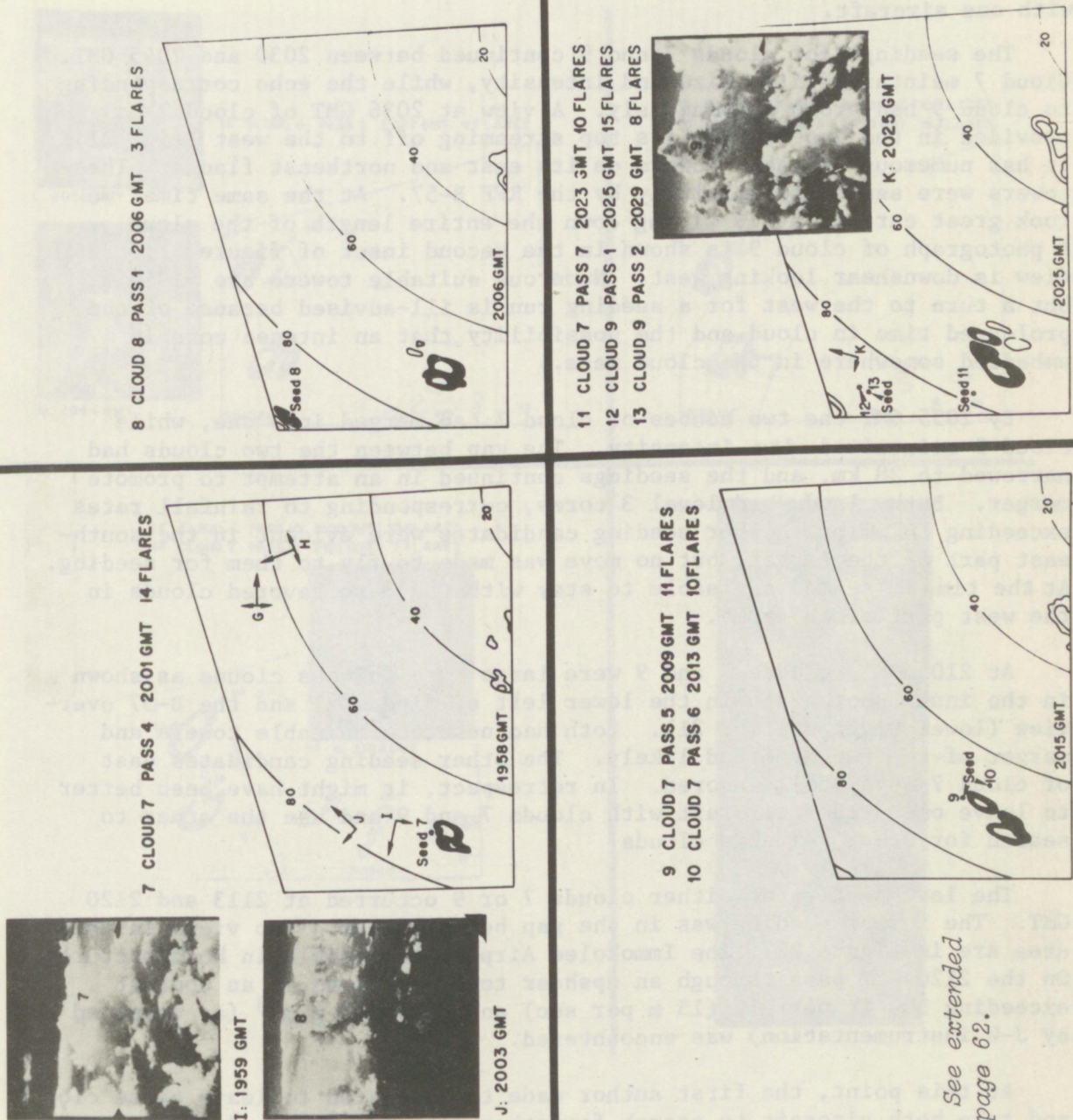


Figure 20. See extended caption, page 62.

By 2025 GMT the scientists aboard the DC-6 had found another seeding candidate (cloud 9) as shown in the inset just before seeding in the lower right of figure 20. It was seeded at 2025 and 2029 GMT although the cloud had no echo presentation. With the exception of clouds 7 and 9 that were being seeded by the B-57 and DC-6, respectively, there were very few other seeding candidates in the area at this time. However, in view of the 46 km separation between clouds 7 and 9, it would have been impossible to seed both effectively with one aircraft.

The seedings for clouds 7 and 9 continued between 2030 and 2045 GMT. Cloud 7 maintained its size and intensity, while the echo corresponding to cloud 9 had grown tremendously. A view at 2036 GMT of cloud 7 is provided in the inset, with its top streaming off to the west (fig. 21). It has numerous suitable towers on its east and northeast flanks. These towers were seeded repetitively by the RFF B-57. At the same time, we took great care to avoid flying down the entire length of the cloud. A photograph of cloud 9 is shown in the second inset of figure 21; the view is downshear looking west. Numerous suitable towers are visible, but a turn to the west for a seeding run is ill-advised because of the prolonged time in cloud and the possibility that an intense core is embedded somewhere in the cloud mass.

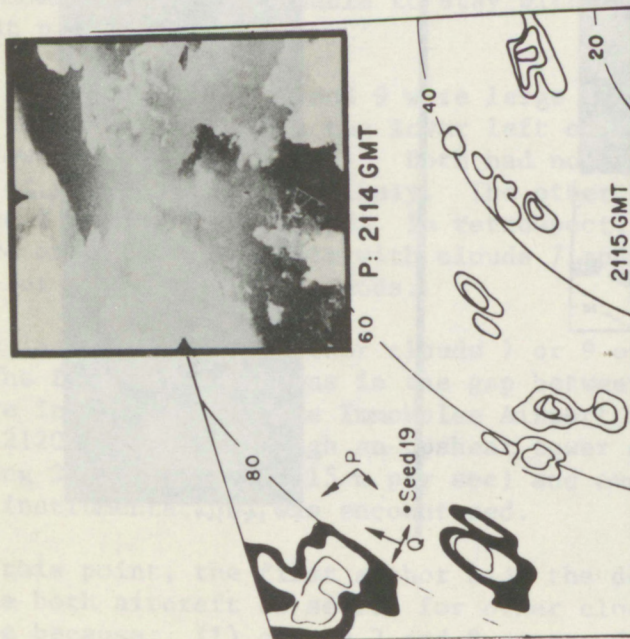
By 2055 GMT the two echoes of cloud 7 had merged into one, while cloud 9 maintained its intensity. The gap between the two clouds had narrowed to 28 km, and the seedings continued in an attempt to promote merger. Both clouds had level 3 cores, corresponding to rainfall rates exceeding 14 mm/hr. Other seeding candidates were evident in the south-east part of the target, but no move was made to fly to them for seeding. At the time it seemed advisable to stay with the more favored clouds in the west part of the area.

At 2105 GMT, clouds 7 and 9 were large cumulonimbus clouds as shown in the inset photograph in the lower left of figure 21 and the B-57 over-view (lower right of fig. 21). Both had numerous suitable towers and merger of the two appeared likely. The other seeding candidates east of cloud 7 were still ignored. In retrospect, it might have been better to leave one seeder aircraft with clouds 7 and 9 and use the other to search for other suitable clouds.

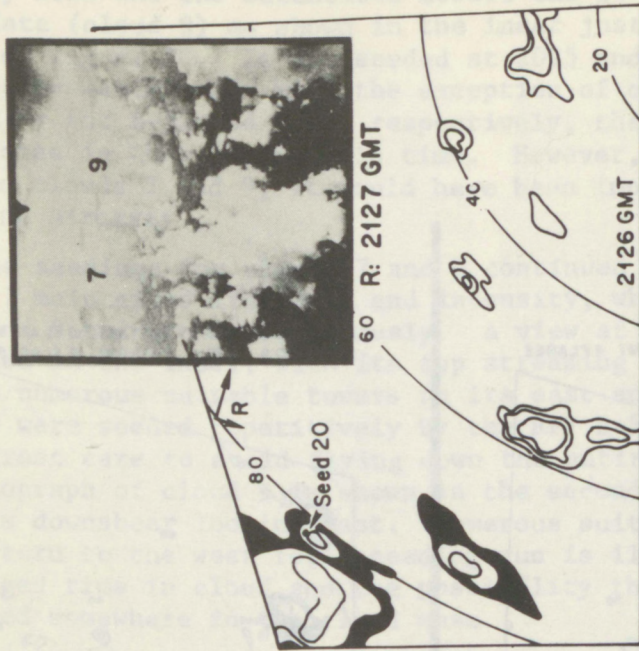
The last seeding of either clouds 7 or 9 occurred at 2113 and 2120 GMT. The former seeding was in the gap between them. Two views in this area are in figure 22. The Immokolee Airport is visible in both pictures. On the 2120 GMT pass through an upshear tower on cloud 9, an updraft exceeding 300 ft per min (15 m per sec) and over 3.0 g m^{-3} (as measured by J-W instrumentation) was encountered.

At this point, the first author made the decision to leave these clouds and take both aircraft to search for other clouds. The decision to leave was made because: (1) clouds 7 and 9 appeared to be destined for eventual merger without further intervention, (2) it appeared that they would leave the area because of their westward drift and, (3) we wanted to expand the floating target by seeding other clouds. In all probability the B-57 would have stayed with clouds 7 and 9 to seed the many vigorous new towers

19 CLOUD 7 PASS 12 2113GMT 7 FLARES



20 CLOUD 9 PASS 6 2120GMT 12 FLARES



Q: 2122 GMT

Figure 22. See extended caption, page 62.

on the two clouds if it had not used 89 of its 104-flare complement. With only 15 flares remaining on this aircraft, it appeared that they might be used more effectively elsewhere.

In the search for other seeding candidates, great care was taken not to contaminate the floating target by seeding mature precipitating systems. In the 2126 GMT radar depiction (fig. 22) a cloud candidate marked by its echo exists southeast of cloud 7. However, it was a mature cumulonimbus at this time, with a top height exceeding 50,000 ft (15.2 km) and it made little sense to claim it for seeding by expending a nominal number of flares in it. Rather, the search was concentrated in the east center of the target. The cloud mass corresponding to clouds 7 and 9 is shown in the inset; cloud 7 is in the center background and the edge of cloud 9 is on the right. The echo of cloud 9 is now massive in the northwest corner of the target area.

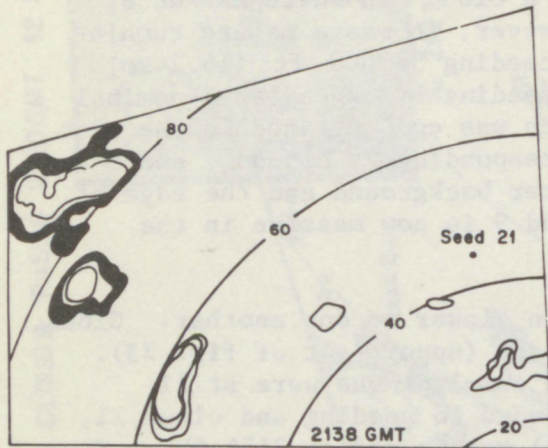
At 2138, clouds 7 and 9 approached even closer to one another. Cloud 10 was seeded at 2142 GMT, but it had no echo (upper left of fig. 23). At 2147, clouds 7 and 9 and the unmodified cumulonimbus were still vigorous entities. Cloud 10 had not responded to seeding and cloud 11, shown in the inset (upper right of fig. 23) was seeded at 2151 GMT. The first echo of cloud 11 appeared at 2152 GMT and it was seeded again at 2202 GMT and 2211 GMT (lower left of fig. 23). It grew in height following seeding, but never exhibited the explosive growth mode. Clouds 7 and 9 had nearly combined at this time and many unmodified echoes formed a broken north-south line east of these clouds.

By 2220 GMT, cloud 11 remained as it was, but clouds 7 and 9 had weakened considerably, while the new echoes southeast of cloud 7 grew and merged (lower right of fig. 23). This trend continued at 2230 GMT and 2240 GMT, and by 2301 GMT all of the seeded echoes had disappeared from the target area (fig. 24). The natural activity continued to grow to the northeast while dying in the southwest portion of the target, and by 0005 GMT on 15 July 1971 (fig. 24) the only echoes were in the extreme northeast corner of the target. All echoes disappeared from the target area at about 0005 GMT.

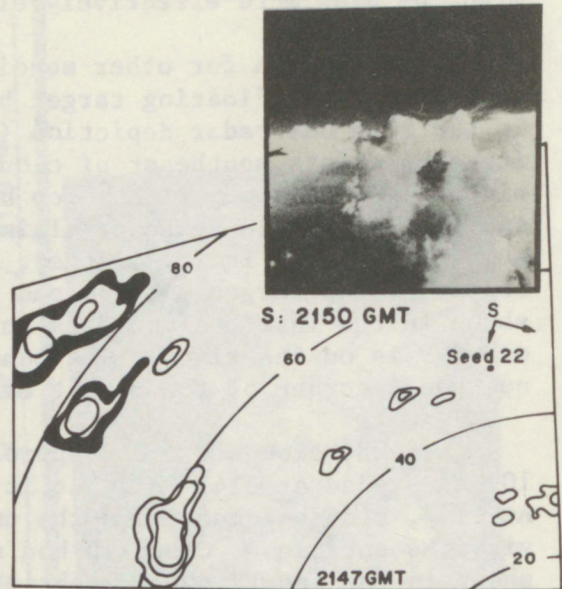
The seeder aircraft left the target area between 2200 and 2300 GMT, the B-57 at 2206 GMT and the DC-6 at 2225 GMT. The first and last seedings of the day were at 1841 GMT and 2211 GMT, respectively. Twenty-four actual seeding passes were made, 14 by the DC-6 and 10 by the B-57. A total of 256 flares were expended, 152 by the DC-6 and 104 by the B-57.

The floating and total target echo areas and volumetric rainfalls in 10-minute intervals for the 6 hours after initial seeding are shown in figure 25. The volumetric rainfalls were converted to area mean cumulative rain depths and they are plotted at the bottom of figure 25. Whenever possible the radar-derived rainfalls have been adjusted by rain-gages as described by Woodley et al. (1975). Seeding times are plotted at the top to serve as an easy reference. Similar plots for all FACE experimental days since 1970 are provided in appendix B.

21 CLOUD 10 PASS 1 2142 GMT 8 FLARES



22 CLOUD 11 PASS 1 2151 GMT 7 FLARES



23 CLOUD 11 PASS 2 2202 GMT 12 FLARES

24 CLOUD 11 PASS 3 2211 GMT 16 FLARES

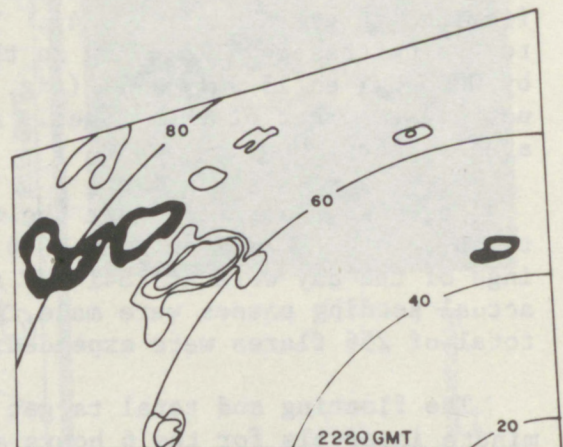
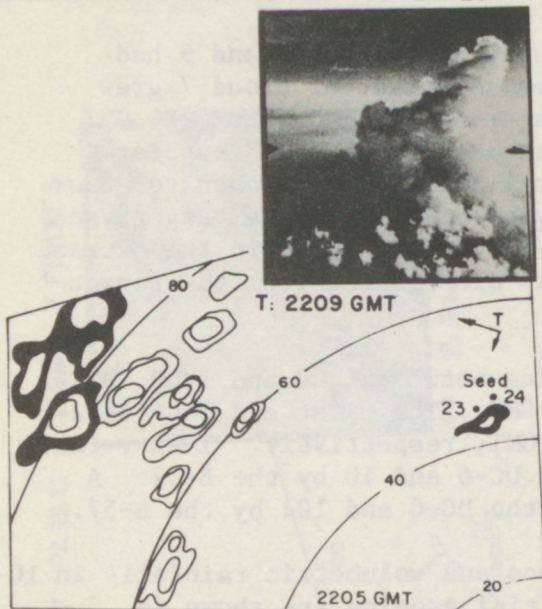


Figure 23. See extended caption, page 62.

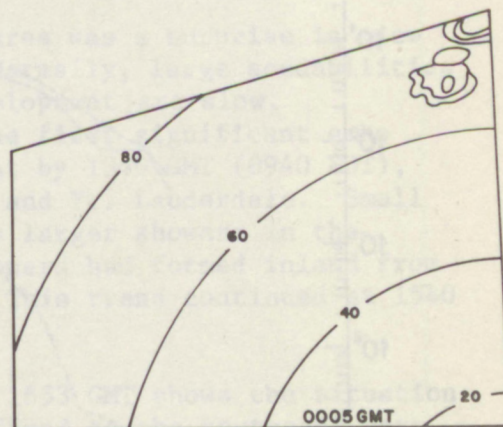
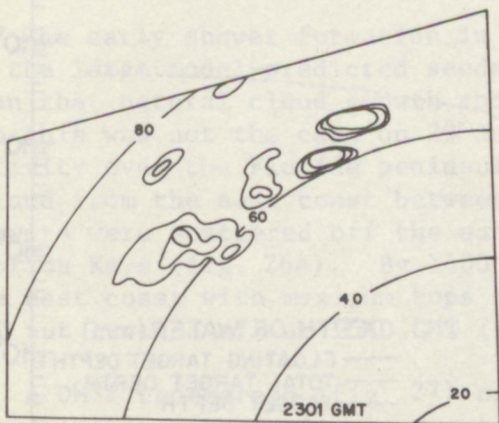
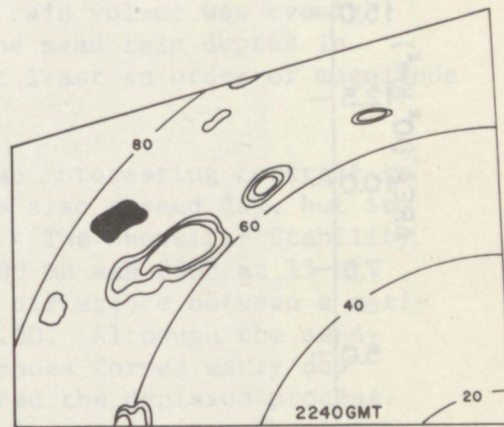
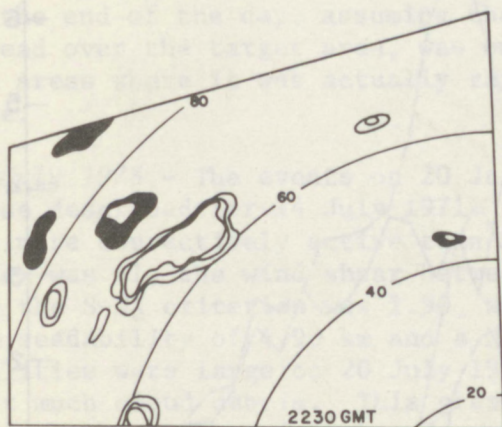
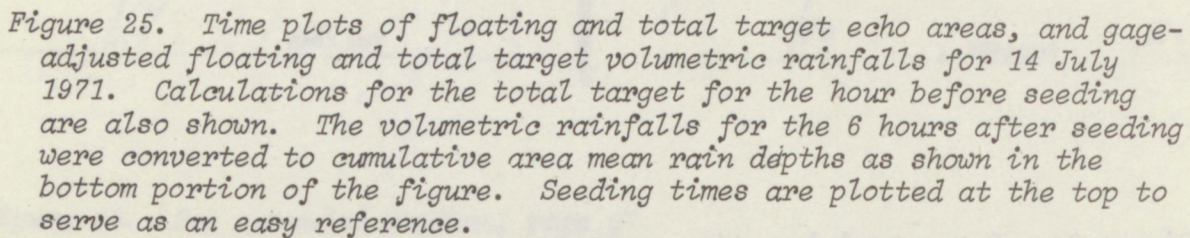


Figure 24. See extended caption, page 62.



The floating and total target echo areas and rainfalls on 14 July 1971 peaked in the middle of the 6-hour evaluation period, and well before the last seeding of the day. The floating target area and rainfall made up a large portion of the total target area and rainfall early in the day, decreasing to insignificance at the time of the last seeding. The maximum floating and total target areas during the period of evaluation were $0.95 \times 10^3 \text{ km}^2$ and $1.7 \times 10^3 \text{ km}^2$, respectively, or only 10 to 15 percent of the overall target area. The mean depth of rain for the target area by the end of the day, assuming that the total rain volume was evenly spread over the target area, was only 5 mm. The mean rain depths in the areas where it was actually raining were at least an order of magnitude more.

20 July 1973 - The events on 20 July 1973 are an interesting contrast to those described for 14 July 1971. This day was also a seed day, but it was more convectively active than 14 July 1971. The Showalter Stability Index was +1, the wind shear between 850 and 200 mb was 030° at 13 kt, and the $S-N_e$ criterion was 1.90, which was the difference between a maximum seedability of 4.90 km and a N_e value of 3.00. Although the seedabilities were large on 20 July 1973, target echoes formed early and left much cloud debris. This greatly complicated the decision process. After much deliberation, this day was qualified for analysis. The lone seeder (RFF C-130) took off at 1655 GMT and returned to base at 2355 GMT after making 29 cloud penetrations through 10 cloud complexes with the expenditure of 232 flares. The first seeding was at 1913 GMT and the last at 2317 GMT. Target developments are treated here.

The early shower formation in the target area was a surprise in view of the large model-predicted seedabilities. Normally, large seedabilities mean that natural cloud growth and shower development are slow, but this was not the case on 20 July 1973. The first significant echo activity over the Florida peninsula was present by 1340 GMT (0940 EDT), inland from the east coast between Palm Beach and Ft. Lauderdale. Small showers were scattered off the east coast with larger showers in the Florida Keys (fig. 26a). By 1400 GMT more showers had formed inland from the east coast with maximum tops near 12 km. This trend continued at 1540 GMT but leveled off at 1640 GMT (fig. 26).

A DMSP photograph (fig. 27) of Florida at 1653 GMT shows the situation very clearly. The main cloud activity is confined to the southeast part of the peninsula with evidence of dual convergence lines in the area southeast of Lake Okeechobee. The most active cloud area is between Lake Okeechobee and the east coast. If we assume that the alinement of small cumuli is an indicator of the low level wind, the flow over the south part of the peninsula was from the southeast, veering to the south over central Florida. Echo motion in the target area was 090° at 10 kt most of the day, but echo propagation was also important.

At 1740 GMT the echo activity over the target had actually decreased, although there were still cumulonimbus masses near the Miami VOR and

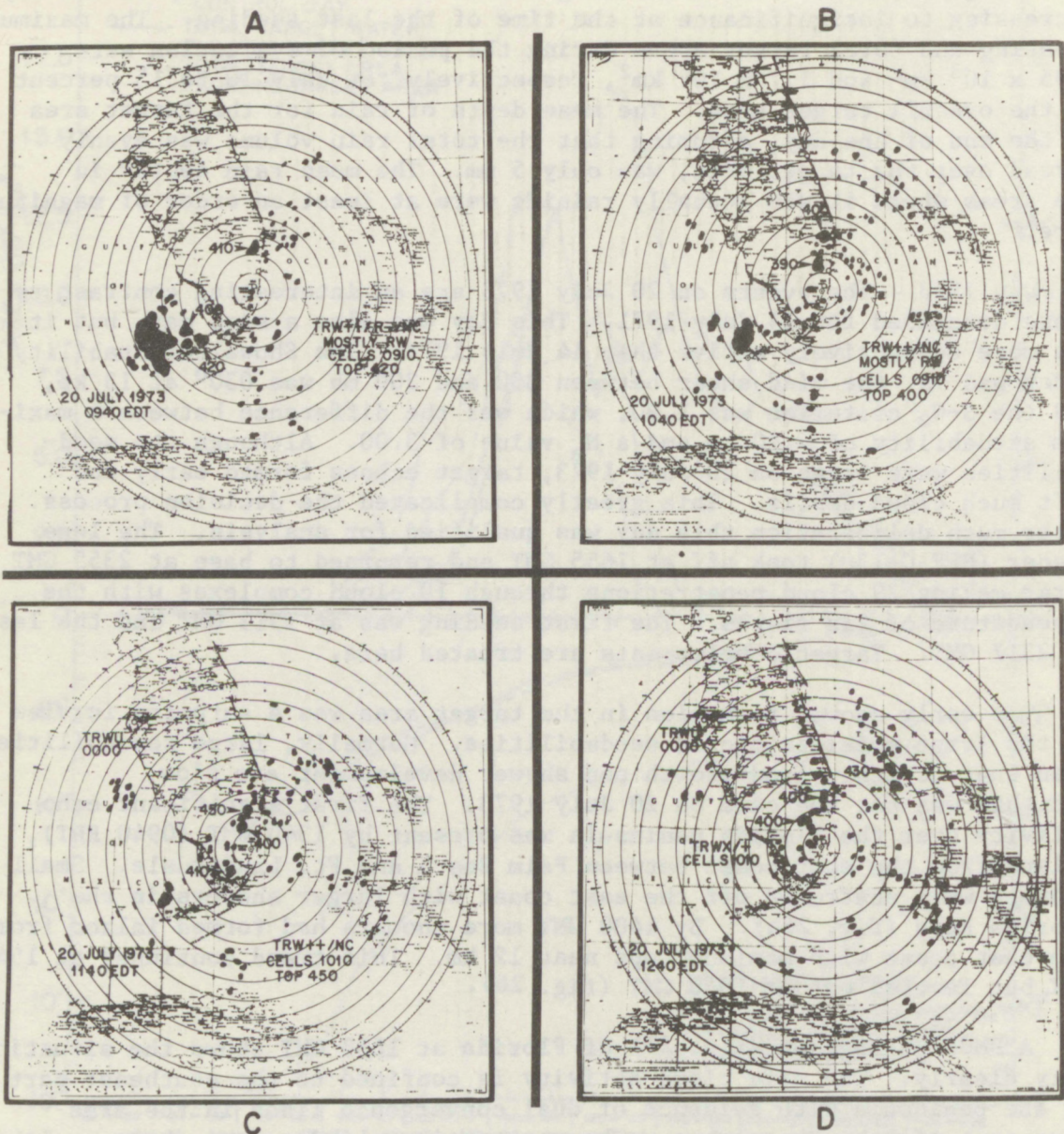


Figure 26. Tracings of the PPI presentation on the scope of the WSR-57 radar of the National Hurricane Center on 20 July 1973 (times as shown). Selected top heights (in hundreds of feet) measured when the radar was operated in the RHI mode are shown on the PPI presentation. Echo intensity, tendency and movement are as indicated in the lower right of each depiction.



20 JULY 1973
1653 GMT

Figure 27. Photograph from the DMSP satellite on 20 July 1973.

northeast of Lake Okeechobee. The latter cloud mass had a maximum top near 14.6 km (48,000 ft). The C-130 seeder had now been airborne for approximately 1 hour and the scientists aboard were momentarily disillusioned by the large, early cloud developments. The cirrus blowoffs from the morning activity were particularly bothersome.

Detailed documentation of target echo developments on 20 July 1973 is provided in figures 28 to 34. This is the same type of presentation as that for 14 July 1971, although the research radar in 1973 was the WSR-57 instead of the UM/10-cm. The rainfall rates for the various contours are as indicated in the extended caption.

At 1823 GMT echo developments were present in the extreme southwest, southeast and northeast portions of the target, but most of the target remained free of showers (upper left of fig. 28). However, old cumulonimbus anvil debris covered much of the target as shown in the inset photograph. This broken upper level cloud layer held down the temperature of the target surface to about 35°C as measured by a downward-looking infrared radiometer aboard the RFF DC-6 that was flying at cloud base. Without cloud cover, 40°C is the usual midafternoon temperature of the target surface. This momentary temperature deficiency beneath the anvils inhibited cumulus development. In addition, the C-130 at 6.1 km (20,000 ft p. alt) was flying in and out of the bases of this cloud debris, further frustrating the project scientists. At the time there was some sentiment for cancelling operations because of these problems. In retrospect it is fortunate that we persevered, because the weather conditions improved considerably during the day.

By 1903 GMT the percentage coverage of the target area had not changed appreciably, but the centers of action were re-arranged (upper right of fig. 28). The echo masses in the southeast and northeast corners of the target had dissipated leaving only anvil debris as shown in the inset photograph. Shower development continued in the southwest corner in an area virtually devoid of upper cloudiness. No seedings were contemplated for this area because of our wish to maintain an uncontaminated floating target, and the seeding of a large natural cumulonimbus complex was not consistent with this philosophy.

The first seeding took place in the center of the target area at 1913 GMT with two other unmodified echo entities in the near vicinity (lower left of fig. 28). Merger of the seeded cloud with its southern neighbor had occurred by 1921 GMT, while the other unmodified echo to the northeast had decreased in intensity (lower right of fig. 28). A picture of the subject cloud mass is provided in the inset. Another view of this cloud, 7 minutes later, is in the inset in the upper left of figure 29. Two cloud towers are still evident even though the echo entity contains

Figures 28 through 33.

*Extended Caption for Radar and Photographic Documentation of
Target Developments on 20 July 1973*

The WSR-57 radar depictions are the for times shown. Floating target echoes are identified by the solid block MDS contour. The contours correspond to the following approximate rainfall rates: first contour or MDS = trace; second contour = 2.5 mm/hr; third contour = 13.7 mm/hr; fourth contour = 30.2 mm/hr; fifth contour = 66.5 mm/hr; sixth contour = 190.8 mm/hr. Comparison of gage and radar volumetric rainfalls for this day (as described by Woodley et al., 1975) suggest that the VIP unit overestimated the rainfall by a factor of 1.67. Consequently, the rainfall rates given above for the contours are probably too high.

The seeding positions are marked by numbers on the radar depictions. Relevant seeding information for a number can be found in the legend above the radar depiction. Letters on the radar depiction refer to the position of the aircraft at the times of the inset photographs. The letters on the map correspond to the letters just below the photographs. The times when the pictures were taken are as marked. Aircraft heading and camera direction at the time of each photograph are indicated by the long and short arrows, respectively. The photographs from the RFF C-130 were taken by 35-mm side cameras while the aircraft was flying at 6.1 km.

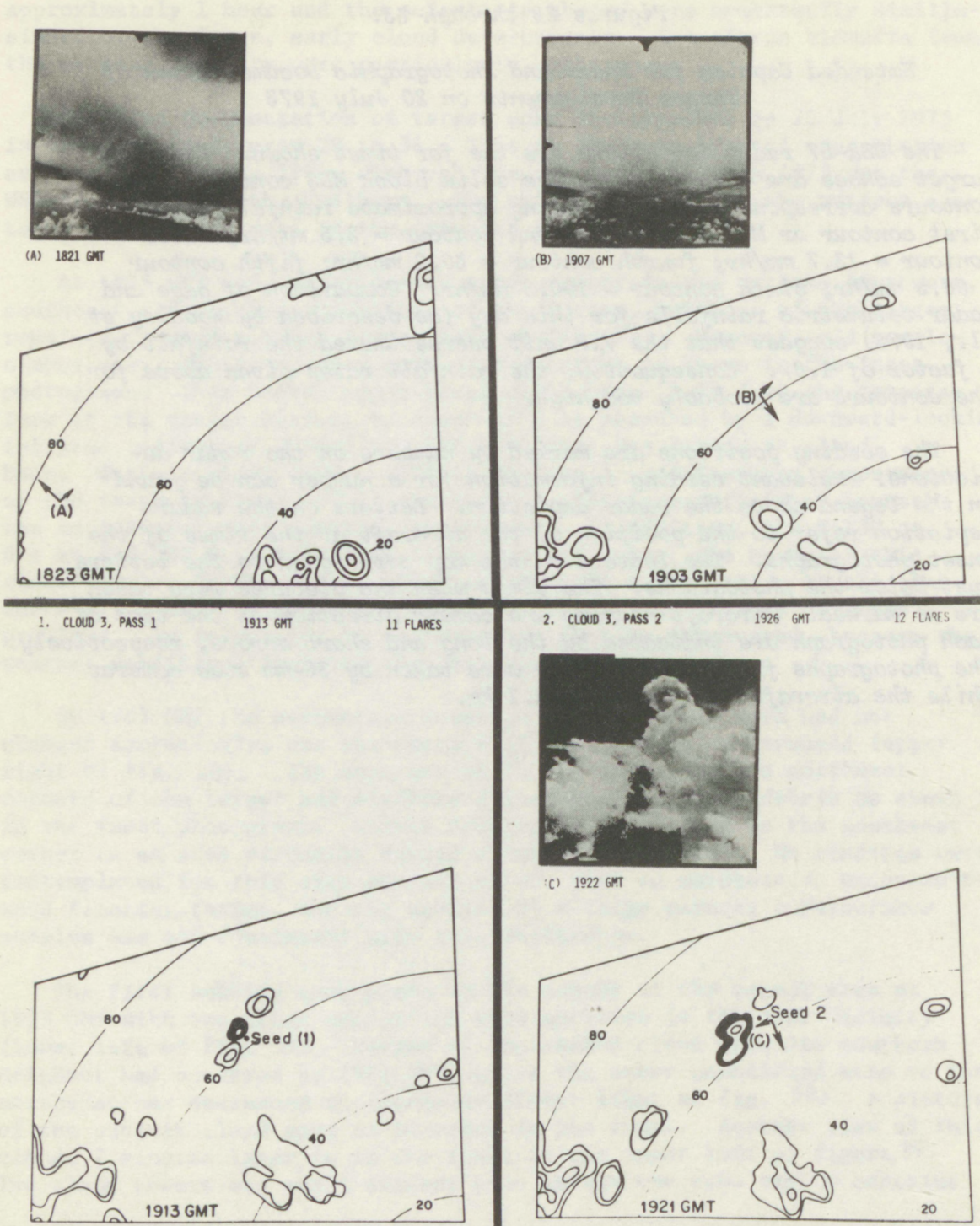


Figure 28. See extended caption, page 79.

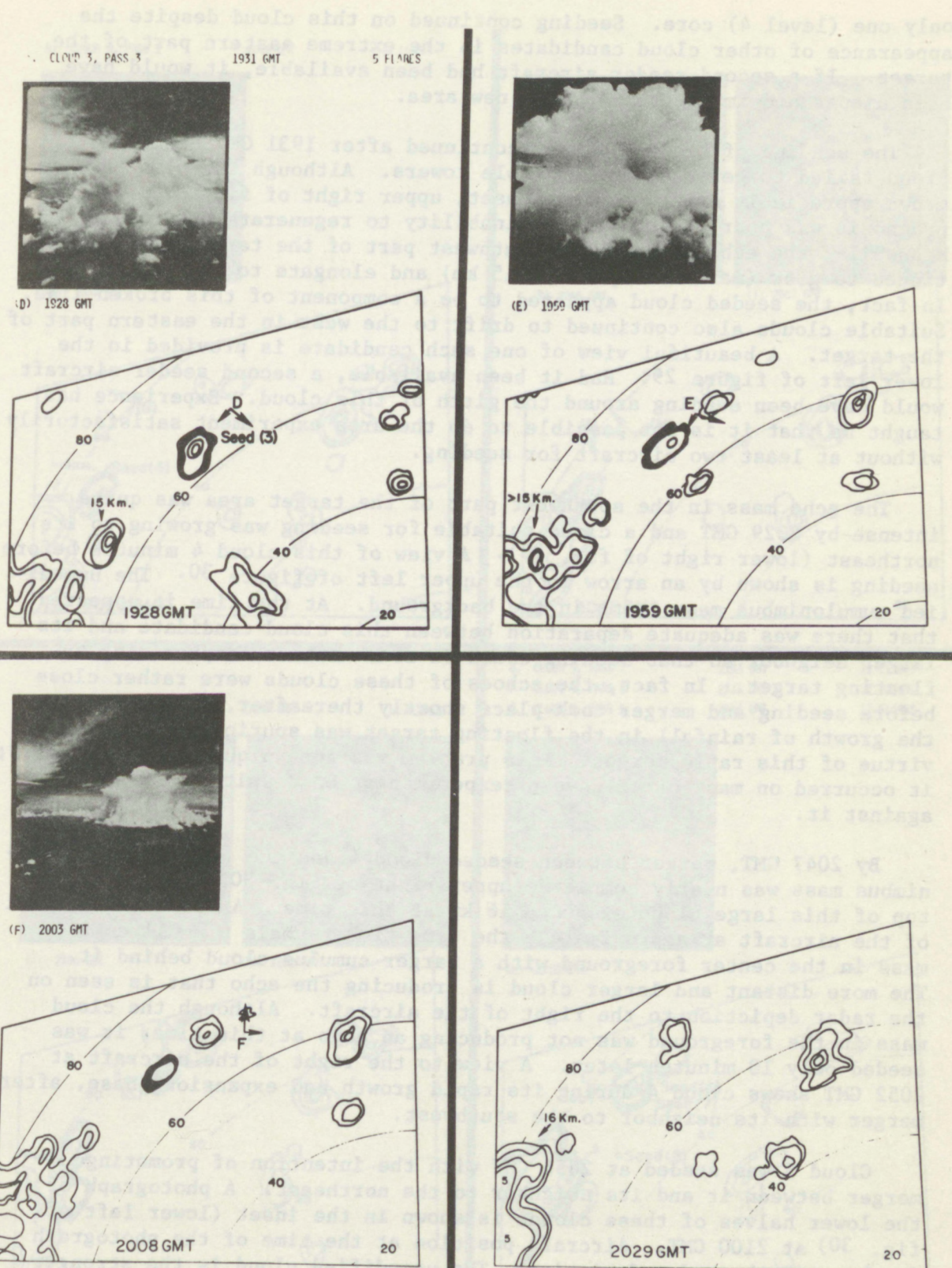


Figure 29. See extended caption, page 79.

only one (level 4) core. Seeding continued on this cloud despite the appearance of other cloud candidates in the extreme eastern part of the target. If a second seeder aircraft had been available, it would have been dispatched immediately to the new area.

The seeding of cloud 3 was discontinued after 1931 GMT because the cloud failed to generate new suitable towers. Although the cloud had grown appreciably after seeding (inset, upper right of fig. 29). its prognosis was poor because of its inability to regenerate new towers. Meanwhile, the echo mass in the southwest part of the target area continued to grow (maximum top above 15 km) and elongate to the northeast. In fact, the seeded cloud appeared to be a component of this broken line. Suitable clouds also continued to drift to the west in the eastern part of the target. A beautiful view of one such candidate is provided in the lower left of figure 29. Had it been available, a second seeder aircraft would have been seeding around the girth of this cloud. Experience has taught us that it is not possible to do the area experiment satisfactorily without at least two aircraft for seeding.

The echo mass in the southwest part of the target area was quite intense by 2029 GMT and a cloud suitable for seeding was growing to its northeast (lower right of fig. 29). A view of this cloud 4 minutes before seeding is shown by an arrow in the upper left of figure 30. The unmodified cumulonimbus mass looms in the background. At the time it appeared that there was adequate separation between this cloud candidate and its larger neighbor so that seeding could be done without compromising the floating target. In fact, the echoes of these clouds were rather close before seeding and merger took place shortly thereafter. Consequently, the growth of rainfall in the floating target was spuriously large by virtue of this rapid merger. This problem was not unique to 20 July 1973; it occurred on many other days of experimentation despite precautions against it.

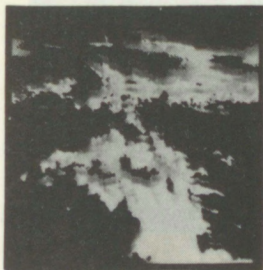
By 2047 GMT, merger between seeded cloud 4 and the unmodified cumulonimbus mass was nearly complete (upper right of fig. 30). The maximum top of this large cloud exceeded 16 km at this time. A view to the right of the aircraft at approximately the same time reveals a small cumulus mass in the center foreground with a larger cumulus cloud behind it. The more distant and larger cloud is producing the echo that is seen on the radar depiction to the right of the aircraft. Although the cloud mass in the foreground was not producing an echo at this time, it was seeded only 10 minutes later. A view to the right of the aircraft at 2052 GMT shows cloud 4 during its rapid growth and expansion phase, after merger with its neighbor to the southwest.

Cloud 5 was seeded at 2056 GMT with the intention of promoting merger between it and its neighbor to the northeast. A photograph of the lower halves of these clouds is shown in the inset (lower left of fig. 30) at 2100 GMT. Aircraft position at the time of the photograph is shown in the radar depiction. The unmodified cloud is the stronger

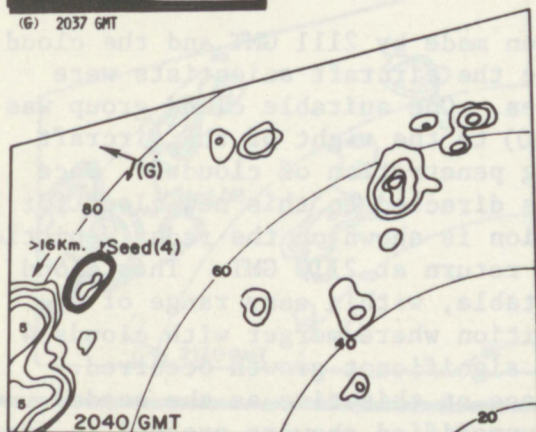
4. CLOUD 4, PASS 1

2042 GMT

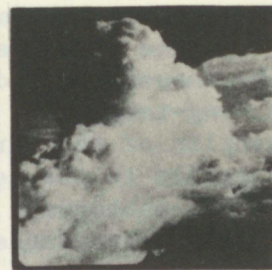
11 FLARES



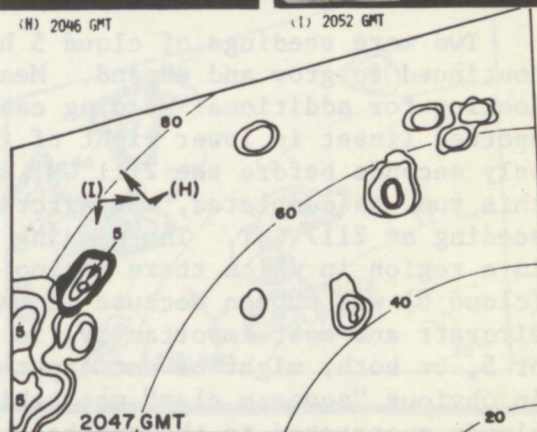
(G) 2037 GMT



(H) 2046 GMT



(I) 2052 GMT



5. CLOUD 5, PASS 1

2056 GMT

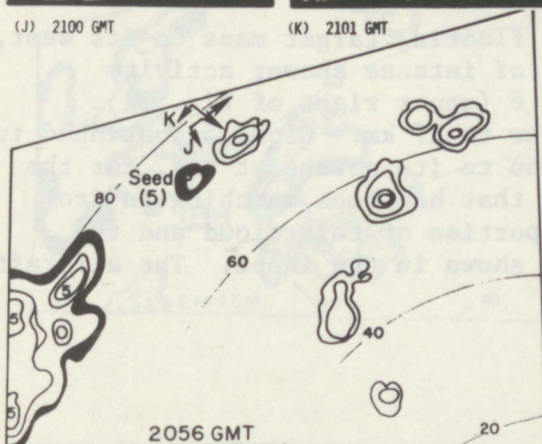
14 FLARES



(J) 2100 GMT



(K) 2101 GMT



6. CLOUD 5, PASS 2

2103 GMT

12 FLARES

7. CLOUD 5, PASS 3

2111 GMT

7 FLARES

8. CLOUD 6, PASS 1

2117 GMT

17 FLARES



(L) 2110 GMT

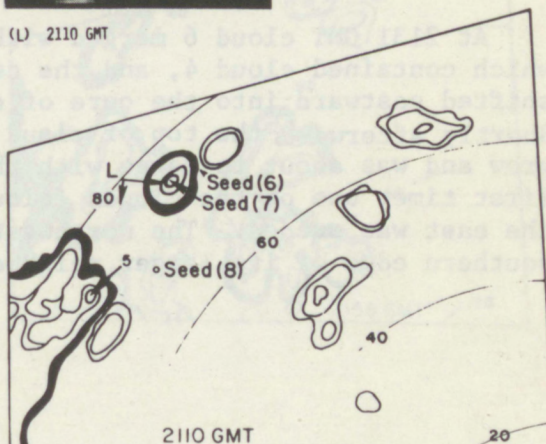


Figure 30. See extended caption, page 79.

on radar, but visually the seeded cloud showed greater promise by virtue of the many new suitable towers that were growing on its upshear or north flank. At the time, we planned to fly northeast to southwest tracks (and vice versa) and seed the upshear towers on both clouds. However, the unseeded cloud collapsed before this plan could be implemented. A long-range look at the portion of the floating target in the southwest section of the target area is in the second inset. The tendency for propagation to the nearest, despite echo motion to the west, is obvious in the photograph as well as in the radar depiction. There were numerous seeding candidates in the target area at this time.

Two more seedings of cloud 5 had been made by 2111 GMT and the cloud continued to grow and expand. Meanwhile the aircraft scientists were looking for additional seeding candidates. One suitable cloud group was spotted (inset in lower right of fig. 30) to the right of the aircraft only seconds before the 2111 GMT seeding penetration of cloud 5. Once this run was completed, the aircraft was directed to this new cloud for seeding at 2117 GMT. The seeding position is shown on the radar depiction in a region in which there was no radar return at 2110 GMT. This cloud (cloud 6) was chosen because it was suitable, within easy range of the aircraft and most importantly, in a position where merger with clouds 4 or 5, or both, might be anticipated, if significant growth occurred. An obvious "squeeze play" was taking place at this time as the seeded clouds propagated to the northeast and unmodified showers pressed in from the east. With a second seeder aircraft to work the clouds in the east, we would have had the situation rather well in hand.

Cloud 6 grew rapidly after seeding as shown in the upper left of figure 31. A view of the hard growing towers on the north side of the echo mass is shown in the inset. This cloud was seeded a second time in this area at 2123 GMT. A view of cloud 5 under its anvil, looking upshear, is in the second inset. At this point the mergers of clouds 4, 5 and 6 appeared to be a possibility. The pinching from the east continued with the unmodified echoes pressing ever closer to the seeded clouds, a situation that is tailor-made for seeding operations. Unfortunately, the seeder aircraft could not be everywhere at once.

At 2131 GMT cloud 6 merged with the floating target mass to its west, which contained cloud 4, and the center of intense shower activity shifted eastward into the core of cloud 6 (upper right of fig. 31). Shortly afterward, the top of cloud 6 grew to 17 km. Cloud 5 continued to grow and was about to merge with the echo to its northeast and, for the first time, one of the clouds (cloud 7) that had been marching in from the east was seeded. The northwestern portion of this cloud and the southern edge of its larger neighbor is shown in the inset. The aircraft

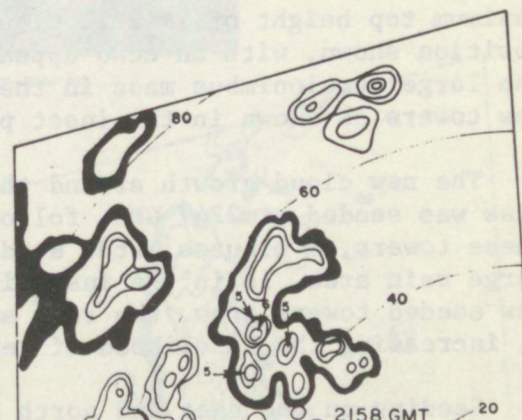
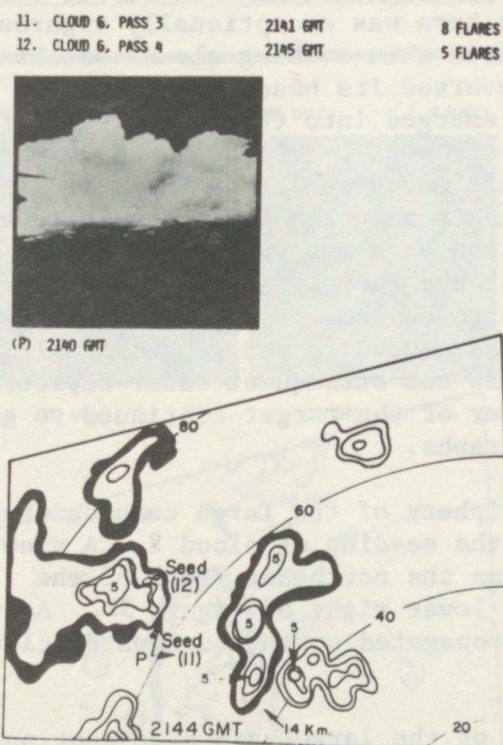
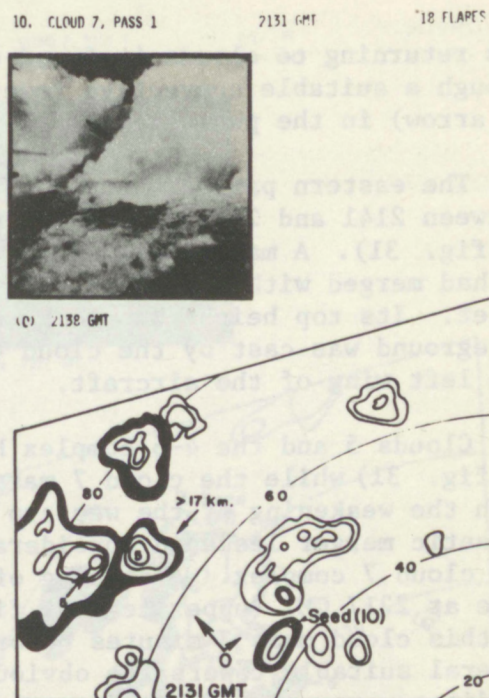
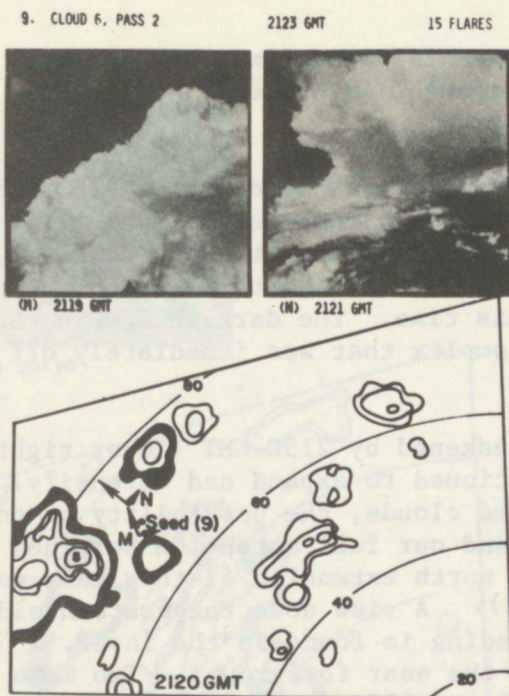


Figure 31. See extended caption, page 79.

was returning to clouds 4, 5 and 6 when this picture was taken, even though a suitable convective tower on cloud 7 is evident (marked by an arrow) in the photograph.

The eastern part of the cloud 4-6 complex was seeded two more times between 2141 and 2145 GMT as the pincer action continued (lower left of fig. 31). A magnificent view of cloud 7 in bright sunlight after it had merged with its unmodified neighbor to the north is shown in the inset. Its top height was 14 km at this time. The dark shadow in the foreground was cast by the cloud 4-6 complex that was immediately off the left wing of the aircraft.

Clouds 5 and the 4-6 complex had weakened by 2158 GMT (lower right of fig. 31) while the cloud 7 mass continued to expand and intensify. With the weakening of the western seeded clouds, the possibility of one gigantic merger lessened considerably and our full attention switched to the cloud 7 complex. A seeding of the north extension of this mass was made at 2217 GMT (upper left of fig. 32). A view down the western side of this cloud mass 3 minutes before seeding is found in the inset. Several suitable towers are obvious in the near foreground. Two more seedings were made in this area at 2222 and 2229 GMT in the region marked by an arrow in the inset photograph (upper right of fig. 32). The north-west portion of this cloud mass as seen here was exceptionally vigorous at this time. Caution should be exercised when working clouds of this type. In this instance the aircraft reversed its heading, penetrated the hard growing tower for seeding and emerged into the clear region to its northeast without encountering the stronger core behind and to the right of the growing tower. The aircraft moved away from the main cloud mass by 2233 GMT (lower left of fig. 32) in a search for suitable towers to its north and northeast. The intention here was to promote cloud growth in the north-center of the target and thereby increase the potential of merger with the main cloud mass to the south, which now had a maximum top height of 17 km. Cloud 8 was seeded in the geographical position shown, with an echo appearing in the subsequent radar depiction. The large cumulonimbus mass in the center of the target continued to grow new towers as shown in the inset photographs.

The new cloud growth around the periphery of the large cumulonimbus mass was seeded at 2247 GMT, following the seeding of cloud 8. A view of these towers, 9 minutes after seeding, on the northeast flank of the large rain area, is in the inset in the lower right of figure 32. As the new seeded towers grew, the rain area propagated northward towards cloud 8, increasing the likelihood of merger.

Seeding on the east and north flank of the large rain area continued between 2300 and 2305 GMT with two seedings of cloud 9 (upper left of fig. 33). Cloud 8 weakened, but new towers grew to its west, setting the stage for a seeding of cloud 10 in this area at 2316 GMT (upper right of fig. 33). The C-130 seeder aircraft terminated seeding operations after this seeding and headed for home.

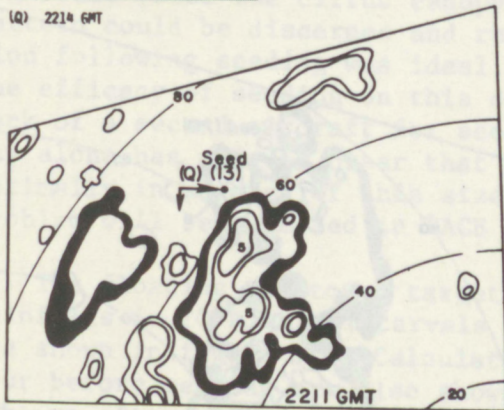
13. CLOUD 7, PASS 2

2217 GMT

10 FLARES



(Q) 2214 GMT



14. CLOUD 7, PASS 3

2222 GMT

25 FLARES

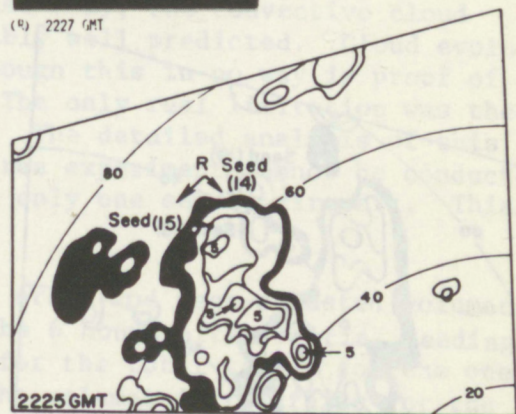
15. CLOUD 7, PASS 4

2224 GMT

16 FLARES



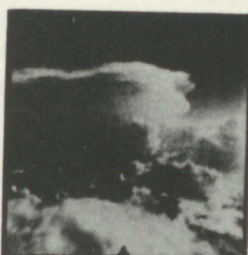
(R) 2227 GMT



16. CLOUD 8, PASS 1

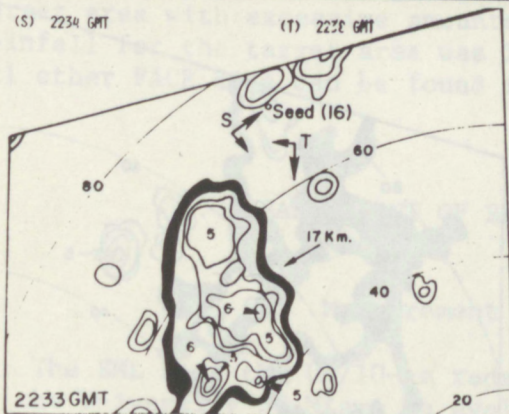
2235 GMT

7 FLARES



(S) 2234 GMT

(T) 2236 GMT



17. CLOUD 7, PASS 6

2247 GMT

10 FLARES



(U) 2256 GMT

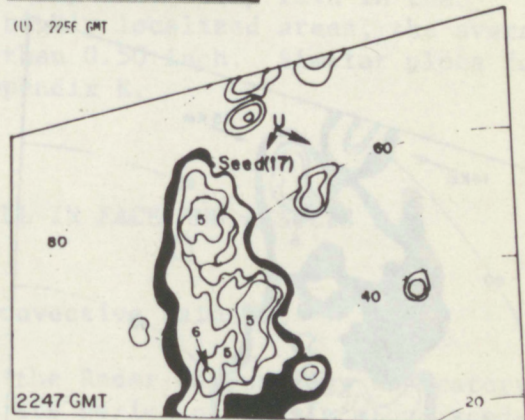
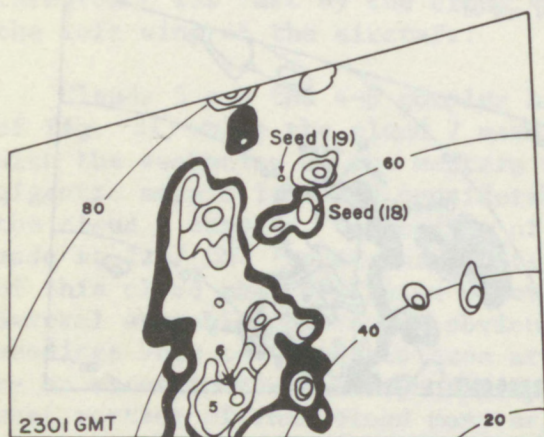


Figure 32. See extended caption, page 79.

18. CLOUD 9, PASS 1
19. CLOUD 9, PASS 2

2301 GMT
2308 GMT

12 FLARES
8 FLARES



20. CLOUD 10, PASS 1

2316 GMT

3 FLARES

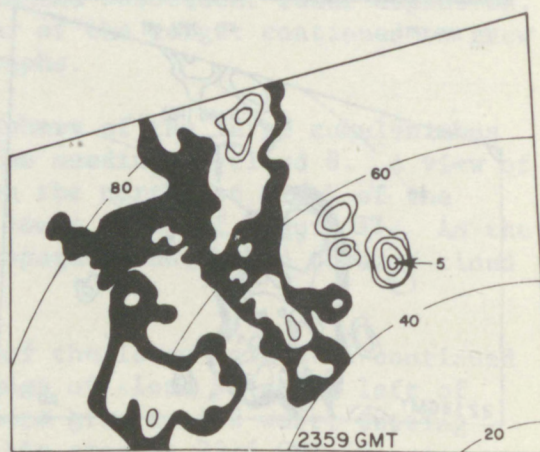
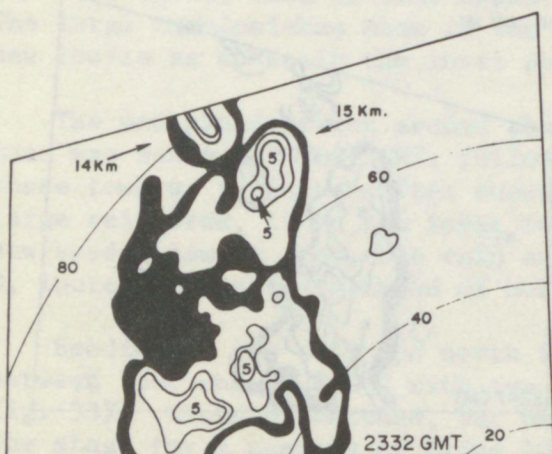
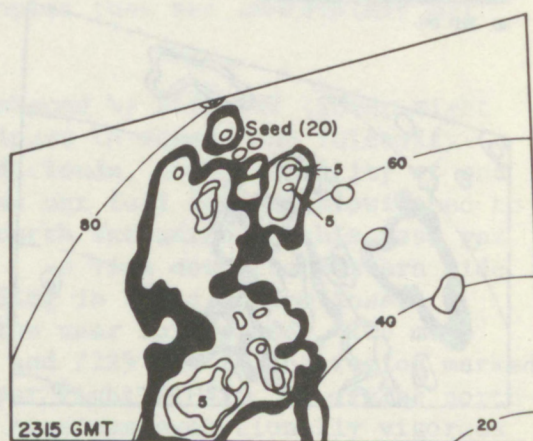


Figure 33. See extended caption, page 79.

A merger of clouds 7, 9 and 10 had occurred by 2332 GMT (lower left of fig. 33). Just before merger, the top height of clouds 9 and 10 were 14 km and 15 km, respectively. By 2359, the rain area had weakened considerably. This downward trend continued to the end of the 6-hr period of rain calculation. False echo due to anomalous propagation became a problem by 0030 GMT (21 July 1973). Fortunately, most of the rain in the target area had ended by this time.

The 20th of July 1973 was an ideal day for seeding despite its poor beginnings. The seedability was large and the towers were long-lived and vigorous. Once the cirrus canopy burned away, the convective cloud pattern could be discerned and reasonably well predicted. Cloud evolution following seeding was ideal, although this in no way is proof of the efficacy of seeding on this day. The only real limitation was the lack of a second aircraft for seeding. The detailed analysis of this day alone has made it clear that the area experiment cannot be conducted optimally in an area of this size with only one seeder aircraft. This problem will be remedied in FACE 1975.

The floating and total target echo areas and gage-adjusted volumetric rainfalls in 10-minute intervals for the 6 hours after initial seeding are shown in figure 34. Calculations for the total target for the one hour before seeding are also shown. The volumetric rainfalls for the 6 hours after seeding were converted to area mean cumulative rain depths and they are plotted at the bottom of figure 34. Seeding times are plotted at the top to serve as an easy reference.

The floating target area and rainfall did not show significant growth until 90 minutes after the initial seeding, but by 120 minutes after seeding the floating and total target rainfalls were virtually equal. The floating and total target rainfalls reached double peaks at 210 and 280 minutes after initial seeding, or 20 and 90 minutes after the final seeding, respectively. The area mean rainfalls for the floating and total targets were near 30 mm, but the area average for the target area was near 10 mm. Even though this was a day with heavy rain in the target area with excessive amounts in highly localized areas, the average rainfall for the target area was less than 0.50 inch. Similar plots for all other FACE days can be found in appendix E.

6. MEASUREMENT OF RAINFALL IN FACE AND RESULTS

6.1 Measurement of Convective Rainfall

The EML used the UM/10-cm radar of the Radar Meteorology Laboratory of the University of Miami to evaluate its series of single cloud seeding experiments between 1968 and 1971. The UM/10-cm and WSR-57 radars of the National Hurricane Center (NHC) were used concurrently in 1972, and

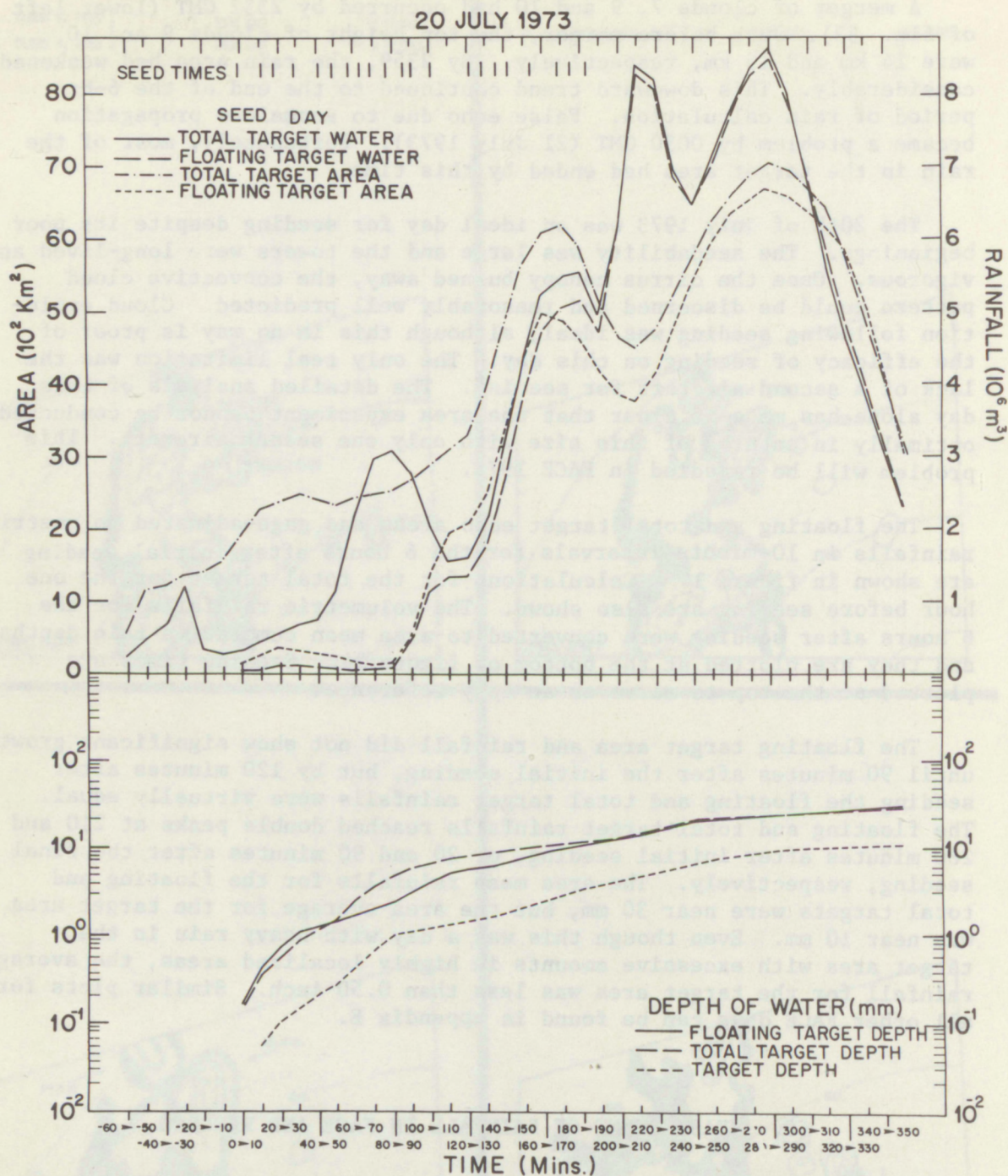


Figure 34. Time plots of floating and total target echo areas and gage-adjusted floating and total target volumetric rainfalls for 20 July 1973. Calculations for the total target for the hour before seeding are also shown. The volumetric rainfalls for the 6 hours after seeding were converted to cumulative area mean rain depths as shown in the bottom portion of the figure. Seeding times are plotted at the top to serve as an easy reference.

by 1973 EML's primary research radar was the NHC WSR-57. The EML chose radar for the evaluation of its single cloud seeding experiments because gage measurement of rainfall from individual clouds (base echo areas generally 250 km²) could not have been accomplished without a totally unacceptable expenditure of money and logistic effort. Further, seed and control clouds were obtained on each day of experimentation so, despite radar inaccuracies, intraday relative differences (seed versus control) should still have been valid. With the advent of the area experiment and interday randomization instead of intraday randomization cloud-by-cloud, radar is not as obvious a choice, particularly if the radar exhibits great interday variability. Woodley et al. (1975) treat this problem in detail, concluding that radar is the best tool for the evaluation of rainfall in FACE, provided the radar estimates are adjusted by raingages.

Before 1973, we calculated target rainfall in FACE by manually planimetering scope photographs of the areas within the contours of each radar echo as described by Woodley (1970). In 1973, a conversion was made to computer processing. In 1970, 1971 and for one nonrandom control day in 1972, the UM/10-cm radar (Senn and Courtright, 1971) of the University of Miami's Rosenthal School of Marine and Atmospheric Sciences made the reflectivity measurements that were used for rain calculation. For 3 nonrandom control days in 1972, and for all days of experimentation in 1973, the WSR-57 radar (Rockney, 1958) of NOAA's National Hurricane Center was used for rain calculation. Both radars are capable of the iso-echo contouring that is necessary for manual rain calculation; the UM/10-cm uses a four-level device (Senn and Andrews, 1968) and the WSR-57 is equipped with a six-level video integrator and processor (Shreeve, 1969).

The rain estimates by radar in FACE-70 were not adjusted by raingages and those in FACE 1971 were adjusted uniformly by a factor of 1.75 based on gage and radar comparisons. In 1972 and 1973, the radar rain estimates were adjusted using raingage clusters, and the resulting values are certainly more accurate than those of earlier years. Based on the analysis of Woodley et al. (1975), it is likely that the calculations from the first two years (1970 and 1971) of area experimentation are accurate to within a factor of 2. However, one or two undetected outliers may exist in this data sample.

Because of intra-agency cooperation in 1973, the EML was able to use the NHC WSR-57 radar for its research without compromising the operational requirements of the NHC. Although the basic radar remained the same as in 1972, the radar output was digitally quantized and tape recorded. This major step was made possible by the cooperation of NHC in conjunction with the collaborative expertise of scientists, from the National Severe Storms Laboratory (NSSL), Norman Oklahoma, the Radar Meteorology Laboratory of the University of Miami, and the EML. Sirmans and Doviak (1973) provide a comprehensive theoretical analysis of the integration and processing techniques necessary to

digitize and record the power returned to the WSR-57 radar. Wiggert and Ostlund (1975) provide specific details on the EML-NHC digitized radar system, including a description of hardware and a description and listing of the software programs for reading and processing the taped data. Calibration of the radar and digitizer are also treated.

The combined radar and digitizer system provides range-normalized average power (in dBm) in each bin. These observations are the data source of the programs designed to process the radar observation to meet specific needs within EML. For the first time since beginning their studies in Florida, scientists in EML could now make their radar-rain calculations more quickly and efficiently by processing digitized radar observations on a computer.

Before we changed to a system of computer processing the radar observations, we had to test the manual and computer methods of rain calculation for comparability. Even though both methods of rain calculation rely on the same radar, the two need not agree because both the VIP and the digitizer must undergo their own calibrations. The method of rain calculation is another potential source of disagreement. If any systematic differences should be evident upon comparison, it would then be possible to make an adjustment so that the rain results generated manually before 1973 are comparable to those generated by computer in 1973 and in subsequent years.

Target rainfalls calculated by two methods of radar-rain estimation were compared for each day of multiple cloud seeding in FACE the manual method of obtaining radar estimates of rainfall, the radar scope photographs were projected on a map of the target, and the contoured echoes were traced at about 10-minute intervals. The echo contour areas were measured with a planimeter, plotted versus time, and integrated. Water volume was obtained by multiplication of each integrated area-time value by a mean rainfall rate and an appropriate constant, and then by summation. Contour rainfall rates were derived from the Miami Z-R relationship:

$$Z = 300 R^{1.4} \quad (5)$$

that has been used throughout the EML experiments (Woodley, 1970). The mean rainfall rate between any two successive contours is one-half the sum of the contour values.

There are many procedural differences between the manual and computer methods of rain calculation, but in principle the techniques are similar. Wiggert and Ostlund (1975) describe the computer processing of the taped radar output to obtain rainfall. When the taped radar data are unpacked, the digitizer response in each bin is converted to power with the transfer curve from the digitizer calibration run. Range normalization to correct for decreased power density with range is done at this time. These range-normalized average powers in bins 2° by $1/2$ n mi are then used with

the KART and RSUM programs to compute rainfall in areas of interest. KART takes the average power per bin, converts it to rainfall rate using the radar equation with appropriate constants and the Miami Z-R relationship. KART then interpolates the bin rainfall rates into a Cartesian grid system of 1 n mi squares, writes a tape, and displays the rainfall rates in 1 n mi squares for each scan. The RSUM program uses the tape created by KART and calculates the total rain depth and volume in the target area for selected periods within the day.

Target rainfall results that have been calculated by means of the two methods are presented in table 4 and figure 35. In the former are tabulations of the target rainfall in the hour before seeding, and floating and total target rainfalls in the 6 hours after seeding. In the latter are plots of total target rainfalls in the 6 hours after initial seeding as generated by the VIP and the digitizer. Because the computer calculations of floating target (FT) rainfall were not made, floating target rainfall was generated artificially by forming the ratio of floating target to total target rainfall derived from the film and multiplying the total rainfall (TT) from the digitizer by this ratio:

$$(FT)_{\text{dig}} = TT_{\text{dig}} \left(\frac{FT}{TT} \right)_{\text{film}}$$

Table 4. Unadjusted Radar-Rainfall Calculations (Units in $m^3 \times 10^7$)

Date	Rainfall from digitizer and computer			Rainfall from VIP with planimeter		
	-1 Hr	Floating target	Total target	-1 Hr	Floating target	Total target
June 26	0.053	2.40	4.21	0.004	3.09	5.42
July 7	0.068	1.62	2.87	0.002	2.00	3.55
July 9	* 0.175	3.26	6.05	* 0.068	3.43	5.52
July 16	0.810	4.32	9.40	0.670	4.55	9.90
July 17	0.709	2.39	5.49	0.831	2.45	5.63
July 20	0.264	8.36	10.58	0.456	13.27	16.79
July 25	0.107	1.06	1.81	0.063	1.50	2.57
July 26	0.336	2.23	4.66	0.370	3.61	7.53
Aug. 6	0.051	3.21	6.71	0.028	2.20	4.60
Aug. 9	Unreliable because of AP			0.109	5.05	6.68
Aug. 11	0.139	3.14	3.81	0.076	1.77	2.15
Aug. 14	0.120	13.97	19.59	0.076	9.31	13.06
Aug. 22	0.037	2.74	3.52	0.025	1.39	1.82
Aug. 25	0.858	3.94	6.17	0.499	3.00	4.71
Aug. 26	0.317	2.31	6.32	0.280	1.50	4.09
Aug. 27	0.179	0.43	0.95	0.119	0.31	0.70
Aug. 28	0.131	0.37	1.31	0.094	0.25	0.92
Sept. 9	* 0.048	0.15	0.46	* 0.003	0.13	0.40
Sept. 10	A.P. Unreliable			0.140	1.02	1.48

*Floating and total target rainfall values for 4 hours.

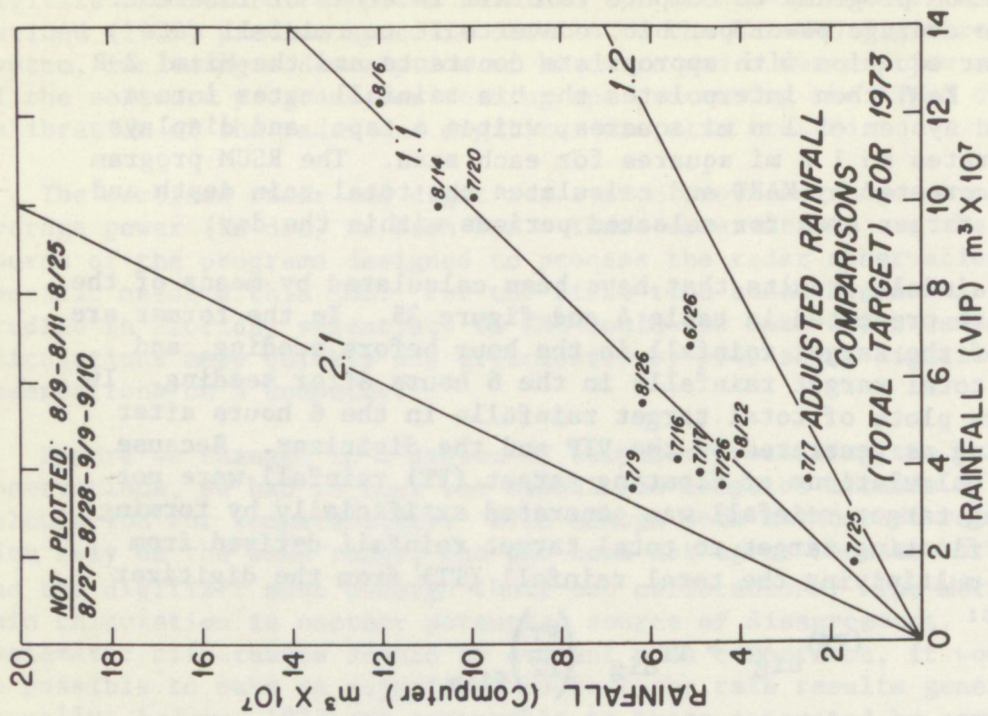
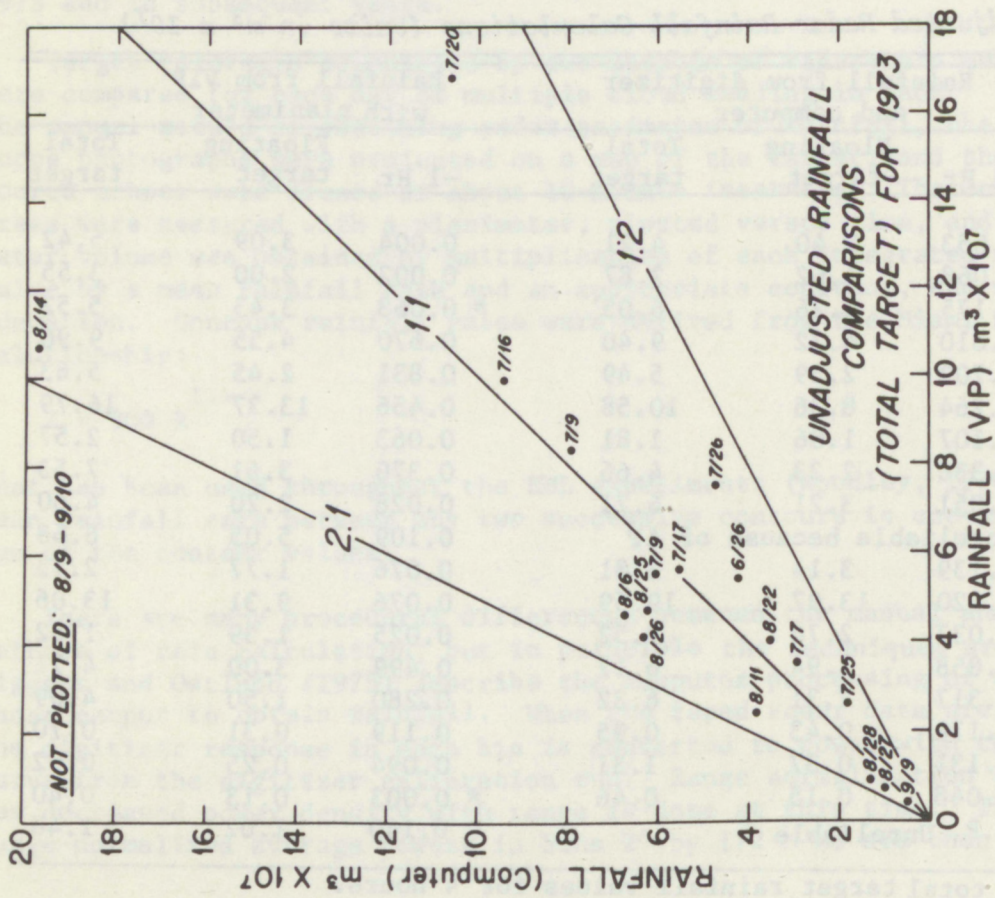


Figure 35. Comparison between rainfall as calculated by computer (on ordinate) and as calculated manually using filmed observations from the Video Integrator and Processing (VIP) unit (on abscissa). On the left are the unadjusted rainfall calculations; on the right are the calculations after having been adjusted by rainages. The month and day in 1973 are indicated near each plotted point.

In FACE-75, the floating target rainfall from the digitizer will be obtained from a computer program called TRACK or from a modification of the RSUM program.

Anomalous propagation (AP) resulting in false echo or ground clutter was a distinct problem for the computer calculation of rainfall. Although a trained individual can distinguish between real echo and ground clutter in most instances, this recognition cannot be programmed into a computer as yet. Consequently, rain estimation could not be accomplished on 9 August and 10 September 1974 because of persistent ground clutter. AP also wreaked havoc in the last 2 hours of the 6 hours of calculation on 9 July and 9 September 1973. On these days, the two methods of rain calculation were compared for only 4 hours after the initial seeding. AP was certainly a problem for brief periods on other days but no adjustments to the computer calculations have been made.

Despite problems with AP, there is reasonable agreement between the computer and planimeter calculations of total target rainfall. All comparisons are within a factor of 2, although there are two disturbing outliers (20 July and 14 August). The correlation between the two methods of calculation is 0.83. No systematic bias of one method with respect to the other is evident, suggesting that if one corrects for AP, the rain results generated by computer are comparable to those generated by hand in past years. Because of this, no adjustment to the rain calculations from past years appears warranted.

The outliers are a problem with no ready explanation. On 14 August, the computer calculation of rainfall exceeded that derived with the planimeter by nearly a factor of 2 and AP is not the cause of the discrepancy. On 20 July, the situation is reversed and the manual rain estimate exceeds that from the digitizer by a factor of 1.6. This is still unexplained. On both days, only one of the two values is the better approximation of the rain that actually fell on that day, but it was impossible to select the more accurate value without additional information. Raingages are the key for resolving this dilemma.

Since 1972, the EML has systematically adjusted its radar estimates of rainfall in the target area based upon the comparison of gage and radar rainfalls in small discrete arrays contained within the target area (Woodley et al, 1975). With this combination of gages and radar, the radar provides the distribution of rainfall within the target area and a first estimate of its magnitude and gages provide for its adjustment. Continuing work with the observations from FACE-73 indicates that this results in the most accurate rain measurements that are possible. A real test of this method is its utility in determining the true value for the outliers discussed above.

All raingage observations from all arrays (fig. 1) were used to adjust the radar estimates of rainfall that were derived manually and by computer (Woodley et al, 1975). One adjustment ratio was obtained for each method for each day and no attempt was made to determine an adjustment within the day as a function of space or time. This daily adjustment ratio was obtained

Table 5. Adjusted Radar-Rainfall Calculations (Units in $m^3 \times 10^7$)

Date	Rainfall from digitizer and computer			Rainfall from VIP with planimeter		
	-1 Hr	Floating target	Total target	-1 Hr	Floating target	Total target
June 26	0.063	2.86	5.01	0.005	3.87	6.78
July 7	0.060	1.42	2.52	0.001	2.10	3.70
July 9	0.162	3.00	5.51	0.042	2.03	3.51
July 16	0.463	2.47	5.37	0.284	1.93	4.20
July 17	0.632	2.13	4.89	0.582	1.72	3.94
July 20	0.247	7.83	9.91	0.276	8.02	10.16
July 25	0.087	0.87	1.49	0.043	1.03	1.76
July 26	0.315	2.09	4.36	0.179	1.73	3.61
Aug. 6	0.091	5.73	11.98	0.075	5.87	12.28
Aug. 9	Unreliable because of AP			0.058	2.67	3.54
Aug. 11	0.087	1.96	2.38	0.076	1.77	2.15
Aug. 14	0.066	7.65	10.74	0.058	7.17	10.06
Aug. 22	0.042	3.08	3.96	0.060	3.29	4.30
Aug. 25	*0.858	3.94	6.17	*0.499	3.00	4.71
Aug. 26	0.311	2.26	6.19	0.370	2.02	5.53
Aug. 27	*0.178	0.43	0.95	*0.119	0.31	0.70
Aug. 28	*0.131	0.37	1.31	*0.094	0.25	0.92
Sept. 9	*0.048	0.15	0.46	*0.003	0.13	0.40
Sept. 10	AP Unreliable			0.140	1.02	1.48

*Not adjusted; same value as in table 4.

by summing the array rain volumes from gages and radar, and then dividing the former by the latter. A daily adjustment ratio was calculated both for the digitizer and for the manual calculations of radar rainfall. Based upon these ratios, an adjustment was made to the total target rainfalls as provided by computer and by hand. Results are presented in table 5 and plotted in figure 35. Five days that appear in figure 35a do not appear in figure 35b because we lacked sufficient gage information to formulate a gage adjustment for these days. Woodley, et al. (1975) indicate that more than gage cluster with rain is necessary for the formulation of a reliable ratio.

The use of gages improves the agreement between the two methods of radar-rain estimation, particularly for the two outliers of 20 July and 14 August (compare the plots in fig. 35a with those in fig. 35b). The correlation between the methods improves from 0.83 to 0.95 after adjustment. The gages suggest that both manual and computer processing resulted in overestimates of the rainfall on 20 July, with the former overestimating more than the latter. On 14 August the gages indicate that the manual method was very nearly correct and that the computer processing resulted in a gross overestimate of the total target rainfall. The radar estimates of rainfall for 6 August were also changed by the gage-radar comparisons.

With adjustment upward, the two methods are brought into better agreement. This day (a random control) is then the wettest day in FACE-73.

The one exception to the general improvement brought about by gage adjustment is 9 July. On this day, rather good agreement (fig. 35) is degraded by adjustment. However, AP was serious problem on this day and the agreement before adjustment may have been fortuitous. If so, adjustment would certainly degrade the agreement between the two methods of radar-rain estimation.

In most cases the unadjusted radar estimates of rainfall are a reasonable estimate of the actual rainfall, and even for the worst outliers they are probably not in error by more than a factor of 2. However, this accuracy is not acceptable for the evaluation of a seeding experiment in which the expected effect of seeding is less than a factor of 2. Adjustment by gages improves radar accuracy, especially so when the radar estimates of rainfall are grossly in error. Such adjustment is necessary if one is to determine the effect of seeding in the shortest possible time.

There is still some disagreement between the results produced by the two methods of radar rain estimation even after adjustment by gages. We were faced with the dilemma of choosing the more accurate of the two values. In instances where there was no additional information to facilitate a choice, the mean of the values provided by the manual and computer methods was chosen as the final rain value. Thus, in most cases, the final rain results presented later represent an average of the adjusted rain values in table 5. With the exception of 9 July, the manual and digitizer-generated rain values do not differ by more than a factor of 1.31, so this is a reasonable compromise. On 9 July, the factor of difference between methods before averaging is 1.84. All floating and total target values in table 5 are for 6 hours after initial seeding. In the two instances (9 July and 9 September) when a computer calculation could not be carried out to 6 hours, the 6-hour digitizer value before averaging is a combination of a 4-hour computer estimate and a 2-hour estimate that was manually calculated from the film. The final rain values on 9 August and 10 September are adjusted planimeter calculations, because AP precluded computer calculation on these days. On 4 days the rainfall in the hour before real or simulated seeding is the adjusted manual calculation, because the computer calculation was either not available or not reliable due to AP. Even with these few manipulations and approximations, it is certain that the final target rain results from FACE-73 are the most accurate that the EML has produced to date.

6.2 Area Rainfall Results From FACE

For all FACE experimentation as of the end of 1973 there were 14 seed days and 23 controls (floating target analysis on 22 of the 23) of which 10 are random and 13 nonrandom. Nonrandom controls were flown in

a light aircraft on days suitable for the experiment on which a seeder aircraft was unavailable. The flights were necessary to ensure that adequate numbers of seedable clouds were present in the target area, to select floating targets, and to simulate flare releases. Results for all days of experimentation are presented in table 6, and means and standard deviations for all experimental periods are presented in table 7.

Day-by-day examination of the results shows that the natural rainfall varies by a factor of 62 in the floating target and 25 in the total target. It is an interesting, but not new, result in table 7 that the standard deviations are comparable to, and in some cases exceed, the mean rainfall values.

For the floating target, the overall seed-control ratio is 1.4, while it is 0.99 for the total target. The seed-control differences in table 7 are not significant by six classical tests, nor is the difference between random and nonrandom controls. A puzzling feature of table 7 is that for floating targets, the nonrandom controls are 16 percent wetter than the random controls. This may be due to unconscious bias on the part of the Project Director (the first author) in leaning over backwards to select wet floating targets on nonrandom control days.

The sample size in FACE is still much too small to determine the effect of seeding. Both Simpson et al. (1973) and Olsen and Woodley (1975) show that at least 50 pairs of cases (seed and control) will be necessary to resolve a seeding effect of 1.5 to 1.7 in total target rainfall. If the seeding factor is less than this, as indicated by our current calculations, more experimental days will be necessary. The situation is much more hopeful for the floating target.

Simpson and Woodley (1975) did a sensitivity test of the FACE rainfall results to the small sample size and "heavy tailed" (produced by a few heavy rain days) rainfall distributions. Several Bayesian approaches were used to estimate a probability distribution of a multiplicative seeding factor, based on gamma rainfall distributions with the same slope parameters for seeded and control populations. Using the data in table 6, the best estimates of the mean multiplicative seeding factors for the floating and total targets were 1.52 and 1.05, respectively. The sensitivity of these results was tested as follows. On 14 August 1973, the only available seeder aircraft was forced to abort. The authors went to great effort to fly a nonrandom control on that day, which proved to be the third wettest in the entire 4-year sample for both floating and total target. If the seeder had flown on that day, and the remainder of the randomized instructions had been executed in order, this could have changed wet 14 August 1973 from a control to a seed day, and dry 28 August 1973 from a seed to control, leaving the remaining instructions unchanged. If the rainfall data were unaltered in the process, the new best estimates of the mean multiplicative seeding factors would become 2.09 and 1.26 for the floating and total targets, respectively. The

Table 6. FACE Rain Results

Date	Action	S-Ne	Echo coverage %	Target rainfall in hr before seeding	Floating target $\times 10^7$	Total target m^3	Cate- gory
1970							
June 29	S	3.00	3	0.208	0.20	3.97	1
June 30	NS	1.10	13	0.468	3.97	8.55	2
July 2	S	5.00	2	0.072	1.37	2.39	2
July 7	NS	3.20	2	0.080	0.96	9.26	2
July 8	S	3.90	4	0.210	12.13	14.64	2
July 17	RC	2.80	2	0.019	-	5.74	2
July 18	S	2.70	~0	0.066	5.61	10.36	2
1971							
June 16	S	2.40	~0	0	0.28	0.31	1
July 1	NS	1.70	2	0.041	0.32	1.94	1
July 12	NS	2.50	1	0.003	0.43	9.27	2
July 13	S	3.40	2	0.001	1.94	3.68	1
July 14	S	2.60	1	0.007	2.05	6.03	1
July 15	NS	2.40	3	0.100	1.18	2.31	1
July 16	RC	3.40	~0	0.034	1.23	8.61	2
1972							
July 21	RC	2.00	~0	0.192	0.12	0.27	1
Aug. 4	RC	1.35	~0	0	0.28	0.32	1
Aug. 9	RC	1.70	~0	0.011	2.64	3.74	1
Aug. 18	RC	1.30	~0	0.096	1.41	3.33	1
1973							
June 26	RC	2.25	1	0.005	3.37	5.90	1
July 7	S	2.00	3	0.001	1.80	3.17	2
July 9	RC	2.60	1	0.101	3.67	6.59	2
July 16	NS	3.30	5	0.374	2.20	4.79	2
July 17	NS	2.60	3	0.607	1.93	4.42	1
July 20	S	1.90	4	0.262	7.93	10.04	1
July 25	S	3.40	2	0.080	0.95	1.63	1
July 26	RC	3.75	2	0.247	1.91	3.99	2
Aug. 6	NS	1.95*	1	0.083	5.80	12.13	2
Aug. 9	NS	1.60	23	0.058	2.67	3.54	1
Aug. 11	RC	3.95	1	0.082	1.87	2.27	1
Aug. 14	RC	2.85	3	0.062	7.41	10.40	2
Aug. 22	S	2.85	~0	0.051	3.19	4.13	1
Aug. 25	S	1.80	3	0.678	3.47	5.45	1
Aug. 26	RC	0.80*	1	0.341	2.14	5.86	1
Aug. 27	S	2.40	2	0.149	0.37	0.83	1
Aug. 28	S	5.05	3	0.113	0.32	1.12	1
Sept. 9	NS	3.55	1	0.026	0.16	0.48	1
Sept. 10	RC	M	M	0.140	1.02	1.48	1

RC = nonrandom control

NS = random control

* = value doubtful

Table 7. FACE Rain Results 1970-1973: Means and Standard Deviations

	n	Floating target		n	Total target	
		\bar{R}	σ		\bar{R}	σ
		(x 10 ⁷ m ³)			(x 10 ⁷ m ³)	
All seed	14	2.97	3.45	14	4.84	4.18
All control	22*	2.11	1.84	23	4.88	3.43
All fair controls**	20*	2.00	1.88	21	4.77	3.49
All random controls	10	1.94	1.78	10	5.67	3.87
All fair random controls**	8	1.62	1.84	8	5.57	4.17
All non-random controls	12*	2.25	1.95	13	4.50	3.07

* There was no floating target on July 17, 1970.

** Fair day defined as 1400 LDT echo coverage <13%.

resultant probability curves would not only be different from those obtained with the real data, but ironically enough, the floating target would be "significant" at the 5 percent level with the Maximum Likelihood and Optimal C(α) tests.

The search for covariates and predictors -- As we have seen in section 2.4.1 the primary obstacle to evaluation of seeding effects in cumulus experiments is enormous natural variability coupled with poor areal rainfall correlations. In addition, the possibility of dynamic contamination may preclude dual target designs, so that ways of coping with natural rain variation (amounting to factors of 50 to 100) in a single target must be found. The only answer to this dilemma is covariates, predictors or data stratification. There are ways to reduce the effects of natural variability by estimates of the rainfall in the seeded target if it had not been seeded, or at least, by stratification to reduce the variability from a factor of 10 or less by a two-way classification. Of course, the reduction in sample size must always be weighed against the variability

decrease when stratification is undertaken. Furthermore, physical understanding of a statistically significant stratification must be sought, optimally in terms of a quantitative model or numerical simulation.

Covariates in an experiment may be derived from models, from physical hypotheses, by systematic trial and error (stepwise regression) or they may arise from intuition, usually based on experience.

Scientists working on the FACE problem have worked hard to find covariates in the area experiment. Many that were useful for single clouds in Florida and/or area experiments elsewhere were tried and failed to provide significant regressions. Examples are rainfall in the area before seeding time, rain upwind of the area, rain surrounding the area, one-dimensional model-predicted seedability or rain production, or both, three-dimensional mesoscale model moisture influx predictions, area echo coverage, and numerous others, singly and in combinations.

Knowledge of the behavior of heated islands (Malkus, 1963) combined with a suggestion that a "heavy-tailed" rain distribution might usefully be treated as two separate distributions, led to a breakthrough in data stratification. Over flat, heated islands, days with strong wind flow generally do not permit the build up of towering clouds and heavy showers; the Pielke Florida model also shows weak vertical moisture fluxes in the EML target with strong winds impinging on the peninsula.

Upon examining the radar echo motions with these concepts in mind, we found that the GO days were readily separable into "marching" and "stationary" days of radar echo behavior. Days could usually be classified using the radar scope tracings and notes thereon provided routinely by the National Weather Service radar observers. The same category (1 for marching and 2 for stationary) was reached by independent analysis on most occasions before 1400 hours local time, or before the time when the first seeding usually occurred. Examination of the radar film itself resolved the few ambiguous cases.

Recently, Simpson and Woodley (1975) demonstrated that the category, as defined, is a significant covariate for FACE rainfall. Although this finding does not give us direct or immediate information regarding the effects of seeding, it has made possible a sharper identification of seeding effects with existing data, and it will be even more useful in the future with expanded data sets.

The category for each day is listed in the last column of table 6. For the rain measurement period, total target rainfall (seed and control combined) in category 2 averaged about 2.5 times that in category 1. The two rain distributions differed at a significance level better than 0.001 with the Mann-Whitney-Wilcoxon test. Mean seeded and control rainfall for all FACE days as a function of category is presented in table 8.

Table 8. Stratification of Cases into Marching (1) and Stationary (2)
Radar Echoes

Comparison of mean rainfalls (x 10 ⁷ m ³)			
Category 1: 10 seed and 13 control			
	\bar{R}_s	\bar{R}_{ns}	\bar{R}_s/\bar{R}_{ns}
A. Floating target	2.07	1.49	1.39
B. Total target	3.72	2.76	1.35
Category 2: 4 seed and 10 control			
A. Floating target	5.23	3.04	1.72
B. Total target	7.64	7.94	0.96

There are, of course, too few cases in each category to draw any conclusions regarding seeding effect, nor are the ratios of seed to no-seed presented as estimators. Nevertheless, table 8 suggests a possibility for further exploration; namely, that the seeding effect might be different on the two types of days. One of the major lessons learned in modification programs is that the effects of seeding commonly differ with the initial conditions of the cloud environment system, and that a vital key to success is the selection of those conditions favorable to the modification hypothesis.

6.3 Results of Single Cloud Analyses in FACE

FACE scientists have pursued any analysis that might clarify the effect of seeding in the area experiment. At the suggestion of Dr. Anthony Olsen, formerly a statistician at EML, we analyzed all individual experimental clouds obtained on FACE days. This was done to determine whether the effect of dynamic seeding on individual clouds as documented by Simpson and Woodley (1971) was persisting in FACE. Of course, exact comparability was not expected because the motivation and experimental procedures were different in the two experiments. In the single cloud experiments of 1968 and 1970, only relatively isolated clouds were selected for experimentation, approximately 1 kgm of silver iodide was expended in each cloud, and the aircraft stayed with each cloud until its demise. In the FACE program, clouds with merger potential were selected, a variable amount of

silver iodide was expended in each cloud, and the seeder aircraft roamed from cloud to cloud with no set pattern. In both experiments the subject clouds could easily be followed on radar.

Analysis procedures for single clouds on all FACE days were the same as those described by Woodley (1970) for the single cloud experiments of 1968 and 1970. In all instances, rain calculations were terminated when the experimental echo merged with a neighbor at the second contour above MDS. This analysis restriction is at odds with the intent of the FACE procedures, which were to promote merger. Nevertheless, it is necessary to insure comparability with the single cloud studies of 1968 and 1970 and to ensure an objective determination of single cloud rainfall.

All FACE single cloud rainfall calculation was done at the Cumulus Group, and statistical calculations are being done in the Cumulus Group and at the University of Virginia. The calculations were done by hand using the contoured video as described by Woodley (1970). Rainfall results by cloud are presented in appendix B. Mean results are presented in tables 9 and 10.

The results for the FACE single clouds that grew and died without ever merging are shown in table 9. Clouds in this category are most comparable to the single clouds of 1968 and 1970. For all years with and without the disturbed days, the mean seed to no-seed ratio of rain volumes is near 2, in excellent agreement with the original single cloud studies that indicated a seeding factor between 2 and 3. Note that this result holds true even for 1973 by itself, even though the FACE area results show no such effect of seeding.

The rainfall results for the FACE single clouds that merged are presented in table 10. Examination of the results for all years reveals a much more diminished effect of seeding. This is puzzling at first until one notices that the mean lifetime of the single clouds before merger was 27 minutes for the seeded clouds and approximately 40 minutes for the controls. Consequently, the apparent seeding effect is smaller for this category because, in the mean, the rainfall analysis of seeded single clouds was terminated 13 minutes earlier than the controls.

The disparity in mean seeded and control cloud lifetimes before merger is an important finding. It has significance at better than the 1 percent level, suggesting a real effect of seeding. The more rapid merger of seeded clouds on seed days is encouraging, since one of the goals of the experiment is to promote merger by seeding. Whether or not more rapid merger of seeded clouds leads to greater rainfall over the target area must still be determined in FACE.

This single cloud analysis with FACE clouds was worth the effort. It demonstrated that dynamic seeding is continuing to produce more rainfall from single clouds and that seeded clouds are merging more rapidly

Table 9. Mean Rainfalls from Single Clouds ($m^3 \times 10^3$) Dissipating Without Merger

Seeded clouds										Unseeded clouds					
Year	n	Lifetime (min)	\bar{R}_V	Random controls			Non-random controls			All controls					
				Lifetime (min)	\bar{R}_V	\bar{R}_{Vs}	Lifetime (min)	\bar{R}_V	\bar{R}_{Vs}	Lifetime (min)	\bar{R}_V	\bar{R}_{Vs}			
1970	18	34.4	403.8	9	43.1	296.6	1.36	0		9	43.1	296.6			
without 6/30	18		403.8	5	36.4	56.4	7.16	0		5	36.4	56.4			
1971	15	35.9	202.9	16	35.9	182.5	1.11	3	31.7	117.3	1.73	19	35.2	172.2	
1972	0			0				18	42.0	128.3		18	42.0	128.3	
1973	26	43.6	475.8	21	40.9	148.7	3.20	20	26.0	275.6	1.73	41	33.6	220.7	
w/o 8/9	26	43.6	475.8	21	40.9	148.7	3.20	20	26.0	275.6	1.73	41	33.6	220.7	
all	59	38.9	384.5	46	39.6	189.4	2.03	41	33.4	199.3	1.93	87	36.7	194.1	
years	59	38.9	384.5	42	38.4	150.6	2.55	41	33.4	199.3	1.93	83	35.9	179.7	
w/o dist. days															

Table 10. Mean Rainfalls from Single Clouds ($m^3 \times 10^3$) Merging Clouds

Seeded clouds										Control clouds							
Year	\bar{n}	Lifetime (min)	\bar{R}_V	\bar{n}	Lifetime (min)	Random Controls \bar{R}_V	\bar{R}_{Vs}	\bar{R}_{Vns}	\bar{n}	Lifetime (min)	Non-Random Controls \bar{R}_V	\bar{R}_{Vs}	\bar{R}_{Vns}	All Controls Lifetime (min)	\bar{R}_V	\bar{R}_{Vs}	\bar{R}_{Vns}
1970	14	22.7	338.9	6	34.7	459.3	*		0					6	34.7	459.3	*
without 6/30	14	22.7	338.9	2	27.5	110.9	3.06		0					2	27.5	110.9	3.06
1971	9	38.8	494.9	6	29.2	258.0	*		6	30.3	375.1	*		12	29.8	316.6	*
1972	0			0					12	49.2	369.3	-		30	44.9	224.7	-
1973	25	25.2	265.1	29	43.5	262.7	*		23	38.7	535.8	*		52	41.4	383.5	*
without 8/9	25	25.2	265.1	23	41.8	160.7	*		23	38.7	535.8	*		46	40.3	358.3	*
all years w/o dist. days	48	27.0	329.7	41	40.1	290.8	*		41	40.5	463.6	*		82	40.3	377.2	*
	48	27.0	329.7	31	38.4	176.3	*		41	40.5	463.6	*		72	39.6	339.9	*
all years (adj.) w/o dist. days	48	40	488.4**	41	40.1	290.8	1.68		41	40.5	463.6	1.05		82	40.3	377.2	1.29
	48	40	488.4	41	38.4	176.3	2.77		41	40.5	463.6	1.05		72	39.6	339.9	1.44

* Either R_{Vs} or R_{Vns} underestimated because of inadequate time history. The ratio is calculated if the time discrepancy is less than 5 min.

** All year value (329.7) multiplied by 40/27.

than control clouds as intended. It is still not known whether these effects will manifest themselves as more rainfall in the target area, but there is every reason to expect that they will.

An analysis of the effect of seeding on rain intensity in FACE is described in appendix B.

7. THE 1975 FACE PROGRAM

The accomplishments at the Cumulus Group since the end of FACE-73 warrant continued experimentation in 1975. In planning our next effort, we have incorporated what we have learned, and we intend to concentrate on areas where understanding is lacking. We will obtain the maximum number of experimental days without violating our suitability criteria, and at the same time press our search for predictors and covariates to reduce the high natural rainfall variability that is inherent in these experiments. Our method of convective rain measurement is adequate and we can shift even more emphasis to documenting cloud processes. The large-scale effects of dynamic seeding in Florida will receive scrutiny for the first time using satellite imagery. Environmental studies will be continued and expanded. Specific plans and operational procedures are detailed in the FACE Planning Document and Operations Plan. Both documents are available upon request.

The FACE-75 field effort is pivotal because it may well determine the future course of cloud modification in NHEML. Certainly, we must be much closer to knowing the effect of dynamic seeding on areal rainfall if experimentation in the same vein is to be continued beyond 1975.

7.1 The Randomized Core Seeding Effort

The randomized seeding effort forms the core of FACE-75. This phase of the program will be conducted over the target area (fig. 1) as in the past, but with some minor, yet potentially significant, changes.

Suitable days will be selected using the same $S - N_e \geq 1.50$ criterion as in the past (Simpson et al., 1973). This criterion is a necessary, but not a sufficient, condition for the selection of a day for experimentation. The final decision will be determined in the air after evaluating the supercooled cloud populations, including their patterning, heights, numbers and their internal properties such as liquid water contents, updrafts, ice particle contents and the duration of the microphysically-favorable conditions for seeding. The actual seed decision will be determined aboard the aircraft with only the randomizer knowing the content of the envelope. Project personnel concerned with the seeding will not know the seed decisions until the end of FACE 1975.

Although this project design has been approved by statisticians, it would be desirable to determine the suitability of a day for experimentation and the seed decision on the ground. However, this has proven impossible to date because appropriate predictor variables for the accurate definition of a suitable day have not been found. Consequently, it has been necessary to fly for final determination of an experimental day.

One change will be made in the decision process leading to qualification of a day for analysis. In the past, a day did not qualify as an experimental day until at least six clouds had been seeded and/or 60 flares had been expended. This final proviso was designed to reduce the natural rain variability by eliminating those days when the clouds disappeared from the target area and those days when natural rainfall was rampant early in the experimental process. As described in an earlier section, the reduction of natural rain variability is a prime goal in FACE. Unfortunately, it is not clear that this final proviso reduced the rain variability enough to outweigh the disadvantages that included a loss of experimental days and a prolonged period of uncertainty on each flight day as the experimenters deliberated on a correct course of action.

In FACE-75, the six cloud and/or 60-flare proviso for qualifying a day (the old ground rules) for experimentation and analysis will be eliminated. On any day in FACE-75, ejection of one pyrotechnic flare (real or simulated) will qualify a day as a GO day regardless of the subsequent course of meteorological events. However a stratification of the data based upon the 60-flare criteria will still be performed. Mechanical failures that end the seeding early in the day will still be grounds for rejection of a day for analysis as long as the individuals conducting the experiment do not know the seed decision. The randomized seeding instructions for FACE-75 have been prepared through the collaboration of Mr. Glenn Brier of Colorado State University and Dr. Ron Biondini of the University of Virginia.

The slight relaxation of the stipulations as to what qualifies a day as a GO day makes our goal of 25 GO days in FACE-75 a realistic one. In FACE-73, alone, seven additional GO days would have been obtained had the old ground rules not been in effect. However, one must recognize that in eliminating the cloud and/or flare proviso to obtain more days, some relatively unsatisfactory days will be included in the data set. This should not be a major problem as long as such days are evenly distributed in the seed and no seed categories. For an objective determination of the distribution of such days, the scientists will state just before ejection of the 60th flare whether they would have qualified the day had the 60-flare proviso been in effect. It will still be possible to stratify the days depending on whether they met the 60-flare criterion.

Based on previous years, two seeder aircraft are required to conduct the seeding efficiently with a minimum of missed opportunities. Optimum use of aircraft would dictate that the C-130 and DC-6 do the seeding between 19000 and 21000 ft MSL. The flight patterns and seeding procedures will be similar to those employed in FACE-73, and described in this

report. Seeding will be done to maximize cloud growth, merger and rainfall in the manner described herein. The instrumentation on the seeder aircraft is listed in section 7.2

There will be no flights to obtain nonrandom control days in FACE-75 for two reasons:

- a) These flights in 1973 greatly exhausted key flight personnel to the point where they had difficulty performing other duties.
- b) The floating target rainfalls on the nonrandom control days were wetter than those on the random control days even though the situation was reversed in the total target. This suggests a subconscious bias on the part of the person conducting the flights to obtain the nonrandom control days.

7.2 Intensive Phase Microphysical Investigation

7.2.1 Motivation

The dynamic seeding of suitable cumulus clouds for the purpose of augmenting rainfall within a target area is predicated upon a chain of three events. First is the conversion of a sufficient quantity of super-cooled water to release enough heat to significantly increase cloud buoyancy and lead to invigorated vertical and horizontal expansion of the bubble volume. Second is the downward "communication" of the seeding level buoyancy increase within the bubble to the low-level boundary layer inflow tapping the moisture source. Third is the organization of the inflow to allow for continual regeneration of cells and a prolonged processing of the available moisture resulting in longer cloud life and more precipitation. The above reasoning chain is obviously only as credible as its weakest link.

Because the technology to investigate in detail the microphysics, dynamics and kinematics of developing convective clouds had not progressed to the degree necessary to attempt to resolve the problems posed above, the bulk of previous FACE research has been directed at changes in cloud top height and rainfall induced by seeding. This largely statistical approach led to a great gain in physical insight during the early single cloud work, but it is inadequate, by itself, when the expected effects of seeding are small compared to the natural variability of GO-day rainfall as appears to be the case in the FACE multiple cloud work. At present, our best attempts at meteorological stratification of seed and no-seed experimental days are inadequate to minimize the effects of natural rain variability, and, without the discovery of useful predictor variables or covariates, it has been calculated that a purely statistical evaluation of seeding effect on rainfall may well require more than 50 pairs of seed-control cases to bring the results to an acceptable level of significance (Simpson, 1974).

Fortunately, technology has now provided cumulus experimenters with some new tools with which to earnestly begin an examination of the sequential links²⁵ in the seeding hypothesis. This will allow for an evaluation of seeding effect based not only upon the strength of statistics, but also upon the strength of physical measurements. Furthermore, and perhaps most important, a detailed investigation into the effect of seeding on the morphology of the cloud microphysics, dynamics, and kinematics would most certainly bring to light incorrect assumptions or procedures and, in the final analysis, would lead to a much more confident assessment of man's potential to alter cumulus development.

7.2.2 Instrumentation

Three fully-instrumented research aircraft, the NOAA C-130, the NOAA DC-6, and the NCAR Queen-Air will be available for the FACE-75 program²⁶. A much expanded surface mesometeorological network will also be in operation. It is planned that the following specialized instrumentation will be utilized to investigate the evolution and morphology of the microphysics, dynamics and kinematics of cumulus system:

on the C-130

- a) Johnson-Williams cloud water content
- b) nimbiometer total liquid water content
- c) INS with AWRS-computation of air vertical velocity
- d) foil impactor
- e) Knollenberg particle spectrometer
- f) Lyman alpha total water content
- g) Mee continuous ice particle counter

on the DC-6

- a) Johnson-Williams cloud water content
- b) nimbiometer total liquid water content
- c) INS with Datacom computation of air vertical velocity
- d) foil impactor
- e) Formvar replicator
- f) Knollenberg particle spectrometer
- g) Mee continuous ice nucleus counter
- h) Mee continuous ice particle counter
- i) UW continuous ice particle counter
- j) Mee continuous cloud condensation nucleus

²⁵a) conversion of water to ice; b) communication of buoyancy to the boundary layer; c) enhanced organization of inflow and more efficient processing of the available moisture.

²⁶The NCAR Queen Air is available for only one month.

- k) APCL continuous ice nucleus counter
- l) APCL cloud condensation nucleus counter
- m) APCL continuous Aitken nucleus counter
- n) Barnes IR radiometer
- o) Lyman alpha total water
- p) APCL aerosol filter system

on the NCAR Queen-Air

- a) NCAR aerosol filter system
- b) NHEML-NRL rainwater scoop
- c) Barnes IR radiometer
- d) NCAR continuous ice nucleus counter
- e) continuous Aitken nucleus counter

ground resources

- a) UM dual doppler radar system
- b) NCAR doppler radar
- c) NOAA/NHC S-band radar
- d) Joss distrometer
- e) surface meteorological network
- f) FOS and Miami radiosonde

A description of the characteristics of some of the specialized cloud physics instrumentation to be used in FACE 1975 is in appendix D.

7.2.3 Procedures

Although we anticipate that cloud penetrations by the two upper level (-10°C) NOAA aircraft during the "core" seeding program will yield a wealth of important cloud physics data, it is only through concerted effort, and through the conscientious repenetration of individual towers that we can achieve a good insight into the evolution of microphysical parameters. Accordingly, an "Intensive Phase" cloud physics study will be conducted as a subprogram of FACE-75. On days without randomized seeding from 16 June to 31 July 1975, a decision will be made whether or not to launch the NOAA DC-6²⁷ aircraft on an Intensive Phase mission. On such occasions, the DC-6 will operate for part of the flight at low levels to collect nuclei data but, for the major portion of the flight, it will be at high levels (-4°C to -10°C) penetrating and repenetrating cloud towers to obtain information on the evolution of the water-ice budget, the interrelationship of microphysical parameters with cloud

²⁷The DC-6 was chosen over the C-130 as the Intensive Phase aircraft because its wing hard points insure that instrumentation can be mounted for excellent exposure to the free air stream.

updraft structure, the partitioning of water substance, the potential for secondary ice crystal production, and the continuity of the tower's life cycle. Seeding will be carried out on a randomized paired-cloud basis, both to determine cloud response and to evaluate nucleation characteristics of the pyrotechnic composition.

7.2.4 Impact on Planning

At the very least, the Intensive Phase results should provide considerable insight, not only into the natural glaciating behavior of Florida cumuli, but also into the capabilities of the dynamic seeding technology for inducing changes prescribed by the hypothesis. The failure to find a significant difference would certainly force a re-evaluation of the techniques, procedures, and resources used in FACE. The nucleating characteristics of three pyrotechnics²⁸ will be investigated in terms of ice crystal production inside clouds. Sufficient duplication of the instrumentation exists on board the DC-6 so that it should be possible to make a judgment of data reliability.

If, as expected, the microphysical studies reveal a much more rapid conversion of water to ice within individual cumuli that are seeded, the logical next step would be to intensively investigate the problem of buoyancy communication to the boundary layer. Such an investigation will need to include one or two gust probe-equipped aircraft at subcloud, and possibly midcloud, levels.

8. FUTURE COURSE OF FACE

8.1 Should We Continue?

From a scientific standpoint there is no question that we should continue with FACE-75, since there are too few cases to make an intelligent decision to redesign or discontinue the experiment altogether. However, at this point it is well to examine the question of whether the potential dividends outweigh the cost of supporting the program. The FACE-73 effort cost NOAA nearly one million dollars²⁹ and FACE-75 will cost somewhat more because of inflation. What is the likely return on this investment?

We must first recognize that NOAA is under continual pressure to advise the people of the world on cloud seeding for drought mitigation. Such advice has been offered without any proof that the proposed seeding

²⁸Olin X-1055/WM105, Navy WMU9/TB-1, and NEI TB-1 (appendix C).

²⁹These figures include all costs to operate the research aircraft.

methodology will work under the existing conditions. Not even NOAA's lone effort has established the efficacy of dynamic seeding for area-wide rain enhancement. Despite this uncertainty, NOAA conducted a drought mitigation program at the request of the State of Florida during the spring of 1971. If NOAA intends to continue in this advisory capacity, it is imperative that its basic cloud seeding research program be brought to a definitive conclusion as soon as scientifically feasible.

Potential benefit-to-cost considerations also dictate continuation of FACE. Simpson and Woodley (1973) suggest that the potential benefit-to-cost ratio for FACE may be in the 10-to-100 range when the seeding technology is applied operationally. If so, this certainly would dictate continuance.

Even if the direct practical benefits prove much smaller than this, the potential scientific benefits from solving this problem in themselves justify its pursuit. So far, only one seeding experiment (Dennis et al., 1975) on fair weather cumuli in tropical air has been brought to a conclusive positive result. Moreover, the merger process, at the focus of FACE, is a key problem in atmospheric dynamics and severe weather prediction. Dynamic seeding, as developed at the old EML, is now the cornerstone of the current "Stormfury" hypothesis. This consideration, alone, underscores the importance of continuing with all aspects of the FACE program as presently conceived.

8.2 Plans

The goals of the FACE 1975 program include: (1) increasing the sample of experimental days with a doubling of the seeded sample, (2) obtaining the observations of cloud and environmental processes that are necessary to derive, verify and update numerical models, and (3) obtaining a covariate or predictor, or both, to diminish the importance of natural rain variability in Florida.

Several milestones are anticipated for this program. The most important milestone should be continued progress in resolving the effect of seeding in the floating target. The effect is positive, but not significant now, and major regression from this position after doubling the seeded sample would be very serious. If this regression should occur, the analysis of all observations should be expedited in order to explain it. With this eventuality, the analysis will be particularly critical to Project "Stormfury" in which an attempt will also be made to alter convective cloud systems on the mesoscale.

Concurrent with the analysis of the effect of seeding in the target in FACE-75 will be an effort to determine whether there are any extra-area effects as well. This will be done using a method newly developed at the Cumulus Group to estimate rainfall from satellite imagery. The method is comparing very favorably with the system of combined gage and

radar groundtruth that was also developed at the Cumulus Group in 1973. Fortunately, the method can also be applied retroactively to past FACE days. Consequently the sample size for the study of extra-area effects will be nearly as large as the entire FACE sample of experimental days. The study to determine if there are large scale effects of dynamic seeding is a new initiative at the Cumulus Group. It had to wait until a tool to tackle the problem was available. Now that such a methodology is available, it will be applied in all past and future FACE programs.

The FACE-76 effort will be similar to FACE-75 in terms of budget and personnel, but the emphasis in the effort will depend upon analyses of FACE-75 observations.

A Cloud Physics Workshop has been suggested as a new initiative in FACE-76. It is a vehicle whereby prominent, active cloud physicists might interact with NHEML scientists to provide a complete description of the internal structure of Florida convective clouds. The internal cloud microstructure data at several levels resulting from such a workshop program, when analyzed and interpreted, would be essential input to the multi-dimensional cumulus modeling work within NOAA.

After analysis of all rainfall measurements through FACE-76, a reassessment will be made once again. At this point, the effect of seeding in the floating target must be nearly established and of practical value. If the effect is established but small, then we must determine whether continued experimentation along the same lines is warranted.

After FACE-76, it will be time to carefully examine the total target. If the total target effect of seeding is negligible despite a definitive positive effect in the floating target, it would then appear that the increases in one area are at the expense of another. At this point a physical explanation of this finding must be sought and continued experimentation should be delayed until it is resolved.

The most probable status of FACE after 1976 is a nearly definitive result for the floating target and a positive but smaller and ill-defined effect for the total target. This is a critical decision point for the scientists and management in NOAA. Whether or not to push on without establishing the size of the positive seeding effect in the total target is a decision of some import. One might argue that if the seeding effect is positive, although not significant, in both areas, then the problem is resolved and we can move on to the new initiative whereby dynamic seeding for areal rain enhancement is transferred to other areas.

This is an option, but hardly a viable one. First, it will not permit a realistic estimate of the benefit-to-cost ratio for an operational program. Second, bypassing the total target will mean that basic studies will receive less emphasis as well. This is especially risky because such studies are necessary to understand the mechanisms whereby the rain is increased. Without this understanding, extrapolation of dynamic seeding methodology to other areas becomes a hit or miss proposition.

The best course of action is to continue with FACE in 1977 in conjunction with a Boundary Layer Workshop. The boundary layer data will be essential for the proper numerical description of convective processes on the mesoscale and will have a vital impact on the NOAA cloud modeling work. With information on changes in total target rainfall induced by seeding, a complete description of Florida mesoscale systems, and the development and testing of convective cloud models, FACE scientists will be in a position to bring dynamic seeding to other areas. Realistically, this may not be possible until 1980. At this point, the Florida work will have a major impact on SESAME and other such programs devoted to the understanding and mitigation of severe storms.

9. CONCLUSIONS

The Florida Area Cumulus Experiment is a continuing program with a mandate for research that probably cannot be completed until at least 1980. Theory, modeling and observations lag far behind our ability to conduct seeding experiments. These foundations must catch up in order to continue progress in FACE. The program must be flexible to accommodate increases in our knowledge of how this experiment can best be carried out.

The sample of experimental days in FACE is still too small to hope for definitive results. Nevertheless, the experiment is moving in the right direction as evidenced both by the factor of 2 increase in rainfall from single clouds in FACE and the greater tendency of the seeded clouds to merge. The observational data base for FACE has been greatly expanded since 1973, and several milestones have been reached.

Probably not until after FACE-76 will the effect of seeding on the floating target be determined, and not until after FACE-77 will the limits on the effect in the total target be specified. Alternative courses of action have been mapped should these expectations prove unfounded.

It may well take until 1980 before an adequate description of Florida convective systems is possible using observations and models. However, by then the effect of seeding in FACE, in and outside of the target area, should be known and, most importantly, the mechanism whereby this effect is produced should be understood. This will then permit transfer of the seeding methodology to other areas and the use of the Florida results to better understand and perhaps mitigate severe storms.

The path in FACE is difficult and the pace sometimes seems agonizingly slow. However, the stakes for this country and the world are too great for us to falter as long as there is a reasonable expectation of definitive results. All indications now warrant continuation of the experiment and every effort should be made to expedite this important work as quickly as is scientifically feasible.

10. ACKNOWLEDGMENTS

Several hundred individuals and numerous organizations have contributed to the FACE effort. Although we have acknowledged many of these contributions in a number of FACE-related publications, we wish to summarize them here.

This major Technical Report is dedicated to Dr. Joanne Simpson, former Director of the Experimental Meteorology Laboratory, who guided us through the early cumulus modification efforts and who continues to make invaluable contributions to the FACE program. We are also grateful to ERL management, particularly in recent years, for support and encouragement of the FACE effort.

Several Federal agencies outside of ERL contributed to the FACE. The National Hurricane Center (NHC) under the direction of Dr. R. H. Simpson and Dr. Neil Frank provided assistance in several areas. They permitted and encouraged research use of the NHC WSR-57 radar. Mr. Alvin Samet and Mr. Ansel Bryan, supervisors of the radar operations and electronic technicians, respectively, deserve our thanks for keeping the radar system operating. Others of NHC who helped with FACE include the district and aviation forecasters and the personnel in the Communications Branch. The staff of the National Weather Service Station at Miami International Airport very capably provided special radiosonde releases during FACE 1973. Personnel at the National Weather Service Stations in Lakeland and Palm Beach, Florida also provided help with various aspects of FACE. The National Environmental Satellite Service, particularly the Miami Satellite Field Services Station under Mr. Don Gaby helped FACE personnel with the satellite subprograms during FACE. The Public Information Office of NOAA ably handled the public relations aspects of all FACE field programs.

The university community played a major role in all aspects of FACE. The Radar Meteorology Laboratory of the University of Miami under Dr. Homer Hiser provided radar observations through 1972 and Mr. George Andrews of that laboratory did most of the work in assembling and building the radar digitizer used in FACE 1973. Dr. Roger Lhermitte of the University of Miami provided dual doppler radar observations of convective clouds in FACE 1973. Dr. Michael Garstang and his crews from Florida State University (FACE 1971) and from the University of Virginia (FACE 1973) played a major role in installing, maintaining, operating and dismantling the surface meteorological network of FACE-71 and -73. The Space Science Engineering Center at the University of Wisconsin is acknowledged for coordinating aspects of the FACE satellite subprograms. Dr. Doug Segar of the Chemical Oceanography Department of the University of Miami supervised the analyses of water samples collected in rainfall from experimental clouds during FACE-73. We are grateful to Dr. Dennis Garvey of Colorado State University's Department of Atmospheric Science for carrying out the comprehensive pyrotechnic testing at the CSU Cloud Chamber Facility.

The private sector also contributed to FACE. We are most grateful to the land owners in the target area for providing us access to their property to set up our surface networks in 1971, 1972 and 1973. Others in the private sector assisted as cooperative observers in FACE.

Much of the support for FACE efforts through 1973 came from within ERL. The Research Flight Facility under the direction of Mr. Howard Mason and Dr. James McFadden went beyond the call of duty in all FACE programs to keep the research aircraft in the air with all systems functioning properly despite many difficulties and punishing flight weather conditions. The National Severe Storms Laboratory, under the direction of Dr. Edwin Kessler, lent its considerable expertise for the design and construction of a radar digitizer that was attached to the NHC WSR-57 and for methods of assessing the taped digitized data. We are grateful to Dr. Farn Parungo of ERL's Atmospheric Physics and Chemistry Laboratory for her help in analyzing characteristics of the pyrotechnics used in FACE. We also acknowledge the many contributions of the National Hurricane Research Laboratory and the Boundary Layer Dynamics Group during past FACE efforts. In particular, Mr. Paul Willis and Mr. Terry Schriker of NHRL participated actively in most of the FACE 1973 flights in order to collect cloud physics data. The entire staff of the Experimental Meteorology Laboratory devoted many long hours to the FACE program, and this group formed the core around which the program was built. We are greatly appreciative of their efforts. We wish to especially acknowledge the tireless, dedicated effort which the EML staff of senior scientists (Dr. Bill Cotton, Dr. Roger Pielke, Mr. Al Miller, Mr. Ron Holle, and Mr. Victor Wiggert) devoted to the FACE-71 and -73 programs. Without their leadership, insight, and expertise, it would have been difficult to develop a balanced conceptual view of the FACE program.

11. REFERENCES

- Brier, G. W., G. F. Cotton, J. Simpson, and W. L. Woodley, 1972: Cloud seeding experiments: lack of bias in Florida series. Science, 176, 163-164.
- Bryant, G. W., J. Hallett, and B. J. Mason, 1959: The epitaxial growth of ice on single-crystalline substances. Physics Chem. Solids, 12, 189.
- Carlson, T. N., and R. C. Sheets, 1971: Comparison of draft scale vertical velocities computed from gust probe and conventional data collected by a DC-6 aircraft. NOAA Tech. Memo. ERLTM NHRL 91, 39 pp.
- Cotton, W. R., 1972a: Numerical simulation of precipitation development in supercooled cumuli. Part I. Mon. Wea. Rev., 100, 757-763.
- Cotton, W. R., 1972b: Numerical simulation of precipitation development in supercooled cumuli. Part II. Mon. Wea. Rev., 100, 764-784.
- Cotton, W. R., 1975: On the parameterization of turbulent transport in cumulus clouds. J. Atmos. Sci., 32, 3, 548-564.
- Cotton, W. R., and A. Boulanger, 1975: On the variability of "dynamic seedability" as a function of time and location over South Florida. J. Appl. Meteor., 14, 710-717.
- Dennis, A. S., J. R. Miller, Jr., D. E. Cain, and R. L. Schwaller, 1975: Evaluation by Monte Carlo tests of effects of cloud seeding on growing season rainfall in North Dakota. J. Appl. Meteor., 14, 959-969.
- Dye, J. E., G. Langer, V. Toutenhoofd, T. W. Cannon, and C. A. Knight, 1975: The measurement of microphysical effects of silver iodide seeding. Submitted to J. Appl. Meteor..
- Edwards, G. R., and L. F. Evans, 1960: Ice nucleation by silver iodide: I. Freezing vs. sublimation. J. Meteor., 17, 627-634.
- Fletcher, N. H., 1962: The Physics of Rainclouds. Cambridge University Press, 319 pp.
- Fletcher, N. H., 1969: Active sites and ice crystal nucleation. J. Atmos. Sci., 26, 1266-1271.
- Gagin, A., 1975: The ice phase in winter continental cumulus clouds. J. Atmos. Sci., 32, 8, 1604-1614.

- Garvey, D. M., 1975: Testing of cloud seeding materials at the cloud simulation and aerosol laboratory, 1971-1973. J. Appl. Meteor. 14, 883-890.
- Grossman, R. L., and B. R. Bean, 1973: An aircraft investigation of turbulence in the lower layers of a marine boundary layer. NOAA Tech. Report ERL-291 WMPO-4, 166 pp.
- Guttman, J., and S. S. Wilks, 1965: Introductory Engineering Statistics. John Wiley & Sons, Inc., 340 pp.
- Hallett, and S. C. Mossop, 1974: Production of secondary ice particles during the riming process. Nature, 249, 26-28.
- Hess, W. N., 1974: Weather and Climate Modification. John Wiley & Sons, Inc., 842 pp.
- Hill, G. E., 1974: Factors controlling the size and spacing of cumulus clouds as revealed by numerical experiments. J. Atmos. Sci., 31, 646-673.
- Hobbs, P. V., 1974: Ice Physics. Oxford University Press, 635 pp.
- Khrigian, A. Kh., and I. P. Mazin, 1956: Analysis of methods characterizing raindrop distribution spectra. Tr. Cent. Aerolog. Obs., 17, 38-46.
- Knollenberg, R. G., 1970: The optical array: An alternative to scattering or extinction for airborne particle size determination. J. Appl. Meteor., 9, 86-103.
- Koenig, L. R., 1963: The glaciating behavior of small cumulonimbus clouds. J. Atmos. Sci., 20, 29-47.
- Koenig, R. L., 1966: Numerical test of the validity of the drop-freezing splintering hypothesis of cloud glaciation. J. Atmos. Sci., 23, 726-740.
- Kraus, E. B., and P. Squires, 1947: Experiments on the stimulation of clouds to produce rain. Nature, 159, 489-491.
- Kyle, T., 1974: The dispersal of seeding material in the updraft of storms. Preprints Fourth Conf. Wea. Mod., Ft. Lauderdale, Fla., Amer. Meteor. Soc., 69-72.
- Lhermitte, R., and R. I. Sax, 1974: Use of dual doppler radar in the Florida Area Cumulus Experiment (FACE). Preprints Fourth Conf. Wea. Mod., Ft. Lauderdale, Fla., Amer. Meteor. Soc., 89-94.

- MacCready, P. B., Jr., 1959: The lightning mechanism and its relation to natural and artificial freezing nuclei. Recent Advances in Atmospheric Electricity, 25, 369-381.
- MacCready, P. B., Jr., 1964: Standardization of gustiness values from aircraft. J. Appl. Meteor., 3, 439-449.
- Malkus, J. S., 1963: Tropical rain induced by a small natural heat source. J. Appl. Meteor., 2, 5, 547-556.
- Malkus, J. S., and R. H. Simpson, 1964: Modification experiments on tropical cumulus clouds. Science, 145, 3632, 541-548.
- McCarthy, J. 1974: Field verification of the relationship between entrainment rate and cumulus cloud diameter. J. Atmos. Sci., 31, 1028-1039.
- Mathews, L. A., D. W. Reed, P. St. Amand, and R. J. Stirton, 1972: Rate of solution of ice nuclei in water drops and its effect on nucleation. J. Appl. Meteor., 11, 813-817.
- Merceret, F. J., 1975: Measuring atmospheric turbulence with airborne hot-film anemometers. Submitted to J. Appl. Meteor..
- Merceret, F. J., and T. L. Schriker, 1975: A new hot-wire liquid cloud water meter. J. Appl. Meteor., 3, 319-326.
- Mossop, S. C., R. E. Ruskin, and K. J. Heffernan, 1968: Glaciation of a cumulus at approximately -4°C . J. Atmos. Sci., 25, 889-899.
- Olsen, A. R., and W. L. Woodley, 1975: On the effect of natural rainfall variability and measurement errors in the detection of seeding effect. J. Appl. Meteor., 14, 929-938.
- Östlund, S. S., 1974: Computer software for rainfall analyses and echo tracking of digitized radar data. NOAA Tech. Memo. ERL WMPO-15, 82 pp.
- Parungo, F. P., E. Ackerman, and R. F. Pueschel, 1974: AgI ice nuclei: Physical and chemical properties depending on their generating procedure. Preprints Fourth Conf. Wea. Mod., Ft. Lauderdale, Fla., Amer. Meteor. Soc., 165-172.
- Pielke, R., 1973: A three-dimensional numerical model of the sea breezes over South Florida. NOAA Tech. Memo. ERL WMPO-2, 136 pp.
- Pielke, R., 1974: A three-dimensional numerical model of the sea breezes over South Florida. Mon. Wea. Rev., 102, 115-139.

- Pueschel, R. F., and F. P. Parungo, 1974: Artificial ice nuclei production by evaporation and sublimation of salts in a flame. Preprints Fourth Conf. Wea. Mod., Ft. Lauderdale, Fla., Amer. Meteor. Soc., 173-175.
- Rockney, V. D., 1958: The WSR-57 radar. Proc. Seventh Weather Radar Conf., Miami, Florida, 15-20.
- Sax, R. I., 1969: The importance of natural glaciation on the modification of tropical maritime cumuli by silver iodide seeding. J. Appl. Meteor., 8, 92-104.
- Sax, R. I., 1972: Comments on "Ice-phase seeding potential for cumulus cloud modification in the Western States." J. Appl. Meteor., 11, 1017-1018.
- Sax, R. I., 1974: On the microphysical difference between populations of seeded vs. nonseeded Florida cumuli. Preprints Fourth Conf. Wea. Mod., Ft. Lauderdale, Fla., Amer. Meteor. Soc., 65-68.
- Sax, R. I., and P. Goldsmith, 1972: Nucleation of water drops by Brownian contact with AgI and other aerosols. Quart. J. Roy. Met. Soc., 98, 60-72.
- Sax, R. I., and P. T. Willis, 1974: Natural glaciation characteristics of an ensemble of Florida cumulus clouds. Preprints Conf. on Cloud Physics, Tucson, Ariz., Amer. Meteor. Soc., 152-157.
- Schickedanz, P. T., and F. A. Huff, 1971: The design and evaluation of rainfall modification experiments. J. Appl. Meteor., 10, 502-514.
- Senn, H. V., and G. F. Andrews, 1968: A new, low-cost multi-level iso-echo contour for weather-radar use. J. Geophys. Res., 73, 1201-1207.
- Senn, H. V., and C. L. Courtright, 1971: Cloud Physics Research. Final Report to U. S. Weather Bureau, Contract No. E22062-71(N), 19 pp.
- Sheets, R. C., and F. K. Odencrantz, 1974: Response characteristics of two automatic ice particle counters. J. Appl. Meteor., 13, 148-155.
- Shreeve, K. H., 1969: Video integration and processor. ESSA Tech. Memo. WBTM EDL-8, 17 pp.
- Simpson, J., G. W. Brier, and R. H. Simpson, 1967: STORMFURY cumulus seeding experiment, 1965: Statistical analysis and main results. J. Atmos. Sci., 24, 508-521.
- Simpson, J., and V. Wiggert, 1969: Models of precipitating cumulus towers. Mon. Wea. Rev., 97, 471-489.

- Simpson, J., W. L. Woodley, H. A. Friedman, T. W. Slusher, R. S. Scheffee, and R. L. Steele, 1970: An airborne pyrotechnic and seeding system and its use. J. Appl. Meteor., 9, 109-122.
- Simpson, J., and V. Wiggert, 1971: 1968 Florida cumulus seeding experiment: Numerical model results. Mon. Wea. Rev., 99, 87-118.
- Simpson, J., and W. L. Woodley, 1971: Seeding cumulus in Florida: New 1970 results. Science, 172, 117-126.
- Simpson, J., W. L. Woodley, A. R. Olsen, and J. C. Eden, 1973: Bayesian statistics applied to dynamic modification experiments on Florida cumulus clouds. J. Atmos. Sci., 30, 1178-1190.
- Simpson, J., and A. S. Dennis, 1974: Cumulus clouds and their modification. Weather Modification. W. N. Hess, ed., New York, Wiley, 229-280.
- Simpson, J., and W. L. Woodley, 1975: Florida area cumulus experiments 1970-73 rainfall results. J. Appl. Meteor., 14, 734-744.
- Sirmans, D., and R. J. Doviak, 1973: Meteorological radar signal intensity estimation. NOAA Tech. Memo. ERL NSSL-64, 80 pp.
- St. Amand, P., and S. D. Elliott, Jr., 1972: How to seed cumulus clouds. J. Wea. Mod., 4, 17-49.
- Stommel, H., 1947: Entrainment of air into a cumulus cloud. J. Meteor., 4, 91-96.
- Sulakvelidze, G. K., 1969: Rainstorms and Hail. IPST Press, Jerusalem, 234-250.
- Warner, J., 1970: On steady-state one-dimensional models of cumulus convection. J. Atmos. Sci., 27, 1035-1040.
- Weinstein, A. I., 1972a: Ice-phase seeding potential for cumulus cloud modification in the western United States. J. Appl. Meteor., 11, 202-210.
- Weinstein, A. I., 1972b: Reply (to Sax 1972). J. Appl. Meteor., 11, 1018.
- Wiggert, V., and S. S. Östlund, 1975: Computerized rain assessment and tracking of South Florida weather radar echoes. Bulletin AMS, 56, 17-26.

- Woodley, W. L., 1970: Precipitation results from a pyrotechnic cumulus seeding experiment. J. Appl. Meteor., 9, 242-257.
- Woodley, W. L., and A. Herndon, 1970: A raingage evaluation of the Miami reflectivity-rainfall rate relation. J. Appl. Meteor., 9, 258-264.
- Woodley, W. L., and R. Williamson, 1970: Design of a multiple cloud seeding experiment over a target area in South Florida. ESSA Tech. Memo. ERLTM-AOML 6, 24 pp.
- Woodley, W. L., J. Simpson, A. H. Miller, J. J. Fernandez-Partagas, and W. Riebsame, 1971: Florida cumulus seeding experiment for drought mitigation, April-May, 1971. NOAA Tech. Memo. ERL OD-9, 160 pp.
- Woodley, W. L., A. R. Olsen, A. Herndon, and V. Wiggert, 1974: Optimizing the measurement of convective rainfall in Florida. NOAA Tech. Memo ERL WMPO-18, 99 pp.
- Woodley, W. L., A. R. Olsen, A. Herndon, and V. Wiggert, 1975: Comparison of gage and radar methods of convective rain measurement. J. Appl. Meteor., 14, 909-928.

APPENDIX A

SEED DECISION: RANDOMIZATION AND INFERENCE*

A.1 Randomization in FACE

Randomization of the seeding decision is an integral and necessary feature of the FACE design to insure against bias in cloud selection. In FACE-70 and -71, the randomized seeding instructions were prepared by Gerald Cotton of the Air Resources Laboratory. After the fact, it was learned that the randomization included a slight bias in favor of the seed decision with precautions against not more than two of the same seed decisions in succession. At the end of each day of experimentation in 1970 and 1971, the project scientists were told the seed decision.

In FACE-73, the seeding instructions were prepared by Anthony Olsen of EML. Once again there was a slight bias in favor of the seed decision, but no precautions were taken against consecutive runs of the same seed decision. This produced four decisions to seed in succession, a highly undesirable result. In FACE-73, project scientists were not informed of the seed decision on the days of experimentation until the conclusion of the program.

Although project scientists are not in a position to prepare the randomized seeding instructions, they are in the best position to suggest an optimal randomization. Based on extensive FACE experience, an optimal randomization scheme would contain the following features:

- 1) instructions weighted slightly in favor of the seed decision,
- 2) guards against long runs of the same seed decision,
- 3) randomization in pairs for consecutive experimental days with new instruction selected after each pair, (if experimental day do not come in pairs, a seeding instruction is selected for each day),
- 4) flights on all days regardless of seed decision, and
- 5) retention of the randomized instruction for the next suitable day if it is not used.

The decision to fly on all days regardless of the seed decision is necessary to preserve the floating target analysis. Although the ultimate test of the area experiment will be based on total target comparisons, the floating target is an important interim step. Any effect of seeding must be evident first in the floating target, and if it is not evident here after a reasonable period of experimentation, then all of FACE should be

redesigned or scrapped. The floating target is our stopgap against years of fruitless experimentation. To discard it to save flight hours is false economy in the long run. The floating target is also our main opportunity to identify experimental clouds and to study merger processes. Only until a suitable covariate is found should serious consideration be given to dropping the floating target.

A.2 Inferring the Seed Decision

There is always the temptation to try to guess the seed decision when conducting dynamic seeding operations, especially so, when one considers that the method should produce a recognizable change in cloud behavior. Of course, recognition of a seeded cloud presumes the ability to anticipate cloud behavior without seeding. Some are more adept than others in identifying seeded clouds. Recording of one's guesses while conducting the seeding operations has proven to be an interesting exercise.

In FACE-71, Simpson and Woodley guessed the seed decision on each day of experimentation upon which they were immediately informed of the actual seeding decision. As shown in table A1, they made only 3 correct guesses out of 11, a record worse than chance (Simpson et al., 1973). The two interpretations of the rather poor guessing performance were: (1) the effect of seeding in the target area was unrecognizable or (2) those guessing were biased because they knew the previous seed decision; that is, they were unknowingly trying to outguess the randomizer and not guessing based upon what they saw. At the time, the first interpretation appeared to be the correct one, but based on experience in FACE-73, the second interpretation is more likely.

In FACE-73, no one except the statistician who compiled the seed instructions, and the randomizer on the aircraft who armed the flare racks, knew the sequence of seeding decisions until after the entire seeding program. In retrospect, this plan had its advantages and disadvantages. Unfortunately, it limited the learning experiences of the project scientists and allowed no compensation for long runs of the same seed decision under the same weather regime. The same effect could have been obtained by keeping only the scientist directing the flight and doing the seeding (Woodley, in this case) uninformed of the seed decision.

On the other hand, ignorance of the seed decision until project termination permitted guesses of the seed decision without the bias that could come from knowledge of decisions for the previous days of experimentation. Thus, the guesses were based on what was seen and not on what one believed should have been the case.

The guessing performance improved dramatically in 1973 as shown in table A2, with 10 correct guesses out of 12, and on the 2 days with

Table A1. *Guessing the Treatment Decision - 1971 Multiple Cloud Seeding Experiment*

Date	Simpson	Woodley	Decision
16 June	*	Seed	Seed
1 July	Seed	Seed	No Seed
12 July	Seed	Seed	No Seed
13 July	Seed	Seed	Seed
14 July	No Seed	No Seed	Seed
15 July	Seed	Seed	No Seed
Score	$\frac{3 \text{ correct}}{11 \text{ guesses}} = 27\%$		

*Not on aircraft.

erroneous guesses, low confidence in the guess was expressed. The reason for each guess and the point at which a decision was reached is also indicated in table A2. The performance in 1973 has two possible interpretations: (1) the effect of seeding was more recognizable in 1973, or (2) no knowledge of prior decisions removed the possibility of subconscious bias resulting in more objective guesses in 1973 than in 1971. The first interpretation is unlikely because there was apparently a more positive effect of seeding on rainfall in 1971 than in 1973. If true, the effect of seeding should have been more recognizable in 1971. The second interpretation is the more likely, suggesting that the scientist probably conducts a more objective experiment if he is ignorant of the preceding seed decisions. Regardless of interpretation, there is every indication that an unbiased student of convective clouds can recognize anomalies in cloud behavior as a result of seeding. Of course, this does not necessarily mean that these anomalies will manifest themselves as increased rainfall in the target area.

Table A2. Attempt to Recognize Seeding Effect in FACE-73

Date	Guessed seed decision	Actual seed decision	Reason for guess of seed decision (written down by Woodley at end of day)
July 7	S	S	Experimental clouds grew intensely after seeding. However, other clouds in target grew as well. Guessed by midday.
July 16	NS	NS	Wet day, but experimental clouds did not grow much after seeding. Clouds did not respond as expected. Guessed early in day.
July 17	S	NS	Wet day, clouds appeared to grow after seeding. However, clouds later in day did not grow following the seeding pass. Low confidence in guess. Never really sure.
July 20	S	S	Clouds grew following seeding pass. First seeded clouds grew much higher than expected. "Knew" by ~ 1530 EDT.
July 25	NS	S	Dry day. Lack of confidence in guess because of stable upper troposphere and warm seeding temperature (about -8°C). Never sure.
Aug. 6	NS	NS	Low seedabilities and strong up-drafts (>4000 ft/min). Experimental clouds were little different from neighboring clouds. Never sure.
Aug. 9	NS	NS	Target covered with cb-derived cloudiness. Weak cloud towers. Experimental clouds did not grow anomalously. Thought I knew by late in day.

Table A2. Attempt to Recognize Seeding Effect in FACE-73 (Continued)

Date	Guessed seed decision	Actual seed decision	Reason for guess of seed decision (written down by Woodley at end of day)
Aug. 22	S	S	Rather dry day. Some experimental clouds grew following seeding. Probably influenced by three prior NS guesses. Never knew.
Aug. 25	S	S	Experimental clouds grew following seeding. Fairly confident guess. Knew early, by second cloud.
Aug. 27	S	S	Initially guessed NS but changed mind overnight. Early experimental clouds did not grow, but two, late in day, grew anomalously. Dry day. Never knew.
Aug. 28	S	S	Dry day. Experimental clouds grew well. Much more confident of guess than on previous day. Knew early in day.
Sept. 9	NS	NS	Rather dry day, but wet cloud towers. Clouds did not grow as explosively as would have been expected if we were seeding. Made up my mind late in day.

Guessed 10 correct out of 12.

APPENDIX B

SUPPLEMENTARY FACE RAIN ANALYSES AND TABULATIONS

B.1 Calculation of Target Rainfalls in 1973 and 1974

Target rainfalls were calculated for selected days in 1973 and 1974 to: (1) determine the natural variability of rainfall for this area, and (2) serve as a standard for the search for predictors and covariates of target rainfall. The computations were made of target rainfall in the manner described in section 6 of this report. The cumulative hourly target rainfall calculations are presented in table B1. All tabulated rainfalls are unadjusted. Multiplication of these values by the suggested adjustment for each day will improve the accuracy of the target rain measurements. Extreme caution is advised in working with the rainfall during hours when false echo due to anomalous propagation was present in the target area. Echo motion, which is apparently a significant covariate for target rainfall (Simpson and Woodley, 1975), is also tabulated in the last column of table B1.

Upon examination of the suggested adjustments to the radar measurements of rainfall, it is obvious that the radar showed no tendency to systematically underestimate or overestimate the rainfall in 1973, but that it consistently overestimated the rainfall in 1974. This is readily explained. With a proper calibration of the radar and digitizer system, errors should tend to be random as was the case in 1973. However, no calibration was done in 1974 until after the processing of the 1974 radar observations was nearly completed using the calibration for 1973. After comparing the digitizer calibrations for 1973 and 1974, it was obvious that the use of the 1973 calibrations for radar observations obtained in 1974 would result in a systematic overestimate of the rainfall by roughly a factor of 2. This agrees very well with our findings upon comparing gages and radar. The suggested gage adjustment should be used to improve the accuracy of the radar measurements.

B.2 Tabulation of Single Cloud Rainfall Obtained on FACE Days

The motivation, procedures and results of a study of single experimental clouds obtained in the context of FACE have been described in section 6.3. Tabulations of single cloud rainfall are presented in table B2. Relevant variables included in table B2 are: (1) the suggested adjustment (G/R) to be applied to the unadjusted single cloud rainfalls, (2) echo motion and speed, (3) echo position with respect to the WSR-57 radar, (4) the seed decision, (5) the number of flares expended in clouds that were actually seeded, (6) whether the clouds merged or dissipated without merger, (7) cloud duration before merger or dissipation, (8) maximum echo area before merger or dissipation, (9) the rainfall in the 10

Table B1. Unadjusted Hourly Rainfall for FACE Target in 1973 (All Times EDT)

Date	G/R	Suggested adjustment	(units: m ³ x 10 ⁶)												Echo motion		
			0900 Rv	0900 1000 Rv	0900 1100 Rv	0900 1200 Rv	0900 1300 Rv	0900 1400 Rv	0900 1500 Rv	0900 1600 Rv	0900 1700 Rv	0900 1800 Rv	0900 1900 Rv	0900 2000 Rv	0900 2100 Rv	Degree	Speed
June																	
165/14	-		**	**	27.96	33.17	47.78	54.23	62.84	69.13	76.69	107.08	114.88	No Motion			
166/15	1.01 (1)	1.01	.51	.85	11.25	19.92	34.95	59.71	78.63	94.16	142.63**	167.95**	190.56**	No Motion			
167/16	1.68	1.68	.23	.72	4.89	7.79	10.97	15.36	20.74	32.92	62.20	83.46**	99.05**	No Motion			
168/17	0.74/(1)	1.00	.32	.82	2.33	4.52	5.48	7.03	9.63	17.33	22.88	**	**	No Motion			
169/18	1.89	1.89	1.17**	1.72	3.88	7.72	20.03	41.53	63.27	77.00	105.59**	147.98**	166.73**	No Motion			
170/19	-		-	-	41.29	62.39	70.91	74.35	80.72	90.86	103.01	108.44	110.53	No Motion			
171/20	1.11*	1.11	10.46	10.87	19.23	30.1	27.70	51.34	70.05	78.41	80.45	82.17**	97.32**	No Motion			
172/21	-	1.61	.64	1.01	3.01	11.34	27.70	51.34	70.05	78.41	80.45	82.17**	97.32**	No Motion			
173/22	1.61	1.61	-	-	8.34	13.10	22.22	27.66	36.98	56.04	70.39	73.27	-	280 15			
174/23	-		.24	1.62	4.35	8.34	13.10	22.22	27.66	36.98	56.04	70.39	73.27	284 12			
175/24	1.88	1.88	.45	.84	1.29	2.21	3.16	4.40	8.12	14.65	20.18	25.22	32.00	243 11			
176/25	0.62	0.62	.45	.84	1.29	2.21	3.16	4.40	8.12	14.65	20.18	25.22	32.00	243 11			
177/26	1.19	1.19	.35	.71	1.24	2.17	3.98	5.44	10.93	22.62	35.08	44.27	45.36	260 12			
178/27	1.46	1.46	.35	.71	1.24	2.17	3.98	5.44	10.93	22.62	35.08	44.27	45.36	260 12			
179/28	1.94	1.94	.89	2.18	2.77	11.47	14.84	23.86	32.10	41.17	45.43	45.88	46.03	230 13			
180/29	1.56	1.56	.37	.78	1.24	3.87	3.91	3.95	4.18	4.33	4.88	6.12	8.40	241 15			
181/30	1.61 (1)	1.61	.22	.68	2.59	4.86	8.36	13.88	15.88	17.10	18.67	26.00	31.07	261 11			
182/ 1	1.80	1.80	.11	.52	1.45	1.90	2.92	6.76	13.04	24.33	35.06	38.13	39.61	270 07			
183/ 2	1.64*	1.64	.35	.71	1.99	12.25	41.93	74.14	133.69	181.85	55.74	57.21	60.72	43 8			
184/ 3	0.89	0.89	.33	1.09	4.44	13.65	21.62	41.37	50.79	52.57	57.21	58.73	60.72	81 9			
185/ 4	1.47	1.47	.010	.42	2.26	7.49	18.80	48.63	88.84	111.81	117.57	120.80	125.09	73 9			
186/ 5	2.58 (1)	1.34	.18	1.52	2.07	2.49	3.74	5.02	6.10	8.03	18.88	31.55	58.46**	No Motion			
187/ 6	1.20	1.20	.43	.83	4.06	5.73	13.19	33.93	46.69	48.32	49.94	54.69	56.98	260 11			
188/ 7	0.92	0.92	.47	1.05	2.17	5.32	11.83	17.64	24.35	28.93	30.95	33.07	34.49	No Motion			
189/ 8	1.80*	1.80	.038	.43	4.09	14.08	37.46	82.15	110.49	132.87**	148.71**	180.34**	268.98**	No Motion			
190/ 9	0.92	0.92	.39	.77	1.18	1.61	2.05	3.80	14.81	27.36	41.03	64.28	87.80**	No Motion			
191/10	0.64	0.64	.20	1.02	2.23	7.85	22.66	36.56	55.64	85.31	108.12	140.38**	232.00**	237 14			
192/11	1.99	1.99	3.50	4.69	5.38	5.91	6.89	11.80	16.60	25.28	34.08	42.23	44.77	224 15			
193/12	0.98	0.98	1.34	6.43	19.09	35.34	45.76	58.16	78.93	98.82	109.10	115.49	117.26	236 17			
194/13	-	-	-	-	-	-	-	-	-	-	-	-	-	214 12			
July																	

** Rainfall unreliable due to AP

✓ Rainfall in clusters $< 10^{-5} m^3$

- Not available

* Only clusters available; no mesonet

(1) Only one cluster available without mesonet

Table B1. Unadjusted Hourly Rainfall for FACE Target in 1973 (All Times EDT) (Continued)

Date	G/R	Suggested adjustment	(units: m ³ x 10 ⁶)												Echo motion		
			0900 R _V	0900 1000 R _V	0900 1100 R _V	0900 1200 R _V	0900 1300 R _V	0900 1400 R _V	0900 1500 R _V	0900 1600 R _V	0900 1700 R _V	0900 1800 R _V	0900 1900 R _V	0900 2000 R _V	0900 2100 R _V	Degree	Speed
July 195/14	-	-	-	.36	.92	2.86	4.53	8.14	22.01	47.51	77.67	95.55	107.49	121.99**	172.75**	240	9
196/15	0.79	0.79	.48	.96	.96	1.45	3.04	11.37	27.72	52.08	74.17	90.72	99.57	117.38**	160.30**	190	10
198/17	0.89✓	0.89	.44	.90	.90	1.66	3.56	7.79	14.64	28.63	52.10	63.29	66.84	69.46	-	No Motion	
199/18	0.51	0.51	.56	.20	.41	21.47	24.26	29.59	31.31	33.03	34.63	46.39	47.37**	52.96**	60.94**	80	12
200/19	1.72	1.72	.023	.023	.029	.41	2.12	3.00	6.34	12.65	23.03	34.32	54.75	85.96	86.57	85	11
201/20	0.92✓	0.92	.38	.72	.72	2.33	4.59	7.25	10.15	21.92	45.26	68.42	93.72	106.74	115.93	90	10
202/21	1.99*	1.99	.41	1.66	1.66	3.20	14.17	24.10	29.77	30.53	31.08	32.09	36.79	41.44	47.08**	96	16
203/22	1.12	1.12	.63	2.33	3.26	4.41	10.15	36.21	64.29	97.84	132.37	161.63	176.91	182.28		181	14
204/23	0.57	0.57	2.81	3.59	9.44	15.83	25.35	35.83	47.70	53.14	54.62	56.53	57.00	57.46		99	16
205/24	0.41	0.41	.48	1.00	3.44	12.83	26.34	34.04	36.88	38.93	41.69	43.46	44.19**	45.85**		96	16
206/25	0.82	0.82	.45	.87	1.29	2.36	4.76	7.60	9.87	14.71	17.82	20.50	24.04	28.18**		80	10
207/26	0.94	0.94	.41	.80	1.65	5.76	9.12	16.11	25.23	35.38	39.67	50.91	55.73	65.58		No Motion	
208/27	1.07	1.07	2.62	3.45	13.63	28.14	49.51	65.28	68.40	73.76	78.56	81.89**	90.43**	103.52**		143	5
209/28	1.35	1.35	.081	.51	.98	1.58	6.65	15.59	28.77	40.66	57.20	71.20	91.96**	107.94**		No Motion	
210/29	1.40	1.40	.14	.56	1.02	2.32	6.15	13.83	39.15	55.80	77.65	84.53	88.87**	105.19**		No Motion	
211/30	0.83*	0.83	.56	.70	2.41	5.03	8.27	15.70	24.81	30.80	32.05	32.83	35.63**	41.24**		188	10
212/31	1.38*	1.38	1.20	7.25	16.49	24.81	29.12	33.05	37.37	46.49	68.03	84.45	91.40	99.56		194	12
Aug. 213/ 1	1.00✓	1.00	7.11**	10.68	21.11	30.45	34.36	41.33	53.13	63.59	74.34	86.19	102.22	122.53**		194	12
214/ 2	1.11	1.11	-	-	.20	.99	15.09	33.44	50.12	61.79	68.12	29.44	71.11	83.61**		189	12
215/ 3	1.04	1.04	1.87	3.54	7.27	13.71	27.60	63.87	92.30	102.64	108.85	113.14**	127.58**	142.74**		166	13
216/ 4	0.82	0.82	3.98	4.01	6.90	12.00	24.11	62.20	114.40	140.97	150.97	154.34	158.77	162.87		140	12
217/ 5	0.59	0.59	.24	1.58	1.58	13.32	25.28	37.63	47.81	48.46	48.92	49.37	51.66	58.70	71.39	133	11
218/ 6	1.79✓	1.79	.062	1.72	1.72	1.80	2.20	5.55	10.47	16.00	24.38	44.68	69.31	88.55	98.11	No Motion	
219/ 7	1.51*	1.51	.13	.48	1.03	2.58	8.79	11.85	21.56	30.76	36.04	37.40	38.01	39.85**		80	8
220/ 8	1.17*	1.17	46.92**	47.58	48.18	49.08	52.01	63.68	82.76	138.88	206.91	231.40	**	**		57	11
221/ 9	0.93*	0.93	.14**	.75**	1.94**	5.24**	9.80**	28.45**	50.58**	67.41**	88.02**	109.07**	123.23**	125.69**		70	8
222/10	0.84	0.84	3.74	4.39	10.35	36.50	79.29	122.13	143.36	149.01	151.48	153.48	155.77	156.46		198	11
223/11	0.63	0.63	.53	1.00	1.49	2.11	3.50	7.82	22.82	32.98	39.44	41.59	48.41	49.80**		130	15
224/12	0.62✓	0.62	.30	.99	1.63	2.21	2.78	5.35	8.55	19.67	28.49	30.58	32.68	39.04**		93	26

* Only clusters available; no mesonet
(1) Only one cluster available without mesonet

✓ Rainfall in clusters < 10⁵m³
- Not available

**Rainfall unreliable due to AP

Table B1. Unadjusted Hourly Rainfall for FACE Target in 1973 (All Times EDT) (Continued)

Date	G/R	Suggested adjustment	(units: m ³ x 10 ⁶)												Echo motion Degree Speed
			0900 R _V	0900 1100 R _V	0900 1200 R _V	0900 1300 R _V	0900 1400 R _V	0900 1500 R _V	0900 1600 R _V	0900 1700 R _V	0900 1800 R _V	0900 1900 R _V	0900 2000 R _V	0900 2100 R _V	
Aug. 225/13	1.17	1.17	1.01	3.53	3.61	4.59	10.45	15.22	19.97	23.82	28.33	32.32	33.99	35.77**	107 16
226/14	0.55	0.55	.63	1.22	1.95	3.14	8.18	30.88	86.18	151.12	177.32	199.06	221.17	227.11**	93 6
227/15	-	-	-	-	-	-	-	-	-	-	-	-	-	-	197 9
228/16	1.05*	1.05	2.11	3.82	7.94	13.92	20.57	22.77	25.55	29.17	31.88	32.56	34.28	38.56**	140 9
229/17	-	-	-	-	-	-	-	-	-	-	-	-	-	-	80 15
230/18	0.91*	0.91	.84	2.05	2.85	3.72	6.90	10.73	15.37	24.42	35.33	52.79	63.80	73.43**	119 15
231/19	1.29*	1.29	.31	2.58	6.66	15.36	22.71	58.96	120.97	136.52	151.31	168.88	180.41**	198.46**	109 10
232/20	1.00*	1.00	1.55	7.72	20.60	29.65	34.77	44.44	47.54	51.78	-	-	-	-	135 12
233/21	1.68*	1.68	3.61	5.58	7.77	12.66	54.69	95.29	114.25	119.33	120.19	120.83**	123.62**	146.05**	230 10
234/22	1.13*	1.13	124.84**	125.52	126.27	127.03	128.52	132.20	138.04	140.82	146.44	155.23	163.99**	167.46**	260 15
235/23	-	-	-	-	-	-	-	-	-	-	-	-	-	-	239 16
236/24	0.87*	0.87	9.81	29.72	56.78	76.18	81.61	87.92	10.85	133.29	150.30	160.99	170.12	172.72	227 17
237/25	0.73 (1)	0.93	.94	2.32	2.48	4.91	13.50	32.11	52.38	64.77	70.68	73.69	75.26	76.91	160 11
238/26	0.98*	0.98	.94	2.19	4.14	7.31	19.39	45.30	57.66	63.50	66.51	70.48	75.56	77.30	110 12
239/27	0.83√(1)	1.00	.76	1.45	2.18	2.94	4.72	7.35	10.00	12.34	13.34	14.20	15.56	16.10**	70 12
240/28	1.62√(1)	1.00	.73	1.45	2.27	3.30	4.61	7.29	9.11	11.05	13.82	16.16	17.68	19.15	40 14
241/29	1.92*	1.92	1.79	9.43	16.25	20.67	26.40	32.47	34.38	35.38	37.24	38.81	39.80	40.88	109 15
242/30	1.33*	1.33	1.77	8.02	9.11	11.08	16.33	34.95	60.00	76.37	86.29	96.16	-	-	123 12
243/31	1.58*	1.58	3.26	5.60	9.53	15.71	27.46	33.13	38.87	42.90	54.24	65.49	70.26	71.82	160 13
Sept. 244/ 1	1.77*	1.77	1.22	3.52	4.59	8.17	15.18	21.16	27.58	34.69	37.13	39.45	39.43	40.07	124 17
245/ 2	1.53*	1.53	.58	2.16	7.95	11.15	15.66	17.39	19.14	20.50	22.00	23.33	24.65	25.62	111 20
246/ 3	1.35*	1.35	.30	2.64	5.55	9.32	18.11	28.17	31.24	39.14	46.00	50.71	54.00	54.77	130 17
247/ 4	1.44*	1.44	.48	1.02	1.96	3.75	7.07	10.37	14.48	21.29	27.36	30.47	31.37	32.10	141 12
248/ 5	2.12 (1)	1.32	2.00	5.88	11.26	12.88	14.31	15.69	17.49	19.36	24.45	29.79	31.26	32.16	135 15
249/ 6	1.19*	1.19	.58	2.29	6.58	11.73	18.23	30.93	53.38	64.27	65.35	66.42	67.35	68.46	123 19
250/ 7	1.15√(1)	1.15	1.05	4.92	7.92	8.57	9.03	10.15	13.26	15.17	16.13	16.62	17.09	17.72	141 16
251/ 8	-	-	-	-	-	-	-	-	-	-	-	-	-	-	170 15
252/ 9	-	-	.40	.86	1.37	1.86	2.34	2.97	4.12	5.74	6.99	8.48	12.08	14.54	No Motion
253/10	1.63 (1)	1.00	-	-	-	-	-	6.57**	12.46	23.56	34.04	60.91**	74.63**	77.19**	315 19
254/11	-	-	5.55	1.03	12.98	13.77	15.39	15.40	15.46	15.96	17.54	22.09	26.28	29.26	301 11
255/12	-	-	.70	1.48	2.62	3.99	5.62	8.00	22.26	34.74	39.64	42.23	-	-	

* Only clusters available; no mesonet
(1) Only one cluster available without mesonet

✓ Rainfall in clusters < 10⁵ m³
- Not available

** Rainfall unreliable due to AP

Table B1. Unadjusted Hourly Rainfall for FACE Target in 1973 (All Times EDT) (Continued)

Date	R radar mm	R gages mm	G/R	Suggested adjustment	0900 1000	0900 1100	0900 1200	0900 1300	0900 1400	0900 1500	0900 1600	0900 1700	0900 1800	0900 1900	Echo motion Degree Speed
1974															
Aug.								(units: m ³ x 10 ⁶)							
213/1	73.47	40.54	.55	0.55	-	.05	.56	4.46	17.53	61.58	152.36	211.35	241.55	273.56	160°
214/2	.16	.05	.19	0.52	.44	1.64	3.43	4.66	5.90	7.12	8.62	9.32	11.37	14.74	12
215/3	5.15	2.58	.50	0.50	-	.05	1.32	18.59	50.86	70.31	80.92	91.32	94.64	95.19	20
216/4	4.77	2.04	.43	0.43	.55	2.58	3.75	5.23	23.10	54.30	75.20	82.30	90.79	97.68	18
217/5	17.20	12.09	.70	0.70	.27	2.33	6.86	17.78	36.76	61.33	83.37	107.26	127.96	-	17
218/6	.37	.05	.14	0.55	.07	.60	1.57	2.96	4.77	6.11	8.54	9.49	9.98	10.51	16
219/7	23.45	9.13	.39	0.39	5.05	7.70	11.45	14.70	26.88	47.05	77.36	117.36	148.00	160.00	15
220/8	6.19	3.08	.50	0.50	.09	.66	2.36	8.76	17.18	27.48	35.73	42.10	47.26	52.97	12
221/9	13.41	7.83	.58	0.58	.13	.66	1.74	3.74	7.60	12.32	22.49	28.17	32.01	34.36	12
222/10	14.22	9.31	.65	0.65	-	.11	.63	2.98	7.60	11.97	20.35	37.13	65.28	92.03	110
223/11	+	+	+	+	+	+	DID NOT USE		+	+	+	+	+	+	+
224/12	3.30	1.60	.48	0.48	.21	.68	2.27	6.11	13.63	23.67	47.04	75.65	109.40	130.48	90
225/13	14.09	7.01	.50	0.50	.91	.75	3.50	7.14	15.52	37.45	60.72	88.00	117.40	137.72	60
226/14	4.87	2.61	.54	0.54	.50	1.09	1.89	2.96	4.66	8.11	13.70	28.31	55.46	81.38	180
227/15	18.61	14.35	.77	0.77	.56	1.12	1.68	4.09	12.81	28.17	53.17	102.95	166.02	-	140
228/16	3.96	2.16	.54	0.54	.35	.87	1.44	2.01	2.60	3.59	5.86	16.44	52.05	74.44	170
229/17	.91	.47	.52	0.52	.07	.33	1.21	2.09	3.71	12.34	29.35	39.71	63.20	88.90	240
230/18	8.18	4.11	.50	0.50	-	-	-	-	.86	2.23	5.27	12.61	25.36	30.67	260
231/19	5.40	2.14	.40	0.40	.65	2.46	5.57	10.57	18.95	29.17	43.11	89.90	100.73	106.37	250
232/20	2.90	.99	.34	0.34	.65	2.46	5.57	10.57	18.95	29.17	43.11	89.90	100.73	106.37	250
233/21	16.92	11.50	.68	0.68	78.24	79.65	81.43	83.61	86.21	89.28	120.51	160.90	189.87	197.95	90
234/22	16.92	10.23	.60	0.60	51.09	16.71	26.75	41.10	58.94	63.68	66.76	82.77	103.76	123.22	90
235/23	11.27	5.83	.52	0.52	2.09	12.59	39.16	78.02	87.48	89.19	91.97	100.97	109.03	110.74	120
236/24	.83	.64	.78	0.78	.06	.60	18.08	3.03	5.24	10.92	15.59	25.10	38.57	50.29	120
237/25	10.14	8.22	.81	0.81	-	-	3.51	16.51	39.08	55.01	61.34	63.38	65.58	70.46	120
238/26	4.10	2.25	.55	0.55	.55	1.21	1.98	3.98	9.68	16.20	25.81	36.25	50.49	60.48	80
239/27	14.20	5.92	.42	0.42	.53	1.08	1.83	4.82	18.67	41.09	53.63	59.82	64.33	65.47	80
240/28	14.78	6.59	.45	0.45	.80	1.51	2.23	5.36	20.82	33.86	45.05	73.02	125.62	155.85	90
241/29	.26	.07	.27	0.50	.05	.27	.93	1.79	4.20	9.53	12.09	14.88	18.10	18.68	120
242/30	.04	0	0	0.50	.55	1.06	1.56	1.94	1.94	-	-	-	-	2.00	110
243/31	1.51	.53	.35	0.50	.60	1.16	1.71	2.26	3.07	13.36	37.59	48.30	49.40	51.74	90
Sept.															
244/1	.22	0	0	0.50	-	.46	.55	1.09	1.67	2.42	3.05	3.65	4.26	2.76	110
245/2	4.35	.77	.18	0.40	.55	1.09	1.70	3.92	8.70	16.23	19.93	23.18	25.43	26.61	110
246/3	13.34	4.80	.36	0.50	1.14	1.78	2.43	3.54	7.70	19.32	35.55	70.91	113.10	167.75	170
247/4	3.17	.86	.27	0.50	-	.13	.90	4.11	19.19	37.85	57.82	69.95	74.65	85.03	180
248/5	2.48	1.41	.57	0.57	7.41	9.00	9.80	16.05	26.16	36.79	46.61	54.31	62.78	72.80	160
249/6	2.41	1.56	.65	0.65	1.66	2.69	4.13	4.78	5.47	9.11	10.90	11.81	12.38	14.17	180
250/7	3.01	.31	.10	0.50	.37	1.00	1.77	5.88	1.98	42.46	54.10	70.09	89.11	98.84	150

Table B1. Unadjusted Hourly Rainfall for FACE Target in 1973 (All Times EDT) (Continued)

Date	R radar mm	R gages mm	G/R	Suggested adjustment	(units: $m^3 \times 10^6$)										0900 R _V	0900 1800 R _V	0900 1900 R _V	Echo motion Degree Speed
					0900 R _V	0900 1100 R _V	0900 1200 R _V	0900 1300 R _V	0900 1400 R _V	0900 1500 R _V	0900 1600 R _V	0900 1700 R _V	0900 1800 R _V	0900 1900 R _V				
1974																		
Sept.																		
251/8	11.22	2.84	.25	0.40	35.71	10.16	1.75	74.60	98.23	117.77	131.33	137.72	181.00	189.75	130	12		
252/9	7.16	3.42	.48	0.48	1.24	.88	.45	1.71	2.72	6.76	13.07	29.40	43.03	54.27	230	12		
253/10	1.05	.07	.07	0.40	1.87	1.21	.57	2.60	3.36	4.41	8.38	13.00	22.57	29.05	30	10		
254/11	3.53	1.12	.32	0.32	1.55	.94	.40	2.48	4.10	6.89	8.21	9.15	15.12	19.24	70	10		
255/12	.71	.21	.30	0.40	6.85	2.42	.78	8.04	10.17	14.69	15.42	15.85	17.18	19.16	100	12		
256/13	15.21	4.94	.32	0.32	1.97	1.36	.72	2.65	3.64	11.40	44.48	117.72	193.34	251.66	120	8		
257/14	11.66	7.54	.65	0.32	1.46	.63	.06	2.85	3.92	4.94	8.01	22.81	48.17	79.19	No Movement			
258/15	13.49	8.86	.66	0.66	1.51	.58	.05	5.44	16.71	41.27	68.27	91.33	96.43	98.41	90	13		
259/16	.27	.02	.06	0.50	1.64	1.06	.51	2.28	3.16	4.93	5.85	6.58	7.80	8.20				
260/17	.81	.33	.41	0.50	3.04	1.04	.17	3.81	4.44	5.03	6.08	7.20	8.05	9.03				
261/18	6.53	2.27	.35	0.35	1.89	1.07	.52	2.74	4.01	6.92	18.25	28.38	39.29	43.44				

Table B2. 1970 - 1973 Rain Table

Date	G/R	Echo motion Direction	Echo motion Speed	Cloud position Azimuth	Cloud position Range	Seed days only # flares	Merger/ dissipate	Duration (min) before dissipate or merger	Max echo area (km ²)	Rain (m ³ x 10 ³) in 10 min before action	Total rain (m ³ x 10 ³) until dis- sipation/merge
6/29/70	1	280	09	296	54	Seed	D	30	76.6	51.9	319.21
				310	51	26	D	68	84.7	223.7	693.30
				320	34	9	D	46	80.6	.98	366.28
				326	41	8	D	10	16.1	1.2	1.28
				335	28	9	D	16	32.3	28.1	51.30
				335	57	13	D	32	68.6	303.4	302.85
				334	56	2	D	9	44.2	11.9	4.03
				335	54	18	D	5	16.1	.74	1.00
				322	59	No seed	D	60	80.6	86.7	673.44
				323	54		D	78	80.6	15.8	1248.81
6/30/70	1	0	0	292	72		M	21	137.2	2.0	541.90
				290	64		M	12	52.4	.44	57.60
				305	81		M	73	84.7	39.0	771.61
				307	72		M	47	112.8	59.0	1163.08
				310	67		D	32	44.2	.49	150.11
				302	84		D	36	116.6	119.1	314.81
				321	45	8	M	10	40.5	2.2	31.96
				323	39	15	M	11	24.3	2.2	7.36
				337	54	24	M	104	165.3	64.1	2190.81
				287	70	7	D	55	96.7	7.1	340.50
7/02/70	1	0	0	292	60	7	D	15	32.2	8.1	37.15
				338	50	10	D	50	326.5	534.2	2360.08
				290	64		D	20	8.2	2.0	12.34
				347	52	4	D	86	40.4	8.9	214.1
				340	37	No seed	D	59	32.2	1.4	44.7
				342	48		D	17	16.1	.71	10.2
				331	36		D	8	4.1	1.4	.54
				338	45		M	48	44.2	4.5	83.01
				327	34		D	12	28.1	7.7	12.4
				332	29		M	7	338.9	66.2	138.68
7/08/70	1	0	0	308	64	48	D	58	52.5	13.8	170.6
				313	67	10	D	15	24.4	3.1	17.9
				315	60	9	M	58	52.5	5.9	1647.19
				325	55	5	M	34	44.2	17.1	198.8
				323	54	4	D	6	12.0	2.1	1.6
				326	60	5	M	13	161.2	69.6	449.7
				314	41	49	M	55	174.9	34.2	1658.6
				341	38	10	D	35	16.1	3.7	24.1
				337	39	7	M	25	28.1	.62	53.7
				333	38	5	M	5	16.1	5.0	6.6
7/18/70	1	0	0	325	38	7	M	15	52.5	1.2	16.9
				340	62	3	M	30	52.5	31.4	446.4
				338	48	9	M	12	48.3	1.1	62.8
				326	43	17	D	45	76.4	4.6	373.1
				346	57	20	M	20	23.1	1.2	11.4
				345	54	7	M	10	20.2	4.3	15.8
				324	30	29	M	20	56.3	1.2	137.2

Table B2. 1970 - 1973 Rain Table (Continued)

Date	G/R	Echo motion Direction	Speed	WSR Cloud position Azimuth Range	Seed days only S/NS # Flares	Merger/ dissipate	Duration (min) before dissipate or merger	Max echo area (km ²)	Rain (m ³ x 10 ³) in 10 min before action	Total rain (m ³ x 10 ⁵) until dis- sipate/
6/16/71	1.75	250	13	338	Seed	D	42	72.7	0	51.85
				326	54	D	25	20.2	9.5	16.72
				328	45	D	46	32.2	2.2	180.4
				354	67	D	5	48.4	31.8	10.08
7/01/71	1.75	120	12	311	38	D	99	229.8	41.8	1316.45
				319	46	D	10	19.9	9.6	5.24
				327	41	D	19	19.9	5.1	16.74
				297	44	D	24	44.2	.90	72.02
				313	64	D	19	56.3	1.4	64.02
				331	55	D	78	108.7	7.4	326.25
				296	47	D	4	8.2	2.8	.60
				327	62	M	47	161.2	.52	315.80
				329	62	D	40	32.2	1.5	36.40
				347	32	M	23	60.4	12.1	280.5
				346	28	M	17	40.4	2.3	83.2
				339	26	M	6	19.9	0	4.7
7/12/71	1.75	0	0	311	71	D	45	104.9	58.3	228.4
				315	77	D	41	56.2	48.3	94.7
				315	44	D	87	133.0	16.2	518.7
				318	34	D	22	12.0	1.5	6.66
				324	20	D	90	165.3	4.2	1624.88
				326	25	D	5	12.0	1.5	1.51
				328	24	D	55	32.3	.90	77.81
				356	62	D	9	40.5	25.6	6.73
				309	39	D	36	40.5	19.5	96.99
				346	31	M	85	112.9	2.2	665.58
				314	37	D	86	76.6	1.1	355.02
				346	37	M	54	302.4	19.3	960.47
				345	47	M	15	60.4	1.1	56.65
				345	50	M	20	48.4	16.9	85.76
				340	54	M	22	28.1	.75	34.47
				344	68	D	70	88.7	27.6	430.67
				347	58	D	5	16.1	.75	.37
				344	56	M	6	20.2	20.2	4.92
7/13/71	1.75	100	12	324	20	Seed	54	12.0	1.5	1.51
				326	25	Seed	55	32.3	.90	77.81
				328	24	Seed	9	40.5	25.6	6.73
				356	62	Seed	36	40.5	19.5	96.99
				309	39	Seed	85	112.9	2.2	665.58
				346	31	Seed	86	76.6	1.1	355.02
				314	37	Seed	54	302.4	19.3	960.47
				346	37	Seed	15	60.4	1.1	56.65
				345	47	Seed	20	48.4	16.9	85.76
				345	50	Seed	22	28.1	.75	34.47
				340	54	Seed	70	88.7	27.6	430.67
				344	68	Seed	5	16.1	.75	.37
				347	58	Seed	6	20.2	20.2	4.92

Table B2. 1970 - 1973 Rain Table (Continued)

Date	G/R	Cloud position Direction	Cloud position Speed	WSR Azimuth	Cloud position Range	S/NS	Seed days only # Flares	Merger/ dissipate	Duration (min) before dissipate or merger	Max echo area (km)	Rain ($m^3 \times 10^3$) in 10 min before action	total rain ($m^3 \times 10^3$) until dissipate/ merger
7/14/71	1.75	105	10	296	84	Seed	15	D	14	16.1	3.0	5.7
				293	70		15	M	62	173.4	1.8	607.5
				307	88		57	D	9	24.4	3.0	5.5
				305	83		23	M	45	253.8	.90	1784.7
				346	43		36	D	42	72.4	3.4	179.2
				297	69		6	M	40	116.9	8.1	254.2
7/15/71	1.75	160	08	299	68	No seed		M	19	121.0	29.2	414.02
				299	75			D	19	28.1	3.2	13.92
				295	75			D	9	16.1	1.8	3.90
				355	56			D	30	92.7	192.0	214.85
				308	70			M	42	76.6	22.0	449.85
				336	61			D	28	12.0	.30	7.70
7/16/71	1.75	0	0	332	21	No seed		D	10	8.2	1.9	1.49
				345	23			M	70	128.9	9.9	1017.25
				331	23			D	52	44.2	18.9	191.40
				349	36			M	15	20.2	.37	6.35
				356	51			M	15	24.3	10.3	18.29
				354	47			M	5	48.3	11.2	11.20
				352	68			M	50	137.1	1.1	626.43
				350	69			M	27	125.0	1.2	570.95
				346	60			D	33	52.4	6.7	159.00
7/21/72	1	80	13	299	54	No seed		D	61	80.6	11.5	94.19
				293	67			D	5	7.8	.52	.43
				328	65			D	50	56.2	18.2	42.48
				328	63			D	30	48.4	4.3	66.94
				307	73			D	36	32.2	2.1	17.14
				325	59			D	28	44.2	50.6	21.37
				321	65			D	72	40.5	4.3	43.22
				328	57			D	16	32.2	20.3	27.73
				311	81			D	6	32.2	38.1	2.05
				311	76			D	8	16.1	1.7	1.37
7/04/72	1	50	10	337	54	No seed		M	75	84.7	1.2	128.71
				341	56			D	22	20.2	1.7	4.66
				337	54			M	34	100.5	2.1	97.12
				358	42			D	13	7.9	.43	1.11
				342	57			M	47	306.5	16.7	478.87
8/09/72	.97	120	12	352	66	No seed		D	65	108.7	55.1	187.03
				342	59			D	80	44.3	9.9	74.50
				332	60			D	150	201.6	1.7	852.6
				350	68			D	70	201.6	80.1	851.4
				322	70			M	70	669.2	2.5	1524.7
				329	70			D	20	32.2	4.5	4.14
				323	67			M	20	24.0	2.5	8.27
				314	62			M	50	129.0	2.0	245.9

Table B2. 1970 - 1973 Rain Table (Continued)

Date	G/R	Echo motion Direction	Echo motion Speed	WSR Cloud position Azimuth Range	S/NS	Seed only # flares	Merger/ Dissipate	Duration (min) before dissipate or merger	Max echo area (km ²)	Rain (m ³ x 10 ³) in 10 min. before action	Total rain (m ³ x 10 ³) until dis- sipate/merger
8/18/72	1	90	08	347 327 324 326 311 328 303 294 289 292 300 302 297 315 354 286 351 356 359 344 359 339 293	No seed		M M M M M M D M M D D D M M M D M M M M D D D	69 139 42 14 10 10 24 59 49 22 82 8 56 132 115 38 5 9 31 59 28 83 18 34 38 24 46 9 39 23 34 9 39 23 34 9 23 23 12 36 8 16 48	309.1 161.3 72.3 16.1 7.9 7.9 40.5 141.1 201.6 72.3 641.4 12.0 104.6 423.4 225.8 282.2 24.4 225.7 16.1 141.0 108.7 527.5 584.4 40.1 375.0 72.4 137.1 168.1 168.1 64.5 145.1 64.5 225.7 197.6 19.8 483.9 28.1 157.3 326.6	148.8 9.1 5.1 1.2 1.2 1.2 5.3 30.0 22.0 15.7 96.7 1.5 13.2 6.1 7.0 7.2 1.5 139.9 2.1 4.2 10.0 189.9 69.1 25.4 61.4 15.8 32.4 1.7 1.4 6.2 1.4 3.9 1.5 5.9 1.2 50.1 4.9 79.5 7.9	1108.90 809.04 26.23 2.40 .86 .86 17.68 420.8 617.6 22.8 4406.1 1.2 10.5 4450.5 2932.6 1220.2 4.4 157.0 2.1 185.6 185.4 2157.3 102.5 46.8 644.4 56.2 307.4 2.0 7.9 30.3 114.6 3.5 177.3 156.6 1.4 598.9 3.8 347.2 888.1
6/26/73	1.19	270	12	347 327 324 326 311 328 303 294 289 292 300 302 297 315 354 286 351 356 359 344 359 339 293	No seed		M M M M M M D M M D D D M M M D M M M M D D D	69 139 42 14 10 10 24 59 49 22 82 8 56 132 115 38 5 9 31 59 28 83 18 34 38 24 46 9 39 23 34 9 23 23 12 36 8 16 48	309.1 161.3 72.3 16.1 7.9 7.9 40.5 141.1 201.6 72.3 641.4 12.0 104.6 423.4 225.8 282.2 24.4 225.7 16.1 141.0 108.7 527.5 584.4 40.1 375.0 72.4 137.1 168.1 168.1 64.5 145.1 64.5 225.7 197.6 19.8 483.9 28.1 157.3 326.6	148.8 9.1 5.1 1.2 1.2 1.2 5.3 30.0 22.0 15.7 96.7 1.5 13.2 6.1 7.0 7.2 1.5 139.9 2.1 4.2 10.0 189.9 69.1 25.4 61.4 15.8 32.4 1.7 1.4 6.2 1.4 3.9 1.5 5.9 1.2 50.1 4.9 79.5 7.9	1108.90 809.04 26.23 2.40 .86 .86 17.68 420.8 617.6 22.8 4406.1 1.2 10.5 4450.5 2932.6 1220.2 4.4 157.0 2.1 185.6 185.4 2157.3 102.5 46.8 644.4 56.2 307.4 2.0 7.9 30.3 114.6 3.5 177.3 156.6 1.4 598.9 3.8 347.2 888.1
7/07/73	.92	0	0	347 327 324 326 311 328 303 294 289 292 300 302 297 315 354 286 351 356 359 344 359 339 293	Seed	38 5 9 31 59 28 83 12	M M M M M M D M M D D D M M M D M M M M D D D	69 139 42 14 10 10 24 59 49 22 82 8 56 132 115 38 5 9 31 59 28 83 18 34 38 24 46 9 39 23 34 9 23 23 12 36 8 16 48	309.1 161.3 72.3 16.1 7.9 7.9 40.5 141.1 201.6 72.3 641.4 12.0 104.6 423.4 225.8 282.2 24.4 225.7 16.1 141.0 108.7 527.5 584.4 40.1 375.0 72.4 137.1 168.1 168.1 64.5 145.1 64.5 225.7 197.6 19.8 483.9 28.1 157.3 326.6	148.8 9.1 5.1 1.2 1.2 1.2 5.3 30.0 22.0 15.7 96.7 1.5 13.2 6.1 7.0 7.2 1.5 139.9 2.1 4.2 10.0 189.9 69.1 25.4 61.4 15.8 32.4 1.7 1.4 6.2 1.4 3.9 1.5 5.9 1.2 50.1 4.9 79.5 7.9	1108.90 809.04 26.23 2.40 .86 .86 17.68 420.8 617.6 22.8 4406.1 1.2 10.5 4450.5 2932.6 1220.2 4.4 157.0 2.1 185.6 185.4 2157.3 102.5 46.8 644.4 56.2 307.4 2.0 7.9 30.3 114.6 3.5 177.3 156.6 1.4 598.9 3.8 347.2 888.1
7/09/73	.92	0	0	347 327 324 326 311 328 303 294 289 292 300 302 297 315 354 286 351 356 359 344 359 339 293	No seed		M M M M M M D M M D D D M M M D M M M M D D D	69 139 42 14 10 10 24 59 49 22 82 8 56 132 115 38 5 9 31 59 28 83 18 34 38 24 46 9 39 23 34 9 23 23 12 36 8 16 48	309.1 161.3 72.3 16.1 7.9 7.9 40.5 141.1 201.6 72.3 641.4 12.0 104.6 423.4 225.8 282.2 24.4 225.7 16.1 141.0 108.7 527.5 584.4 40.1 375.0 72.4 137.1 168.1 168.1 64.5 145.1 64.5 225.7 197.6 19.8 483.9 28.1 157.3 326.6	148.8 9.1 5.1 1.2 1.2 1.2 5.3 30.0 22.0 15.7 96.7 1.5 13.2 6.1 7.0 7.2 1.5 139.9 2.1 4.2 10.0 189.9 69.1 25.4 61.4 15.8 32.4 1.7 1.4 6.2 1.4 3.9 1.5 5.9 1.2 50.1 4.9 79.5 7.9	1108.90 809.04 26.23 2.40 .86 .86 17.68 420.8 617.6 22.8 4406.1 1.2 10.5 4450.5 2932.6 1220.2 4.4 157.0 2.1 185.6 185.4 2157.3 102.5 46.8 644.4 56.2 307.4 2.0 7.9 30.3 114.6 3.5 177.3 156.6 1.4 598.9 3.8 347.2 888.1
7/16/73	.57	190	10	347 327 324 326 311 328 303 294 289 292 300 302 297 315 354 286 351 356 359 344 359 339 293	No seed		M M M M M M D M M D D D M M M D M M M M D D D	69 139 42 14 10 10 24 59 49 22 82 8 56 132 115 38 5 9 31 59 28 83 18 34 38 24 46 9 39 23 34 9 23 23 12 36 8 16 48	309.1 161.3 72.3 16.1 7.9 7.9 40.5 141.1 201.6 72.3 641.4 12.0 104.6 423.4 225.8 282.2 24.4 225.7 16.1 141.0 108.7 527.5 584.4 40.1 375.0 72.4 137.1 168.1 168.1 64.5 145.1 64.5 225.7 197.6 19.8 483.9 28.1 157.3 326.6	148.8 9.1 5.1 1.2 1.2 1.2 5.3 30.0 22.0 15.7 96.7 1.5 13.2 6.1 7.0 7.2 1.5 139.9 2.1 4.2 10.0 189.9 69.1 25.4 61.4 15.8 32.4 1.7 1.4 6.2 1.4 3.9 1.5 5.9 1.2 50.1 4.9 79.5 7.9	1108.90 809.04 26.23 2.40 .86 .86 17.68 420.8 617.6 22.8 4406.1 1.2 10.5 4450.5 2932.6 1220.2 4.4 157.0 2.1 185.6 185.4 2157.3 102.5 46.8 644.4 56.2 307.4 2.0 7.9 30.3 114.6 3.5 177.3 156.6 1.4 598.9 3.8 347.2 888.1
7/17/73	.89	80	12	347 327 324 326 311 328 303 294 289 292 300 302 297 315 354 286 351 356 359 344 359 339 293	No seed		M M M M M M D M M D D D M M M D M M M M D D D	69 139 42 14 10 10 24 59 49 22 82 8 56 132 115 38 5 9 31 59 28 83 18 34 38 24 46 9 39 23 34 9 23 23 12 36 8 16 48	309.1 161.3 72.3 16.1 7.9 7.9 40.5 141.1 201.6 72.3 641.4 12.0 104.6 423.4 225.8 282.2 24.4 225.7 16.1 141.0 108.7 527.5 584.4 40.1 375.0 72.4 137.1 168.1 168.1 64.5 145.1 64.5 225.7 197.6 19.8 483.9 28.1 157.3 326.6	148.8 9.1 5.1 1.2 1.2 1.2 5.3 30.0 22.0 15.7 96.7 1.5 13.2 6.1 7.0 7.2 1.5 139.9 2.1 4.2 10.0 189.9 69.1 25.4 61.4 15.8 32.4 1.7 1.4 6.2 1.4 3.9 1.5 5.9 1.2 50.1 4.9 79.5 7.9	1108.90 809.04 26.23 2.40 .86 .86 17.68 420.8 617.6 22.8 4406.1 1.2 10.5 4450.5 2932.6 1220.2 4.4 157.0 2.1 185.6 185.4 2157.3 102.5 46.8 644.4 56.2 307.4 2.0 7.9 30.3 114.6 3.5 177.3 156.6 1.4 598.9 3.8 347.2 888.1
7/20/73	.92	90	10	347 327 324 326 311 328 303 294 289 292 300 302 297 315 354 286 351 356 359 344 359 339 293	Seed	28 11 33	M M M M M M D M M D D D M M M D M M M M D D D	69 139 42 14 10 10 24 59 49 22 82 8 56 132 115 38 5 9 31 59 28 83 18 34 38 24 46 9 39 23 34 9 23 23 12 36 8 16 48	309.1 161.3 72.3 16.1 7.9 7.9 40.5 141.1 201.6 72.3 641.4 12.0 104.6 423.4 225.8 282.2 24.4 225.7 16.1 141.0 108.7 527.5 584.4 40.1 375.0 72.4 137.1 168.1 168.1 64.5 145.1 64.5 225.7 197.6 19.8 483.9 28.1 157.3 326.6	148.8 9.1 5.1 1.2 1.2 1.2 5.3 30.0 22.0 15.7 96.7 1.5 13.2 6.1 7.0 7.2 1.5 139.9 2.1 4.2 10.0 189.9 69.1 25.4 61.4 15.8 32.4 1.7 1.4 6.2 1.4 3.9 1.5 5.9 1.2 50.1 4.9 79.5 7.9	1108.90 809.04 26.23 2.40 .86 .86 17.68 420.8 617.6 22.8 4406.1 1.2 10.5 4450.5 2932.6 1220.2 4.4 157.0 2.1 185.6 185.4 2157.3 102.5 46.8 644.4 56.2 307.4 2.0 7.9 30.3 114.6 3.5 177.3 156.6 1.4 598.9 3.8 347.2 888.1

Table B2. 1970 - 1973 Rain Table (Continued)

Date	G/R	Echo motion Direction	Speed	WSR Cloud position Azimuth	Range	S/NS	Seed days only # Flares	Merger/ Dissipate	Duration (min) before dissipate or merger	Max echo area (km ²)	Rain (m ³ x 10 ³) in 10 min before action	Total rain (m ³ x 10 ³) until dis- sipate/merger
(7/20/73 cont'd)				323	59		20	M	14	161.2	121.3	130.3
				297	68		{51}	M	10	92.6	22.6	29.4
				304	65		79	M	11	116.6	42.0	46.2
				302	44			M	13	120.7	60.9	81.7
				326	70		3	M	45	96.7	31.0	184.2
7/25/73	.82			356	52	Seed	25	M	5	44.2	24.2	3.7
				348	64		14	D	152	463.7	25.2	3736.2
				344	52		26	D	13	84.7	7.4	9.5
				322	44		5	M	30	92.6	41.0	163.6
				309	59		96	D	19	52.1	12.6	22.4
7/26/73	.94	0	0	328	65	No seed		M	94	205.8	85.5	1016.7
				334	34			D	29	100.4	81.2	154.3
				332	24			M	21	80.6	41.0	181.2
				345	30			M	14	16.1	2.6	5.0
				319	30			M	28	104.8	2.0	380.7
				290	44			D	25	68.5	28.4	288.7
				288	53			D	15	24.0	2.4	3.7
8/06/73	1.79	0	0	322	56	No seed		D	11	60.4	23.8	12.5
				333	45			D	119	262.1	20.8	1062.1
				320	57			D	12	16.1	3.0	3.5
				325	47			M	96	60.3	16.8	163.4
				320	32			M	77	100.5	20.6	194.2
				309	34			M	15	19.9	9.1	5.7
				314	36			M	15	36.0	13.0	10.1
				332	41			D	15	12.0	2.3	3.3
				335	52			D	15	52.1	9.9	14.9
				327	52			D	88	221.8	48.9	431.2
				311	46			D	37	68.3	17.6	41.3
				345	48			M	37	241.9	83.8	237.8
				320	39			D	19	7.9	2.2	2.8
				333	39			M	19	7.9	3.0	2.8
				337	42			M	19	3.4	1.5	1.5
				337	48			D	19	7.9	2.3	2.8
				332	32			D	18	12.0	10.0	4.2
				307	47			D	18	7.9	2.3	2.6
				305	36			M	99	40.1	4.6	103.8
				340	36			M	16	36.0	6.8	11.0
				310	41			M	83	44.2	2.3	92.6
				310	25			M	83	193.6	36.7	243.0
				334	49			D	15	19.8	3.9	5.7
				343	54			D	10	32.2	2.2	6.1
				289	62			M	73	411.6	26.2	1618.9
				341	28			M	19	4.0	4.6	8.6
				305	46			M	27	36.0	4.6	18.4
				298	41			M	27	16.1	3.1	8.4
				301	31			M	27	44.2	8.4	22.7
				291	43			M	13	16.1	3.1	4.0

Table B2. 1970 - 1973 Rain Table (Continued)

Date	G/R	Echo direction	Echo motion	Cloud azimuth	WSR Range	S/NS	Seed days only # flares	Merger/dissipate	Duration (min) before dissipate or merger	Max echo area (km ²)	Rain (m ³ x 10 ³) in 10 min before action	Total rain (m ³ x 10 ³) until dissipate/merger
8/09/73	93	70	08	329	62	No seed		M	49	177.4	55.9	201.3
				329	55			M	13	56.2	15.9	20.5
				304	70			M	142	746.0	98.2	3061.1
				312	76			M	39	145.1	30.9	129.0
				307	90			M	39	358.9	119.3	507.7
				335	38			M	14	64.5	16.4	8.4
8/11/73	.63	135	15	316	67	No seed		D	43	153.0	35.7	70.9
				299	60			M	22	96.7	14.8	69.4
				285	64			D	18	52.1	4.0	6.2
				302	63			M	10	169.1	82.1	46.5
				296	55			M	20	205.5	21.5	56.6
				312	62			M	52	108.7	1.9	102.6
				302	62			M	13	19.9	1.4	1.7
				321	77			M	13	7.8	.54	.70
8/14/73	.55	0	0	324	37	No seed		M	75	173.2	28.6	183.6
				312	40			D	56	124.9	2.8	62.0
				312	45			D	16	12.0	.72	1.0
				310	33			M	29	84.4	2.8	18.7
				330	29			D	16	24.0	1.4	2.2
				328	38			M	12	32.2	1.9	27.0
				322	29			D	12	7.9	.47	.56
				330	28			D	27	52.1	.47	8.7
				340	26			D	9	16.1	.94	.88
				316	72			M	51	500.0	3.2	578.8
				300	34			M	29	197.6	4.2	39.2
8/22/73	1.13	260	15	311	68	Seed	18	D	36	177.3	9.2	97.2
				294	55		43	D	107	895.1	510.2	3834.7
				302	62		8	D	35	56.6	1.9	26.6
				303	53		6	D	35	44.2	4.3	42.8
				291	59		12	D	16	20.2	4.3	3.7
				339	56		34	M	55	120.7	8.7	89.7
				312	69		11	D	12	44.2	5.3	6.2
				321	65		11	D	12	76.5	9.1	10.9
				329	64		{31}	D	27	24.4	.95	8.8
				319	74			M	46	782.0	35.2	1217.7

Table B2. 1970 - 1973 Rain Table (Continued)

Date	G/R	Echo motion Direction	Speed	WSR Cloud position Azimuth	Range	S/NS	Seed days only # flares	Merger/ dissipate	Duration (min) before dissipate or merger	Max. echo area (km ²)	Rain (m ³ x 10 ³) in 10 min before action	Total rain (m ³ x 10 ³) until dis- sipate/merger
8/25/73	1	160	11	311	57	Seed	11	M	45	459.7	127.8	741.9
				325	55		56	M	29	302.4	113.6	373.0
				324	53		9	M	22	40.1	4.3	14.0
				331	55		20	M	11	92.6	23.1	25.3
				332	50		11	M	11	64.4	11.9	7.5
8/26/73	.98	110	12	314	44		31	M	60	435.5	16.4	950.6
				310	68			M	12	36.0	3.8	4.5
				317	54	No seed		M	15	403.2	260.9	214.6
				317	50			M	39	161.3	36.0	245.2
				307	62			M	20	76.5	68.9	90.4
8/27/73	1	70	12	316	69	Seed	56	D	53	185.5	127.8	196.0
				297	70		31	M	15	152.9	67.8	74.1
				327	64		10	D	48	116.6	42.0	193.2
				319	63		6	D	58	84.7	32.2	63.7
				309	57		12	D	41	129.0	50.3	86.8
8/28/73	1	40	14	306	50	Seed	58	M	59	298.4	30.4	541.9
				303	52		12	D	45	100.5	16.4	101.8
				303	79		16	D	29	72.4	17.7	25.2
				350	48		9	D	14	16.1	3.0	2.3
				299	46		8	D	28	36.0	10.7	10.5
9/09/73	1	0	0	336	38		1	M	22	108.7	44.8	19.6
				329	33		4	D	48	362.9	53.8	315.9
				301	45		24	M	31	290.3	5.1	250.1
				320	57	No seed		M	72	108.7	3.1	197.4
				323	53			D	12	7.8	.85	1.0
9/10/73	1	330	17	347	62			D	185	233.9	43.7	834.4
				339	59			D	32	60.4	6.4	14.0
				324	51			D	117	108.9	15.9	321.9
				324	56			M	27	48.4	5.2	13.7
				302	37	No seed		D	28	60.4	31.7	59.1

minutes before the seeding, and (10) the total rain produced by the cloud until dissipation of merger.

B.3 Time Plots of Target Variables on FACE "GO" Days³⁰

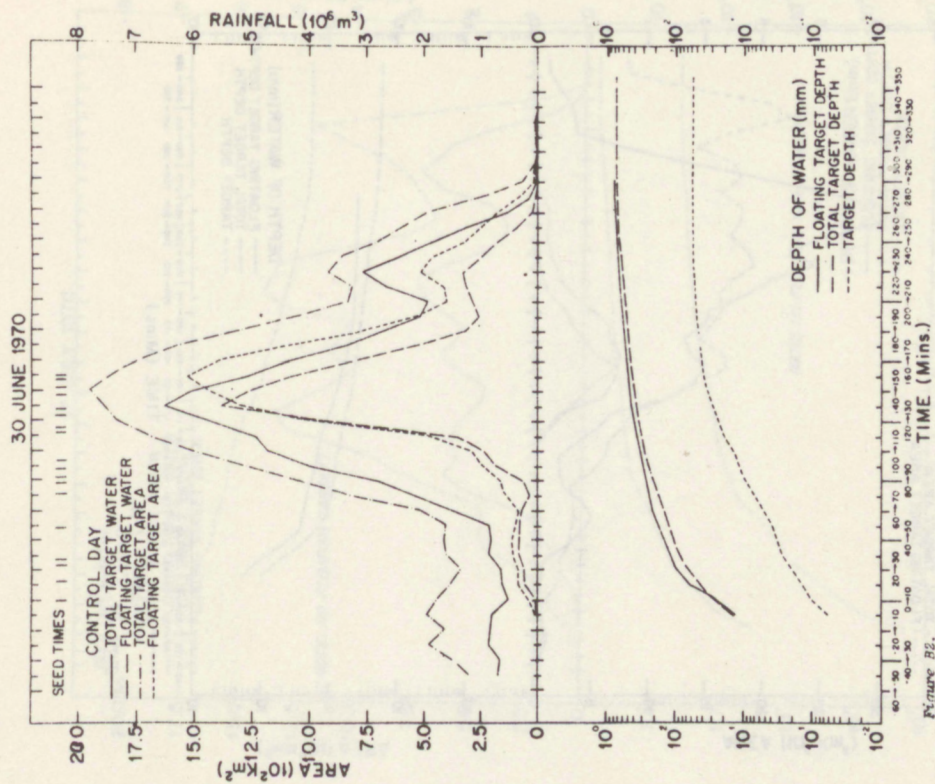
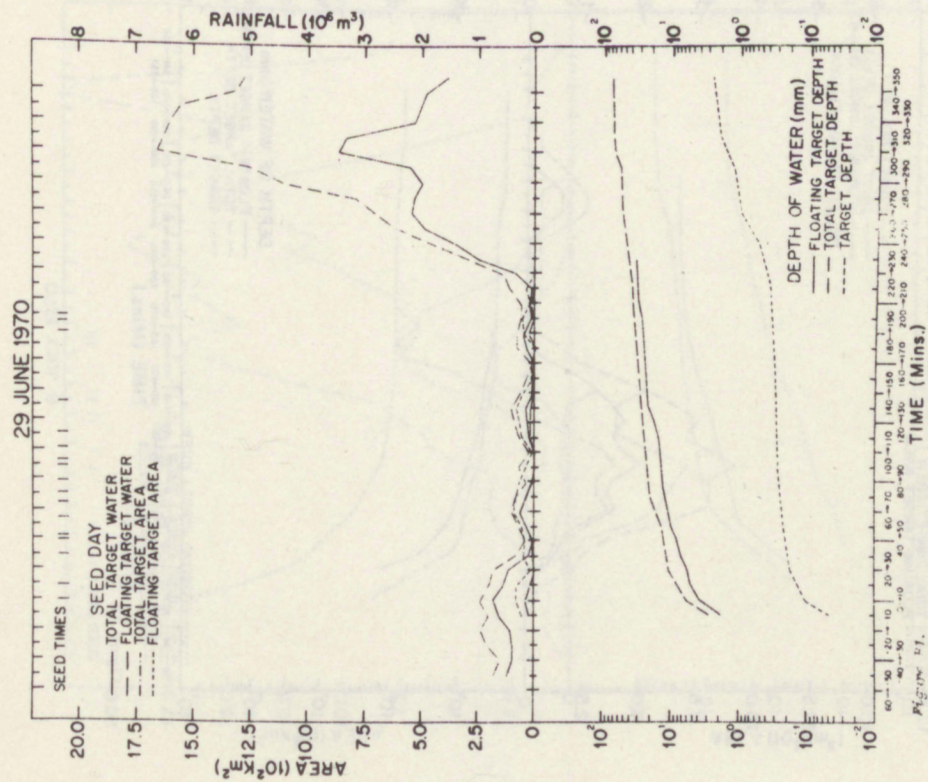
Time plots of floating and total target echo areas, and gage-adjusted floating and total target volumetric rainfalls, are provided in figures B1 through B37. Calculations for the total target for the hour before seeding are also shown. The volumetric rainfalls for the 6 hours after seeding were converted to cumulative area mean rain depths, and they are plotted in the bottom portion of the figures. Seeding times are plotted at the top to serve as an easy reference.

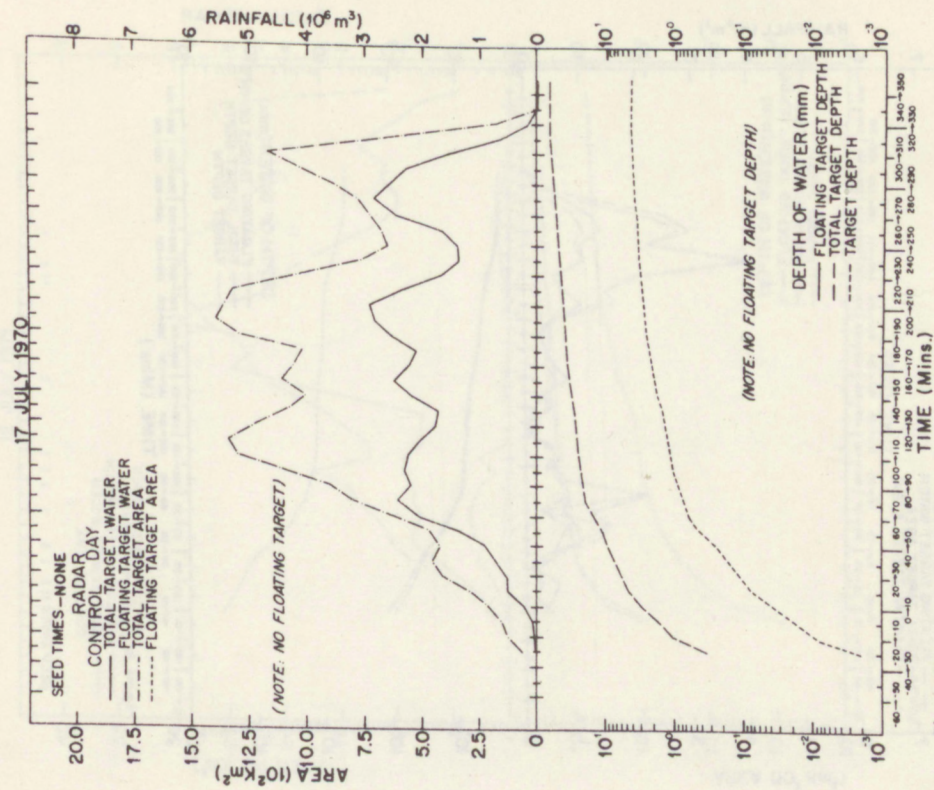
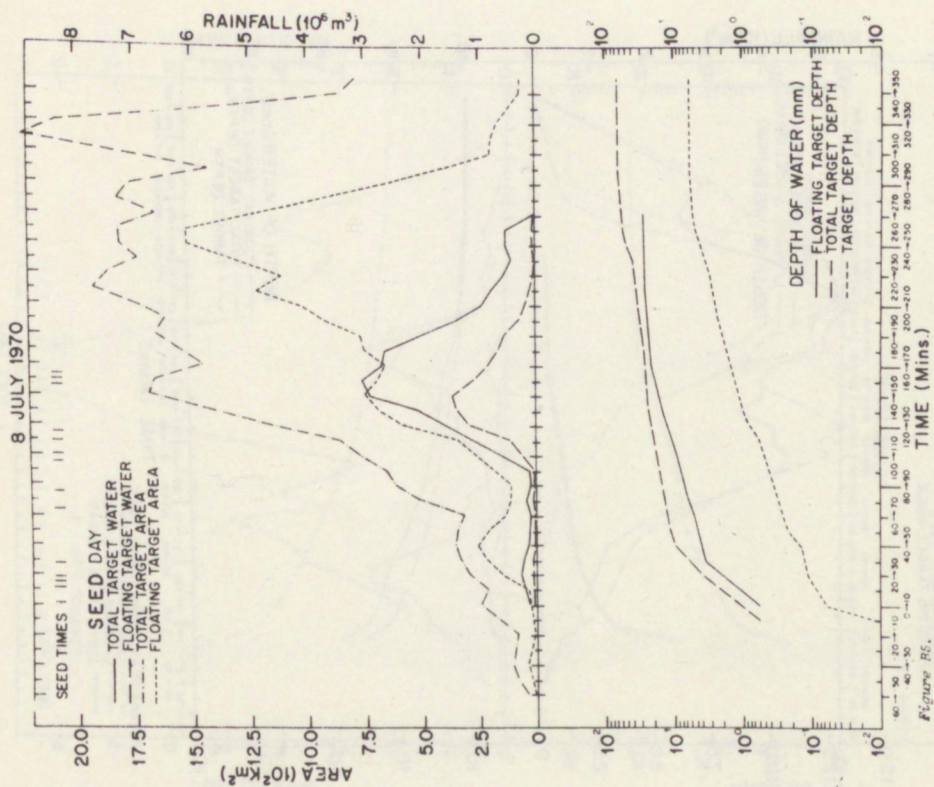
Caution is urged when comparing floating and total target cumulative rain depths for days in different years. Because the floating and total targets are defined by echo coverage, these targets will cover a greater area in the mean in 1972 and 1973 than in 1970 and 1971. Consequently, the rain depths, obtained by dividing rain volume by echo area, will be systematically smaller in 1972 and 1973 than in 1970 and 1971. There is no problem with target rain depth because it is determined by dividing available rain volume by a constant target area. Therefore, comparison of cumulative target rain depths among days in different years is valid.

The systematic disparity in the sizes of the floating and total target areas in the two early FACE years as compared to the later two FACE years is readily explained. In 1970 and 1971, rainfall was estimated using the UM/10-cm radar, but in 1972 and 1973 the WSR-57 was the main research radar. The minimum discernible signal (MDS) of the WSR-57 is several dB more sensitive than the UM/10-cm, with the result that echo areas for the WSR-57 are larger than those detected by the UM/10-cm. However, rain volumes calculated for echoes viewed by both radars are little different because the coverage of echo at the MDS makes an insignificant contribution to the calculated rain volume.

The cumulative rain depths for the floating and total targets in 1971 suffer from an additional problem. The UM/10-cm radar underestimated the true rainfall (as determined by raingages) by a mean factor of 1.75 during this year. The reason for this problem was never determined. Consequently, the radar measurements of volumetric rainfall in the target were increased by a factor of 1.75. The echo areas were undoubtedly underestimated as well, but the magnitude of the underestimation was impossible to quantify. Rather than make an arbitrary adjustment to the

³⁰Data in this section were compiled with the assistance of Mr. Jack Thomas of the Cumulus Group.





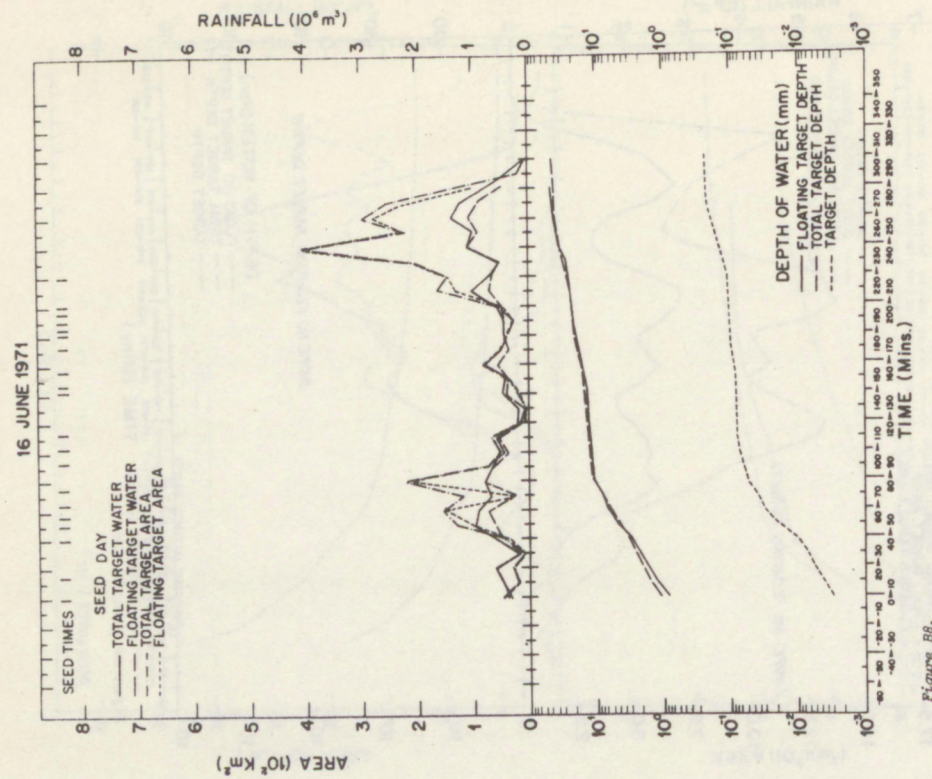


Figure B6.

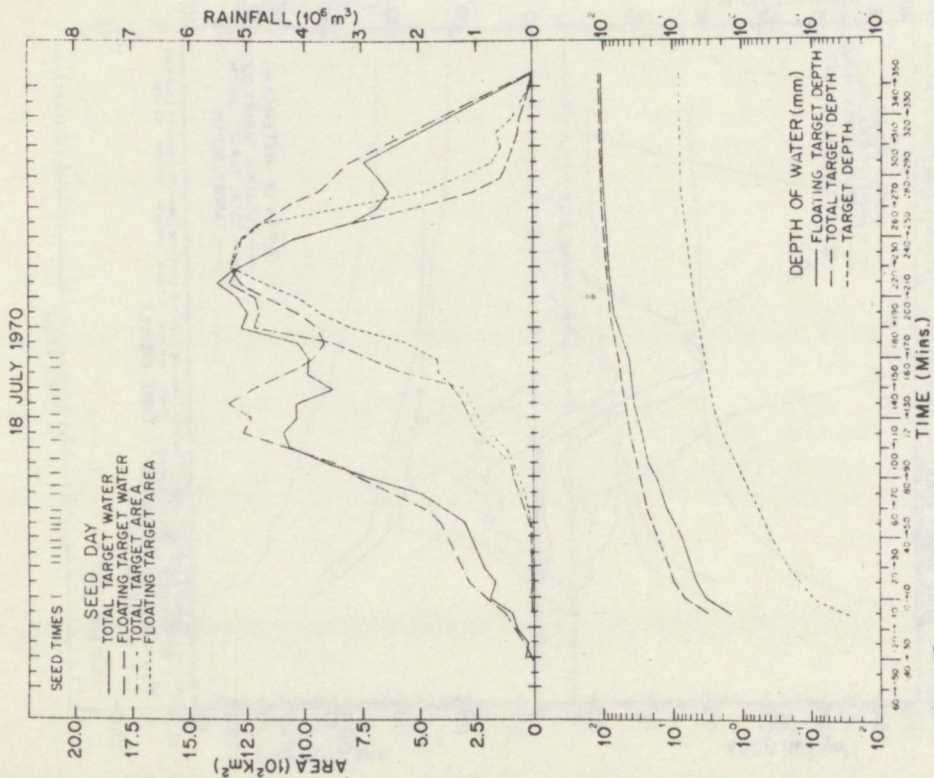


Figure B7.

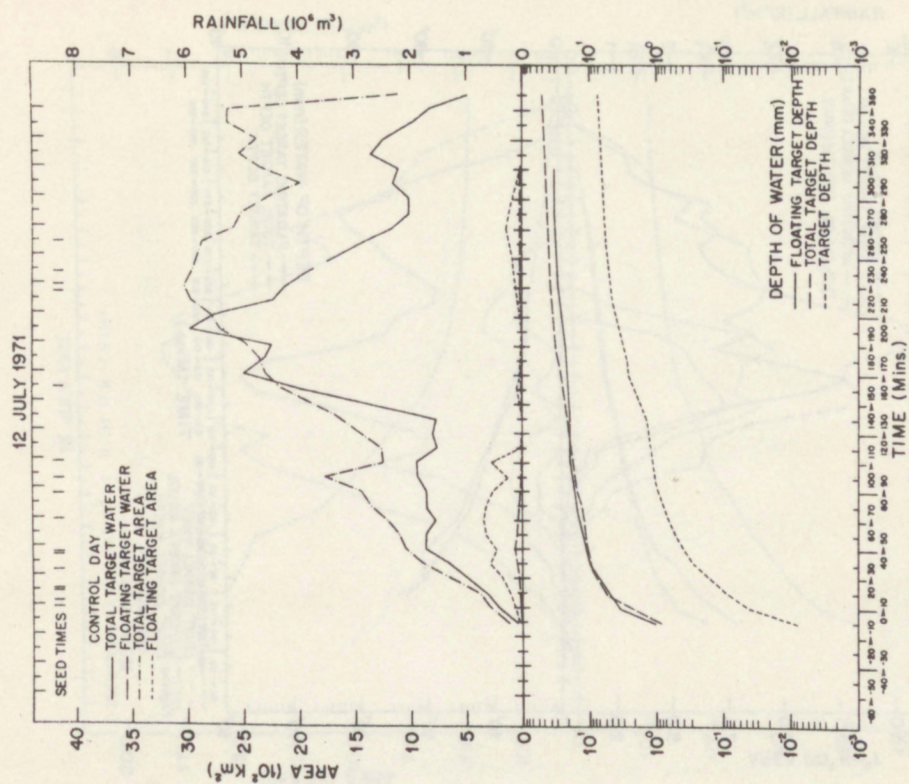


Figure B10.

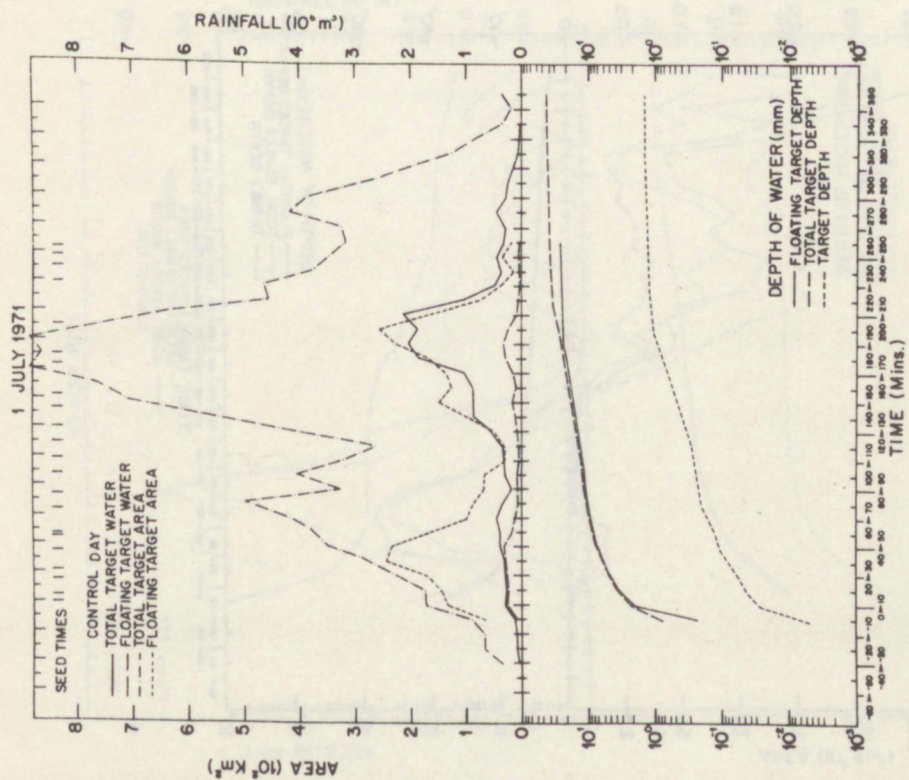


Figure B9.

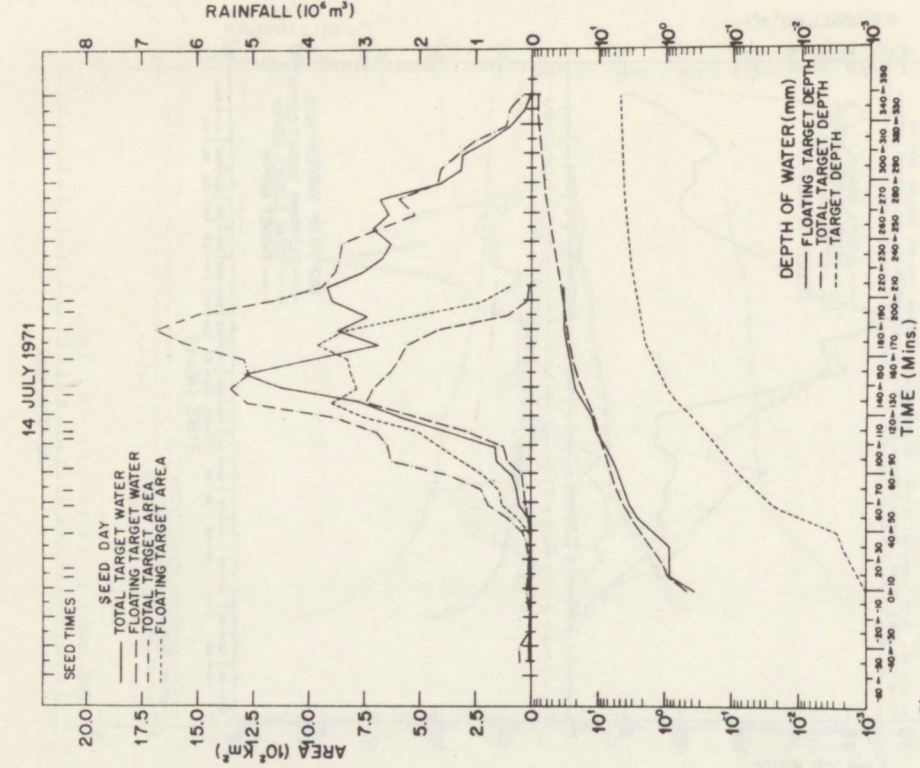


Figure B12.

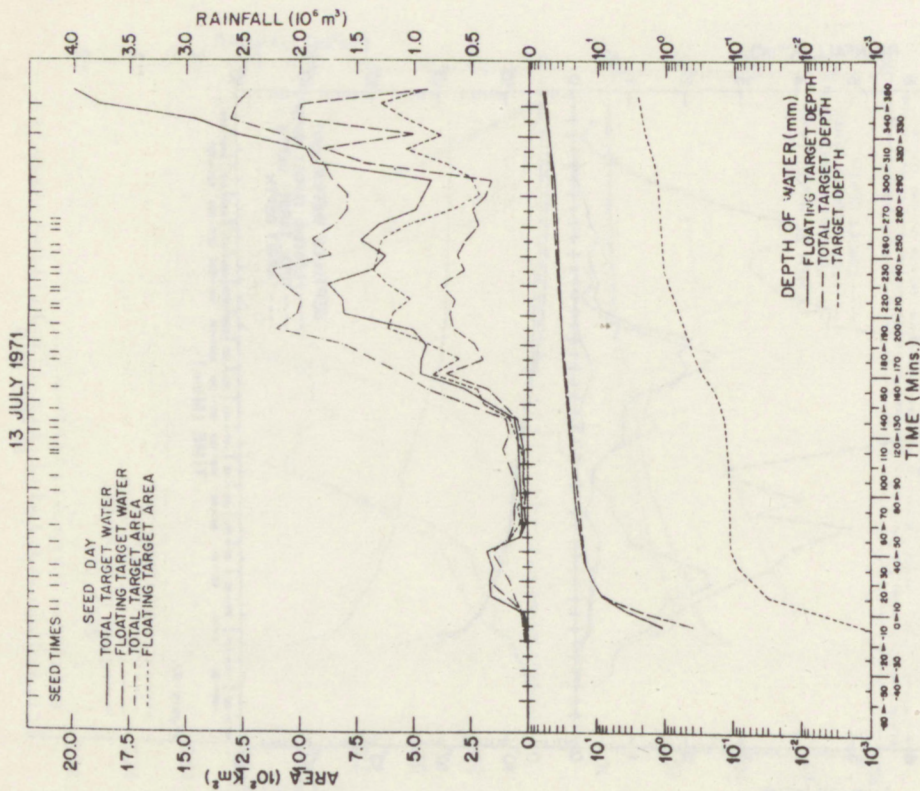


Figure B11.

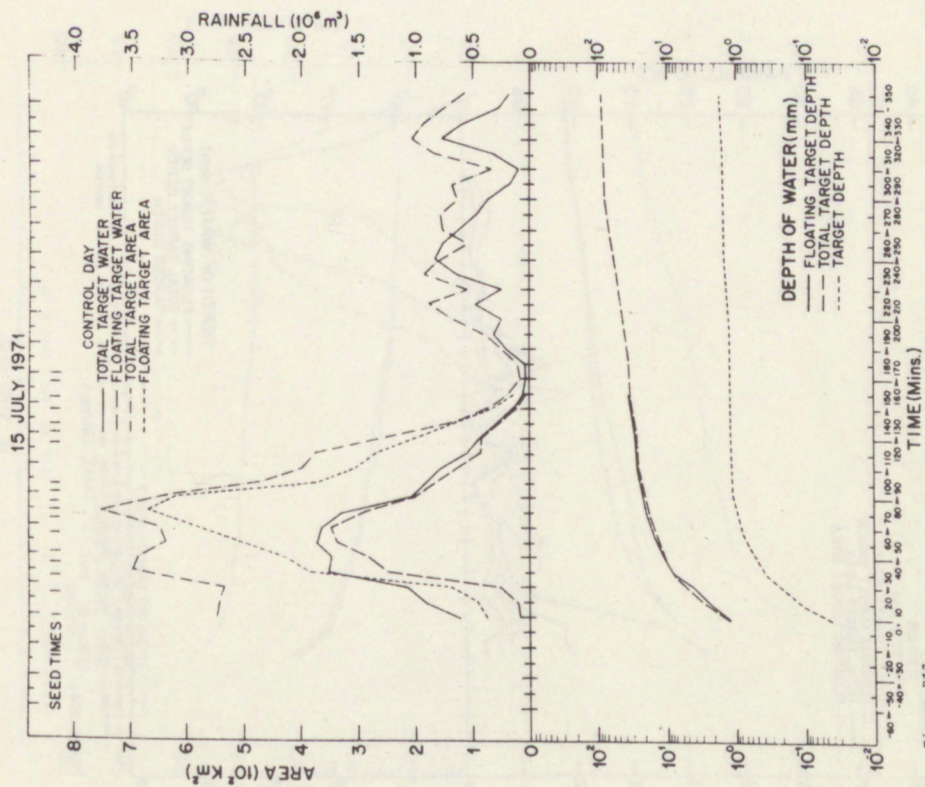


Figure B13.

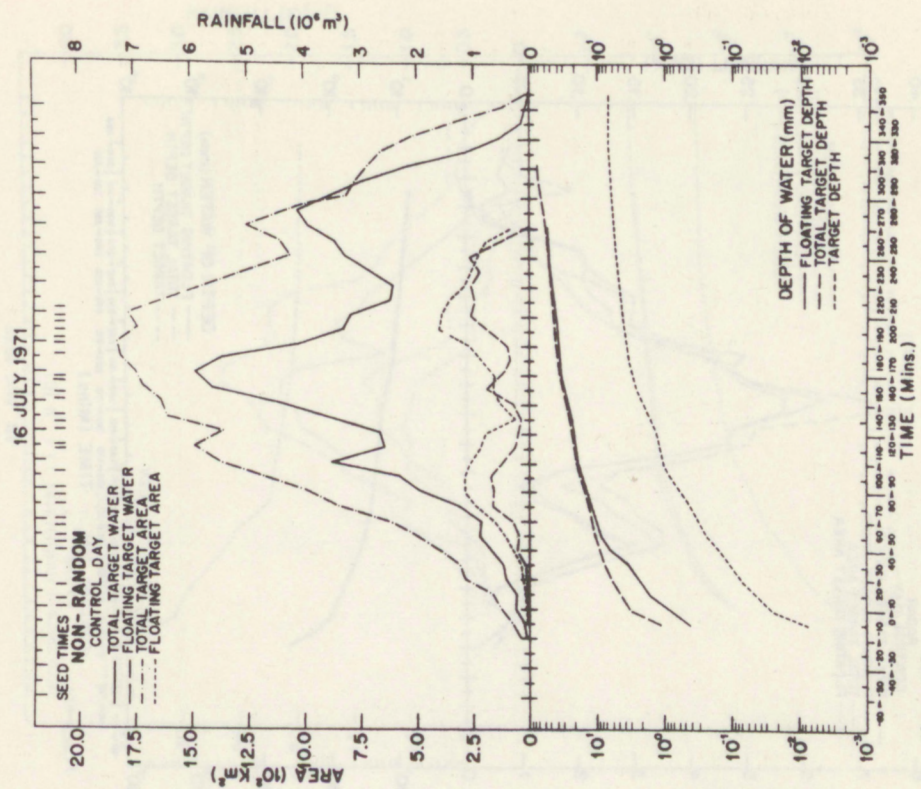


Figure B14.

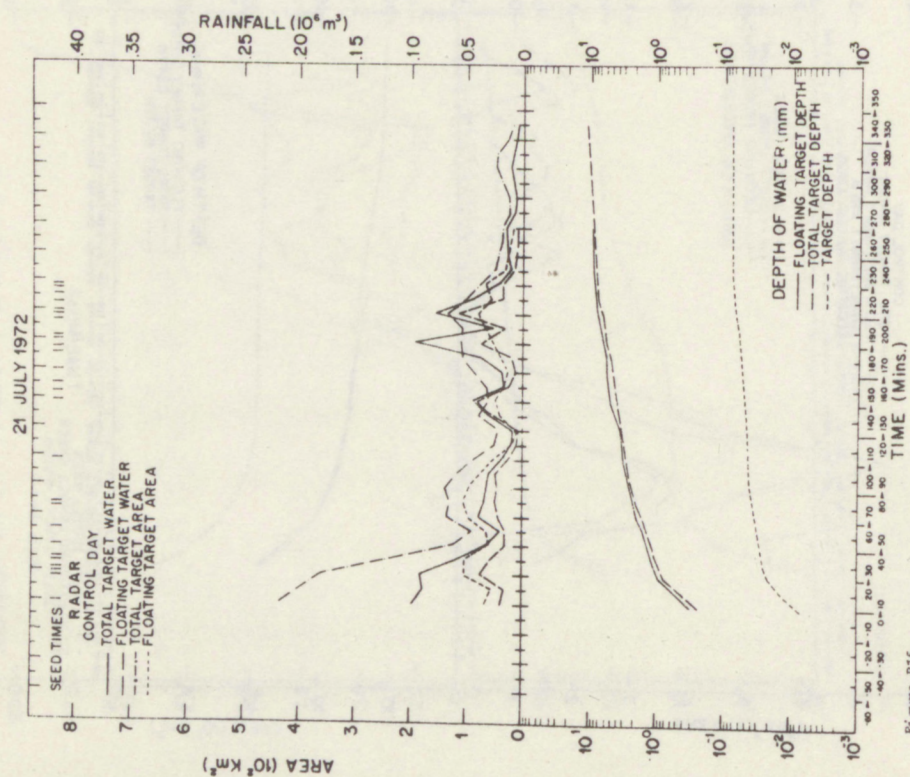


Figure B75.

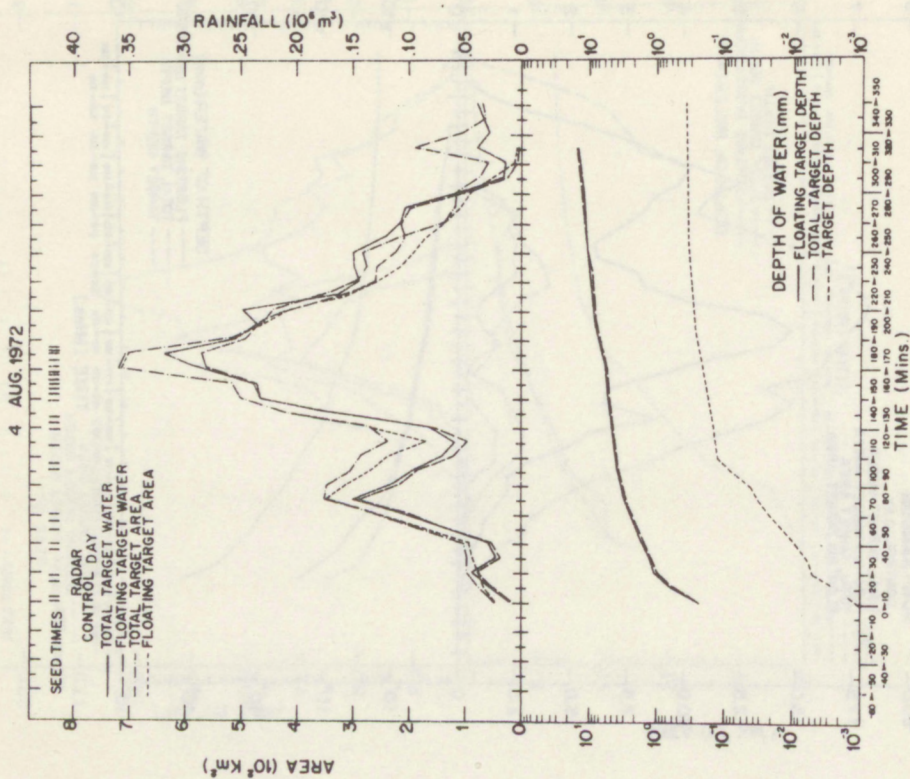


Figure B76.

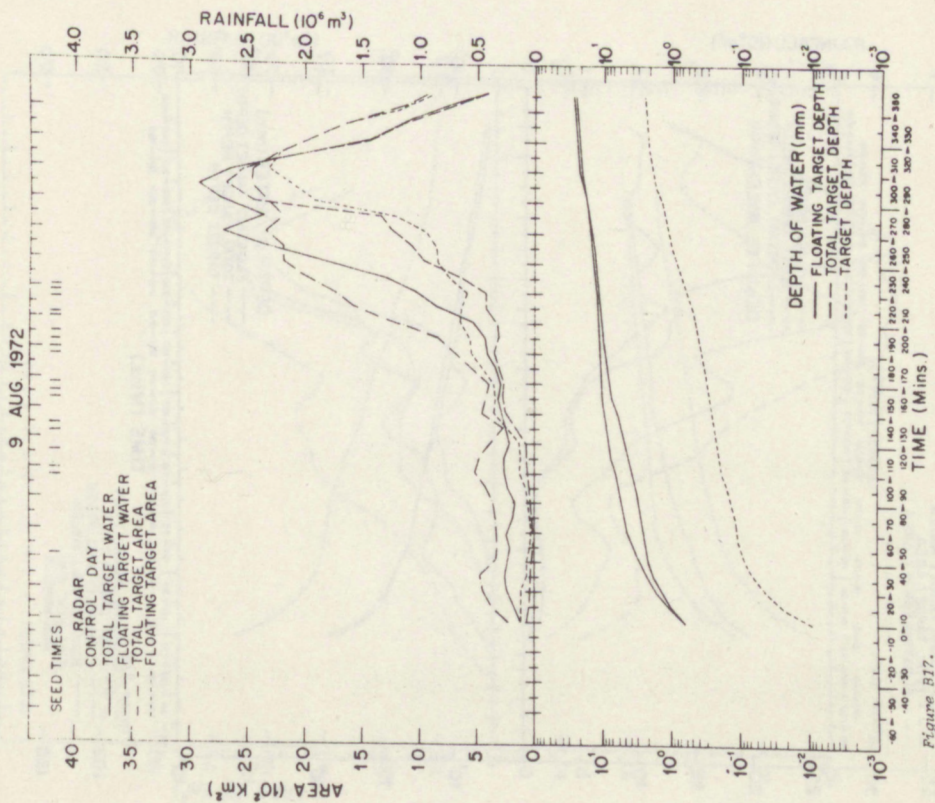


Figure B17.

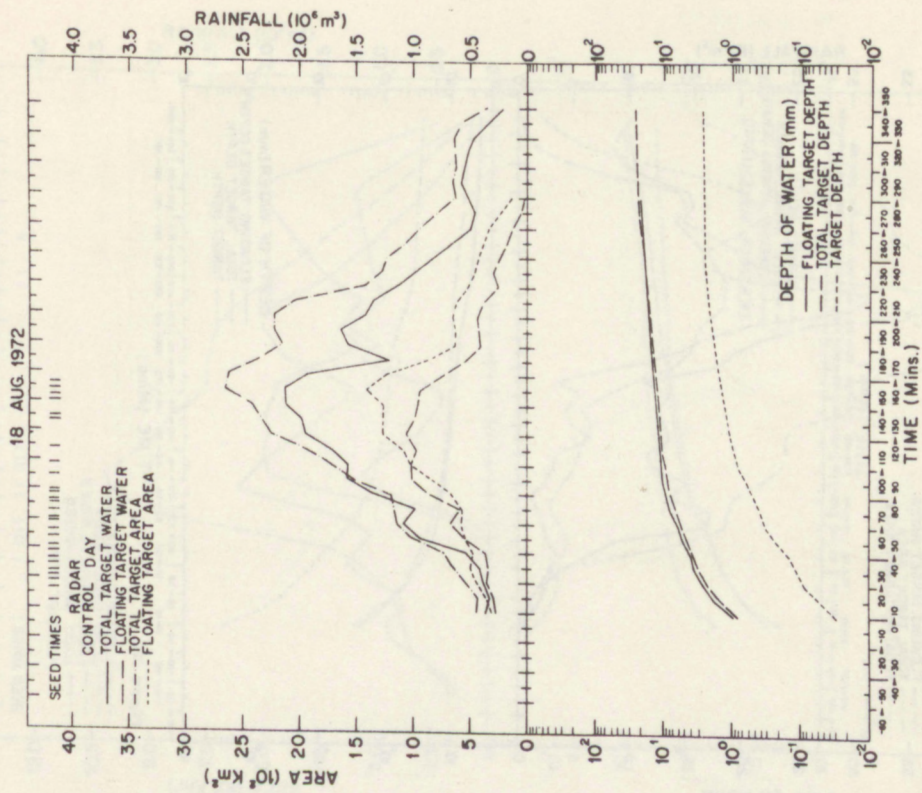


Figure B18.

26 JUNE 1973

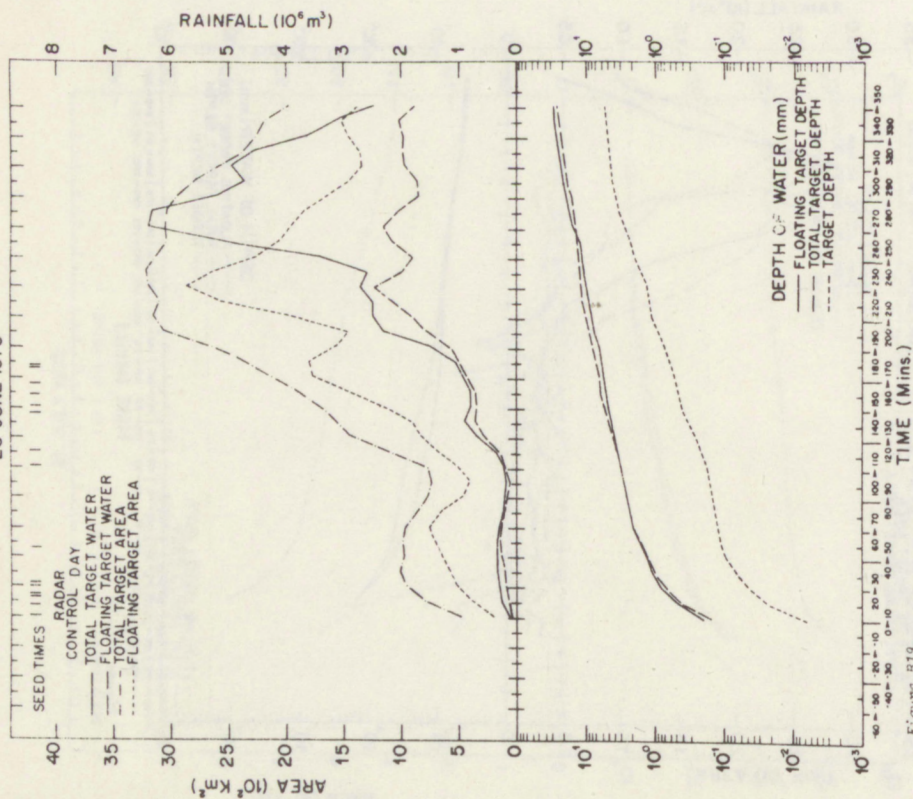


Figure B19.

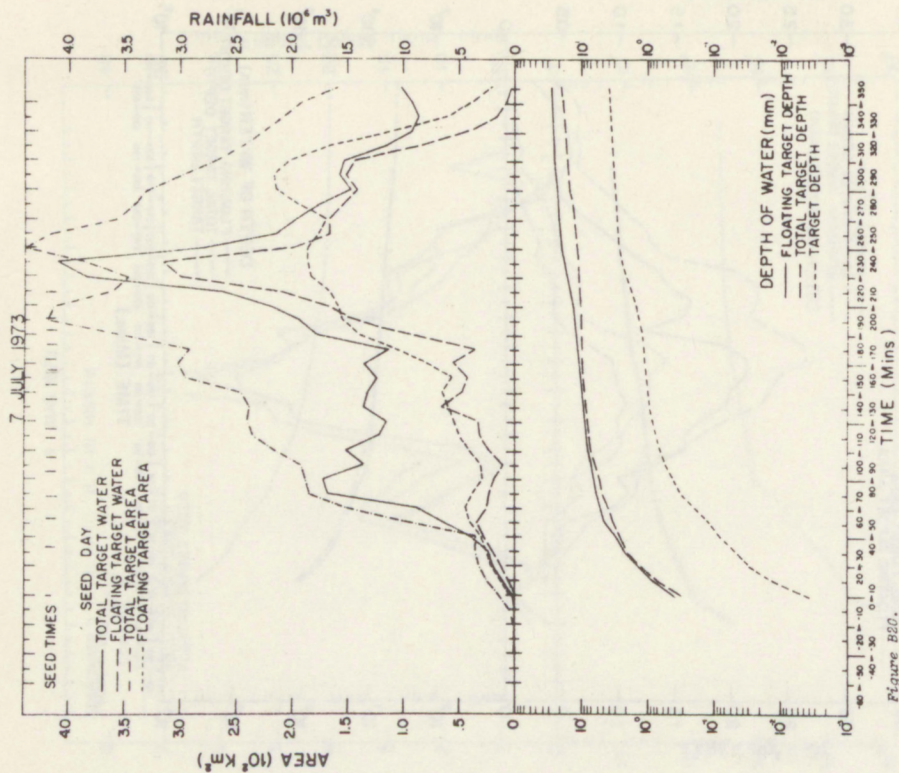
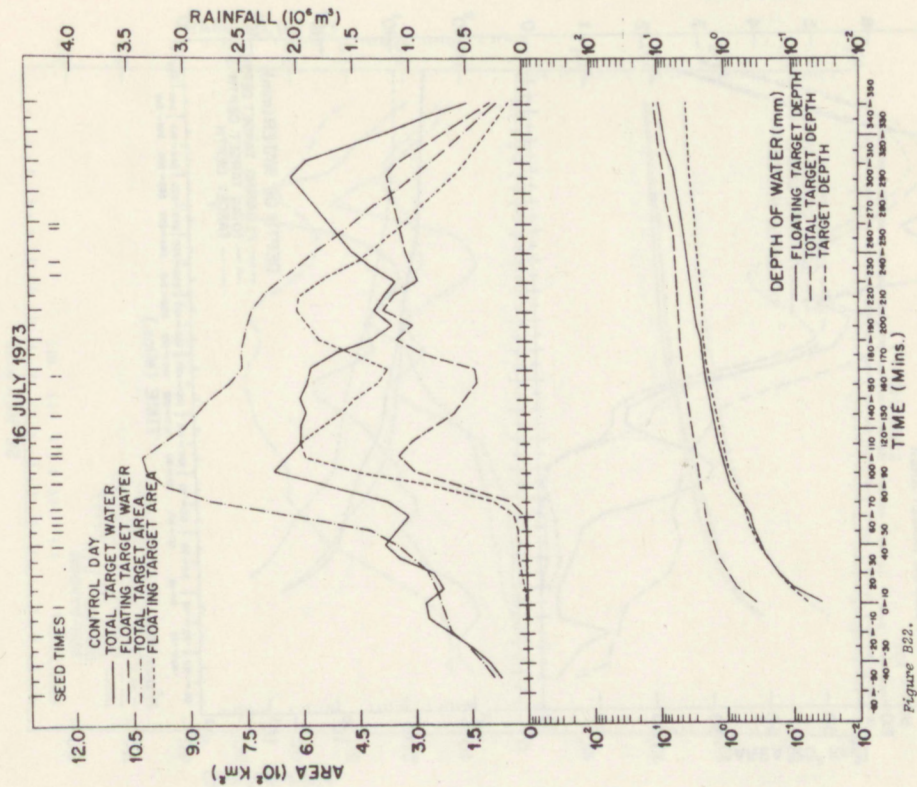
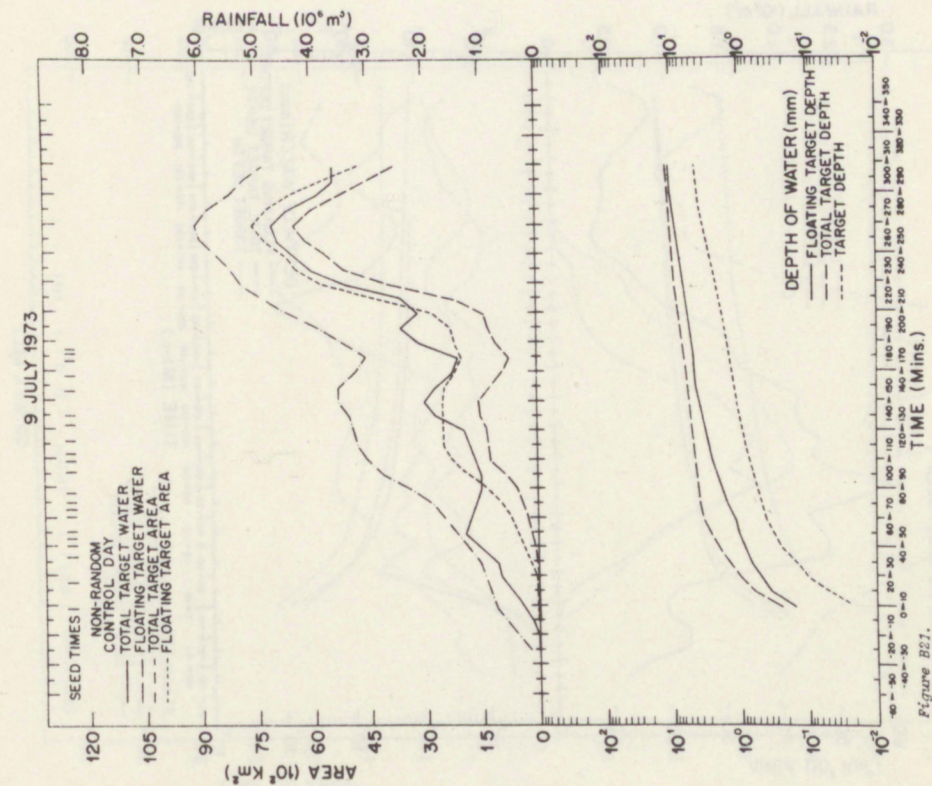


Figure B20.



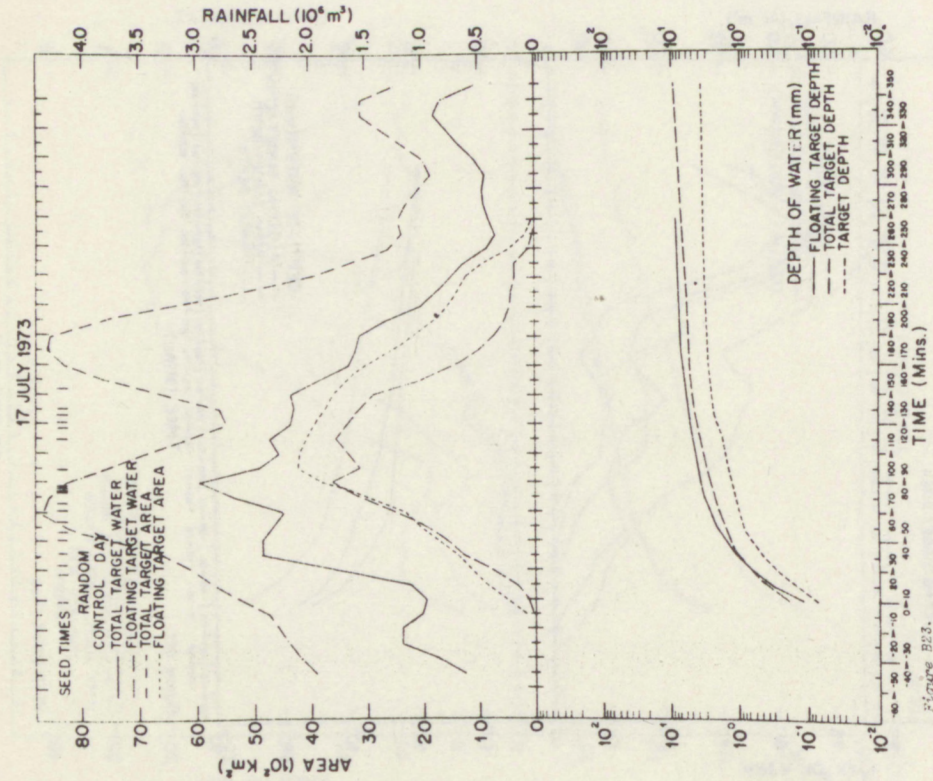


Figure B23.

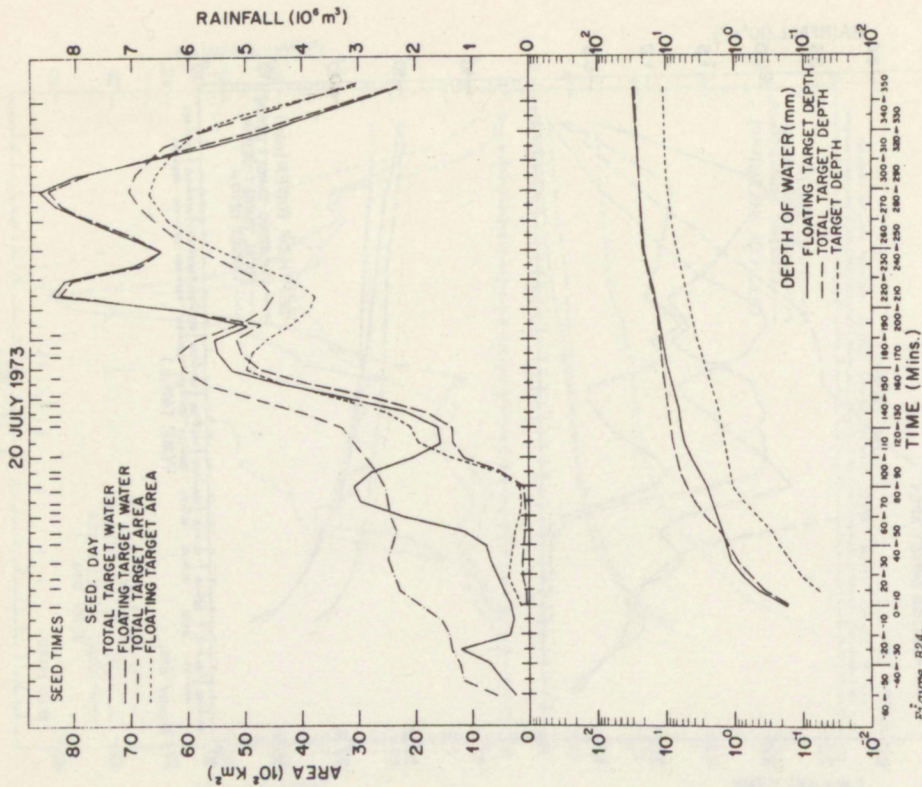
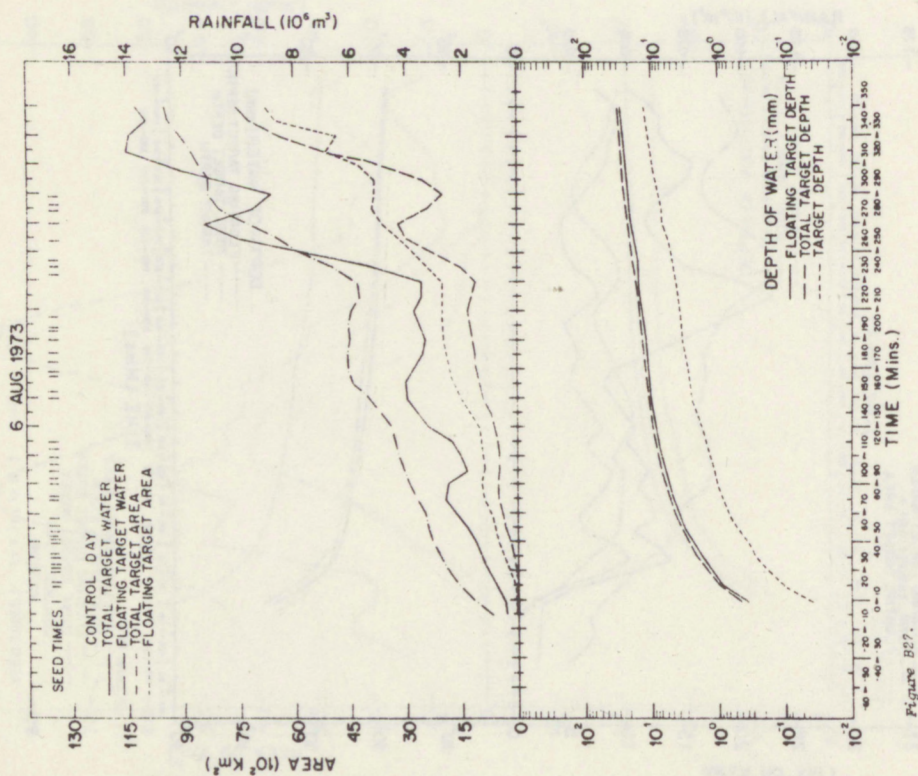
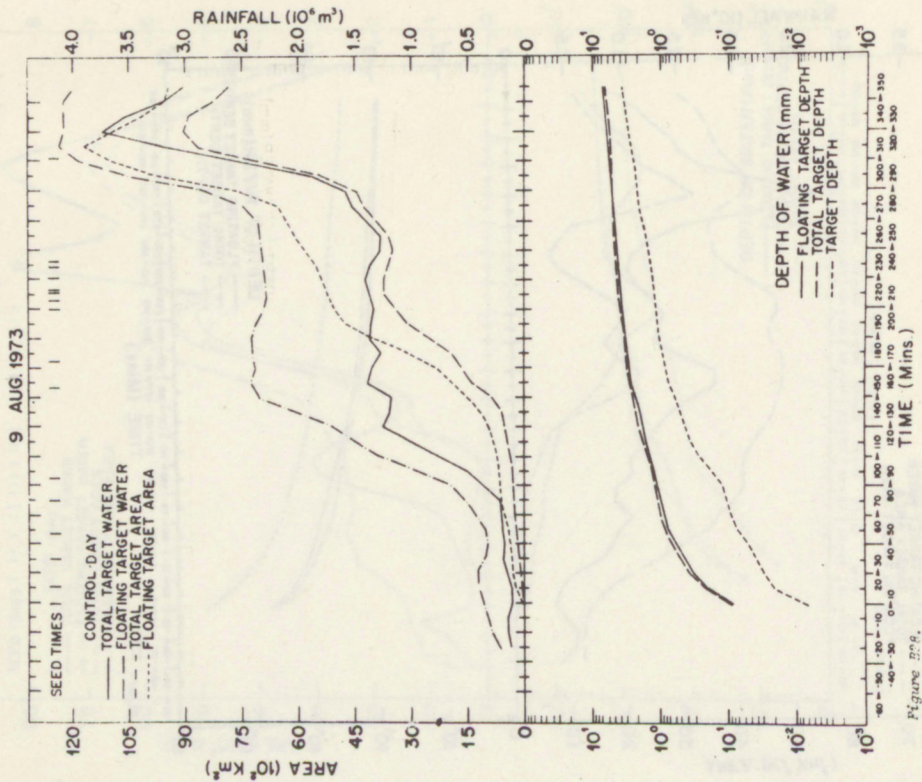
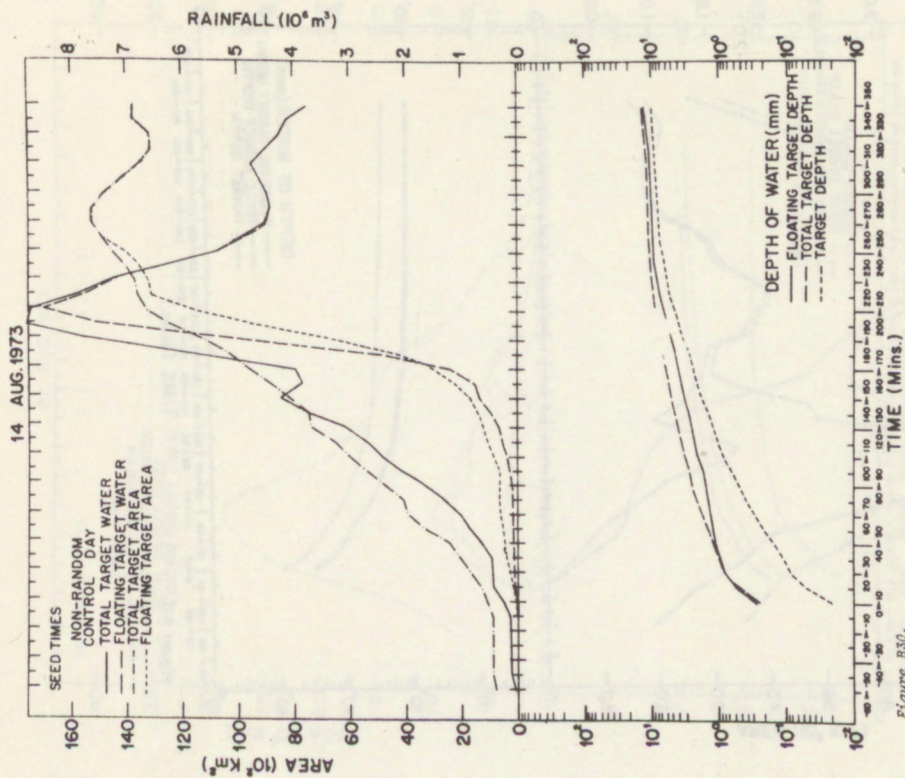
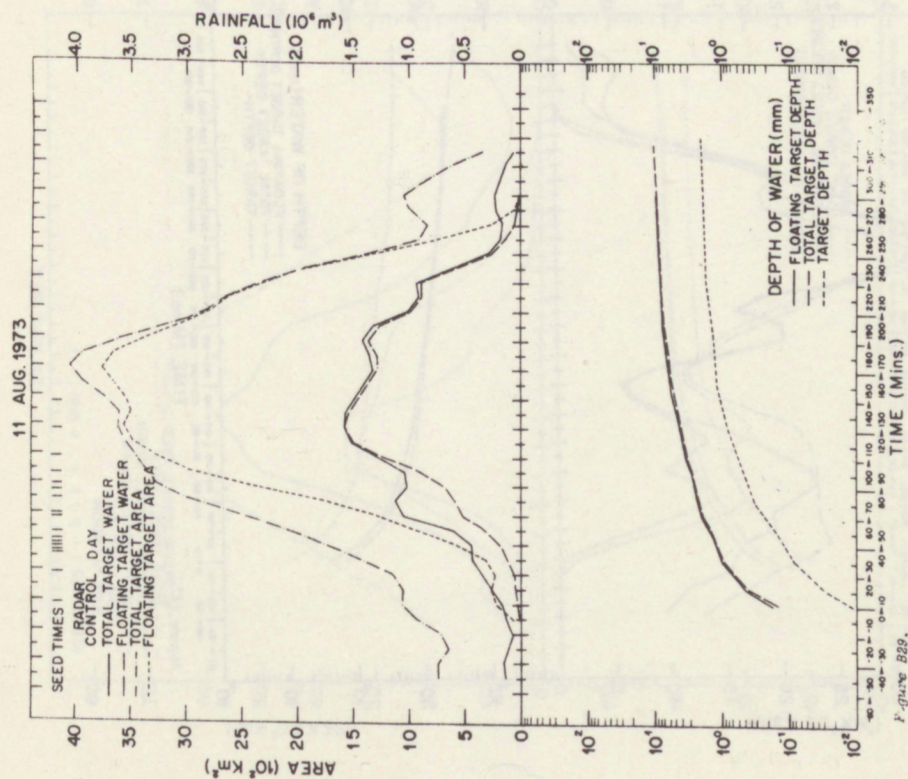
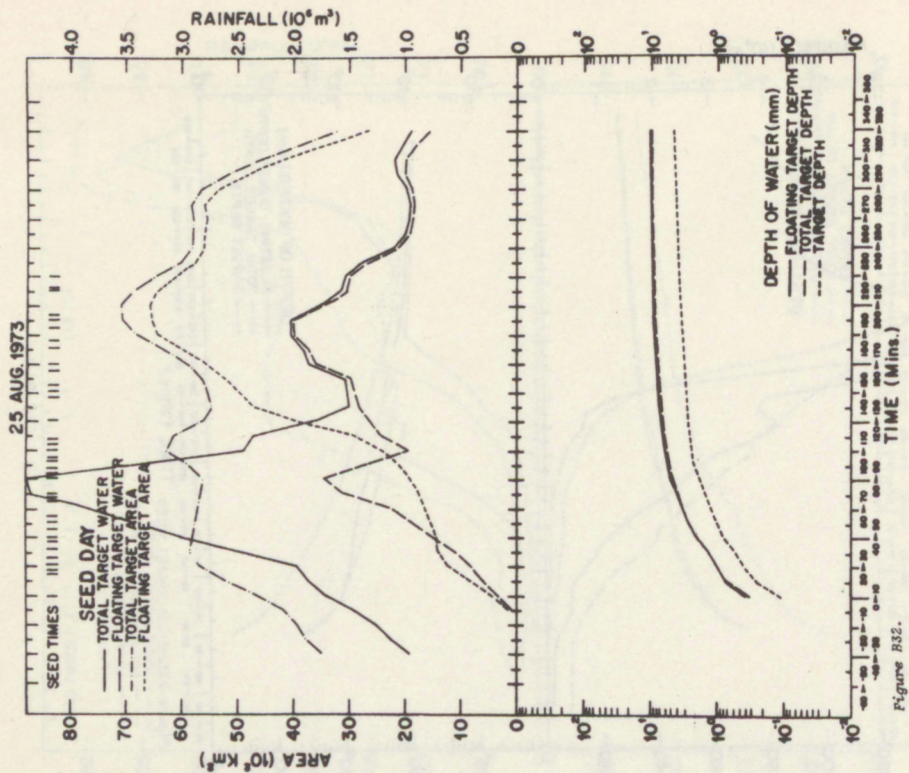
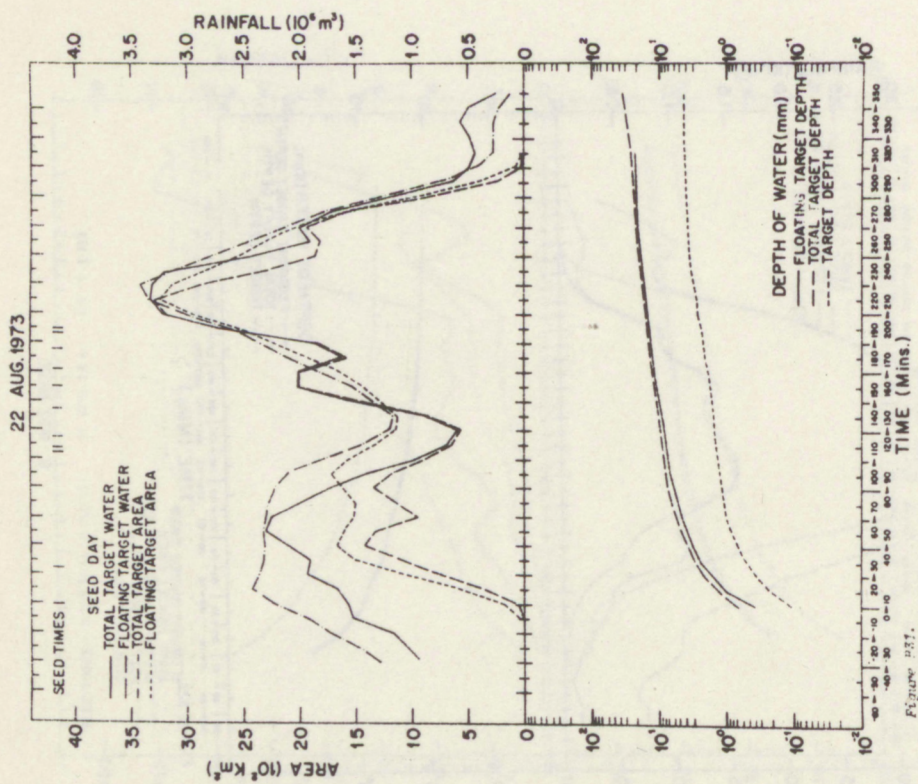


Figure B24.







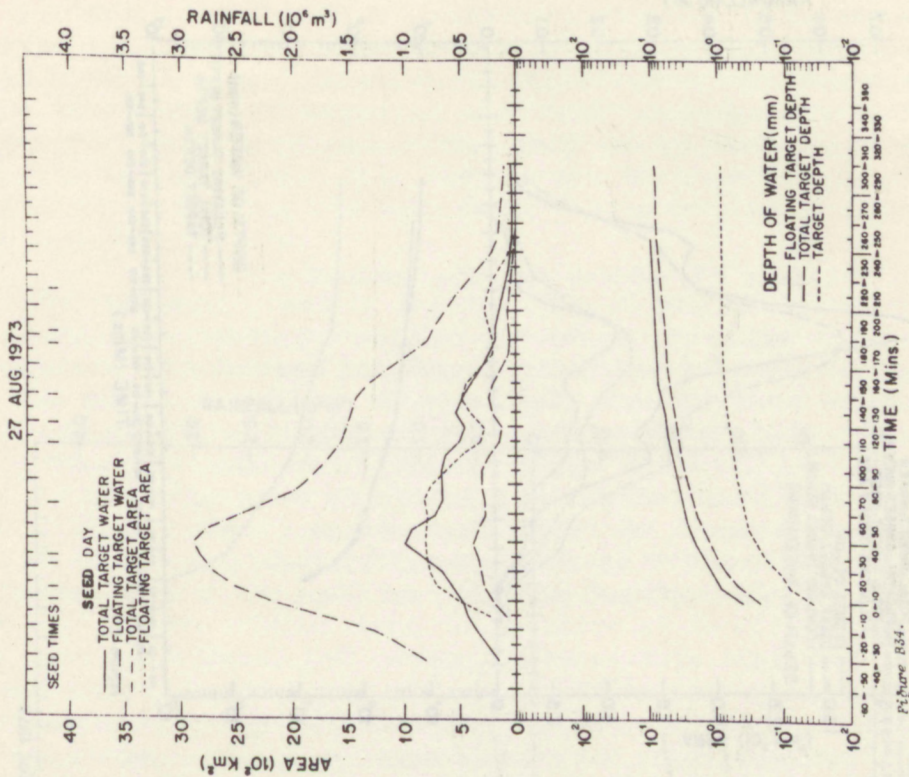


Figure B34.

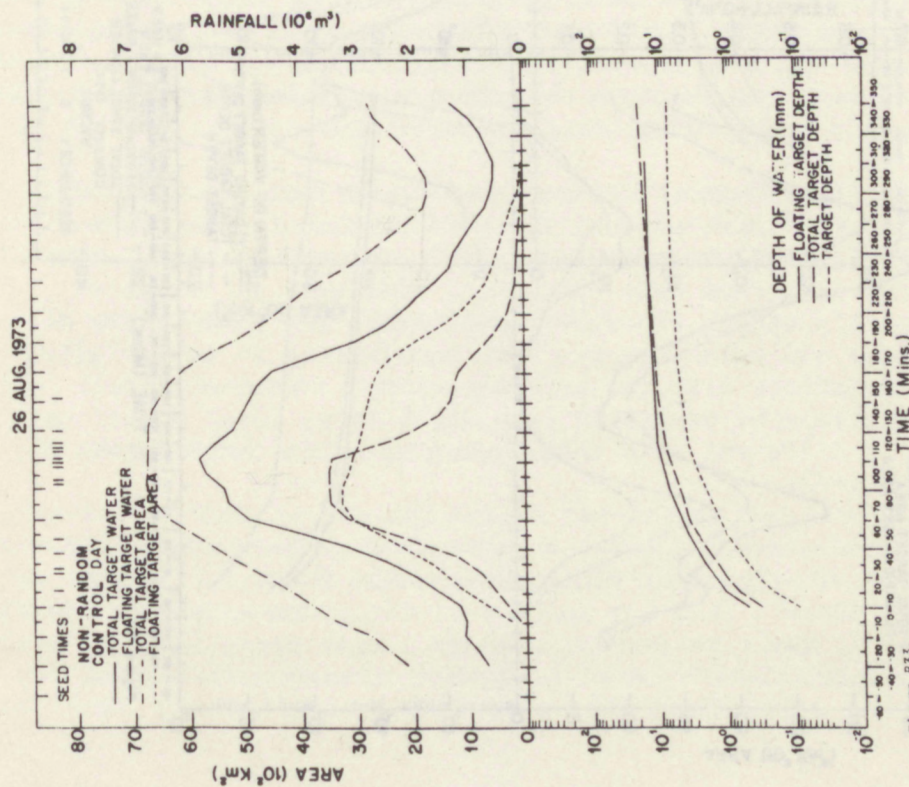
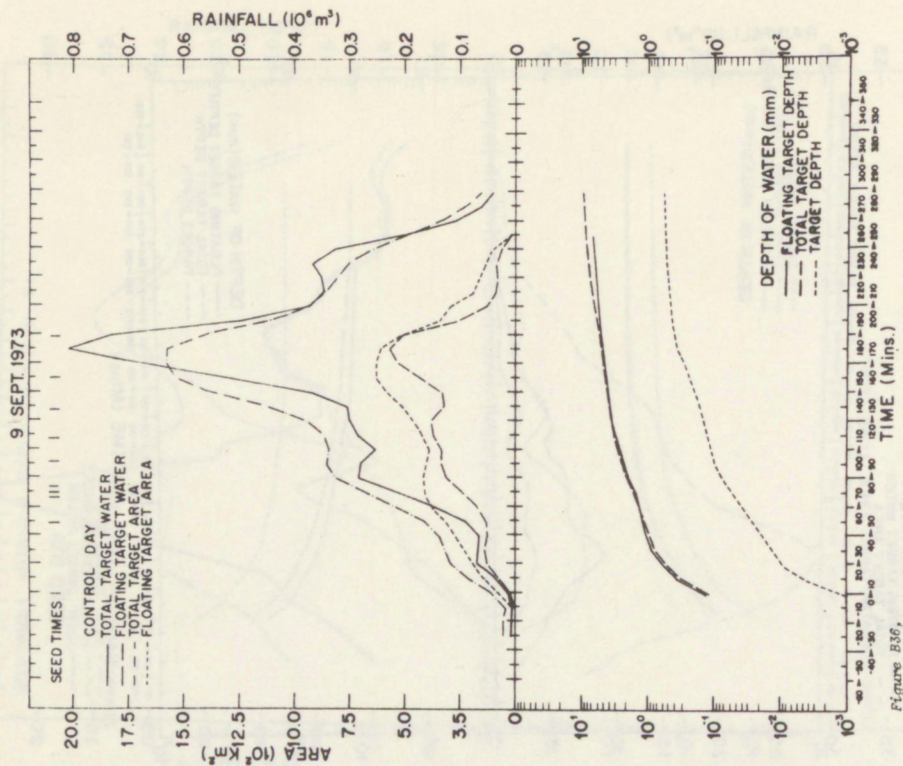
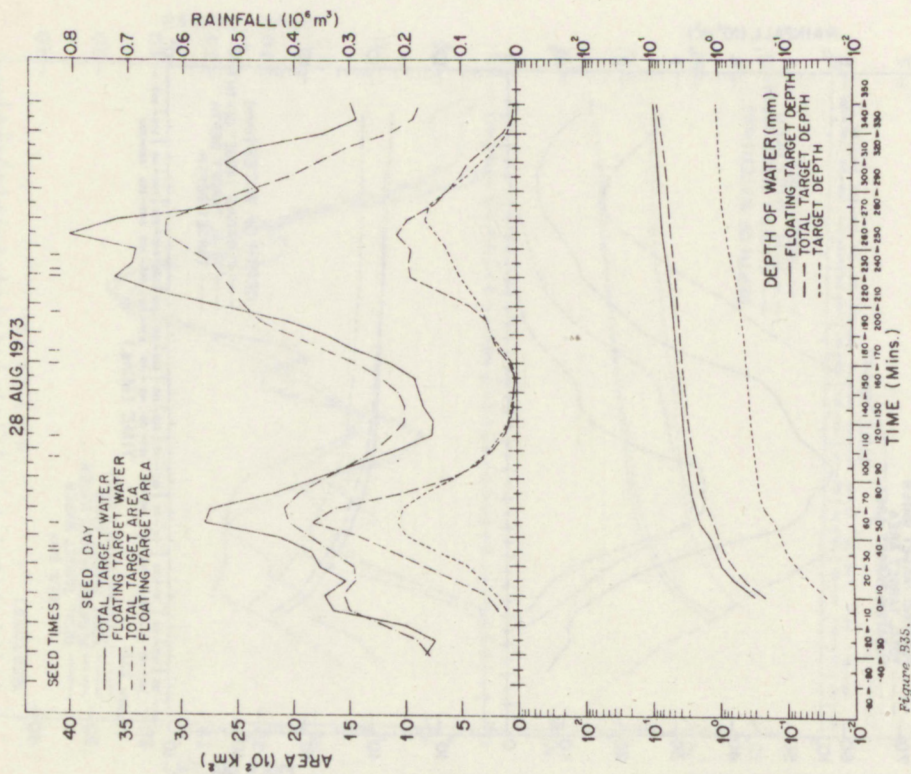


Figure B33.



10 SEPT. 1973

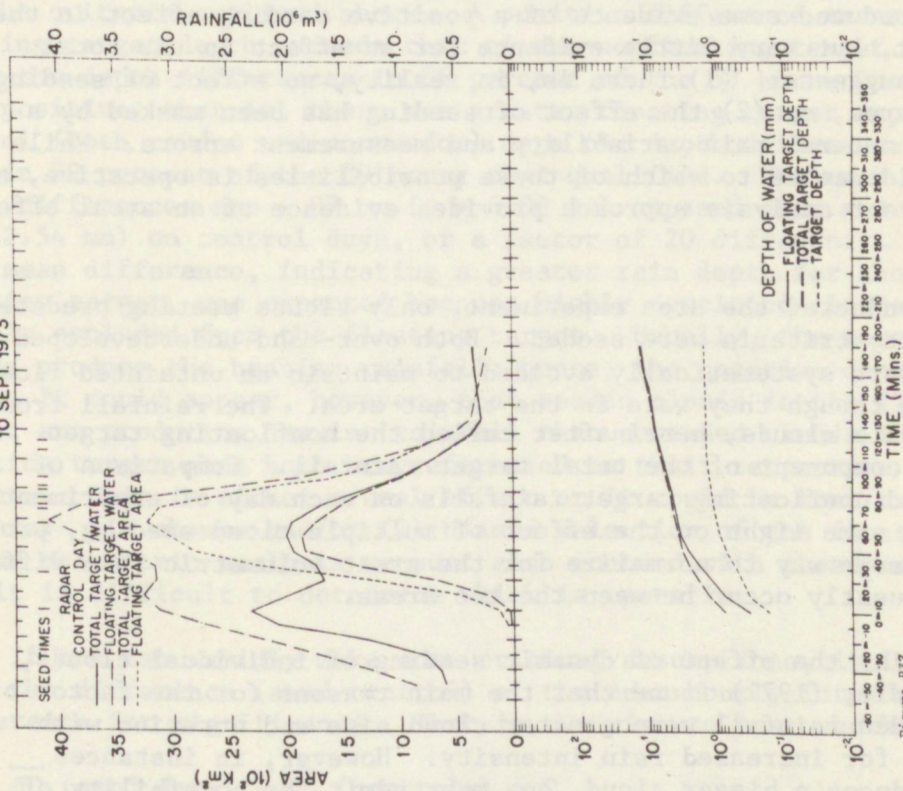


Figure B.37.

echo areas, none was made. With an increase in rain volume by a factor of 1.75 and no adjustment of echo area, the calculated floating and total target rain depths are spuriously large. They should not be compared to those calculated in other years. This does not apply to target rain depth because it is obtained by dividing rain volume by a fixed target area.

B.4 Effect of Seeding on Rain Intensity

The results of multiple cloud seeding to date have been examined by making volumetric rain comparisons between seed and control days. This approach has produced some evidence of a positive seeding effect in the floating target, but very little evidence for an effect in the total target. This suggests: (1) there is, in reality, no effect of seeding in the target area, or (2) the effect of seeding has been masked by a combination of natural rain variability and measurement errors. While there is no evidence as to which of these possibilities is operative, a somewhat different analysis approach provides evidence of an areal effect of seeding.

When we conducted the area experiment, only clouds meeting predetermined suitability criteria were seeded. Both over- and underdeveloped cloud systems were systematically avoided to maintain an untainted floating target even though they were in the target area. The rainfall from these unacceptable clouds, hereinafter called the nonfloating target rainfall, is a component of the total target rainfall. Comparison of the floating and nonfloating target rainfalls on each day of experimentation might shed some light on the effect of multiple cloud seeding, provided there is some way to normalize for the great volumetric rain differences that frequently occur between the two areas.

In evaluating the effect of dynamic seeding of individual clouds, Simpson and Woodley (1971) found that the main reasons for the factor of 3 increased seeded rainfall were greater cloud size and duration with little evidence for increased rain intensity. However, in instances when seeding induces a bigger cloud, one must admit the possibility of increased rain rates and rain depths. This possibility is investigated with the rain calculations from the area experiment. Fortunately, approaching the analysis by examining rain depth is an ideal way of normalizing for vastly different rain volumes and areas in the floating and nonfloating target areas.

Hourly rain depths were calculated for each day of experimentation for the 6 hours after real or simulated seeding for the floating and nonfloating target areas. This was done by dividing the hourly rainfalls in the two targets by their respective maximum target areas (over 10 min) within the hour. Thus, the effect of greatly differing rain volumes for

the two targets is removed by normalizing by the target areas. This removes the effect of differences in rain duration. Because this is an intraday comparison, this aspect also diminishes the importance of longer term radar inaccuracies. A further restriction was that the maximum rain coverage in one area had to be at least 5 percent of the rain area in the other. This restriction is intended to eliminate the absurdity of comparing the rain depth from a very small echo with that of a massive rain area.

The rain depth results for each day of multiple cloud experimentation are presented in table B3. The values presented are differences between the floating and nonfloating target depths for each hour that met the criteria outlined above. A positive difference means that the floating target depth exceeds that of the nonfloating target. On seed days, the depth differences in 56 percent of the 57 hours that qualified were positive; that is, there was greater floating target depth. On control (both random and nonrandom) days the depth differences were positive in 39 percent of the 89 hours that qualified. The mean hourly depth differences are $-.07$ mm ($\sigma = 6.00$ mm) on seed days and -1.39 mm ($\sigma = 2.54$ mm) on control days, or a factor of 20 difference. A negative mean difference, indicating a greater rain depth for the nonfloating target, was expected because highly developed clouds were frequently excluded from the floating target. Usually, the more massive clouds produce the heavier rainfall; hence, the negative depth difference. It would appear, however, that seeded clouds in the floating target are producing heavier rainfall than unseeded clouds in the floating target when both are referenced to their respective nonfloating targets. This is either a real effect or it could be from two other factors: (1) chance and/or (2) biased selection of the floating targets. In the volumetric analysis we must also contend with these uncertainties, and it is difficult to determine which is operative.

If one can validly make some critical assumptions, it is possible to test the difference (seed-control) of the mean hourly intraday depth difference for significance. That is, we wish to test whether:

$$\overline{\Delta D} \text{ (seed days)} - \overline{\Delta D} \text{ (controls)} = 0$$

against the alternative that

$$\overline{\Delta D} \text{ (seed days)} - \overline{\Delta D} \text{ (controls)} > 0$$

The one-tailed test is justified here because it has always been postulated that seeding would increase rain intensity to some extent, but that increased rain intensity was apparently not the major explanation for increased seeded rainfall.

To test, one must assume that the hourly mean depth differences are independent and that they come from normal populations. Usually, what

Table B3. Hourly Rain Depth Difference (D)

(Floating target depth - Nonfloating target depth)													
Seed ΔD (mm)							Control ΔD (mm)						
Hour w.r.t. Seeding	1	2	3	4	5	6	Hour w.r.t. Seeding	1	2	3	4	5	6
Date	Date						Date	Date					
7/07/73	3.00	-1.04	0.46	9.08	4.65	-0.72	8/06/73	-1.20	-0.05	-0.07	0.16	-2.03	0.57
7/20/73	-2.43	-29.2	5.13	--	3.22	--	8/09/73	-0.71	0.41	-0.38	1.24	0.08	-1.75
7/25/73	2.09	3.03	0.51	-0.76	0.42	4.75	7/26/73	-1.74	1.06	4.97	0.79	-0.24	2.43
8/22/73	9.44	0.62	1.10	--	--	--	6/26/73	1.46	1.65	1.47	14.84	-13.37	-5.65
8/25/73	-0.35	0.23	1.49	1.49	--	0.63	7/09/73	-6.18	0.84	-0.17	-4.69	-0.26	-0.81
8/27/73	1.50	-0.89	-0.11	0.02	--	--	7/16/73	-7.59	-4.89	-4.81	0.55	--	--
8/28/73	-0.09	-0.18	0.59	0.70	-0.30	--	7/17/73	1.30	2.28	2.08	-0.19	--	--
6/16/71	1.98	--	--	4.14	--	--	8/11/73	-1.34	--	2.55	--	--	--
7/13/71	--	--	3.34	-2.11	-5.78	3.61	8/14/73	-0.89	-2.49	-7.08	--	--	--
7/14/71	-0.21	3.46	7.08	-15.0	--	--	8/26/73	-0.34	1.75	-2.28	-1.42	--	--
6/29/70	-4.00	0.30	-2.70	0.50	--	--	9/09/73	2.17	0.62	-0.54	-1.67	--	--
7/18/70	--	-7.50	6.90	--	--	-5.00	9/10/73	-7.77	1.76	--	--	--	--
7/08/70	--	-14.7	8.50	4.50	-0.30	--	8/09/72	-0.80	-1.88	-1.34	1.54	-8.28	3.17
7/02/70	4.10	-5.70	-6.50	--	--	--	8/04/72	--	--	--	--	1.63	--
							8/18/72	2.35	0.97	-1.14	-0.45	-1.18	--
							7/01/71	3.22	0.82	-0.63	-4.81	--	--
							7/12/71	-0.27	-1.43	--	--	--	--
							7/15/71	1.67	2.16	2.02	--	--	--
							7/16/71	-0.23	1.13	-1.56	7.28	-4.43	--
							6/30/70	-11.50	-5.50	-7.20	-11.35	-3.88	--
							7/07/70	-6.70	-9.40	-0.90	-14.90	-15.30	--

$n = 57$
 $\Delta D = -0.07$ mm
 $\sigma = 6.00$ mm

n = 89
 $\Delta D = -1.39$ mm
 $\sigma = 2.54$ mm

n = 57
 $\Delta D = -0.07$ mm
 $\sigma = 6.00$ mm

-- Precipitation Area in either FT or N-FT; < 5% of other

one assumes about the variances is critical, but in this case it makes little difference whether one assumes that the variances are known, or equal but unknown. The crucial question would appear to be the independence of the hourly rain differences within a day. Examination of the hourly depth differences (table B1) for each day reveals a rather surprising lack of correlation of the sign of the depth difference from 1 hour to the next. This gives weight to the assumption of independence.

The development of the test and its use for problems of this type is described by Gutman and Wilks (1965; pp. 165-169). The test examines the means of two normal distributions having either known, or equal but unknown, variances. Substitution of the appropriate parameters into the test equations yields a test statistic between 1.40 and 1.50 depending on the assumption about the variances, which suggests ΔD (seed) and ΔD (control) are different at the 5 to 10 percent levels of significance.

Test details are not important here, nor is more sophisticated testing warranted. The important fact gleaned from this exercise is further evidence of an effect of seeding. However, somewhat increased rain intensity does not necessarily mean an overall increase in rainfall in the target area. This crucial question must still be resolved.

APPENDIX C

CHARACTERISTICS OF THE NUCLEATING AGENT

C.1 Modes of Nucleation of a Silver-Iodide Aerosol

In general, the effectiveness of a substance as an ice nucleus is determined by its ability to force adsorbed or condensed water molecules to assume an ice-like configuration. This may be a result of the crystalline lattice structure in the case of inorganic compounds, or the nature and configuration of exposed bonding groups in the case of organic compounds. Other physical or chemical properties such as ionic structure and surface topography also play a role. Since its discovery as an ice-nucleating agent in 1947, silver iodide (AgI) has been found to have the highest activation temperature (about -4°C) of any inorganic compound tested.

A nucleating substance can be activated in the atmosphere in at least three principle ways ("immersion freezing," "depositional freezing," and/or "contact freezing"). If the particle is large enough, or contains soluble material, a layer of liquid can condense on its surface. This liquid layer can subsequently be nucleated as the particle is carried upward into colder temperatures. This process has been termed "immersion freezing" since the nucleating material is completely immersed within a layer of liquid before the onset of nucleation. For a particle to be activated while immersed in bulk liquid, it is necessary that the rate of dissolution of the substance in relation to the rate of nucleation not be great enough to destroy the surface or structural features that enable the material to be effective as an ice nucleus. Silver iodide is hydrophobic and very nearly insoluble (3×10^{-7} grams in 100 ml in cold water). These characteristics theoretically make it very difficult for submicron-sized particles of pure AgI to acquire a liquid layer through condensation at the very small supersaturations likely to be encountered in the atmosphere (see Fletcher, 1962). Once immersed, however, pure AgI particles will dissolve relatively slowly. Mathews et al. (1972) have calculated that a $0.01 \mu\text{m}$ particle of pure AgI can survive for more than 5 minutes immersed in a cloud droplet in excess of $40 \mu\text{m}$. However, if the AgI particle is complexed with more soluble material, as is oftentimes the case in ordinary generation procedures, it is not likely that even $0.1 \mu\text{m}$ particles can survive for more than a fraction of a second if immersed in cloud droplets of $10 \mu\text{m}$ or greater. The implications of this theoretical work relating the time needed to completely dissolve (and hence definitely deactivate) AgI particulate matter to the nucleating behavior of artificially-produced AgI aerosol is controversial³¹, but suffice it to say that the longer the material is immersed within liquid water, the less likely that it will be effective as an ice nucleating agent. It would appear, therefore, that

³¹For example, Pueschel et al. (1974) report experiments indicating that the rate of solution of submicron AgI particles is slow enough to preserve their efficiency for several hours while floating on a water substrate.

immersion freezing in the atmosphere has relevance to an AgI aerosol only if the particles are complexed with soluble material and only if they are injected directly into the regions of cloud that are supercooled to temperatures colder than -4°C . In this case, the particles should not be smaller than about $0.1\mu\text{m}$ for optimum effectiveness, and the order of 10^{14} of $0.1\mu\text{m}$ particles can be produced from 1 gram of AgI material.

It has been determined experimentally in the laboratory (Bryant et al., 1959) that at supersaturations in excess of 12 percent with respect to ice (but subsaturated with respect to water) ice could form on an AgI crystalline substrate if the temperature was colder than -12°C . At warmer temperatures or at lower supersaturations no ice was found to form. Since the environment was subsaturated with respect to water, it was logically assumed that the ice was formed by a direct vapor to solid phase change, and the term "deposition freezing" has been coined to describe the mechanism for this type of nucleation. It is possible that the vapor first passes through a transitory liquid phase as molecules are adsorbed into cracks and crevices on the surface of the nucleating substrate, and the term "sorption freezing" is preferred by some to account for this possibility. It has long been considered that regardless of whether nucleating by a deposition or a sorption mechanism (really only an academic distinction) an AgI aerosol owes its great effectiveness at temperatures of about -12°C or colder, at least in part, to a process which can transfer molecules from the vapor to the solid phase. The difficulty arises in extrapolating this type of process to temperatures warmer than -10°C a range of considerable interest to scientists involved in cloud physics or cumulus modification work. From both theoretical calculations and experimental studies, it would appear that submicron-sized AgI particles would have difficulty in causing nucleation through deposition in water-saturated conditions at temperatures warmer than about -10°C . Edwards and Evans (1960) have shown in the laboratory that $0.01\mu\text{m}$ AgI particles are ineffective as sorption nuclei even at -18°C until the humidity relative to water exceeds 110 percent. However, note that because of the large number of particles produced (typically 10^{14} or more per gram of AgI), even if only one in 10^6 (a fraction well below experimental detection) were active by a deposition mechanism there could easily be on the order of 10^8 particles per gram of AgI effective as ice nuclei.

The direct contact of a nucleating substance with a supercooled water droplet is the final mode of nucleation considered here. Sulakvelidze (1969) describes an experiment in which submicron-sized particles of AgI were allowed to coalesce by Brownian diffusion with millimeter-sized water drops suspended in a small cold chamber. It was found that if the AgI aerosol came into contact with the drop at temperatures warmer than -4°C subsequent lowering of the temperature in the chamber did not cause the drop to nucleate until -13°C had been reached. If, however, the AgI aerosol first contacted the drop at temperatures colder than -5°C nucleation occurred immediately. The first case would correspond to an "immersion" type of freezing process, while the second case is referred to as "contact" freezing. Although it is not universally accepted that AgI particles have

higher activation temperatures if allowed to come into direct contact with supercooled drops, the laboratory evidence tends to indicate that such is the case. Sax and Goldsmith (1972) have demonstrated that 1 percent of AgI particles as small as $0.01\mu\text{m}$ are effective as contact nuclei at a temperature of -10°C , 10 percent at -13°C , and 100 percent by -16°C . Contact nucleation may have great importance in the atmosphere because, unlike immersion or deposition processes in which the likelihood of nucleation theoretically decreases markedly with decreasing particle size, the probability of a freezing event actually increases with a decrease in size of the aerosol material. This is due to the far great mobility of small-sized particles. Since most of the atmosphere's natural aerosol is composed of particles in the submicron size range, the probability for interaction with cloud droplets is fairly reasonable on the time scale of cloud processes. In the case of an artificial AgI aerosol, it is shown in the next subsection that a large proportion of particles produced from pyrotechnics are in the size range ($0.01\mu\text{m}$ to $0.1\mu\text{m}$) conducive to an effective contact nucleation mechanism.

C.2 Size Distribution of the AgI Pyrotechnic Aerosol

Parungo et al. (1974) have reported the results of rather extensive pyrotechnic sampling tests conducted in a wind tunnel at an air velocity of 75 m/sec (roughly equivalent to the terminal velocity of the pyrotechnic shortly after ignition). The AgI aerosol was sampled directly with Millipore or Nucleopore filters, and indirectly by passage through a thermal precipitator. With isokinetic flow through the filters, little difference in the size spectra using the various sampling techniques was noted. Sizing analysis was carried out by means of the NCAR transmission electron microscope. The size spectrum of AgI particles produced during the burn of an Olin-Mathieson X-1055/WM105 pyrotechnic (the type and composition exclusively used in the FACE program through 1973) is shown in figure C1. The modal diameter is $0.05\mu\text{m}$, the mean diameter is $0.12\mu\text{m}$ and the median diameter is $0.09\mu\text{m}$. The best-fit curve is in fair agreement with the generalized aerosol size distribution (dotted curve in fig. C1) described by Khigrin and Mazin (1956) which takes the form:

$$n(r) = ar^2e^{-br} \quad (C1)$$

with $b = 3/\bar{r}$ and \bar{r} the mean radius. Some discrepancy between the two curves can be observed at the larger particle sizes, but this deviation may well be due to measurement problems associated with proper identification of the individual components of a coagulated mass of particles.

From the distribution shown in figure C1, we can calculate that 96 percent of the total number of particles are smaller than $0.1\mu\text{m}$ in radius. It can be expected, therefore, that at the supersaturations of less than 2 percent typically encountered in the atmosphere, water could condense on only about 4 percent of any pure AgI particles emitted by this pyrotechnic. Even if the emitted particulate matter is complexed with enough soluble material

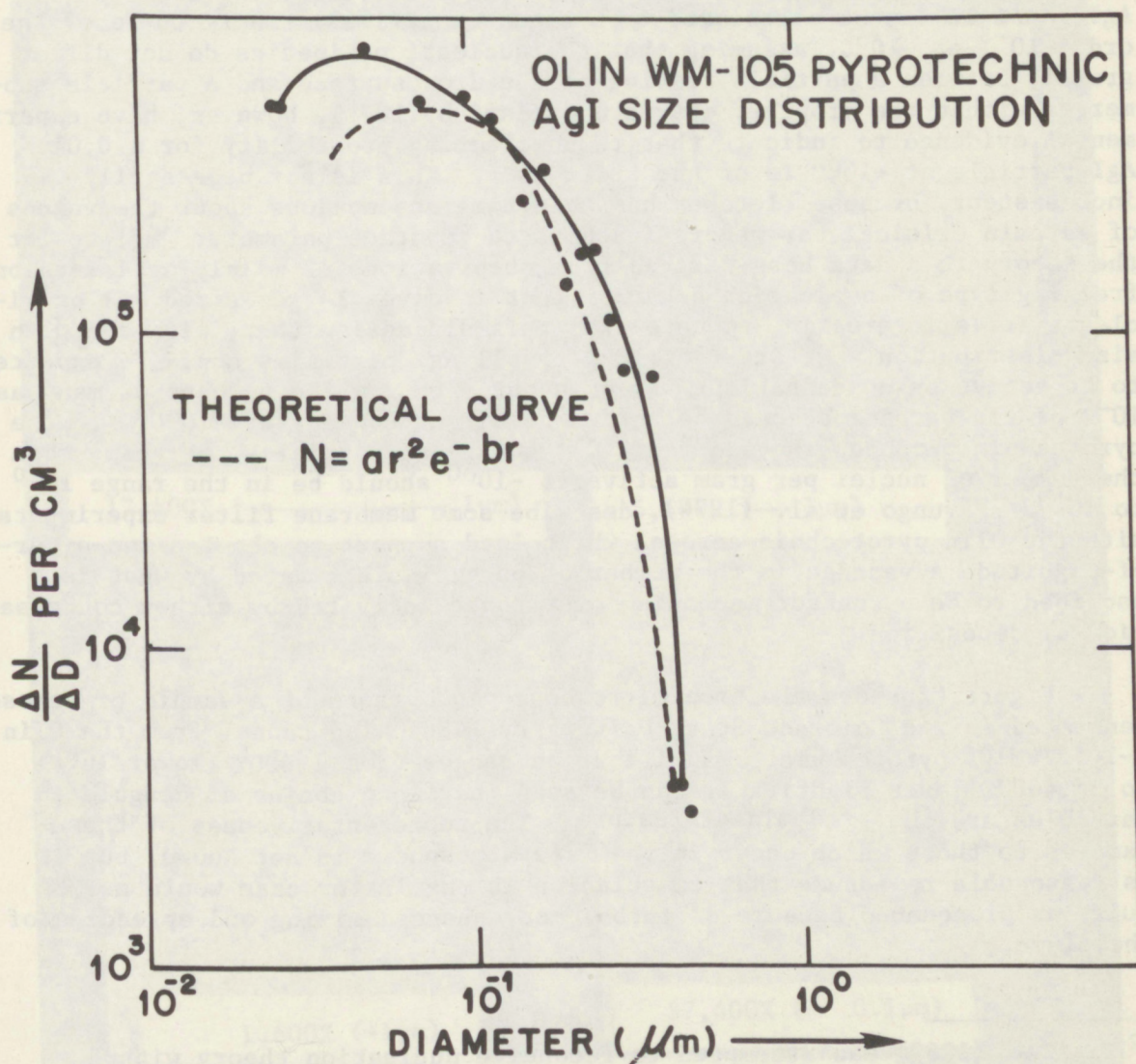


Figure C1. Size distributions of AgI particles produced from the Olin X-1055/WM105 pyrotechnic; theoretical Khrgran-Mazin distribution included for comparison.

to permit condensation to occur, calculations³² by Fletcher (1969) show that the probability of a $0.1\mu\text{m}$ particle being activated once immersed in water is no better than 10^{-3} at -10°C . On the other hand, over 50 percent of the total number of particles produced have a radius smaller than $0.05\mu\text{m}$, and these possess a mobility (diffusion coefficient) great enough to have about a 50 percent probability of coming into direct contact with a cloud droplet within a time span of a half hour by a Brownian diffusion process. The nucleating probability for a $0.01\mu\text{m}$ AgI particle can be calculated from Fletcher's (1969) theory to be of the order 10^{-5} at -10°C , assuming that the nucleation kinetics do not differ greatly between a particle resting on the drop surface and a particle submerged within the droplet. Sax and Goldsmith (1972), however, have experimental evidence to indicate that the nucleating probability for a $0.01\mu\text{m}$ AgI particle at -10°C is of the order 10^{-2} . This is not necessarily inconsistent, because Fletcher has made some assumptions about the values of certain critical parameters (such as the contact parameter "m") to fit the theory to a data base derived from observations of mainly an immersion freezing type of nucleating behavior that involves larger sized AgI particles. It is interesting to note from this discussion that, with the Olin size distribution, the order of 10^{-5} of all AgI particles could be expected to be active by condensational freezing at -10°C , while perhaps as many as 10^{-2} of the particles could be active by direct contact at -10°C . If the pyrotechnic produces the order of 10^{15} total AgI particles per gram, then the number of nuclei per gram active at -10°C should be in the range 10^{10} to 10^{13} . Parungo et al. (1974) describe some membrane filter experiments with the Olin pyrotechnic aerosol which lend support to about a two-order-of-magnitude advantage in the number of particles activated by what is ascribed to be a contact mechanism over those activated by either condensation or deposition.

Figure C2 shows electron microscope photographs of a sample of aerosol generated in the Colorado State University (CSU) wind tunnel from the Olin X-1055/WM105 pyrotechnic. Magnification ranges from 1,600X (lower left) to 37,400X (lower right). It can be seen that long chains of coagulated particles are the predominant feature. The representativeness of these samples to those which occur in the free atmosphere is not known, but it is reasonable to assume that coagulation in the latter case would not be quite as pronounced because of turbulence-enhanced mixing and spreading of the plume.

³²Fletcher (1969) has attempted to reconcile nucleation theory with experimental evidence indicating that a range of probabilities exist for a given size particle to act as an ice nucleus at a given temperature. By assuming a log-normal distribution of very active sites (physically interpreted as re-entrant cavities and mathematically interpreted as conical pits) upon the surface of a particle, one can derive immersion nucleating probabilities for a $0.1\mu\text{m}$ AgI particle ranging from 10^0 at -17°C to 10^{-3} at -10°C .

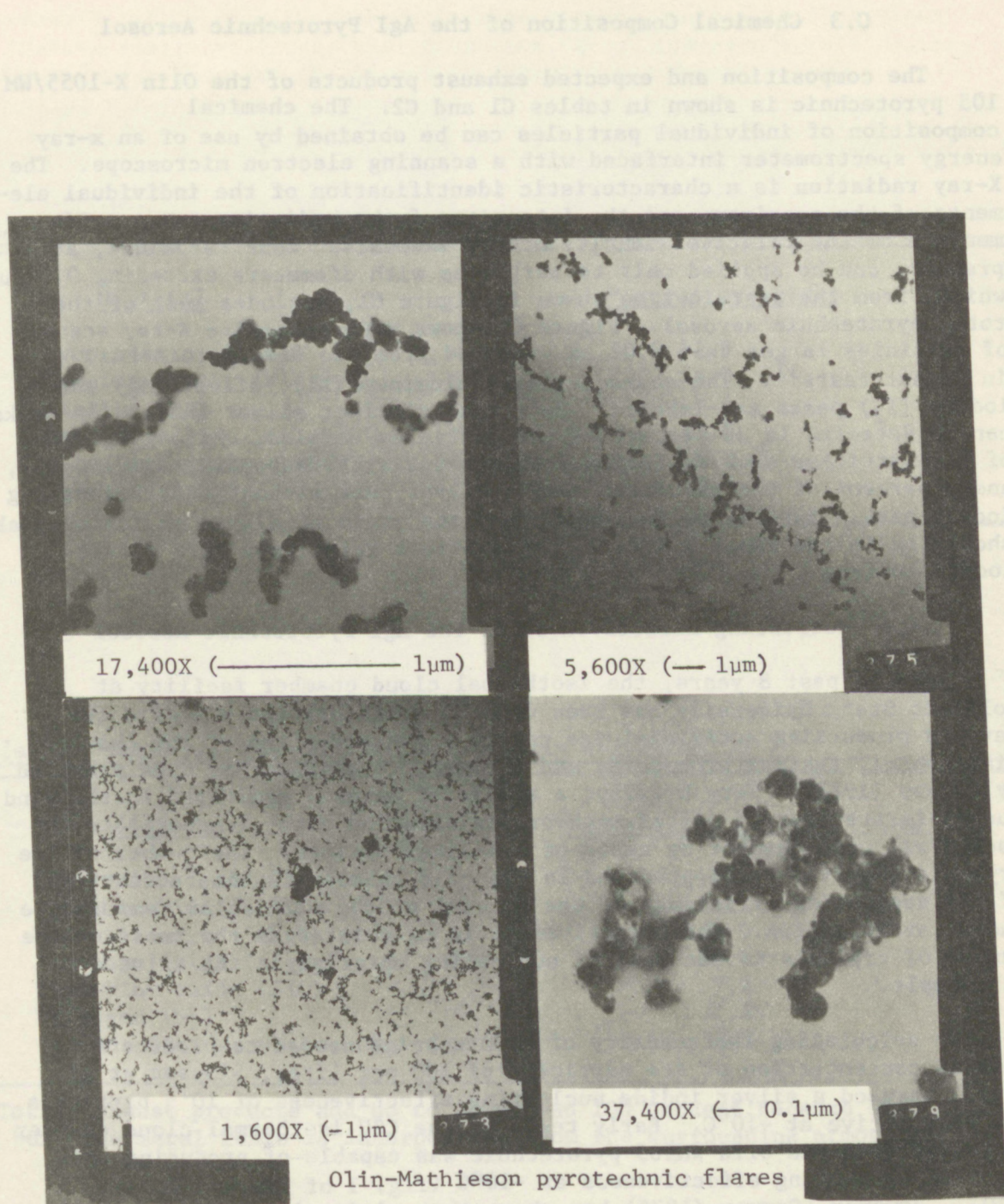


Figure C2. Electron microscope photographs of various magnification showing aerosol produced during burn of Olin X-1055/WM105 pyrotechnic. (Courtesy of NOAA/APCL.)

C.3 Chemical Composition of the AgI Pyrotechnic Aerosol

The composition and expected exhaust products of the Olin X-1055/WM 105 pyrotechnic is shown in tables C1 and C2. The chemical composition of individual particles can be obtained by use of an x-ray energy spectrometer interfaced with a scanning electron microscope. The X-ray radiation is a characteristic identification of the individual elements of the specimen, and the intensity of the radiation can provide a measure of the relative quantity of the elements. This technique, at present, can be applied only to particles with diameters exceeding $0.02\text{ }\mu\text{m}$ which, from the distribution shown in figure C1, includes most of the total pyrotechnic aerosol. Figure C3 shows representative X-ray scans of particles larger than $0.02\text{ }\mu\text{m}$ produced from the Olin pyrotechnic in recent tests³³. The characteristic aluminum (Al), silver (Ag) and iodine (I_2) peaks are labeled. Note that distinct silver and iodine peaks can be detected in 80 percent of the particles sampled, while 15 percent of the particles show an iodine peak without a corresponding silver peak, and 5 percent of the particles show a silver peak without a corresponding iodine peak. Experience indicates that the ratio of silver to iodine peaks should be in the range 1.4 to 1.8 to insure a relatively pure silver iodide surface.

C.4 Nucleating Effectiveness of the AgI Pyrotechnic Aerosol

For the past 8 years, the isothermal cloud chamber facility at Colorado State University has been used as a calibration standard for devices producing artificial ice nuclei. A description of the chamber, wind tunnel, testing procedure, and analysis techniques has been provided by Garvey (1975). Very briefly, a sample of aerosol generated in the wind tunnel is transferred (after appropriate dilution with clean air) to the isothermal cold chamber by means of a 4-liter syringe. The number of ice crystals observed to be produced in the cold chamber is then a function of the nucleating efficiency of the aerosol at the particular temperature under investigation. The effectiveness is calculated as the ratio of the number of crystals to the mass of nucleating material in the diluted air sample.

In calculating the quantity of pyrotechnics needed to produce a desired concentration of ice particles of 100 per liter, Simpson et al. (1970) assumed a silver iodide nucleating effectiveness of 10^{12} particles per gram active at -10°C . Early tests in the CSU isothermal cloud chamber indicated that the Olin WM105 pyrotechnic was capable of producing this required nucleating effectiveness at -10°C (fig. 1 of Simpson et al., 1970). However, Garvey (1975) has shown that mixing in the wind tunnel is not almost instantaneous as had been assumed in the early tests. As a result, the sample of aerosol transferred to the cold chamber is actually much more concentrated than had been calculated in

³³Conducted in May 1975.

Table C1. Composition of Olin X-1055/WM105

<u>Material</u>	<u>Percent by weight</u>
Silver iodate (AgIO_3)	53.0
Potassium iodate (KIO_3)	8.0
Magnesium (Mg)	5.6
Aluminum (Al)	12.9
Strontium nitrate $\text{Sr}(\text{NO}_3)_2$	10.5
Polyester binder	10.0

Table C2. Expected Exhaust Products of Olin X-1055/WM105

<u>Compound</u>	<u>Percent (gm per gm of mix)*</u>
Silver iodide (AgIO)	44.0
Potassium iodide (KI)	6.1
Magnesium oxide (MgO)	9.5
Aluminum oxide (Al_2O_3)	24.1
Strontium oxide (SiO)	7.2
Nitrogen (N_2)	1.4
Carbon dioxide, water, etc.	31.7

* Total exhaust products add up to more than 100 percent because some oxygen to burn the metal fuels is incorporated from the surrounding atmosphere.

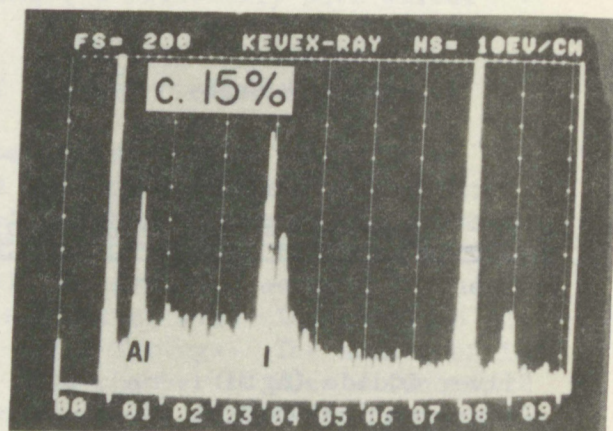
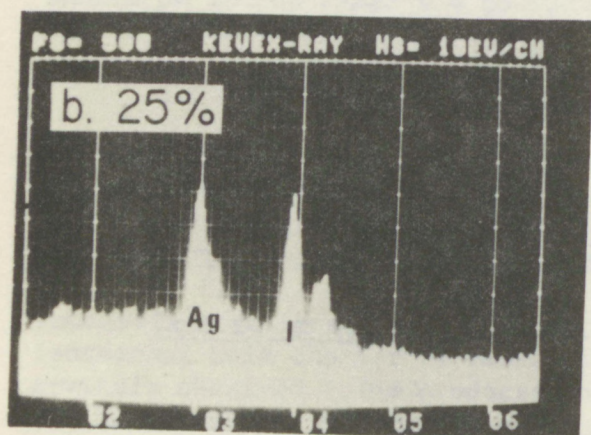
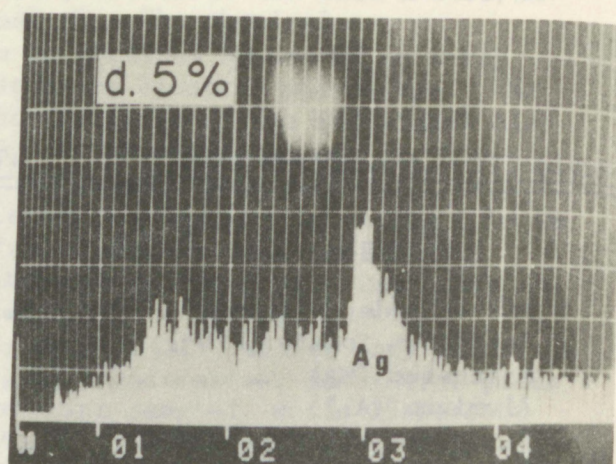
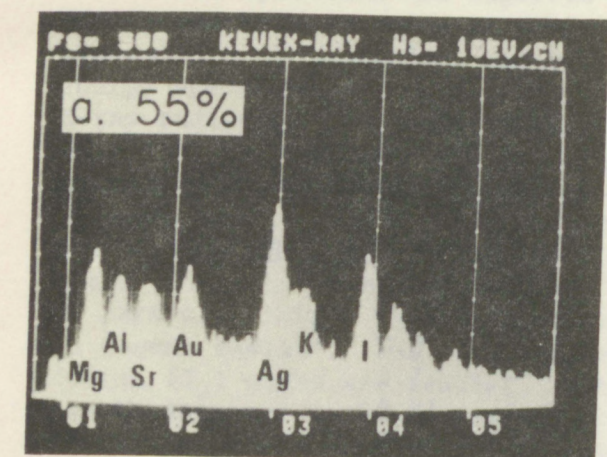


Figure C3. Representative elemental composition of individual particles ($>0.02 \mu\text{m}$) produced by burn of Olin X-1055/WM105 pyrotechnics in wind tunnel; data were obtained using an X-ray energy spectrometer in combination with a scanning electron microscope; percentages shown refer to total number of particles analyzed (e.g., 5 percent of all particles analyzed contained Ag without other elements present). Data courtesy of NOAA/APCL.

experiments before 1973. For the region of the wind tunnel from which the aerosol sample is drawn, the correction factor for pyrotechnic sources is about 0.03. This has the effect of lowering all "uncorrected" nucleating effectiveness calculations by nearly two orders of magnitude, and accounts for the discrepancy between the Simpson et al. (1970) figure 1, and the figure C4 effectiveness curve (next page).

Figure C4 shows a plot of nucleating effectiveness as a function of temperature for cold chamber tests of the Olin WM105 formulation. All values have been corrected to account for a proper wind tunnel dilution factor. With the exception of one test, it can be seen that at -8°C , the nucleating effectiveness is found to be less than 10^{10} particles per gram, but an effectiveness of 10^{12} particles per gram is achieved at -12°C . From the earlier discussion of the physical hypothesis, one might recall that it was considered necessary that 10^{12} particles per gram of nucleating material be effective in order to achieve the criterion of a concentration of 100 nuclei per liter distributed throughout the cloud bubble volume. If glaciation is assumed to occur in the temperature range of -4°C to -8°C , it is obvious that the Olin pyrotechnic does not meet the criterion. If, however, glaciation is assumed to occur from -4°C to -15°C , the Olin WM105 mixture may be producing enough effective nuclei. It can also be noted that the 2-73 batch was tested in January of 1974 and again in May of 1975, and, with the possible exception of the data at -12°C , no evidence for a significant deterioration in effectiveness was observed.

Figure C5 shows the nucleating performance of a type of pyrotechnic mixture originally developed by the Naval Weapons Center and designated TB-1. Some Navy WMU-9/TB-1 and Nuclei Engineering Incorporated (NEI - the commercial firm with patent license to produce TB-1) pyrotechnics were tested in May 1975 at the CSU facility. The Navy flares were produced 4 years ago, while those of NEI were produced recently. A mean Olin activity curve from figure C4 is also included for comparison. It can be seen that the TB-1 mixture is considerably more effective than the WM105 mixture at temperatures warmer than -12°C . In fact, with the NEI/TB-1 mixture, the requirement of producing 10^{12} nuclei per gram effective at -8°C apparently can be achieved. It is necessary at this juncture to emphasize that while the CSU isothermal cold chamber is an excellent testing facility for intercomparing nucleation effectiveness from various types of production devices relative to each other, it is not known with any certainty that the absolute magnitudes of the effectiveness curves resemble those which occur in the real atmosphere. An actual dynamic cloud is very much more complex than the static environment of the cold chamber, and some important processes of nucleation in the atmosphere may not be simulated correctly in the cold chamber. Nevertheless, the data presented here provide the best guidance available. They are accepted and applied with the reservation that the absolute values of nucleating effectiveness are strictly valid only for the testing procedures used.

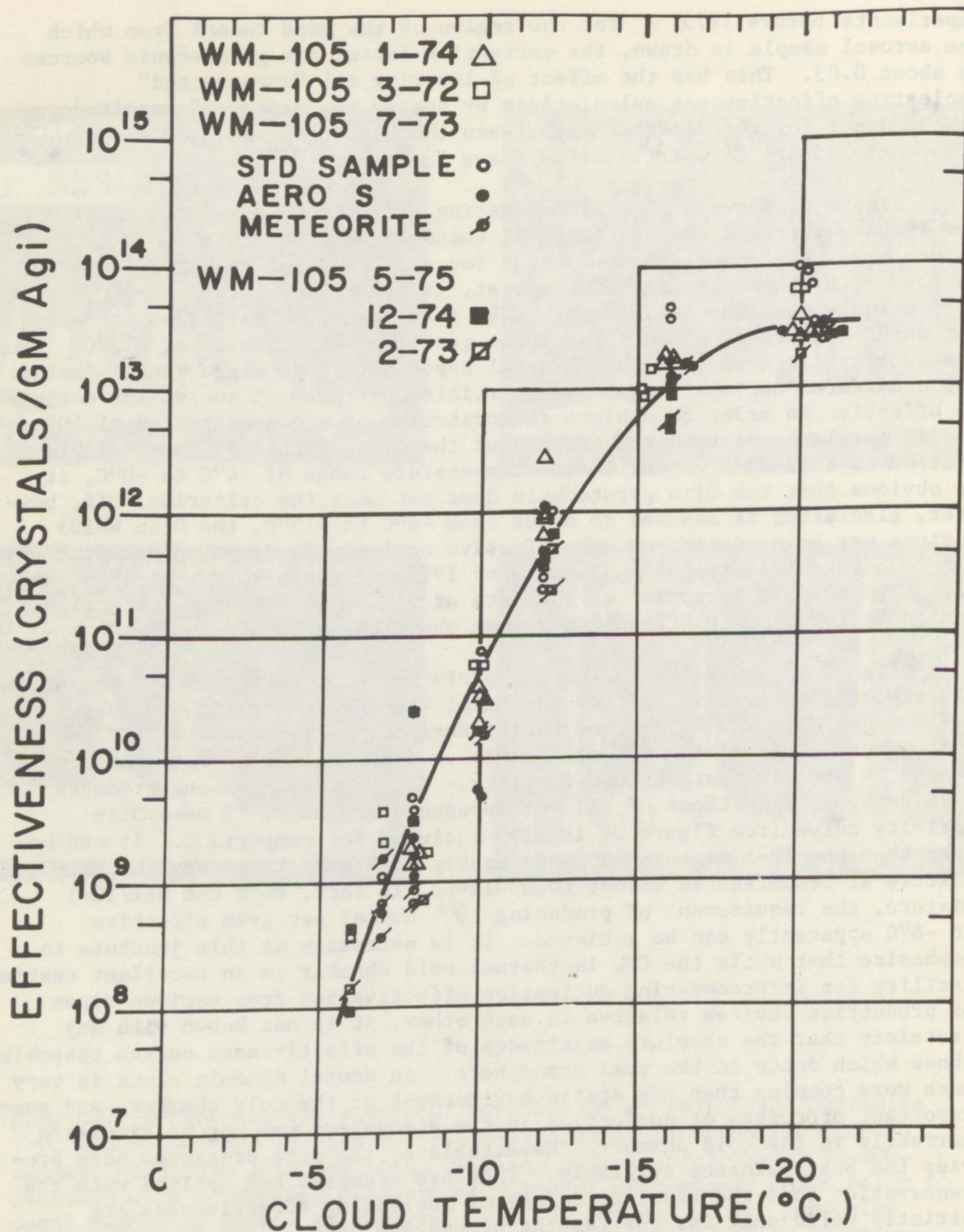


Figure C4. Nucleating effectiveness as a function of temperature for AgI emitted from Olin WM-105 pyrotechnic; all pertinent data from tests conducted at the CSU cold chamber facility in 1972, 1973, 1974, and 1975 are included; note nucleating effectiveness of about 10^{10} at -8°C .

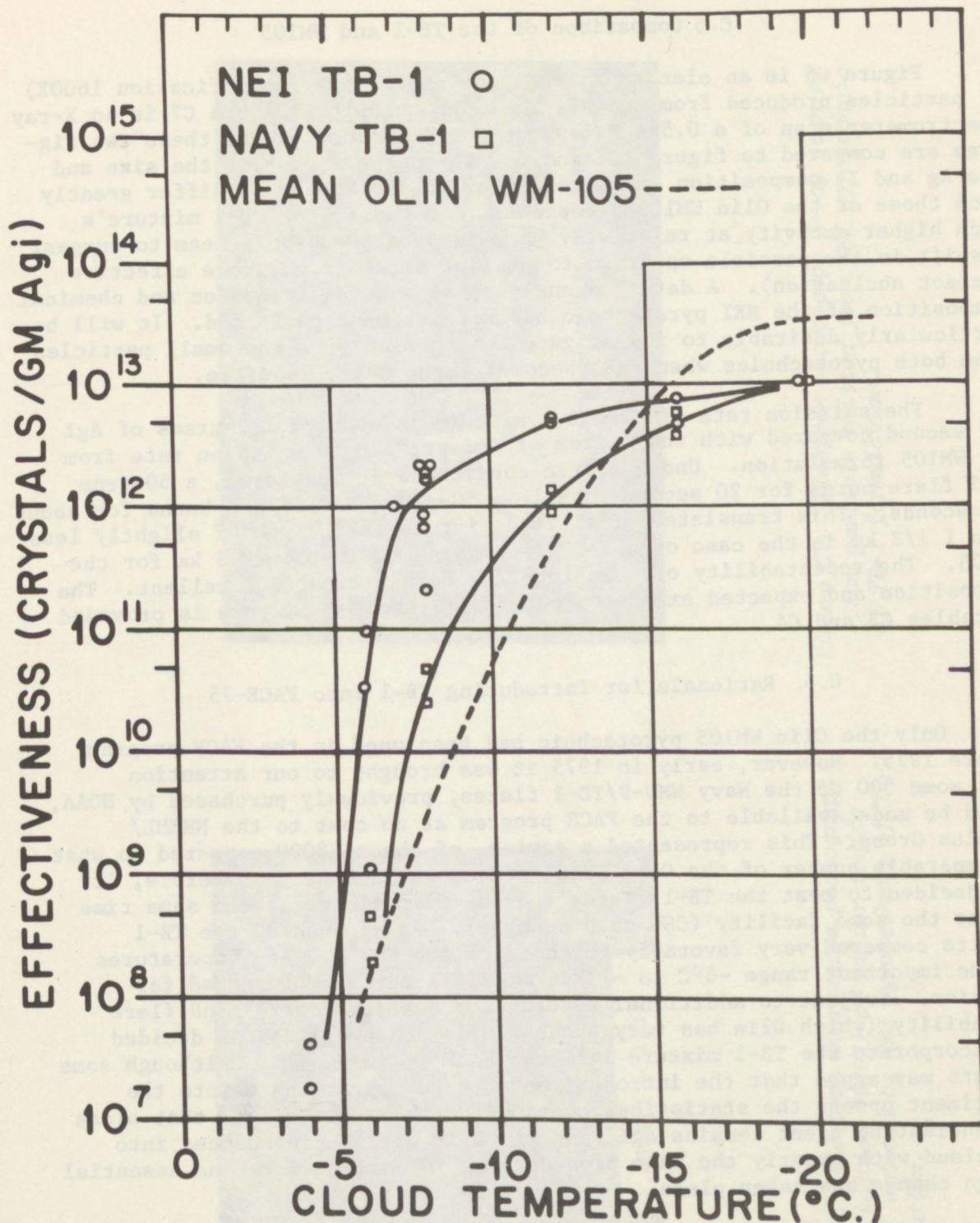


Figure C5. Nucleating effectiveness data for NEI TB-1 and Navy TB-1 pyrotechnic with Olin WM-105 nucleating curve included for comparison. Note orders of magnitude differences between the effectiveness curves at -8°C.

C.5 Comparison of the TB-1 and WM105

Figure C6 is an electron microscope photograph (magnification 1600X) of particles produced from the NEI TB-1 pyrotechnic. Figure C7 is an X-ray spectrometer scan of a 0.5 μ m NEI pyrotechnic product. When these two figures are compared to figures C2 and C3, it can be seen that the size and the Ag and I₂ composition characteristics do not appear to differ greatly from those of the Olin WM105 pyrotechnic. However, the TB-1 mixture's much higher activity at relatively warm temperatures would seem to suggest a shift in the particle spectrum to smaller sizes (i.e., more effective contact nucleation). A detailed analysis of size distribution and chemical composition of the NEI pyrotechnic has not yet been performed. It will be particularly desirable to investigate the chemistry of the small particles from both pyrotechnics when this becomes technically feasible.

The emission rate of the TB-1 mixture is about 2 1/2 grams of AgI per second compared with the 1 gram of AgI per second emission rate from the WM105 formulation. Under static conditions at sea level, a 50-gram TB-1 flare burns for 20 seconds, while a 50-gram WM105 flare burns for about 50 seconds. This translates at altitude into a fall depth of slightly less than 1 1/2 km in the case of the TB-1 compared to just over 3 km for the WM105. The repeatability of burn rate for both flares is excellent. The composition and expected exhaust products of the TB-1 mixture is provided in tables C3 and C4.

C.6 Rationale for Introducing TB-1 into FACE-75

Only the Olin WM105 pyrotechnic had been used in the FACE program before 1975. However, early in 1975 it was brought to our attention that some 500 of the Navy WMU-9/TB-1 flares, previously purchased by NOAA, could be made available to the FACE program at no cost to the NHEML/Cumulus Group. This represented a saving of about \$8000 compared to what a comparable number of the Olin WM105 flares would cost. Therefore, it was decided to test the TB-1 flares and the Olin flares at the same time and at the same facility (CSU cold chamber). As discussed, the TB-1 results compared very favorably to those of the WM105. At temperatures in the important range -6°C to -12°C, the TB-1 activity appeared far superior. Subject to additional testing for quality control and flare reliability (which Olin has very successfully achieved), it was decided to incorporate the TB-1 mixture into the FACE-75 program. Although some purists may argue that the introduction of a new pyrotechnic into the experiment upsets the statistical continuity, the authors feel that since the nucleating agent remains AgI, and since it will be introduced into the cloud with exactly the same procedure as in earlier work, no essential design change has taken place.

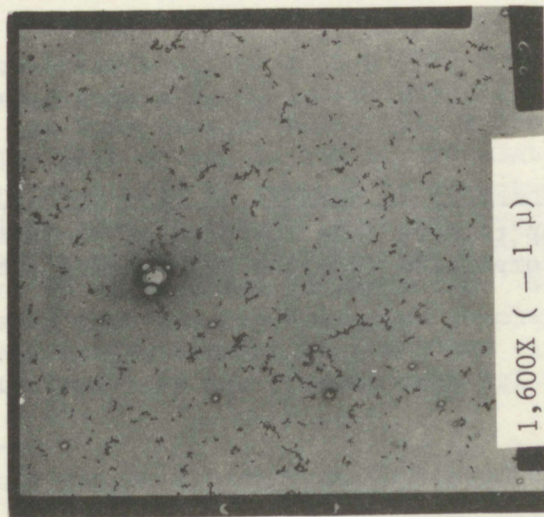


Figure C6. Electron microscope photograph (magnification 1600X) of silver iodide aerosol emitted by NEI pyrotechnic of TB-1 formulation.

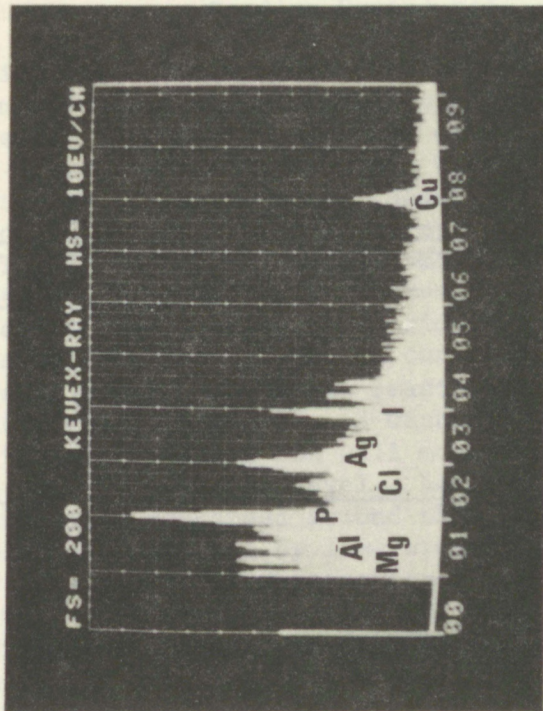


Figure C7. Electron microscope X-ray scan of 0.5 μm particle emitted from NEI pyrotechnic of TB-1 formulation.

Table C3. Composition of TB-1

<u>Material</u>	<u>Percent by weight</u>
Silver iodate (AgIO_3)	78.3
Magnesium (Mg)	5.2
Aluminum (Al)	10.8
Binder	5.7

Table C4. Expected Exhaust Products of TB-1

<u>Compound</u>	<u>Percent (gm per gm of mix)*</u>
Silver iodide (AgI)	64.9
Aluminum oxide (Al_2O_3)	20.4
Magnesium oxide (MgO)	8.6
Carbon dioxide (CO_2)	18.2
Water (H_2O)	7.4

* Total exhaust products add up to more than 100 percent because some oxygen to burn the metal fuels is incorporated from the surrounding atmosphere.

C.7 Nucleating Characteristics in Relation to Optimizing Seeding Procedures

The question often arises as to whether it might be more feasible in the FACE program to inject AgI nucleant into the updrafts at cloud base rather than directly into the supercooled cloud tower. The procedures, techniques, and instrumentation for cloud base seeding have been developed and thoroughly tested in many regions (Hess, 1974), and there is no doubt that this method offers advantages in safety and economics over that requiring penetration of active towers some 5 km above their bases. However, there are certain significant reservations that exist in successfully applying cloud base seeding to Florida cumuli. The most important consideration is whether the AgI nuclei can retain their activity while being carried upward through at least 3 km of "warm" cloud. Theoretically, any particles of AgI complexed with soluble material (NaI or KI) will act as centers for condensation and will most likely be dissolved by the time they reach the 0°C isotherm level. Large (> 0.1µm) particles of pure AgI may also have water condensed around them, but probably would not be totally dissolved and could act by immersion. Small (< 0.1µm) particles of pure AgI should remain dry, if not scavenged by cloud or rain drops.

Since hydrodynamic capture of submicron particulate matter is negligible, it can be assumed that only those particles scavenged by diffusion or phoretic processes (Brownian diffusion, turbulent diffusion, diffusiophoresis, thermophoresis) during ascent through cloud may be lost³⁴ as active ice nuclei. A rough estimate of the proportion of particles contacting water droplets can be obtained through the relationship

$$\frac{dn_p}{n_p} = kwD_p dt / \bar{r}^2 \quad (C1)$$

where k is a constant equal to 1.35×10^6 , w is the cloud liquid water content expressed in g m^{-3} , D_p is the diffusion coefficient of the particles and \bar{r} is the mean droplet size. For a cloud of water content 1.5 g m^{-3} and mean droplet size 15 µm, it can be calculated that only about 6 percent all 0.01µm particles will be removed by Brownian³⁵ capture during a 10-minute ascent from cloud base to the 0°C isotherm level. Therefore, it can be concluded that nearly all pure AgI particles 0.01 to 0.1µm will survive the ascent to supercooled temperatures. Similarly, from (C1) it can be calculated that the cloud droplet population will remove about 3 percent of the small AgI nuclei between the -4°C and -15°C isotherm levels. If a generator at cloud base can produce pure AgI particles of 0.01µm radius

³⁴Even these may retain activity as indicated by Pueschel et al. (1974).

³⁵Other capture processes are thought to be only of secondary importance and will not significantly alter the implications to follow.

with an output of the order 10^{16} particles per gram,³⁶ then approximately 10^{14} particles per gram should be available to be activated by a direct contact mechanism in the -4°C to -15°C temperature range. The effectiveness of such small particles has been found by Sax and Goldsmith (1972) to vary between 10^{-5} at -5°C , 10^{-2} at -10°C , and nearly 10^0 at -15°C . It would appear, therefore, that enough nuclei (10^9 to 10^{14} per gram) would be active by a contact mechanism between -4°C and -15°C to insure the possibility of successful dynamic seeding if the particles produced were not complexed with any soluble material, if they were to reach the correct regions of the cloud at the proper time, and if they were distributed over a large enough area to glaciate a significant portion of the cloud updraft region.

A detailed discussion of these latter requirements is outside the scope of this appendix. Briefly, however, it can be mentioned that in Florida, there are definite logistical problems in selecting proper towers for experimentation from the cloud base level. The continuity of the updraft through deep convection (as in Florida) has not as yet been documented, and the degree of vertical spreading of material by turbulence is not known. Without vertical diffusion, the horizontal plane of AgI material would tend to move upwards with the updraft and would nucleate only in a region of relatively narrow depth. Finally, there is considerable advantage in an experimental situation in repeatedly penetrating cumulus towers to determine the effect of seeding on the evolution of the cloud microphysics.

³⁶These criteria have been achieved by the Patten generator (Pueschel et al., 1974).

APPENDIX D

SELECTED DATA FROM THE FACE-73 CLOUD PHYSICS PROGRAM

Since the inception of the program that has become known as the Florida Area Cumulus Experiment (FACE), the importance of obtaining reliable cloud physics data has been recognized. The FACE hypothesis is predicated upon a sequential chain of microphysical and dynamical events, beginning with the massive conversion of supercooled water to ice and culminating in an increase of rainfall over a large area of the surface. Although some collection and analysis of in-cloud microphysical data was carried out in conjunction with the dynamic seeding experiments in the Caribbean in 1963 and 1965, the single cloud seeding experiments in Florida in 1968, and the early FACE studies in 1970 and 1971, it was not until the FACE-73 program that a thorough investigation into the evolution of the cloud's microphysical structure was initiated. There are at least two main reasons why such a study was not initiated earlier. First, the rather limited resources of the former Experimental Meteorology Laboratory were taxed to the fullest in the carrying out of analyses pertaining to the development and refinement of the one-dimensional cumulus model, the verification of model-predicted cumulus growth behavior with that observed from dynamic seeding, and the optimization of field experimental procedures and techniques necessary to establish an effect of seeding on rainfall; second, the instrumentation required to confidently assess changes in ice particle concentrations on a continuous basis was not available before the 1973 FACE program.

Table D1 summarizes the important characteristics of microphysical instrumentation either used in FACE-73, or planned for use in the 1975 FACE program. Instruments (1), (2), (3), (4), (5), (6), (8), (9), (10), (14), (17) and (18) were used to some degree in the FACE-73 program. Top priority was given to an analysis of the cloud updraft structure in conjunction with the partitioning of the water substance as determined by our use of data obtained from the Lyman alpha total water probe, the Johnson-Williams hot wire sensor, the hydrometeor sampler and the MEE ice particle counter.

Table D2 provides a complete summary³⁷ of microphysical data obtained and analyzed from 69 cumulus cloud penetrations carried out at approximately the -10°C isotherm level. These penetrations were selected for detailed study because there was a reasonable certainty that repeat passes were made through roughly the same portion of the tower as the original pass. Thus, the evolution of the microphysics, both in seeded and in unseeded clouds, could be legitimately investigated. The first 29 penetrations (from 1/1 through 29/1) contain

³⁷A value of -77 or -88 in a grouping indicates that the set of data in the group was not available for analysis.

Table D1. Characteristics of Microphysical Instrumentation Used in the FACE Program

Type	Objective of Measurement	Type of Instrument	Principle of Operation	Range	Sampling Volume (100 m/sec airspeed)	Accuracy
(1) Total Water Content Probe	Total water in cloud and in the cloud environment.	Lyman-Alpha	Absorption of Lyman-Alpha radiation by water vapor.	0-15 g/m ³	7.5 l/sec	+10% total water, less on liquid particles at low altitudes.
(2) Nimbrometer Total Liquid Water Probe	Total Liquid Water content of clouds.	Hot Wire	Constant temperature device below boiling point of water.	0-7 g/m ³	250 l/sec	+20% preliminary value - calibration incomplete.
(3) Johnson Williams	Cloud droplet water content.	Hot Wire	Constant current complete water vaporization device.	0-3 g/m ³ at 200 knots	1.5 l/sec	+20% over small drop-let size range of spectrum.
(4) Airborne Hydrometer Sampler	Drop size distributions.	Foil Impactor	Impaction impressions on soft soil.	drops >250µm diameter	19.2 l/frame (fast motor) 29.0 l/frame (slow motor)	+10% of large drop liquid water content.
(5) Continuous Particle Replicator	Droplet distributions and crystal habits.	Formvar Replication	Particle impression on plastic resin.	Function of collection efficiencies for particles.	3.175 l/sec (MEE) 1.2 l/sec (DRI)	Qualitative Indications and relative concentrations only.
(6) MEE Ice Particle Counter	Ice particle concentrations.	Optical	Cross polarization discrimination of pulses produced by ice, count particles above a size threshold.	count particles above 150µm longest dimension	10.0 l/sec	+20% gross number of ice particles above a threshold size. Some ambiguity by liquid drops >1 mm dia.

Table D1. Characteristics of Microphysical Instrumentation Used in the FACE Program (Continued)

Type	Objective of Measurement	Type of Instrument	Principle of Operation	Range	Sampling Volume (100 m/sec airspeed)	Accuracy
(7) UW Ice Particle Counter	Ice Particle Concentrations	Optical	Birefringence property of ice discriminates at 0° scattering angle.	count particles above 100µm longest dimension	2.8 1/sec	100% for ice particles >250µm longest dimension; 50% for ice particles >130µm longest dimension; some ambiguity by liquid drops >3mm dia.
(8) C.S.I. Dew Point	Humidity	Dew/frost point.	Light scattering by dew formed on thermoelectrically-cooled mirror.	-40°C to +40°C		+10% at +40°C +30% at -40°C
(9) Rosemount Temp. Probe	Total Temperature	Platinum Resistor	Heated air due to deicing bleed off.	-60°C to +40°C		+0.5°C out of cloud.
(10) Interface Temp. PRT-5	Ground surface temperatures.	IR Radiometer 9.5-11.5µ	Bolometer type receiver.	-40°C to +40°C		Relative ±.15°C. absolute ±.4°C.
(11) Air/Cloud Temp. radiometer FW 14-330	Air temperatures in cloud temperatures.	IR Radiometer 15µ CO ₂ band	Bolometer type receiver.	-40°C to +40°C		Relative ±.3°C absolute ±.5°C
(12) Knollenberg Cloud drop spectrometer Raindrop spectrometer	Cloud droplet spectrum Raindrop spectra	Optical array cloud droplet spectrometer Optical array cloud droplet spectrometer	Laser beam absorption 14 channels Laser beam absorption 14 channels	20-280µ 300-4500µ	1721/sec for 300µm droplets 551/sec for 4500µm droplets	Theoretically absolute.
(13) Knollenberg 2-D cloud and raindrop spectrometers	Cloud and raindrop spectra and shape discrimination for ice particle spectrum	Optical array	Laser beam absorption with image slicing	25-800µ (cloud probe) 200-6400µ (rain probe)	167 1/sec for all drop sizes	Theoretically absolute with a shape resolution of ~25µm.

Table D1. Characteristics of Microphysical Instrumentation Used in the FACE Program (Continued)

Type	Objective of Measurement	Type of Instrument	Principle of Operation	Range	Sampling Volume (100 m/sec airspeed)	Accuracy
(14) Aitken counter (E-1)	Total particulate concentration (Aitken Nuclei).	Particle Counter	Light beam extinction through cloud formed in water saturated adiabatic expansion chamber.	50 - 1 x 10 ⁷ /ml	30-70 ml/sec	+30%
(15) CCN Counter	Cloud droplet condensation nuclei (CCN) concentration.	CCN Counter	Water saturated thermal diffusion chamber forms droplets on CCN.	50 - 1 x 10 ⁴ /ml	~.02 ml	+10%
(16) IN Counter (NCAR)	Ice nuclei concentration.	NCAR Ice Nuclei Counter-Acoustic	Supercooled cloud chamber, acoustic counter.	.01 - 1 x 10 ³ /l	10 l/min	+20% for natural ice nuclei.
(17) Membrane Filter	Ice nuclei concentration.	Sub Freezing Thermal Diffusion Chamber	Ice nuclei activation at saturated water vapor pressure.	.1 - 1 x 10 ³ /l	~300 l	Internally consistent results only with standardized procedure, equipment and materials.
(18) IN Counter (MEE)	Ice nuclei concentration.	Optical	Cross polarization discrimination of pulses produced by ice, count particles above a size threshold.	Up to 10 ³ /l	10l/min	+20 for natural ice nuclei.

Table D2. FACE 1973 Pass-by-Pass Selected Microphysical Data

CLOUD IDENTIFICATION	716 2	716 9	71613	71616	71710	71712	71793	71717	806 1	806 3
PASS BEGIN TIME	181419	19 543	193312	2034 5	203418	205530	21 2 8	2132 1	171529	172559
ARBITRARY CLOUD/PASS DESIGNATION	1/1	2/1	3/1	4/1	5/1	6/1	7/1	8/1	9/1	10/1
PASS DURATION (SEC)	29	41	33	23	29	58	22	17	15	20
ACTION	NS	NS	NS	NS	NS	NS	NS	NS	NS	NS

VERTICAL VELOCITY STATISTICS										
MEAN VERTICAL VELOCITY (M/SEC)	4.39	4.45	2.29	2.91	.75	2.43	5.02	.96	8.85	6.31
STANDARD DEVIATION (M/SEC)	3.51	7.43	4.18	3.52	5.86	4.09	7.30	3.19	5.75	6.94
MEAN UPDRAFT VELOCITY (M/SEC)	5.00	7.11	4.24	4.06	6.88	4.37	8.38	3.02	9.50	8.34
STANDARD DEVIATION (M/SEC)	3.01	5.63	2.40	2.64	4.42	2.15	6.35	2.41	5.37	5.18
MEAN DOWNDRAFT VELOCITY (M/SEC)	-1.68	-4.83	-4.03	-2.54	-3.15	-3.71	-2.24	-1.98	-.24	-5.18
STANDARD DEVIATION (M/SEC)	2.28	5.27	.86	1.18	3.15	3.24	1.56	1.17	0.00	3.08
RMS VELOCITY (M/SEC)	5.57	8.49	4.66	4.51	5.74	4.72	8.70	3.24	10.45	9.25
MAXIMUM UPDRAFT VELOCITY (M/SEC)	11.94	16.82	7.22	8.47	12.45	9.10	20.21	6.99	15.93	18.95
MAXIMUM DOWNDRAFT VELOCITY (M/SEC)	-3.30	-11.42	-5.27	-3.82	-6.76	-7.72	-4.17	-3.87	-.24	-8.17
MEDIAN VERTICAL VELOCITY (M/SEC)	3.90	3.68	2.50	2.36	-1.45	3.76	3.19	.32	12.24	7.02
PERCENT OF PASS WITH UPDRAFTS	90.91	77.74	76.47	82.61	38.89	76.00	68.42	58.82	93.33	85.00
PERCENT OF PASS WITH DOWNDRAFTS	9.09	22.22	23.53	17.39	61.11	24.00	31.58	41.18	6.67	15.00
PERCENT OF PASS WITH $w > 7.5$ M/SEC	13.64	33.33	0.00	17.39	16.67	4.00	36.84	0.00	60.00	45.00

JOHNSON-STILLMANS CLOUD WATER STATISTICS										
MEAN J_w CLOUD WATER (G/M**3)	1.36	1.73	1.23	1.01	1.50	.39	1.46	1.32	1.11	.72
STANDARD DEVIATION	.66	.60	.35	.79	.62	.31	.65	.57	.52	.46
MAXIMUM J_w CLOUD WATER (G/M**3)	2.16	2.50	1.62	2.13	2.14	1.07	2.22	2.29	1.88	1.61
MEDIAN J_w CLOUD WATER (G/M**3)	1.43	1.77	1.19	.87	1.75	.38	1.56	1.24	1.15	.53
PERCENT OF PASS WITH $J_w > 1.0$ G/M**3	72.73	88.89	94.12	47.83	83.33	2.00	73.68	76.47	66.67	30.00

MFF ICE PARTICLE STATISTICS										
MEAN ICE PARTICLE CONCENTRATION (NO/L)	.08	.13	.52	2.61	1.92	11.53	0.00	.02	1.49	4.30
STANDARD DEVIATION	.11	.33	.77	4.37	2.99	7.19	0.00	.07	1.15	2.74
MAXIMUM ICE PARTICLE CONCENTRATION (NO/L)	.30	1.40	2.20	16.50	9.40	30.10	0.00	.20	3.50	8.40
MEDIAN ICE PARTICLE CONCENTRATION (NO/L)	0.00	0.00	.10	.40	.35	10.80	0.00	0.00	1.70	4.50
PERCENT OF PASS WITH IPC < 2.5 PER LITER	100.00	100.00	100.00	73.91	83.33	14.00	100.00	100.00	80.00	40.00
PERCENT PASS $w > 7.5$, $J_w > 1.0$, IPC < 2.5	13.64	33.33	0.00	8.70	16.67	0.00	31.58	0.00	46.67	10.00

LYMAN-ALPHA TOTAL WATER STATISTICS										
MEAN L- α TOTAL WATER (G/M**3)	4.27	3.59	3.60	4.25	6.39	7.05	6.30	6.50	0.00	0.00
STANDARD DEVIATION	1.23	1.32	1.25	1.11	1.46	2.04	1.11	.43	0.00	0.00
MAXIMUM L- α TOTAL WATER (G/M**3)	5.65	5.48	5.33	5.41	8.49	9.47	7.79	7.23	-88.00	-88.00
MEDIAN L- α TOTAL WATER (G/M**3)	4.46	3.33	3.99	4.69	6.85	8.03	6.38	6.49	-77.78	-77.78

FOUL HYDROMETEOR STATISTICS										
MEAN HYDRO WATER CONTENT (G/M**3)	.13	.02	.18	0.00	.71	1.59	0.00	0.00	0.00	0.00
STANDARD DEVIATION	.14	.03	.34	0.00	.78	1.33	0.00	0.00	0.00	0.00
MAXIMUM HYDRO WATER CONTENT (G/M**3)	.47	.09	1.31	-88.00	2.34	3.57	0.00	-88.00	-88.00	-88.00
MEDIAN HYDRO WATER CONTENT (G/M**3)	.09	.00	0.00	-77.78	.37	1.67	0.00	-77.78	-77.78	-77.78
MEAN CONC DRIPS $D > 0.47$ MM (NO/L)	.29	.04	.38	0.00	1.17	1.79	0.00	0.00	0.00	0.00
MAX CONC DRIPS $D > 0.47$ MM (NO/L)	.93	.22	2.72	-88.00	2.77	5.36	0.00	-88.00	-88.00	-88.00
MEAN CONC DRIPS $D > 0.93$ MM (NO/L)	.07	.01	.07	0.00	.36	.65	0.00	0.00	0.00	0.00
MAX CONC DRIPS $D > 0.93$ MM (NO/L)	.28	.04	.66	-88.00	1.09	1.92	0.00	-88.00	-88.00	-88.00

CORRELATION STATISTICS										
VERTICAL VELOCITY VS JW CLOUD WATER	.49	.42	-.33	-.13	.31	.66	.48	.26	.46	.53
VERTICAL VELOCITY VS ICE PARTICLE CONC	-.14	.33	.03	.31	-.08	.17	88.89	-.34	-.26	.21
VERTICAL VELOCITY VS HYDRO WATER CONTENT	-.29	-.60	-.78	88.89	-.31	.56	88.89	88.89	88.89	88.89
JW CLOUD WATER VS ICE PARTICLE CONC	.20	.01	.40	-.51	.11	-.13	88.89	-.28	-.43	-.11
JW CLOUD WATER VS HYDRO WATER CONTENT	.03	-.55	.07	88.89	-.48	.72	88.89	88.89	88.89	88.89
HYDRO WATER CONTENT VS ICE PARTICLE CONC	.52	-.16	-.21	88.89	-.08	.17	88.89	88.89	88.89	88.89

Table D2. FACE 1973 Pass-by-Pass Selected Microphysical Data (Continued)

CLOUD IDENTIFICATION	720 7	72010	72016	80616	80621	809 2	809 5	909 1	909 6	90911
PASS BEGIN TIME	2056 1	2117 6	2221 41	193126	21 448	1744 4	181539	1825 1	184437	211239
ARBITRARY CLOUD/PASS DESIGNATION	18/1	19/1	20/1	11/1	12/1	13/1	14/1	15/1	16/1	17/1
PASS DURATION (SEC)	39	59	76	52	42	54	49	30	25	26
ACTION	S	S	S	NS	NS	NS	NS	NS	NS	NS
VERTICAL VELOCITY STATISTICS										
MEAN VERTICAL VELOCITY (M/SEC)	3.26	2.82	6.95	2.60	14.95	8.57	2.57	13.34	8.19	6.41
STANDARD DEVIATION (M/SEC)	5.47	8.14	6.24	7.12	9.91	7.81	3.82	10.43	6.70	6.71
MEAN UPDRAFT VELOCITY (M/SEC)	6.79	8.67	8.05	7.09	16.91	3.95	3.95	13.34	9.07	9.24
STANDARD DEVIATION (M/SEC)	3.86	6.22	5.69	5.17	8.16	3.74	3.10	10.43	4.79	5.53
MEAN DOWNDRAFT VELOCITY (M/SEC)	-2.16	-4.20	-1.88	-4.57	-3.69	-6.68	-2.24	0.00	-4.84	-1.27
STANDARD DEVIATION (M/SEC)	1.88	2.73	1.73	2.11	3.29	5.47	1.22	0.00	2.78	1.16
RMS VELOCITY (M/SEC)	6.30	8.49	9.29	7.52	17.87	11.45	4.54	16.72	10.50	9.18
MAXIMUM UPDRAFT VELOCITY (M/SEC)	12.90	21.84	21.38	19.04	30.76	19.02	10.99	39.30	17.38	19.17
MAXIMUM DOWNDRAFT VELOCITY (M/SEC)	-6.35	-9.02	-4.78	-8.47	-7.78	-12.15	-3.87	-9.2	-6.98	-3.34
MEDIAN VERTICAL VELOCITY (M/SEC)	3.27	2.21	5.43	2.16	18.64	10.66	2.35	12.14	8.32	4.64
PERCENT OF PASS WITH UPDRAFTS	60.61	54.55	88.89	61.54	90.48	84.21	77.78	100.00	88.00	78.08
PERCENT OF PASS WITH DOWNDRAFTS	39.39	45.45	11.11	38.46	9.52	15.79	22.22	0.00	12.00	21.92
PERCENT OF PASS WITH W > 7.5 M/SEC	27.27	24.24	46.67	26.92	78.57	73.68	14.81	80.00	56.00	42.31
JOHNSON-WILLIAMS CLOUD WATER STATISTICS										
MEAN JW CLOUD WATER (G/M**3)	1.80	1.43	1.53	.34	1.24	1.86	1.81	1.66	.72	1.58
STANDARD DEVIATION	.68	.64	.60	.41	.84	.58	.47	.71	.77	.47
MAXIMUM JW CLOUD WATER (G/M**3)	2.51	2.26	2.54	1.85	2.34	2.70	2.65	2.45	2.46	2.34
MEDIAN JW CLOUD WATER (G/M**3)	2.00	1.62	1.45	.23	1.48	2.02	1.98	1.97	.53	1.45
PERCENT OF PASS WITH JW > 1.0 G/M**3	88.85	75.76	80.00	9.62	64.29	89.47	96.30	80.00	24.00	92.31
MEE ICE PARTICLE STATISTICS										
MEAN ICE PARTICLE CONCENTRATION (NO/L)	6.01	1.06	.17	11.16	2.71	.67	.50	.07	7.39	.32
STANDARD DEVIATION	9.48	3.20	.36	5.92	2.86	.98	1.02	.10	5.36	.46
MAXIMUM ICE PARTICLE CONCENTRATION (NO/L)	38.10	14.60	1.80	28.00	9.80	3.40	4.00	.30	15.50	2.20
MEDIAN ICE PARTICLE CONCENTRATION (NO/L)	.50	0.00	0.00	16.93	2.03	.20	0.00	0.00	7.30	.20
PERCENT OF PASS WITH IPC < 2.5 PER LITER	63.64	90.91	100.00	5.77	61.90	94.74	92.59	100.00	28.00	100.00
PERCENT PASS W > 7.5, JW > 1.0, IPC < 2.5	21.21	24.24	40.00	5.77	54.76	68.42	14.81	66.67	16.00	42.31
LYMAN-ALPHA TOTAL WATER STATISTICS										
MEAN L-A TOTAL WATER (G/M**3)	1.79	3.50	5.26	0.00	0.00	5.47	4.68	3.81	7.13	6.55
STANDARD DEVIATION	.06	2.06	1.71	0.00	0.00	1.94	1.93	1.86	1.98	.84
MAXIMUM L-A TOTAL WATER (G/M**3)	2.02	6.36	7.58	-88.00	-88.00	8.51	7.47	6.59	9.90	7.85
MEDIAN L-A TOTAL WATER (G/M**3)	1.77	3.09	5.94	-77.78	-77.78	5.40	5.32	3.32	7.58	6.57
FOIL HYDROMETEOR STATISTICS										
MEAN HYDRO WATER CONTENT (G/M**3)	.83	.06	.06	0.00	0.00	.99	.26	.36	0.00	0.00
STANDARD DEVIATION	.93	.16	.12	0.00	0.00	1.30	.41	.60	0.00	0.00
MAXIMUM HYDRO WATER CONTENT (G/M**3)	2.70	1.10	.47	-88.00	-88.00	4.96	1.39	1.76	-88.00	-88.00
MEDIAN HYDRO WATER CONTENT (G/M**3)	.26	0.00	.01	-77.78	-77.78	.36	.01	.00	-77.78	-77.78
MEAN CONC DROPS D > 0.47 MM (NO/L)	.99	.14	.04	0.00	0.00	1.36	.29	.11	0.00	0.00
MAX CONC DROPS D > 0.47 MM (NO/L)	3.70	4.07	.22	-88.00	-88.00	6.08	1.61	.68	-88.00	-88.00
MEAN CONC DROPS D > 0.93 MM (NO/L)	.11	.02	.02	0.00	0.00	.26	.13	.04	0.00	0.00
MAX CONC DROPS D > 0.93 MM (NO/L)	1.68	.38	.15	-88.00	-88.00	1.26	.67	.17	-88.00	-88.00
CORRELATION STATISTICS										
VERTICAL VELOCITY VS JW CLOUD WATER	.53	.45	.13	.44	.75	.41	.52	.30	.54	.46
VERTICAL VELOCITY VS ICE PARTICLE CONC	-.57	-.12	-.13	-.47	-.79	.02	-.25	-.12	-.13	.00
VERTICAL VELOCITY VS HYDRO WATER CONTENT	-.29	-.29	-.44	88.89	88.89	.31	.31	-.05	88.89	88.89
JW CLOUD WATER VS ICE PARTICLE CONC	-.74	-.40	.31	-.33	-.73	.29	-.19	.29	-.47	-.16
JW CLOUD WATER VS HYDRO WATER CONTENT	-.68	-.20	.06	88.89	88.89	.46	.06	.77	88.89	88.89
HYDRO WATER CONTENT VS ICE PARTICLE CONC	.52	.31	.29	88.89	88.89	.35	.62	.35	88.89	88.89

Table D2. FACE 1973 Pass-by-Pass Selected Microphysical Data (Continued)

CLOUD IDENTIFICATION	72019	7251	72514	72517	72520	72522	9125	91212
PASS BEGIN TIME	23 137	174011	18 726	20327	20346	21 0 0	2111 6	185034
ARBITRARY CLOUD/PASS DESIGNATION	21/1	22/1	23/1	24/1	25/1	26/1	27/1	28/1
PASS DURATION (SEC)	59	34	28	23	30	30	66	12
ACTION	S	S	S	S	S	S	S	S
VERTICAL VELOCITY STATISTICS								
MEAN VERTICAL VELOCITY (M/SEC)	6.38	1.77	2.33	3.24	2.52	.61	-1.41	7.50
STANDARD DEVIATION (M/SEC)	6.13	5.11	5.61	2.61	4.86	3.83	2.77	4.99
MEAN UPDRAFT VELOCITY (M/SEC)	8.68	4.62	6.07	3.83	5.16	3.53	2.29	8.28
STANDARD DEVIATION (M/SEC)	4.83	3.65	3.49	2.21	2.49	2.14	2.39	4.39
MEAN DOWNDRAFT VELOCITY (M/SEC)	-1.76	-3.56	-3.49	-6.2	-4.07	-3.05	-2.60	-1.11
STANDARD DEVIATION (M/SEC)	1.58	2.38	2.31	1.46	1.59	1.57	1.68	0.00
RMS VELOCITY (M/SEC)	8.82	5.31	5.96	4.12	5.32	3.77	3.07	8.89
MAXIMUM UPDRAFT VELOCITY (M/SEC)	17.29	12.11	11.24	6.97	8.44	6.98	5.59	14.90
MAXIMUM DOWNDRAFT VELOCITY (M/SEC)	-5.05	-7.45	-6.61	-9.7	-5.46	-4.97	-6.01	-1.11
MEAN VERTICAL VELOCITY (M/SEC)	5.91	1.77	2.12	4.10	4.11	1.14	-1.64	8.26
PERCENT OF PASS WITH UPDRAFTS	77.97	65.22	60.87	85.71	71.43	55.56	24.32	91.67
PERCENT OF PASS WITH DOWNDRAFTS	22.03	34.78	39.13	14.29	28.57	44.44	75.68	8.33
PERCENT OF PASS WITH W > 7.5 M/SEC	42.37	13.04	26.09	0.00	14.29	0.00	0.00	58.33
JOHNSON-WILLIAMS CLOUD WATER STATISTICS								
MEAN JW CLOUD WATER (G/M**3)	.69	1.52	1.84	1.51	1.53	1.77	1.63	1.98
STANDARD DEVIATION	.90	.91	.72	.58	.45	.82	.55	.83
MAXIMUM JW CLOUD WATER (G/M**3)	2.40	2.46	2.53	2.28	2.16	2.28	2.44	2.50
MEAN JW CLOUD WATER (G/M**3)	.24	1.85	2.09	1.72	1.64	2.28	1.79	2.31
PERCENT OF PASS WITH JW > 1.0 G/M**3	27.12	60.87	82.61	85.71	85.71	77.78	89.19	83.33
MEE ICE PARTICLE STATISTICS								
MEAN ICE PARTICLE CONCENTRATION (NO/L)	8.81	.09	.08	.39	.12	.15	.43	.18
STANDARD DEVIATION	7.21	1.49	.23	.61	.32	.31	.69	.29
MAXIMUM ICE PARTICLE CONCENTRATION (NO/L)	27.90	5.90	1.10	2.00	1.20	1.30	2.70	.80
MEAN ICE PARTICLE CONCENTRATION (NO/L)	6.60	.30	0.00	.20	0.00	0.00	.10	.05
PERCENT OF PASS WITH IPC < 2.5 PER LITER	28.81	91.30	100.00	100.00	100.00	100.00	97.30	100.00
PERCENT PASS W > 7.5, JW > 1.0, IPC < 2.5	5.08	13.04	26.09	0.00	14.29	0.00	0.00	50.00
LYMAN-ALPHA TOTAL WATER STATISTICS								
MEAN L-A TOTAL WATER (G/M**3)	6.30	3.37	4.23	4.68	3.23	3.68	3.97	0.00
STANDARD DEVIATION	1.51	1.40	1.00	.81	1.16	1.40	1.59	0.00
MAXIMUM L-A TOTAL WATER (G/M**3)	8.61	5.28	5.22	5.92	4.65	5.90	6.11	-88.00
MEAN L-A TOTAL WATER (G/M**3)	6.50	3.51	4.73	4.78	3.10	4.03	4.57	-77.78
FOIL HYDROMETER STATISTICS								
MEAN HYDRO WATER CONTENT (G/M**3)	0.00	.58	.09	.13	.07	.20	.37	0.00
STANDARD DEVIATION	0.00	.63	.11	.14	.11	.23	.72	0.00
MAXIMUM HYDRO WATER CONTENT (G/M**3)	-88.00	1.76	.34	.50	.43	.66	3.84	-88.00
MEAN HYDRO WATER CONTENT (G/M**3)	-77.78	.32	.05	.08	.02	.02	.08	-77.78
MEAN CONC DROPS D > 0.47 MM (NO/L)	0.00	.90	.12	.30	.29	.43	.55	0.00
MAX CONC DROPS D > 0.47 MM (NO/L)	-88.00	4.40	.34	.79	1.93	1.25	3.82	-88.00
MEAN CONC DROPS D > 0.93 MM (NO/L)	0.00	.25	.04	.04	.02	.10	.21	0.00
MAX CONC DROPS D > 0.93 MM (NO/L)	-88.00	1.01	.12	.13	.05	.34	1.97	-88.00
CORRELATION STATISTICS								
VERTICAL VELOCITY VS JW CLOUD WATER	.59	.75	.21	.66	.37	.41	.39	.06
VERTICAL VELOCITY VS ICE PARTICLE CONC	.08	-.34	-.14	-.15	-.46	.22	-.17	.75
VERTICAL VELOCITY VS HYDRO WATER CONTENT	88.89	.09	-.67	-.72	-.69	-.44	.88.89	88.89
JW CLOUD WATER VS ICE PARTICLE CONC	-.31	-.27	-.13	-.13	-.34	.32	.11	.28
JW CLOUD WATER VS HYDRO WATER CONTENT	88.89	.17	-.04	-.60	-.49	.59	.54	88.89
HYDRO WATER CONTENT VS ICE PARTICLE CONC	88.89	.61	.29	.32	.38	.24	.07	88.89

Table D2. FACE 1973 Pass-by Pass Selected Microphysical Data (Continued)

CLOUD IDENTIFICATION	716 3	71610	71614	71617	71711	71713	71714	71718	806 2	806 4
PASS BEGIN TIME	182011	19 839	193951	203640	203813	21 034	21 556	213943	171934	172819
ARBITRARY CLOUD/PASS DESIGNATION	1/2	2/2	3/2	4/2	5/2	6/2	7/2	8/2	9/2	10/2
PASS DURATION (SEC)	48	35	18	23	23	64	36	46	19	33
ACTION	NS	NS	NS	NS	NS	NS	NS	NS	NS	NS
VERTICAL VELOCITY STATISTICS										
MEAN VERTICAL VELOCITY (M/SEC)	2.15	3.02	1.72	-0.25	-2.21	3.68	-4.89	1.11	3.95	1.63
STANDARD DEVIATION (M/SEC)	4.95	7.19	3.30	2.71	4.55	3.92	2.07	2.94	3.14	2.74
MEAN UPDRAFT VELOCITY (M/SEC)	5.12	7.45	3.68	1.40	2.35	5.04	0.00	2.59	4.75	2.50
STANDARD DEVIATION (M/SEC)	2.72	5.24	2.68	1.06	.98	2.45	0.00	1.57	2.14	2.54
MEAN DOWNDRAFT VELOCITY (M/SEC)	-2.88	-3.94	-1.36	-2.39	-5.13	-2.83	-4.89	-2.82	-2.82	-1.10
STANDARD DEVIATION (M/SEC)	3.59	2.85	.92	2.73	3.30	2.98	2.07	2.52	1.25	.95
RMS VELOCITY (M/SEC)	5.31	7.61	3.64	2.66	4.97	5.35	5.29	3.12	5.00	3.15
MAXIMUM UPDRAFT VELOCITY (M/SEC)	9.33	15.07	8.65	3.22	4.22	10.83	-.98	6.35	7.85	8.33
MAXIMUM DOWNDRAFT VELOCITY (M/SEC)	-10.15	-7.86	-2.25	-7.94	-11.71	-8.20	-9.15	-7.40	-3.71	-2.39
MEDIAN VERTICAL VELOCITY (M/SEC)	3.02	1.62	1.50	.45	-1.71	4.06	-5.25	1.40	4.93	.86
PERCENT OF PASS WITH UPDRAFTS	62.96	61.11	61.11	56.52	39.13	82.69	0.00	69.57	89.47	75.76
PERCENT OF PASS WITH DOWNDRAFTS	37.04	38.89	38.89	43.48	60.87	17.31	100.00	30.43	10.53	24.24
PERCENT OF PASS WITH W > 7.5 M/SEC	14.81	33.33	5.56	0.00	0.00	15.38	0.00	0.00	5.26	6.06
JOHNSON-WILLIAMS CLOUD WATER STATISTICS										
MEAN JW CLOUD WATER (G/M**3)	1.07	1.58	.22	1.09	.04	.13	.81	.29	.07	.11
STANDARD DEVIATION	.85	.44	.29	.71	.07	.17	.50	.16	.06	.17
MAXIMUM JW CLOUD WATER (G/M**3)	2.36	2.09	.74	2.24	.24	.54	1.62	.78	.83	.86
MEDIAN JW CLOUD WATER (G/M**3)	.86	1.73	.02	1.24	.01	.06	.83	.25	.07	.02
PERCENT OF PASS WITH JW > 1.0 G/M**3	44.44	88.89	0.00	60.87	0.00	0.00	28.57	0.00	0.00	0.00
MFE ICE PARTICLE STATISTICS										
MEAN ICE PARTICLE CONCENTRATION (NO/L)	.41	.99	17.46	9.21	18.17	13.42	.05	17.47	12.03	6.12
STANDARD DEVIATION	.74	1.20	8.57	6.21	13.05	9.30	.10	7.71	6.49	3.62
MAXIMUM ICE PARTICLE CONCENTRATION (NO/L)	2.20	4.40	33.60	24.00	40.80	34.50	.40	33.90	26.30	18.10
MEDIAN ICE PARTICLE CONCENTRATION (NO/L)	0.00	.40	20.35	7.80	22.10	12.95	0.00	17.90	11.40	5.80
PERCENT OF PASS WITH IPC < 2.5 PER LITER	100.00	94.44	5.56	17.39	17.39	17.31	100.00	6.52	10.53	12.12
PERCENT PASS W > 7.5, JW > 1.0, IPC < 2.5	7.41	33.33	0.00	0.00	0.00	0.00	0.00	0.00	0.00	0.00
LYMAN-ALPHA TOTAL WATER STATISTICS:										
MEAN L-A TOTAL WATER (G/M**3)	3.45	4.03	5.22	5.39	6.59	6.53	4.89	7.82	0.00	0.00
STANDARD DEVIATION	1.29	1.70	.72	1.45	1.77	1.84	1.05	.73	0.00	0.00
MAXIMUM L-A TOTAL WATER (G/M**3)	5.76	6.56	5.93	6.63	8.72	9.13	6.71	8.79	-88.00	-88.00
MEDIAN L-A TOTAL WATER (G/M**3)	3.19	4.43	5.35	5.85	6.98	6.58	4.87	8.06	-77.78	-77.78
FBIIL HYDROMETEOR STATISTICS										
MEAN HYDRO WATER CONTENT (G/M**3)	.19	.11	0.00	0.00	0.00	1.40	.02	0.00	0.00	0.00
STANDARD DEVIATION	.26	.17	0.00	0.00	0.00	1.54	.04	0.00	0.00	0.00
MAXIMUM HYDRO WATER CONTENT (G/M**3)	.77	.48	-88.00	-88.00	-88.00	6.02	.15	-88.00	-88.00	-88.00
MEDIAN HYDRO WATER CONTENT (G/M**3)	.04	.00	-77.78	-77.78	-77.78	.68	0.00	-77.78	-77.78	-77.78
MEAN CONC DROPS D > 0.47 MM (NO/L)	.52	.24	0.00	0.00	0.00	1.46	.05	0.00	0.00	0.00
MAX CONC DROPS D > 0.47 MM (NO/L)	2.30	1.10	-88.00	-88.00	-88.00	3.08	.30	-88.00	-88.00	-88.00
MEAN CONC DROPS D > 0.93 MM (NO/L)	.11	.05	0.00	0.00	0.00	.48	.01	0.00	0.00	0.00
MAX CONC DROPS D > 0.93 MM (NO/L)	.45	.19	-88.00	-88.00	-88.00	1.39	.12	-88.00	-88.00	-88.00
CORRELATION STATISTICS										
VERTICAL VELOCITY VS JW CLOUD WATER	.50	.43	.24	.23	.14	.58	.50	.49	.20	.64
VERTICAL VELOCITY VS ICE PARTICLE CONC	.27	-.63	-.46	-.31	.28	.12	.10	-.19	-.54	.17
VERTICAL VELOCITY VS HYDRO WATER CONTENT	.72	-.44	88.89	88.89	88.89	-.19	-.55	88.89	88.89	88.89
JW CLOUD WATER VS ICE PARTICLE CONC	.23	-.01	-.71	-.17	-.39	-.45	-.02	-.34	-.02	-.01
JW CLOUD WATER VS HYDRO WATER CONTENT	.10	-.01	88.89	88.89	88.89	-.47	-.49	88.89	88.89	88.89
HYDRO WATER CONTENT VS ICE PARTICLE CONC	.16	.20	88.89	88.89	88.89	.44	-.44	88.89	88.89	88.89

Table D2. FACE 1973 Pass-by-Pass Selected Microphysical Data (Continued)

CLOUD IDENTIFICATION	720 8	720 11	720 17	806 17	806 22	809 3	809 6	909 2	909 7	909 12
PASS BEGIN TIME	21 216	215326	2229 1	193553	211718	173833	182137	182814	184946	211728
ARBITRARY CLOUD/PASS DESIGNATION	18/2	19/2	20/2	11/2	12/2	13/2	14/2	15/2	16/2	17/2
PASS DURATION (SEC)	115	94	89	66	37	27	62	52	16	35
ACTION	S	S	S	NS	NS	NS	NS	NS	NS	NS
VERTICAL VELOCITY STATISTICS										
MEAN VERTICAL VELOCITY (M/SEC)	5.23	2.04	6.35	4.55	13.53	6.98	2.94	.22	6.80	6.05
STANDARD DEVIATION (M/SEC)	7.20	5.07	8.84	7.23	10.31	5.76	2.71	2.70	10.93	6.66
MEAN UPDRAFT VELOCITY (M/SEC)	8.27	4.70	9.82	7.83	14.38	8.35	3.56	2.58	11.64	8.23
STANDARD DEVIATION (M/SEC)	6.23	3.29	8.02	5.45	9.94	5.10	2.33	1.58	9.62	5.54
MEAN DOWNDRAFT VELOCITY (M/SEC)	-2.38	-3.51	-2.51	-4.21	-1.36	-8.9	-1.06	-1.70	-3.86	-2.66
STANDARD DEVIATION (M/SEC)	1.66	3.33	1.95	2.41	1.36	.50	.90	1.62	3.17	1.78
RMS VELOCITY (M/SEC)	8.86	5.44	10.83	8.49	16.93	8.98	3.97	2.66	12.58	8.93
MAXIMUM UPDRAFT VELOCITY (M/SEC)	21.44	13.97	25.99	19.65	33.59	18.29	7.57	4.98	22.65	17.61
MAXIMUM DOWNDRAFT VELOCITY (M/SEC)	-5.72	-11.21	-6.88	-8.78	-2.32	-1.63	-2.40	-5.50	-7.50	-5.44
MEDIAN VERTICAL VELOCITY (M/SEC)	3.50	2.36	2.86	3.88	12.02	6.72	3.00	.15	1.73	4.42
PERCENT OF PASS WITH UPDRAFTS	71.43	67.57	71.88	72.73	94.59	85.19	86.49	44.83	68.75	80.00
PERCENT OF PASS WITH DOWNDRAFTS	28.57	32.43	28.13	27.27	5.41	14.81	13.51	55.17	31.25	20.00
PERCENT OF PASS WITH W > 7.5 M/SEC	33.77	13.51	37.50	33.33	67.57	48.15	2.70	0.00	37.50	37.14
JOHNSON-WILLIAMS CLOUD WATER STATISTICS										
MEAN JW CLOUD WATER (G/M**3)	.98	1.02	1.52	.39	.99	.09	.19	.96	.19	.62
STANDARD DEVIATION	1.06	.75	1.00	.59	.79	.09	.24	.29	.38	.72
MAXIMUM JW CLOUD WATER (G/M**3)	2.59	2.35	2.65	2.15	2.27	.30	1.25	1.56	1.07	2.13
MEDIAN JW CLOUD WATER (G/M**3)	.30	1.02	2.04	.13	1.03	.06	.11	.94	0.00	.20
PERCENT OF PASS WITH JW > 1.0 G/M**3	44.16	51.35	62.50	18.18	51.35	0.00	2.70	41.38	12.50	34.29
MEE ICE PARTICLE STATISTICS										
MEAN ICE PARTICLE CONCENTRATION (NO/L)	7.84	9.51	9.38	9.54	3.40	10.44	8.24	.74	3.44	9.33
STANDARD DEVIATION	9.33	8.20	10.34	5.23	2.80	4.88	4.66	.99	5.07	10.62
MAXIMUM ICE PARTICLE CONCENTRATION (NO/L)	31.80	45.70	35.50	22.20	13.50	21.80	18.30	3.70	14.90	26.00
MEDIAN ICE PARTICLE CONCENTRATION (NO/L)	4.10	7.65	4.60	8.85	3.70	11.40	9.10	.40	8.85	4.30
PERCENT OF PASS WITH IPC < 2.5 PER LITER	41.96	14.86	42.19	10.61	35.11	11.11	18.92	93.10	12.50	48.57
PERCENT PASS W > 7.5, JW > 1.0, IPC < 2.5	18.18	0.00	15.63	1.52	21.62	0.00	0.00	0.00	0.00	28.57
LYMAN-ALPHA TOTAL WATER STATISTICS										
MEAN L-A TOTAL WATER (G/M**3)	2.17	1.26	5.97	0.00	0.00	6.80	6.75	4.21	6.01	6.77
STANDARD DEVIATION	.25	.14	2.43	0.00	0.00	1.15	1.21	1.83	2.19	1.00
MAXIMUM L-A TOTAL WATER (G/M**3)	2.75	1.63	9.28	-88.00	-88.00	8.69	8.46	7.52	8.99	8.26
MEDIAN L-A TOTAL WATER (G/M**3)	2.14	1.25	7.08	-77.78	-77.78	6.84	7.15	4.73	5.94	6.91
FOIL HYDROMETEOR STATISTICS										
MEAN HYDRO WATER CONTENT (G/M**3)	.92	1.24	1.53	0.00	0.00	0.00	2.41	.70	0.00	0.00
STANDARD DEVIATION	1.33	1.11	2.34	0.00	0.00	0.00	3.08	1.19	0.00	0.00
MAXIMUM HYDRO WATER CONTENT (G/M**3)	5.41	3.84	9.68	-88.00	-88.00	-88.00	10.05	4.13	-88.00	-88.00
MEDIAN HYDRO WATER CONTENT (G/M**3)	.39	1.24	.57	-77.78	-77.78	-77.78	.34	.01	-77.78	-77.78
MEAN CONC DROPS D > 0.47 MM (NO/L)	.90	1.39	.92	0.00	0.00	0.00	1.76	.68	0.00	0.00
MAX CONC DROPS D > 0.47 MM (NO/L)	3.38	4.11	4.01	-88.00	-88.00	-88.00	5.71	3.45	-88.00	-88.00
MEAN CONC DROPS D > 0.93 MM (NO/L)	.33	.50	.31	0.00	0.00	0.00	.68	.26	0.00	0.00
MAX CONC DROPS D > 0.93 MM (NO/L)	1.46	1.72	1.18	-88.00	-88.00	-88.00	2.18	1.39	-88.00	-88.00
CORRELATION STATISTICS										
VERTICAL VELOCITY VS JW CLOUD WATER	.69	.53	.72	.77	.66	.74	.17	.33	.74	.77
VERTICAL VELOCITY VS ICE PARTICLE CONC	-.42	-.28	.18	-.03	-.23	-.14	.45	.26	.26	.40
VERTICAL VELOCITY VS HYDRO WATER CONTENT	-.46	-.44	.67	88.89	88.89	88.89	.02	.45	88.89	88.89
JW CLOUD WATER VS ICE PARTICLE CONC	-.49	-.16	-.59	-.19	-.30	-.49	-.30	-.29	-.29	-.66
JW CLOUD WATER VS HYDRO WATER CONTENT	-.61	.63	.52	88.89	88.89	88.89	-.11	-.03	88.89	88.89
HYDRO WATER CONTENT VS ICE PARTICLE CONC	.84	.20	-.20	88.89	88.89	88.89	.28	.02	88.89	88.89

Table D2. FACE 1973 Pass-by-Pass Selected Microphysical Data (Continued)

CLOUD IDENTIFICATION	72020	725 2	725 8	72515	72518	72521	72523	912 6	91213
PASS BEGIN TIME	23 839	174910	1813 0	202649	204230	21 439	211417	19 348	2147 7
ARBITRARY CLOUD/PASS DESIGNATION	21/2	22/2	23/2	24/2	25/2	26/2	27/2	28/2	29/2
PASS DURATION (SEC)	20	138	24	70	17	14	39	29	12
ACTION	S	S	S	S	S	S	S	S	S
VERTICAL VELOCITY STATISTICS									
MEAN VERTICAL VELOCITY (M/SEC)	6.02	-38	-1.31	6.56	-4.74	-2.33	4.30	1.93	-2.93
STANDARD DEVIATION (M/SEC)	5.85	4.26	1.22	7.77	2.15	3.26	5.59	4.92	2.97
MEAN UPDRAFT VELOCITY (M/SEC)	8.17	3.66	.86	11.18	0.00	.99	6.75	5.40	1.81
STANDARD DEVIATION (M/SEC)	4.26	2.63	.55	5.89	0.00	.69	4.29	3.15	.23
MEAN DOWNDRAFT VELOCITY (M/SEC)	-2.59	-3.33	-1.55	-1.51	-4.74	-4.18	-2.64	-2.99	-3.68
STANDARD DEVIATION (M/SEC)	1.59	2.38	1.01	1.08	2.15	2.51	.83	1.53	2.19
RMS VELOCITY (M/SEC)	8.29	4.26	1.77	10.10	5.17	3.91	6.96	5.21	4.08
MAXIMUM UPDRAFT VELOCITY (M/SEC)	14.92	10.39	1.25	19.11	.72	1.85	12.70	10.78	1.97
MAXIMUM DOWNDRAFT VELOCITY (M/SEC)	-4.41	-9.19	-3.90	-3.24	-7.98	-8.04	-3.47	-5.63	-6.56
MEDIAN VERTICAL VELOCITY (M/SEC)	6.24	-.93	-1.18	5.86	-5.11	-1.88	2.71	1.70	-3.36
PERCENT OF PASS WITH UPDRAFTS	80.00	42.16	10.00	63.64	0.00	35.71	73.91	58.62	16.87
PERCENT OF PASS WITH DOWNDRAFTS	20.00	57.84	90.00	36.36	100.00	64.29	26.09	41.38	83.13
PERCENT OF PASS WITH W > 7.5 M/SEC	40.00	3.92	0.00	47.73	0.00	0.00	39.13	13.79	0.00
JOHNSON-WILLIAMS CLOUD WATER STATISTICS									
MEAN JW CLOUD WATER (G/M**3)	1.33	.37	.31	1.31	.44	.27	1.63	.08	.01
STANDARD DEVIATION	.88	.53	.23	1.00	.43	.21	.79	.12	.02
MAXIMUM JW CLOUD WATER (G/M**3)	2.15	2.02	.76	2.66	1.27	.55	2.42	.39	.08
MEDIAN JW CLOUD WATER (G/M**3)	1.86	.15	.30	1.44	.31	.31	2.11	0.00	0.00
PERCENT OF PASS WITH JW > 1.0 G/M**3	65.00	12.75	0.00	56.82	7.14	0.00	65.22	0.00	0.00
MEE ICE PARTICLE STATISTICS									
MEAN ICE PARTICLE CONCENTRATION (NO/L)	3.77	3.87	6.10	3.52	6.72	7.18	2.37	5.52	15.38
STANDARD DEVIATION	5.30	3.32	3.78	3.97	4.90	4.04	1.99	4.62	9.77
MAXIMUM ICE PARTICLE CONCENTRATION (NO/L)	16.70	14.50	16.70	16.70	15.60	14.40	7.60	17.10	26.40
MEDIAN ICE PARTICLE CONCENTRATION (NO/L)	1.45	3.80	6.15	2.00	6.70	6.60	2.20	4.10	17.50
PERCENT OF PASS WITH IPC < 2.5 PER LITER	65.00	41.18	20.00	59.09	21.43	7.14	60.87	31.03	16.87
PERCENT PASS W > 7.5, JW > 1.0, IPC < 2.5	35.00	0.00	0.00	31.82	0.00	0.00	21.74	0.00	0.00
LYMAN-ALPHA TOTAL WATER STATISTICS									
MEAN L-A TOTAL WATER (G/M**3)	5.96	3.39	3.28	4.06	4.16	5.59	4.70	0.00	0.00
STANDARD DEVIATION	1.13	1.07	.60	1.88	.92	1.71	1.80	0.00	0.00
MAXIMUM L-A TOTAL WATER (G/M**3)	6.90	4.95	4.10	6.50	5.14	7.25	6.94	-88.00	-88.00
MEDIAN L-A TOTAL WATER (G/M**3)	6.40	3.67	3.45	5.03	4.46	6.48	5.32	-77.78	-77.78
FOIL HYDROMETEOR STATISTICS									
MEAN HYDRO WATER CONTENT (G/M**3)	0.00	.92	.47	.78	.36	0.00	.51	0.00	0.00
STANDARD DEVIATION	0.00	.92	.41	.93	.47	0.00	.86	0.00	0.00
MAXIMUM HYDRO WATER CONTENT (G/M**3)	-88.00	3.26	1.07	3.39	1.20	-88.00	2.03	-88.00	-88.00
MEDIAN HYDRO WATER CONTENT (G/M**3)	-77.78	.61	.43	.38	.07	-77.78	.06	-77.78	-77.78
MEAN CONC DROPS D > 0.47 MM (NO/L)	0.00	1.86	1.50	1.59	.90	0.00	.58	0.00	0.00
MAX CONC DROPS D > 0.47 MM (NO/L)	-88.00	5.18	3.44	6.46	3.23	-88.00	3.69	-88.00	-88.00
MEAN CONC DROPS D > 0.93 MM (NO/L)	0.00	.45	.17	.37	.17	0.00	.18	0.00	0.00
MAX CONC DROPS D > 0.93 MM (NO/L)	-88.00	1.80	.49	1.92	.59	-88.00	.93	-88.00	-88.00
CORRELATION STATISTICS									
VERTICAL VELOCITY VS JW CLOUD WATER	.74	.41	.39	.77	-.04	.88	.60	.71	.17
VERTICAL VELOCITY VS ICE PARTICLE CONC	-.50	.09	-.43	-.24	-.52	.61	-.03	.62	.18
VERTICAL VELOCITY VS HYDRO WATER CONTENT	88.89	.22	.38	.76	.00	88.89	.15	88.89	88.89
JW CLOUD WATER VS ICE PARTICLE CONC	-.83	-.40	-.40	-.48	-.63	.63	-.41	.60	.36
JW CLOUD WATER VS HYDRO WATER CONTENT	88.89	-.15	-.41	.72	-.53	88.89	.44	88.89	88.89
HYDRO WATER CONTENT VS ICE PARTICLE CONC	88.89	.45	-.28	-.16	-.19	88.89	-.60	88.89	88.89

Table D2. FACE 1973 Pass-by-Pass Selected Microphysical Data (Continued)

CLOUD IDENTIFICATION	716.4	716.11	716.18	717.15	717.19	720.9	725.9	725.16	909.3	909.13	912.14
ARBITRARY CLOUD/PASS DESIGNATION	1/3	2/3	4/3	7/3	8/3	18/3	23/3	24/3	15/3	17/3	29/3
PASS BEGIN TIME	182517	191148	203918	211052	214619	211130	181643	203236	1832.0	212013	215019
PASS DURATION (SEC)	58	54	45	27	73	39	43	62	47	23	11
ACTION	NS	NS	NS	NS	NS	NS	S	S	NS	NS	S
VERTICAL VELOCITY STATISTICS											
MEAN VERTICAL VELOCITY (M/SEC)	1.88	-29	.20	-3.32	.86	9.71	1.64	3.67	-75	9.54	1.92
STANDARD DEVIATION (M/SEC)	3.75	5.49	4.40	2.23	3.64	6.83	2.06	4.27	2.96	5.86	4.34
MEAN UPDRAFT VELOCITY (M/SEC)	3.64	4.33	3.89	1.25	3.43	10.31	2.40	4.71	2.44	10.65	4.62
STANDARD DEVIATION (M/SEC)	2.50	3.28	2.75	.87	1.78	6.48	1.41	4.05	2.58	4.77	4.28
MEAN DOWNDRAFT VELOCITY (M/SEC)	-2.35	-4.37	-3.02	-3.69	-2.62	-1.39	-1.53	-90	-2.10	-2.13	-1.33
STANDARD DEVIATION (M/SEC)	2.74	3.36	2.68	1.86	2.39	6.66	1.00	5.6	1.88	1.44	.32
RMS VELOCITY (M/SEC)	4.16	5.41	4.35	3.98	3.72	11.82	2.60	5.40	3.01	11.13	4.56
MAXIMUM UPDRAFT VELOCITY (M/SEC)	9.11	10.82	9.88	1.86	6.85	26.03	4.78	14.24	7.92	17.98	10.23
MAXIMUM DOWNDRAFT VELOCITY (M/SEC)	-8.66	-12.19	-9.69	-6.79	-10.32	-1.86	-2.56	-2.05	-7.40	-3.14	-1.62
MEDIAN VERTICAL VELOCITY (M/SEC)	1.51	-24	-24	-3.94	1.31	7.80	1.88	2.53	-65	10.26	.40
PERCENT OF PASS WITH UPDRAFTS	70.59	46.88	46.67	7.41	57.53	94.87	80.77	81.48	29.73	91.30	54.55
PERCENT OF PASS WITH DOWNDRAFTS	29.41	53.13	53.33	92.59	42.47	5.13	19.23	18.52	70.27	8.70	45.45
PERCENT OF PASS WITH W > 7.5 M/SEC	5.88	12.50	4.44	0.00	0.00	51.28	0.00	18.52	2.70	73.91	18.18
JOHNSON-WILLIAMS CLOUD WATER STATISTICS											
MEAN JW CLOUD WATER (G/M**3)	.34	.91	.36	.28	.17	.43	.14	.11	.07	1.59	.00
STANDARD DEVIATION	.56	.70	.68	.10	.56	.13	.13	.17	.08	.69	.01
MAXIMUM JW CLOUD WATER (G/M**3)	2.28	2.09	2.42	.43	.38	2.10	.45	.63	.23	2.55	.04
MEDIAN JW CLOUD WATER (G/M**3)	.13	.62	.02	.29	.17	.85	.12	.03	.04	1.64	0.00
PERCENT OF PASS WITH JW > 1.0 G/M**3	11.76	43.75	15.56	0.00	0.00	12.82	0.00	0.00	0.00	78.26	0.00
MEF ICE PARTICLE STATISTICS											
MEAN ICE PARTICLE CONCENTRATION (NO/L)	7.47	9.43	10.71	24.81	14.09	15.03	4.55	7.20	10.58	1.72	3.11
STANDARD DEVIATION	5.86	11.24	9.81	9.12	6.84	8.28	2.72	5.22	12.27	2.51	3.24
MAXIMUM ICE PARTICLE CONCENTRATION (NO/L)	23.50	37.80	33.50	37.20	27.70	31.80	10.10	20.00	56.70	10.50	10.20
MEDIAN ICE PARTICLE CONCENTRATION (NO/L)	6.90	3.60	8.40	26.10	15.70	16.50	4.55	6.40	7.00	7.00	1.40
PERCENT OF PASS WITH IPC < 2.5 PER LITER	25.49	40.63	35.56	3.70	8.22	12.82	30.77	24.07	32.43	73.91	54.55
PERCENT PASS W > 7.5, JW > 1.0, IPC < 2.5	0.00	3.13	2.22	0.00	0.00	0.00	0.00	0.00	0.00	60.87	0.00
LYMAN-ALPHA TOTAL WATER STATISTICS											
MEAN L-A TOTAL WATER (G/M**3)	4.00	4.52	4.51	6.91	7.10	4.61	2.83	4.52	3.22	7.28	0.00
STANDARD DEVIATION	1.05	1.76	1.15	1.19	1.20	1.37	1.04	1.49	1.26	1.05	0.00
MAXIMUM L-A TOTAL WATER (G/M**3)	5.59	6.88	5.95	8.44	8.91	6.15	4.82	6.49	5.93	8.74	-88.00
MEDIAN L-A TOTAL WATER (G/M**3)	4.13	5.09	5.11	6.66	7.61	5.38	2.65	4.65	3.06	7.30	-77.78
FILL HYDROMETER STATISTICS											
MEAN HYDRO WATER CONTENT (G/M**3)	.88	.84	0.00	0.00	0.00	0.00	.49	1.49	.22	0.00	0.00
STANDARD DEVIATION	.79	1.31	0.00	0.00	0.00	0.00	.65	1.37	.47	0.00	0.00
MAXIMUM HYDRO WATER CONTENT (G/M**3)	2.38	5.11	-88.00	-88.00	-88.00	-88.00	2.11	3.65	1.95	-88.00	-88.00
MEDIAN HYDRO WATER CONTENT (G/M**3)	.82	.23	-77.78	-77.78	-77.78	-77.78	.94	.86	0.00	-77.78	-77.78
MAX CONC DROPS D > 0.47 MM (NO/L)	1.90	.77	0.00	0.00	0.00	0.00	.94	2.35	.53	0.00	0.00
MAX CONC DROPS D > 0.47 MM (NO/L)	4.64	3.82	-88.00	-88.00	-88.00	-88.00	3.20	5.83	3.16	-88.00	-88.00
MEAN CONC DROPS D > 0.93 MM (NO/L)	.44	.28	0.00	0.00	0.00	0.00	.24	.77	.11	0.00	0.00
MAX CONC DROPS D > 0.93 MM (NO/L)	1.36	1.55	-88.00	-88.00	-88.00	-88.00	1.11	2.11	1.08	-88.00	-88.00
CORRELATION STATISTICS											
VERTICAL VELOCITY VS JW CLOUD WATER	.25	.36	.58	.21	.51	.73	.65	.76	-.47	.87	.56
VERTICAL VELOCITY VS ICE PARTICLE CONC	.08	.01	.10	-.22	.32	.16	.37	.14	-.21	-.71	.41
VERTICAL VELOCITY VS HYDRO WATER CONTENT	.08	-.55	88.89	88.89	88.89	88.89	.13	.31	-.27	88.89	88.89
JW CLOUD WATER VS ICE PARTICLE CONC	-.31	-.47	-.21	.18	-.29	-.21	-.31	-.21	-.00	-.67	-.72
JW CLOUD WATER VS HYDRO WATER CONTENT	-.31	-.74	88.89	88.89	88.89	88.89	-.02	.36	-.34	88.89	88.89
HYDRO WATER CONTENT VS ICE PARTICLE CONC	.43	.35	88.89	88.89	88.89	88.89	.43	-.06	-.15	88.89	88.89

initial pass data, while the following 29 penetrations (from 1/2 through 29/2) contain second pass data. Only 11 of the cloud towers (see final page of table D2) were penetrated a third time. A composite summary of the microphysical data obtained from the 17 unseeded and 12 seeded towers as a function of first, second and third penetrations has been presented in table 2 of the main text. The main purpose of table D2 is to point out both the variabilities in microphysical data inherent in an ensemble of Florida cumulus towers (even after stratification on the basis of physical appearance³⁸), and the rapidity and magnitude of the microphysical changes from one penetration to another. Of particular interest are the statistics dealing with:

- 1) the percentage of the pass found to contain vertical velocities in excess of 7.5 m/sec,
- 2) JW liquid water in excess of 1.0 g/m³, and/or
- 3) ice particle concentrations of less than 2.5 per liter.

These threshold values have been arbitrarily selected on the basis of experience to represent in-cloud conditions conducive to seeding. It can be seen that in 10 of the 29 towers penetrated for the first time, the three criteria were met simultaneously during at least 25 percent of the pass, with four of those clouds exhibiting the three criteria during at least 50 percent of the pass. On the other hand, in 10 of the 29 towers the three criteria were met simultaneously during 10 percent or less of the pass, with six of those clouds failing to exhibit the three criteria simultaneously during any portion of the penetration. Only in four of the 29 towers penetrated a second time did more than 25 percent of the traverse have the three conditions met simultaneously, while in 19 of the 29 towers, the second penetration failed to show any portion of the cloud with the three conditions coincident. Of the 11 clouds penetrated a third time, only one (17/3) had more than 5 percent of the traverse with all conditions met simultaneously, and 8 of the 11 towers showed no portion of the pass to have these three conditions met at the same time.

The cloud-by-cloud microphysical intercorrelation statistics are also interesting in that they are somewhat surprising. Intuitive reasoning, reinforced by a glance at figures 5, 7 and 12 in the main text, might lead one to suspect that a strong positive correlation should exist between vertical velocity and JW cloud water content, and a strong inverse correlation should exist between vertical velocity and ice particle content. A computation of correlation coefficient based upon a linear best fit to the sample data set indicates, however, that this is not true for all cloud passes. Cloud #80621 (12/1) is an example where such a correlation does exist, while cloud #71616 (4/1) provides an example where the expected correlation not only fails to materialize, but also shows a tendency to be completely reversed.

³⁸ Only those clouds with a hard cauliflower appearance judged suitable for seeding were penetrated initially.

The ice particle data from all second and third penetrations of cloud towers which, on initial penetration, contained a maximum ice particle concentration of less than 3.0 per liter and a mean ice particle concentration not in excess of 0.5 per liter are plotted as a function of time in figures D1, D2 and D3. Data points from 11 seeded and 14 unseeded towers are included. Figure D1 shows the evolution of the mean ice particle concentration and figure D2 shows the evolution of the maximum ice particle concentration. Figure D3 shows how the percentage of the pass with ice particle concentration in excess of 2.5 per liter changes with time. The "zero" time point in each of the three figures corresponds to the time the aircraft entered the tower on the initial penetration.

As discussed in the main text, knowledge of how glaciation proceeds with time in the case of seeded and unseeded cumulus clouds is vital to a proper interpretation of how seeding alters cloud processes. We might expect from the seeding hypothesis that the introduction of massive amounts of silver iodide ice nucleating material should lead to a detectable increase in ice particle concentration in the case of seeded clouds. We can see from figure D1, however, that when the mean ice particle measurements are stratified according to seeded and unseeded towers, no clear-cut trend in the data set emerges. It appears that after 10 minutes, as much ice is present in unseeded towers as in seeded towers. In fact, the three highest mean ice particle concentrations are found in unseeded clouds. The situation improves little when maximum ice particle concentration is considered. No argument could reasonably be made for consistently more ice in seeded clouds during the first 10 minutes. Again, the highest values of maximum ice appeared in unseeded clouds.

It is only when the ice particle data are analyzed in terms of the percentage of the pass with a concentration in excess of 2.5 per liter that some trends in the data set possibly begin to emerge. It can be seen in figure D3 that of the 21 data points in the first 10 minutes, the five lowest pass percentages are all from unseeded towers. During the first 6 minutes, with seven seeded and seven unseeded towers in the data set, the lowest four pass percentages are found in unseeded towers and four of the five highest percentages of the pass with ice are found in seeded towers.

The three figures taken together would seem to suggest that the spread of ice throughout the cloud at a single level is greater in the case of seeded towers, a finding which is not reflected in measurements of mean or maximum values of the concentration. However, this is by no means a certainty and more data will be necessary to determine if the trend is real.

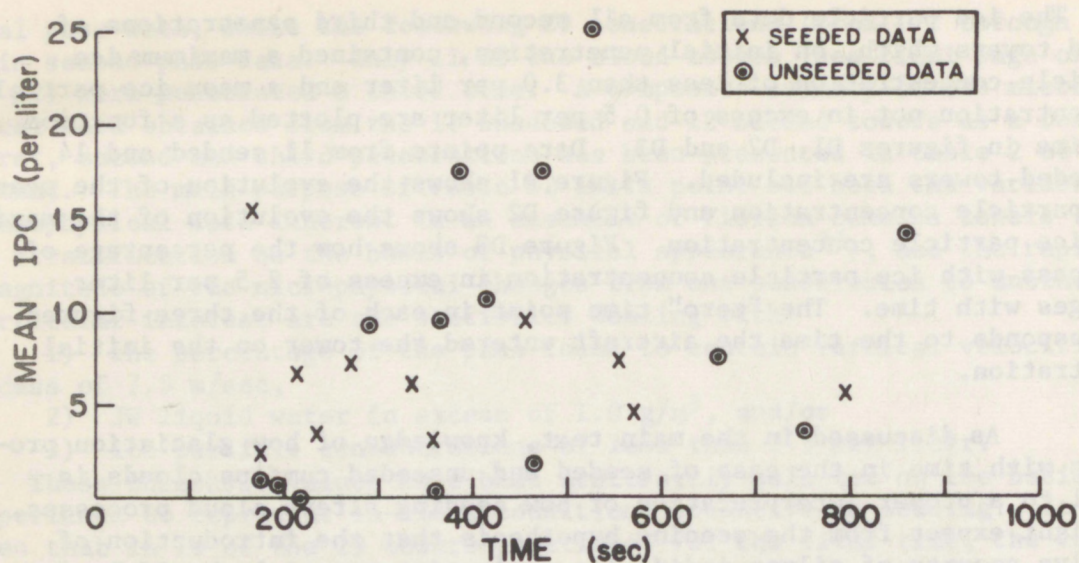


Figure D1. Mean concentration of ice particle concentration (as determined from Mee ice particle instrument) as a function of time for those seeded and unseeded cumulus towers which were penetrated at least twice and had no ice on first penetration.

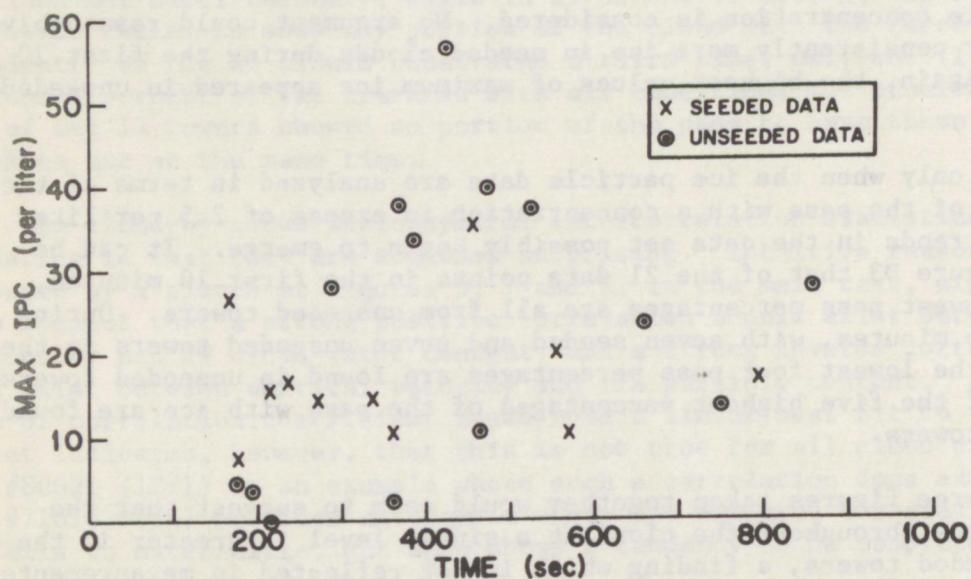


Figure D2. Maximum concentration of ice particle concentration (as determined from Mee ice particle instrument) as a function of time for those seeded and unseeded cumulus towers which were penetrated at least twice and had no ice on first penetration.

Remember, also, that all the data in table D2 and in figures D1, D2 and D3 were obtained from penetrations at a single level near the -10°C isotherm. It is indeed possible, particularly with the pyrotechnics used in FACE-73 (appendix C), that any significant glaciation due to seeding occurred at slightly colder temperatures and thus might not have been sampled at the -10°C level. This possibility will be examined during the FACE-75 program.

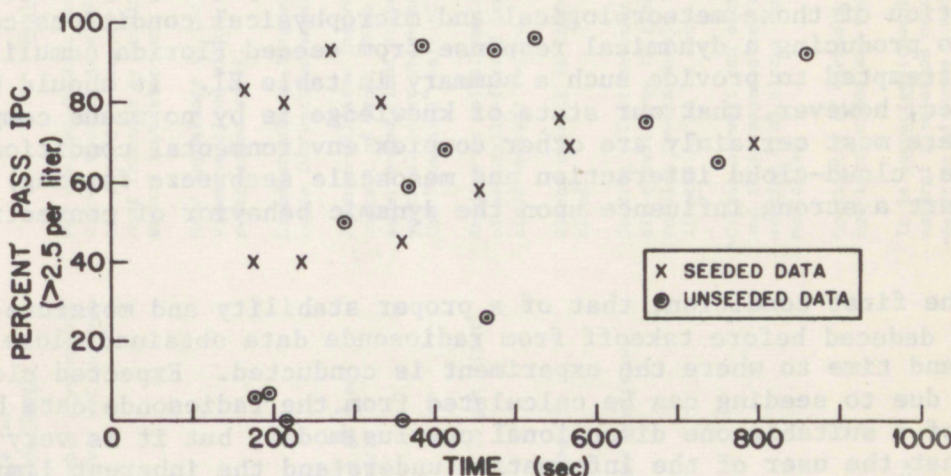


Figure D3. Percentage of the penetration with ice particle concentration (as determined from Mee ice particle instrument) greater than 2.5 crystals per liter as a function of time for those seeded and unseeded cumulus towers which were penetrated at least twice and had no ice on first penetration.

APPENDIX E

SYNOPSIS OF METEOROLOGICAL AND MICROPHYSICAL CONDITIONS JUDGED SUITABLE OR UNSUITABLE FOR DYNAMIC CUMULUS SEEDING IN FLORIDA

NHEML's Cumulus Group is often requested to present a concise summarization of those meteorological and microphysical conditions conducive to producing a dynamical response from seeded Florida cumuli. We have attempted to provide such a summary in table E1. It should be realized, however, that our state of knowledge is by no means complete, and there most certainly are other complex environmental conditions (for example, cloud-cloud interaction and mesoscale seabreeze forcing) which can exert a strong influence upon the dynamic behavior of convective clouds.

The first condition, that of a proper stability and moisture profile, can be deduced before takeoff from radiosonde data obtained close in space and time to where the experiment is conducted. Expected cloud growth due to seeding can be calculated from the radiosonde data by means of a suitable one dimensional cumulus model, but it is very important that the user of the information understand the inherent limitations of the model. Conditions #8 and #9 can also be determined from the radiosonde data or, in the case of #9, from the movement of S-band radar echoes of rainfall. Condition #10 can be determined from radiosonde information in conjunction with an analysis of low-level air trajectories.

Criteria #2, #3 and #7 can be determined from the aircraft prior to penetrating the cloud towers. Although the cloud conditions may not appear suitable initially, it has been our experience that patience is often rewarded as conditions can improve dramatically in an hour or two. Conversely, some days which appear suitable initially become unsuitable later. This is particularly true in the case of days with middle- or upper-level wind shear which can serve to extend cirrus anvils over large portions of the target area.

Criteria #4, #5 and #6 can only be determined from measurements obtained during penetration of the cloud tower. It is desirable to penetrate the cloud to insure proper placement of the nucleant and to confirm impressions gained from visual observations. Oftentimes it is not possible to confidently judge cloud suitability without penetrating. However, on some occasions, a rapidly-rising tower presents such an unambiguously hard appearance that it is feasible to seed over its top without actually penetrating.

Table E1. *Dynamic Seeding Criteria*

Conditions Suitable for "Dynamic" Seeding of Florida Cumuli		Conditions not Suitable for "Dynamic" Seeding of Florida Cumuli	Explanation
1. unstable lower troposphere, stable middle troposphere and unstable upper troposphere with moisture values not too dry or too wet throughout		stable lower troposphere or unstable troposphere through mid-levels; very dry or very wet through large region of troposphere	For optimum dynamic seeding effects, cumulus clouds need to grow naturally to about -10°C but should be stopped by a capping inversion; heat released by seeding allows cloud to grow beyond inversion into unstable layer above.
2. hard cauliflower appearance to clouds		fuzzy appearance to clouds	Hard appearance is indicative of young, vigorous cloud with a copious quantity of supercooled water.
3. tower moving upward through flight altitude		no upward motion to tower	Cloud should be in growing stage of its life cycle for optimum seeding effect.
4. cloud liquid water content in excess of 1.0 gm^{-3} as measured by Johnson-Williams device		cloud water content less than 0.5 gm^{-3} as measured by Johnson-Williams device	Johnson-Williams instrument measures water content of drops $<30\mu\text{m}$ radius; the presence of supercooled cloud drops is indicative of a youthful tower which has not yet started on the "downhill" part of its life cycle.
5. ice particle content less than 7.5 per liter		ice particle content greater than 20 per liter	Seeding is pointless if large concentrations of naturally-formed ice already exist in cloud updraft region.
6. updraft velocity in excess of 7.5 m sec^{-1}		updraft velocity less than 5.0 m sec^{-1}	Strong updraft is indicative of youthful cloud.
7. convection neither very isolated nor very disturbed		suppressed conditions or disturbed conditions	Seeding effect becomes indistinguishable if all clouds grow to great heights, however, cumulus towers should form in close proximity if seeding is to cause mergers.
8. weak wind shear conditions		strong wind shear conditions	^Cirrus blowoff can decrease surface heating and thus suppress new convection; also natural seeding from cirrus anvils can confuse experimentation.
9. weak low-level winds		strong low-level winds	Continuity of thermals destroyed by strong low-level winds and convection is suppressed.
10. continental air mass characteristics		maritime air mass characteristics	It is suspected (though not confirmed) that natural glaciation occurs more readily under maritime air mass conditions.

APPENDIX F

ANSWERS TO QUESTIONS FREQUENTLY ASKED ABOUT FACE

Question 1: What is meant by dynamic cloud seeding?

Dynamic cloud seeding is seeding to alter the circulations that sustain the clouds. In the context of FACE, this is accomplished by massive silver iodide seeding of supercooled convective clouds. Massive seeding in such clouds results in the release of the latent heat of fusion and deposition which acts to increase cloud buoyancy and invigorate the updraft. Under ideal circumstances, invigoration of the cloud updraft results in the invigoration of the entire cloud system.

Question 2: What is meant by massive seeding?

Massive cloud seeding in the context of FACE is the expenditure of silver iodide pyrotechnics into a cloud so that approximately 100 nuclei per liter active at -10°C are distributed in the supercooled cloud volume.

Question 3: Why is seeding conducted at about the 6-km level rather than below cloud base?

It is our opinion that serious uncertainties with regard to targeting, distribution and nucleating effectiveness of the silver iodide would occur if the material had to ascend through 4 km of cloud depth before reaching the freezing level. In addition, penetration of the cumulus cloud at the level of nucleating effectiveness allows us to make the measurements necessary to optimize placement of the nucleant within the tower.

Question 4: What is seedability?

Seedability is the model predicted difference in kilometers between the maximum height of a seeded cloud and the same cloud if not seeded.

Question 5: What is meant by explosive cloud growth?

Explosive cloud growth is the rapid growth of a convective cloud mass following silver iodide seeding. Growth normally occurs in two phases. The first is vertical growth, typically from an altitude of 7 or 8 km to an altitude of 11 to 14 km and normally requires 10 to 15 minutes. The second is horizontal growth that requires another 15 to 20 minutes. Unseeded clouds also can exhibit the explosive growth made.

Question 6: You have shown that dynamic seeding increases the rainfall in isolated convective clouds. Then why bother with an area experiment?

It is true that dynamic seeding is effective in increasing the rainfall from individual clouds. However, most of the rain that falls in Florida at least comes from organized cloud systems. Consequently, if the technique is to have practical use, we must demonstrate that dynamic seeding is effective in increasing cloud organization and rainfall over a large geographical area. This is what FACE is all about.

Question 7: What is meant by cloud merger?

Cloud merger is the joining at a particular rainrate of two or more formerly independent precipitating cloud systems into one coherent echo mass as viewed on radar. In all instances, merger of the visible clouds precedes merger of the echoes that correspond to them. In the FACE program, merger is defined to occur at a rainrate of 1 mm/hr.

Question 8: Why conduct dynamic seeding in Florida when all natural clouds grow to cumulonimbus anyway?

Although it may seem that way, in actuality, not all Florida convective clouds grow to cumulonimbus stature. Nevertheless, Florida is a tremendous generator of such clouds and their existence in this natural state constitutes a source of noise in FACE. This is why project scientists have been so selective in their choice of experimental days. An ideal location for dynamic seeding experiments would be one in which there is large and consistent seedability in an area where large clouds occur rather infrequently, but suitable towers occur on a reproducible basis.

Question 9: Why is the experiment randomized by day instead of by area?

This is an important question. Other researchers have demonstrated that randomization by area, commonly called the crossover design, is much more efficient than the randomization by day. We knew this at the start of our planning for FACE; however, certain conditions precluded the crossover design. Initially, we relied on the University of Miami 10-cm radar for rain measurement. Unfortunately, there were then, and are now, obstructions to the

Question 9: energy radiated by this radar producing blind spots
(cont.) to the west of this radar. Any thoughts of crossover for FACE would have necessitated two areas, one over the Everglades National Park and the other south of Lake Okeechobee. However, with the University of Miami 10-cm radar it was not possible to view the entire southern area. Consequently, the crossover design was precluded by this one consideration. We are now using the 10-cm radar of the National Hurricane Center for our rain measurement, so crossover is now a possible design option. However, there are other considerations that may preclude the crossover design in Florida. One is the contamination problem, whereby the control area is contaminated by activities in the seeded area. This might occur by direct movement of the silver iodide from the seed area to the control or it might by a more subtle contamination whereby cloud growth induced in the seeded area might suppress cloud growth in the nearby control. This has been dubbed "dynamic contamination" by Arnett Dennis at the South Dakota School of Mines. A second consideration of lesser importance that makes the crossover design less desirable is the poor correlation of rain events in one area to rain events in the other. That is, one area might well be covered by intense convection and the other area might have none at all. However, this is the same problem we face in randomization by area, so this one consideration does not of itself preclude the crossover design. At present, the lone consideration that would appear to preclude crossover is the possibility, or perhaps probability, of control area contamination by activities in the seeded area. This is not a closed issue and the crossover design is still a possibility in the FACE program.

Question 10: What do you mean by the floating target?

The floating target is made up of the echoes of experimental clouds and the echoes of clouds with which they merge during the period of rain calculation. The floating target is limited to the area within the fixed target area.

Question 11: Why do you fly on control days? It would be much more efficient to fly on only seed days.

It certainly would be desirable to fly on only seed days. This would minimize the cost and effort expended in such an experiment. However, as we have seen, natural rain variability is the major obstacle to be overcome in FACE and

Question 11: at present the way we hope to overcome this obstacle is through the floating target. The floating target can only be defined by flying on both seed and no seed days. If we should find a suitable predictor or covariate that we can use to minimize the natural rain variability, then it may be possible to eliminate the floating target concept and fly only on seed days. This might be done in the following way: We would determine the suitability of the day as best we could in the usual manner, and fly in the target area to determine whether the clouds are suitable for seeding. At that point, the randomized seeding instruction would be drawn. Regardless of the decision, we would continue to fly until we had expended 60 flares and/or seeded six clouds. Then the seeding decision would be revealed. Should the decision be to seed, we would continue the work knowing we are seeding. Should the decision be not to seed, the day would qualify as a control and we could immediately return to the airport. The analysis would be then a comparison between seeded and nonseeded rainfall for the entire target. This is a very desirable goal. It would be the most efficient use of the resources and it would maximize the learning experience because the individual conducting the experiment would know what he is doing and would be able to compare the response of the seeded clouds to his expectations. Elimination of the floating target concept would also serve to increase the number of cloud towers eligible for seeding. However, until the appropriate covariate or covariates are in hand or until the seeding effect on the floating target is established, it is felt that we must continue with the floating target concept which necessitates flying on both seed and no seed days.

Question 12: In the FACE efforts of 1970 and 1971 the project scientists knew the seed decisions at the end of each day of experimentation. Why was this information denied them in subsequent experiments?

This change was made in order to guard against bias in conducting the experiment and to eliminate bias or prejudice in the analysis of the results. In the early FACE efforts there was some evidence that indicated that the project scientists were anticipating the seed decision based on the seed decision of the previous day. It was reasoned that if the scientists did not know the decision of the previous day, no bias would be possible. The possibility of bias or prejudice in the analysis is a more serious consideration. The rainfall in FACE is and has been obtained using radar observations. In principle, the analysis should be a totally objective process. However, two partly subjective considerations enter into the

Question 12: analysis. The first is the elimination of false echo (cont.) due to anomalous propagation and the second is the adjustment of the radar-derived rainfall using gages. The elimination of false echo due to anomalous propagation is a subjective process, because one must delineate the false echo from the real. The adjustment of the radar representation of rainfall using gages is more objective. Nevertheless, there are elements of subjectivity that enter into this process as well. To eliminate any possibility of bias entering into either process, the seed decisions were kept secret until after both had been accomplished. Although this is an improvement in one sense, it is a major disadvantage in another because it minimizes the learning experience. The scientist or scientists conducting the operation cannot learn from operations on each day because the seed decision is not known. Consequently, it is impossible to tailor the seeding or improve the seeding based on one's experience. Rather, the scientist must wait until the end of the entire operation to know the decision and then rely on an imperfect memory for the learning experience. A solution that might satisfy both points of view is to analyze the rainfall in near real-time, and provide the scientists the seed decision after that analysis has been completed.

Question 13: What are the primary obstacles to the resolution of an area wide seeding experiment for rain enhancement?

The main obstacles to resolution of area seeding effect in FACE are natural rain variability and measurement errors. Natural rain variability is by far the most serious obstacle and every attempt is being made to minimize its effect on the experiment. This can be done by adopting the most efficient experimental design and also by seeking predictors and covariates for the rain analysis.

Question 14: How long must FACE continue before definitive answers are in hand?

This is the question in the mind of everyone affiliated with FACE. The considerations here are the expected seeding effect and obstacles such as natural rain variability and measurement errors. All have been considered in recent years in statistical simulations done at the old Experimental Meteorology Laboratory. In summary, the results indicate that at least 100 total experimental days, 50 seed and 50 no-seed days will be needed to demonstrate a seeding effect of 1.5. Should the effect

Question 14: be less than that, we must resolve to continue for a
(cont.) longer time, redesign the experiment or discontinue
the effort altogether. These are decisions that must
be made in the future.

Question 15: Why is so much effort being expended on measuring and
evaluating internal cloud processes?

FACE is a program designed to investigate the effects of
dynamic cloud seeding on the development and organization
of convective clouds and the rainfall which results from
them. The physical foundation of the experiment is pre-
dictated upon a sequential chain of microphysical and dynam-
ical events which eventually lead to enhanced rainfall. It
is important to determine and document that the physical
foundation is solid, particularly since the natural varia-
bility of rainfall is much greater than the effect which
can most likely be produced through seeding. Without a
thorough understanding of how cloud evolution is altered
by seeding, it would not be possible either to improve
the experimental procedures or to foresee limitations in
exportability of the technique to other locations.

Question 16: What is the environmental impact of the Florida Area
Cumulus Experiment?

In answering this question, one must first remember that
we are talking about a research cloud seeding effort, not
an operational effort. Consequently, the answer
is only valid for this research situation and this matter
should be reconsidered if and when dynamic seeding is used
operationally. Of most concern to the environmentalist is
the silver iodide used in the seeding. In 1973, we began
a program to trace the silver iodide used during the
course of dynamic seeding. We had water collection at the
surface and at cloud base using airborne collectors. In
this limited study, silver concentrations of seed and non-
seed days were far below those specified as dangerous by
the U.S. Public Health Service. In fact, it was noted
during FACE 1973 on several occasions that the silver
concentration was greater on no seed days than on seed
days. At the present time, we have no evidence
to indicate an environmental hazard from the silver iodide
used in the experiment. However, we do not feel that this
is by any means a closed issue and we are presently en-
gaged in an intensive environmental effort in FACE-75.
Once again, water and aerosol collection at cloud base
and at ground is being conducted. After the analysis of

Question 16: the data, we will be able to determine whether our preliminary
(contd.) indications from FACE-73 are valid.

The second environmental problem that could result from dynamic seeding might be increased rainfall at the ground, since this is the goal of this particular experiment. There should be no problem during the research effort. However, should it be possible to increase the rainfall by 15 or 25 percent over the course of a year, then it is possible that the increased rainfall will change the environmental balance of south Florida. If, in fact, this is determined, then the advantages from the seeding should be weighed against any disadvantages that result from the seeding. This problem is one that is left to the future since at this time we have not established that dynamic seeding is effective in increasing rainfall over an area.

☆U.S. GOVERNMENT PRINTING OFFICE: 1976-077-347/1246 REGION NO. 8

ENVIRONMENTAL RESEARCH LABORATORIES

The mission of the Environmental Research Laboratories is to study the oceans, inland waters, the lower and upper atmosphere, the space environment, and the earth, in search of the understanding needed to provide more useful services in improving man's prospects for survival as influenced by the physical environment. Laboratories contributing to these studies are:

Atlantic Oceanographic and Meteorological Laboratories (AOML): Geology and geophysics of ocean basins and borders, oceanic processes, sea-air interactions and remote sensing of ocean processes and characteristics (Miami, Florida).

Pacific Marine Environmental Laboratory (PMEL): Environmental processes with emphasis on monitoring and predicting the effects of man's activities on estuarine, coastal, and near-shore marine processes (Seattle, Washington).

Great Lakes Environmental Research Laboratory (GLERL): Physical, chemical, and biological, limnology, lake-air interactions, lake hydrology, lake level forecasting, and lake ice studies (Ann Arbor, Michigan).

Atmospheric Physics and Chemistry Laboratory (APCL): Processes of cloud and precipitation physics; chemical composition and nucleating substances in the lower atmosphere; and laboratory and field experiments toward developing feasible methods of weather modification.

Air Resources Laboratories (ARL): Diffusion, transport, and dissipation of atmospheric contaminants; development of methods for prediction and control of atmospheric pollution; geophysical monitoring for climatic change (Silver Spring, Maryland).

Geophysical Fluid Dynamics Laboratory (GFDL): Dynamics and physics of geophysical fluid systems; development of a theoretical basis, through mathematical modeling and computer simulation, for the behavior and properties of the atmosphere and the oceans (Princeton, New Jersey).

National Severe Storms Laboratory (NSSL): Tornadoes, squall lines, thunderstorms, and other severe local convective phenomena directed toward improved methods of prediction and detection (Norman, Oklahoma).

Space Environment Laboratory (SEL): Solar-terrestrial physics, service and technique development in the areas of environmental monitoring and forecasting.

Aeronomy Laboratory (AL): Theoretical, laboratory, rocket, and satellite studies of the physical and chemical processes controlling the ionosphere and exosphere of the earth and other planets, and of the dynamics of their interactions with high-altitude meteorology.

Wave Propagation Laboratory (WPL): Development of new methods for remote sensing of the geophysical environment with special emphasis on optical, microwave and acoustic sensing systems.

Marine EcoSystem Analysis Program Office (MESA): Plans and directs interdisciplinary analyses of the physical, chemical, geological, and biological characteristics of selected coastal regions to assess the potential effects of ocean dumping, municipal and industrial waste discharges, oil pollution, or other activity which may have environmental impact.

Weather Modification Program Office (WMPO): Plans and directs ERL weather modification research activities in precipitation enhancement and severe storms mitigation and operates ERL's research aircraft.

NATIONAL OCEANIC AND ATMOSPHERIC ADMINISTRATION
BOULDER, COLORADO 80302